Université de Montréal

Localization and Function of the Endocannabinoid System Throughout the Retinogeniculate Pathway of Vervet Monkeys

Par

Pasha Javadi Khomami

École d'optométrie

Thèse présentée à la Faculté des études supérieures

en vue de l'obtention du grade de doctorat

en Sciences de la Vision

Option Neurosciences de la vision et psychophysique

Janvier 2015

Résumé

Mots-clés: *endocannabinoïdes, vision, singe, CB1R, CB2R, FAAH, NAPE-PLD, DAGL, MAGL, ERG*

Le système endocannabinoïde (eCB) est présent dans le système nerveux central (SNC) de mammifères, incluant la rétine, et est responsable de la régulation de nombreux processus physiologiques. Bien que la présence du récepteur cannabinoïde de type 1 (CB1R) a bien été documenté dans la rétine de rongeurs et primates, il y a encore une controverse quant à la présence du récepteur cannabinoïde de type 2 (CB2R) au niveau du SNC. En utilisant la microscopie confocale, nous sommes les premiers à signaler les patrons d'expression du CB2R dans la rétine de singe. Nos résultats démontrent que le CB2R est exprimé exclusivement dans les cellules de Müller de la rétine du singe. En outre, nous avons comparé les différents patrons d'expression du système eCB dans la rétine de la souris, du toupaye, ainsi que du singe vervet et macaque. Nous rapportons que les distributions de CB1R, FAAH (*fatty acid amid hydrolase*), MAGL (monoacylglycerol *lipase*) et DAGLα (*diacylglycerol lipase alpha*) sont hautement conservées parmi ces espèces alors que CB2R et NAPE-PLD (*N-acyl phosphatidylethanolamine phospholipase D*) présentent différents profils d'expression. CB2R n'a pas été détecté dans les cellules neuronales de la rétine des primates. L'immunoréactivité de NAPE-PLD est présente dans les couches de la rétine de souris et toupayes, mais a été limitée à la couche des photorécepteurs des singes vervet et macaque.

Pour étudier les corrélats neuronaux et le rôle de la signalisation du système eCB dans la rétine, nous avons établi un protocole standard pour l'électrorétinographie (ERG), puis

enregistré la réponse ERG de la rétine après le blocage des récepteurs avec des antagonistes spécifiques pour CB1R (AM251) et CB2R (AM630). Comparé au témoin, dans des conditions photopiques, et à certaines intensités faibles du stimulus, le blocage de CB1R diminue l'amplitude de l'onde-b, alors qu'à des intensités plus élevées, le blocage de CB2R augmente l'amplitude des deux-ondes a et b. De plus, le blocage des récepteurs cannabinoïdes provoque une augmentation de la latence des deux ondes a et b. Dans des conditions d'adaptation à l'obscurité, le blocage de CB1R et CB2R réduit l'amplitudes de l'onde a seulement à des intensités plus élevées et réduit l'onde b à intensités plus faibles. Des augmentations significatives de latence ont été observées dans les deux cas. Ces résultats indiquent que les récepteurs CB1 et CB2 chez les primates non humains sont impliqués dans la fonction rétinienne conditions photopiques.

En outre, nous avons évalué le profil d'expression du CB1R, de FAAH et de NAPE-PLD au-delà de la rétine dans le corps géniculé latéral des singes et nous rapportons pour la première fois que CB1R et FAAH sont exprimés davantage dans les couches magnocellulaires. La NAPE-PLD a été localisée à travers les couches magno- et parvocellulaires. Aucune de ces composantes n'est exprimée dans les couches koniocellulaires.

Ces résultats nous aident à mieux comprendre les effets des cannabinoïdes sur le système visuel qui pourraient nous mener à trouver éventuellement de nouvelles cibles thérapeutiques.

Abstract

Keywords: *endocannabinoid, vision, monkey, CB1R, CB2R, FAAH, NAPE-PLD, DAGL, MAGL, ERG*

The endocannabinoid (eCB) system is present in the mammalian central nervous system, including the retina, and is responsible for the regulation of many physiological processes. Anatomical and functional data collected in the retina indicate that cannabinoid receptors are important mediators of retinal function. Although the presence of the cannabinoid receptor type 1 (CB1R) has been documented in the rodent and primate retina, there is still some controversy regarding the presence of the CB2 receptor (CB2R) within the central nervous system. By using confocal microscopy, we are the first to report the distribution patterns of CB2R in the monkey retina. Our results show that CB2R is expressed exclusively in the Müller cells of the primate retina. Furthermore, we compared the eCB system distribution patterns in the retinas of mice, tree shrews, and vervet and macaque monkeys. We report that CB1R, FAAH, MAGL, and DAGLα distributions are highly conserved among these 3 species whereas CB2R and NAPE-PLD exhibit different expression patterns. CB2R was not detected in the neuroretinal cells of primates. NAPE-PLD immunoreactivity was present in the retinal layers of mice and tree shrews but was restricted to the photoreceptor layer in both species of primates studied.

To study the neural correlates and the role of eCB signaling in the retina, we first established a standard protocol for electroretinography (ERG) and then recorded the ERG response of the retina after blocking receptors with specific antagonists for CB1R (AM251) and CB2R (AM630). Compare to control, in photopic conditions, at certain low flash

intensities, only the blockade of CB1R decreases the amplitude of the a-wave and b-wave, while at some high flash intensities, blockade of CB2R increase the amplitude of both a- and b-waves. Also the blockade of the cannabinoid receptors causes an increase in the latency of both a- and b-waves. In dark-adapted eyes, blockade of the CB1R and CB2R reduces the a-wave only amplitudes in the higher intensities and decrease the b-wave in lower intensities. Some significant increases in latency were observed in both cases. These results indicate that CB1 and CB2 receptors in primates are involved in retinal function under photopic and scotopic conditions.

In addition, we assessed the expression pattern of eCB components CB1R, FAAH, and NAPE-PLD beyond the retina in the dorsal lateral geniculate nucleus (dLGN) of primates and report for the first time that while CB1R and FAAH are more abundantly expressed in the magnocellular layer, NAPE-PLD is distributed throughout both the magno- and parvocellular layers. None of these components are expressed in the koniocellular layer.

These findings augment our understanding of the effects of cannabinoids on the visual system and may lead to novel therapeutics targeted to eCB signaling.

Table of Contents

List of tables

List of figures

List of abbreviations

2-AG	2-arachidonoylglycerol
Abhd12	α, β-hydrolase 12
Abhd6	β-hydrolase 6
AC	adenylyl cyclase
AMD	age-related macular degeneration
AEA	anandamide, N-arachidonoylethanolamine
CaN	Ca2+-sensitive phosphatase calcineurin
CB1R	cannabinoid receptor 1
CB2R	cannabinoid receptor 2
CBC	cannabichromene
CBD	cannabidiol
CBG	cannabigerol
CBN	cannabinol
CBR	cannabinoid receptors
CECD	clinical endocannabinoid deficiency
cGMP	cyclic guanosine monophosphate
CNS	central nervous system
COX-2	cyclooxygenase-2
CRIP1a	cannabinoid receptor interacting protein
DAGL	diacylglycerol lipase
dLGN	dorsal lateral geniculate nucleus
DSE	depolarization-induced suppression of excitation
DSI	depolarization-induced suppression of inhibition
eCB	endocannabinoid
EEG	electroencephalography
ERG	electroretinography
ERK	extracellular signal-regulated kinases
FAAH	fatty acid amide hydrolase
GCL	ganglion cell layer
GFAP	glial fibrillary acidic protein
$G_{i/o}$	inhibitory G-proteins
GPR55	G protein-coupled receptor 55
GS	glutamine synthetase
iGluR	ionotropic glutamate receptors
INL	inner nuclear layer
IOP	intraocular pressure

IPL	inner plexiform layer
JNK	c-Jun N-terminal kinases
LPI	L-α-lysophosphatidylinositol
LTD	long-term depression
MAGL	monoacylglycerol lipase
MST	medial superior temporal area
MT	middle temporal
NADA	N-arachidonoyl-dopamine
NAE	N-acylethanolamines
NAPE	N-acyl-phosphatidylethanolamine
NAPE-PLD	N-acyl phosphatidylethanolamine-specific phospholipase D
NAT	N-acyltransferase
NDS	normal donkey serum
OAE	*Virodhamine* (O-arachidonoyl ethanolamine)
ONL	outer nuclear layer
OPL	outer plexiform layer
PBS	phosphate-buffered saline
PKA	protein kinase A
PKC	protein kinase C
PLC	phospholipase C
RhoA	ras homolog gene family, member A
SC	superior colliculus
SEM	standard error of the mean
SSVEP	steady state visual evoked potential
STD	short-term depression
THC	Δ9-tetrahydrocannabinol
TRPV1	transient receptor potential vanilloid type 1
V1	primary visual cortex
V2	visual areas two
V3	visual areas three
V4	visual areas four
V5	visual areas five
VEP	visual evoked potential
VGLUT1	vesicular glutamate transporter 1
Δ^8-THC	Δ^8-tetrahydrocannabinol
Δ^9- THC	Δ^9-tetrahydrocannabinol

To

Farnoush, Mahnaz and Alireza

Who have made me confident,

in the cloudiest days of life!

Acknowledgments

Numerous people over the years have helped me get here, so there are many people I need to thank. I would never have been able to finish my dissertation without the guidance of my committee members, help from friends, and support from my family and wife.

Foremost, I would like to express my deepest gratitude to my advisor, mentor and friend Professor Maurice Ptito, for the continuous support of my Ph.D study and research, for his patience, energy, motivation, enthusiasm, and immense knowledge. His guidance helped me in all the time not only in my research and writing of this thesis but also in life.

I am deeply indebted to my co-supervisor Dr. Jean-François Bouchard, for the patient guidance, encouragement and advice he has provided throughout my doctorate. His precision, moral and passion persuasively conveyed an interest in my work. I could not have imagined having a better team of advisor and mentor for my Ph.D study.

I would also like to thank all the members of our laboratory, Alexandra, Bruno, Hocine, Hosni, Lea, Laurent, Reza, Sebrina and Vanessa, with whom I have enjoyed working during last years. I am especially thankful to Joseph Bouskila for his valuable science exchange and discussions, and who was not only a great colleague but also a good friend and a wonderful person from whom I have learned a lot.

My special thanks also goes to Drs. Roberta Palmour and Frank Ervin for providing me with the opportunity to work in their lab and for their constant support, and all our colleagues in Behavioral Science Foundation in St. Kits, Amy, Chris, Aybob, Bango, Doris, … for all their helps.

On a more personal note, I would like to send a heartfelt thank to all my friends who made these years very joyful with their friendship and interesting, intellectual and creative ideas Ali, Arash, Armin, Azadeh, Bahador, Behzad, Farrokh, Hazhir, Mahdokht, Mohammad, Mojdeh, Naeim, Pedram, Reza, Sara, Shahab, Shahdad, Shahin, Yasi, Yashar… .

I would like to thank Dr Shahin Zangenehpour who, as a good friend, was always willing to help and give his useful suggestions. He introduced me to the field of neuroscience and Dr Ptito and always provides me with creative idea and fruitful collaboration.

I acknowledge the unconditional support, understanding and care of my in-laws Shahin, Fariborz and Farshad.

I am deeply indebted to my adorable parents, Mahnaz and Alireza, for their absolute love and support, who have always encouraged me to follow my dreams. They are the driving force behind all of my successes. I would like to acknowledge the helps of my brother, Pooya, who was always, patiently, there for me and give me lots of technical supports.

Above all I would like to thank my wife Farnoush for her love and constant support, for all the late nights and early mornings, and for keeping me sane over the past few months. Thank you for being my muse, proofreader, and sounding board. But most of all, thank you for being my best friend and companion. I owe you everything.

CHAPTER 1: Introduction

Historical aspects

We cannot talk about cannabinoid system research and not citing the cannabis plant and marijuana related subjects. Certainly, this is in part due to the ancient history of the cannabis plant. Marijuana has been cultivated as hemp for manufacturing and personal reasons for thousands of years, while recreational use of marijuana as a euphoric agent can be dated back to ancient Zoroastrian rituals (Mechoulam, 1986; Di Marzo, 2006;). It also has an ancient history of prescription as a medicinal herb in North Africa, Middle East, India, and far Asia. Half a century after Napoleon carried the Egyptian cannabis seeds to France (1799), an Irish physician working in Calcutta assessed the therapeutic effects of cannabis scientifically and publicized it to the Western World, setting the foundation for cannabinoid research (O'Shaughnessy, 1840).

Long after, in the middle of 20th century, Gaoni and Mechoulam elucidated the structure of Δ^9-tetrahydrocannabinol (THC), the main psychoactive substances of the cannabis, marking another significant step in cannabinoid research (Mechoulam and Gaoni, 1965). The leading studies in the field during that period focused on the adverse effects of cannabis. Two decades later, the first THC binding site – a G-protein-coupled receptor – Cannabinoid receptor 1 (CB1R), was found (Matsuda et al., 1990). This was followed by a second receptor CB2R (Munro et al., 1993). Later on, the isolation of the endogenous ligands anandamide (AEA) and 2-arachidonoylglycerol (2-AG) revealed their cannabinoid-like behavior (Figure 1-1) (Devane et al., 1992; Mechoulam et al., 1995; Di Marzo, 2006).

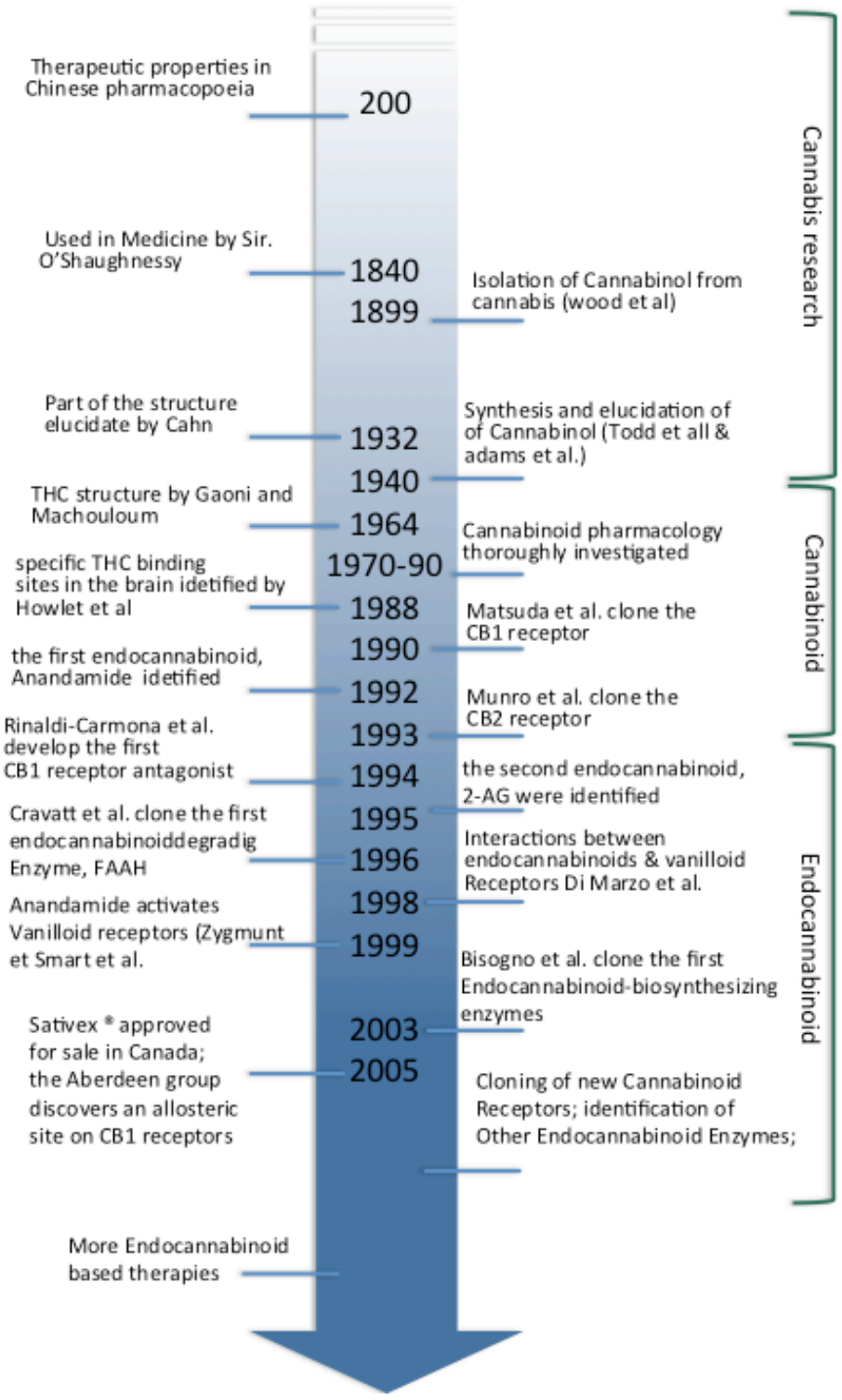

Figure 1-1. Cannabinoid research throughout the history (Di Marzo, 2006)

Chemistry and taxonomy of cannabis

The flowering plant family of Cannabaceae, endogenous to central and south Asia, includes three main different species, *Cannabis sativa*, *indica* and *ruderalis*. Besides for its medicinal and recreational uses, the cannabis plant has been utilized as fiber (hemp), seeds and seed oils for long time (Figure 1-2). Up to more than 525 constituents have been isolated and identified from *C. sativa* among them, 85 cannabinoids, belong to the chemical class of terpenophenolics (El-Alfy et al., 2010). The most common natural cannabinoids are THC, cannabidiol (CBD), cannabigerol (CBG), cannabichromene (CBC), and cannabinol (CBN) that are mostly in a very low quantity and poorly characterized (Figure 1-3).

The ratio of cannabinoid content in different species is dissimilar. *C. ruderalis* has the lowest THC content compared to *C. sativa* or *C. indica*. The cannabidiol (CBD) content of *C. indica* is higher than *C. sativa* strains (Hillig and Mahlberg, 2004).

Figure 1-2 *C. Sativa*. Male flower (1), pollen sac (2 and 3), pollen grain (4), female flower with cover petal (5); female flower (6); female fruit cluster (7), fruit with cover petal (8); seed without hull (13). (Franz Eugen Köhler's drawing 1887)

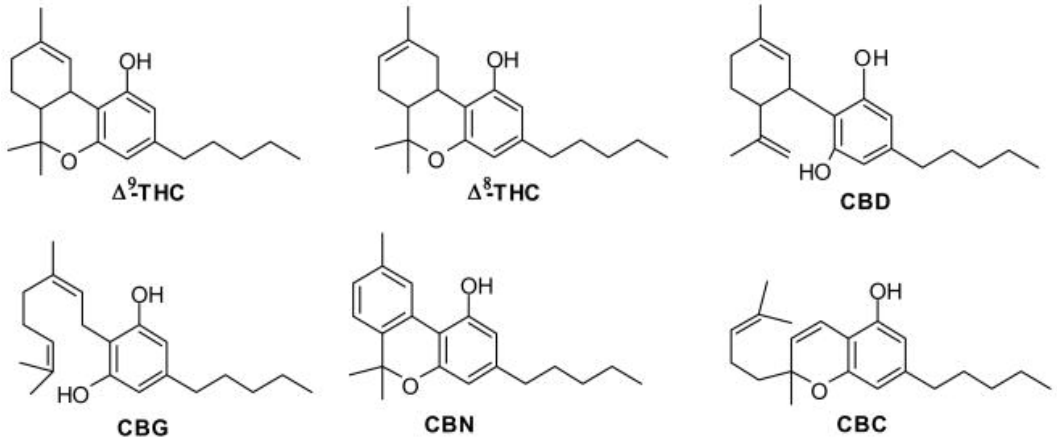

Figure 1-3. Chemical structure of cannabinoids: Δ9-tetrahydocannabinol (Δ9-THC), Δ8-tetrahydrocannabinol (Δ8-THC), cannabidiol (CBD), cannabigerol (CBG), cannabinol (CBN), and cannabichromene (CBC).

Δ^9-tetrahydocannabinol (Δ^9-THC)

The cannabis principal psychoactive constituent, mainly called THC, is a lipophilic aromatic terpenoid that has a very low solubility in water and solubilized thoroughly in organic solvents, lipid and alcohol. The role of the THC in the Cannabis plant is supposed to be a self-defense mechanism of the plant against the herbivores. It might also play a role in protection of the plant from harmful effects of the UV due to its high UV-B (280–315 nm) absorption properties (Lydon et al., 1987). THC produces and affects several positive and negative symptoms such as reducing nausea, fertility, tumor growth, intra ocular pressure (IOP) reduction, analgesia, impaired short-term memory and motor coordination and appetite stimulation (Mechoulam, 2002; Iversen, 2003; Yazulla, 2008).

Δ^8-tetrahydocannabinol (Δ^8-THC)

It is about 20% less active than Δ^9-THC and considered as a THC artifact.

Cannabidiol (CBD)

As the first discovered member of the family is the most abundant cannabinoid in the industrial hemp and accounts for up to 40% of the plant extract. Compare to the main role player in psychoactive symptoms, CBD is believed to have a broad capacity for therapeutic usage (Campos et al., 2012).

Cannabigerol (CBG)

Hemp is rich in this non-psychoactive cannabinoid that is supposed to play a role in reducing the IOP and beneficial to pressure-associated optic neuropathy, glaucoma (Colasanti et al., 1984) and play a role in inflammatory conditions of colon of the large intestine, small intestine and inflammatory Bowel Disease (IBD) (Borrelli et al., 2013).

Cannabinol (CBN)

CBN is poorly characterized. A scant amount of this substance can be found in *C. sativa* and *C. indica*, as the metabolites of CBD and THC.

Cannabichromene (CBC)

CBC is not well characterized although some of the anti-inflammatory, anti-viral and analgesic effects of cannabis have been imputed to CBC (Mechoulam and Gaoni, 1967).

Cannabis effects

The body effects of Marijuana included congestion of the conjunctival blood vessels (red eye), decrease of intraocular pressure, xerostomia (dry-mouth), sensation of hot and cold

in hands and feet, increase in heart rate and muscle relaxation (Ashton, 1999; Green et al., 2003). The psychoactive effects of cannabis are more subjective and difficult to assess due to two main reasons. First, the outcomes are dissimilar in each subject based on the dosages of the drug and its mode of administration. Second, the social setting and expectation results in completely inverse symptoms (Yazulla, 2008). Additionally, brain-imaging and behavioural techniques have been widely used to study the effects of marijuana consumption on brain (Chang and Chronicle, 2007). Cannabis consumption alters the level of consciousness, impairs the short- term memory (Kanayama et al., 2004; Jager et al., 2006; Han et al., 2012), coordination and psychomotor behaviour (Pillay et al., 2004; Rodríguez de Fonseca et al., 2005). It can increase the appetite and craving food (Mattes et al., 1994), relieve nausea (Tramer et al., 2001) and reduce pain (Pini et al., 2012). In some cases, it can block the anxiety feeling and in other cases cause anxiety (Coscas et al., 2013) (Figure 1-4).

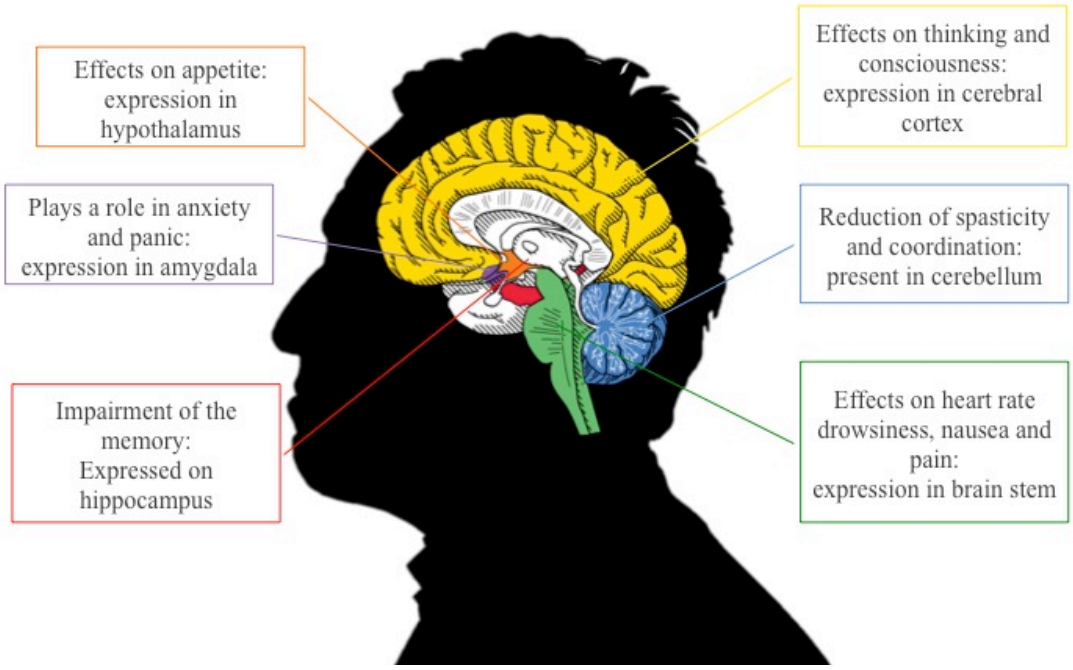

Figure 1-4. Effects of cannabis on the brain with their corresponding area. (Adapted from Maryanne Murray info-graphic and Experimental and Clinical Psychopharmacology, 1994)

The Endocannabinoid System (eCB)

The experience of discovering endogenous ligand for opiate receptors and morphine-like compounds raises this question that the cannabinoids might follow the same track. Devane et al, isolated a brain constituent that binds to the receptors of cannabinoid, arachidonylethanolamide, known as anandamide[1] as the first endogenous cannabinoid with THC-like performance (Devane et al., 1992), later on designated as eCB (Di Marzo and Fontana, 1995).

[1] *Ananda in Sanskrit means joy, bliss, delight*

Function

A number of specific roles have been ascribed to the eCB system in physiological and functions of the synapsis, such as neuroprotection, nociception, motor activity, neurogenesis, synaptic plasticity, in memory (Xu and Chen, 2014), and vision (Yazulla, 2008). The alteration of the normal level of eCBs is considered as a disorder called Clinical eCB deficiency (CECD). CECD is one of the explanation for therapeutic benefits of cannabis in migraine, fibromyalgia, irritable bowel syndrome, and other treatment-resistant conditions (Russo, 2008). More and more, studies suggest that the modulation of eCB activity holds therapeutic promise for a broad range of diseases, including neurodegenerative, cardiovascular and inflammatory disorders (Robson, 2001). Using genetics and pharmacological tools suggests that eCB system plays the role of neuromodulator in various physiological processes (Yazulla, 2008). Among the vast research projects on revealing the roles of endocannabinoid system, particularly in attention, memory, appetite, stress response, inflammation, immune functions, analgesia, sleep and etc., here in this thesis we mainly focus on their visual functions.

Evolution

The cannabinoid receptors are found in many mammals, as well as in various classes of vertebrates and invertebrates, in all major subdivision of bilaterians, in urochordate and cephalochordates, but not in the nonchordate invertebrate phyla like insects (McPartland et al., 2006a; McPartland et al., 2007; Cottone et al., 2013). Thus, it has been suggested that the cannabinoid receptors may have evolved in the last common ancestor of bilaterians with a

secondary loss in insects and other clades (McPartland et al., 2006a). The enzymes responsible for the biosynthesis and degradation of eCBs are present throughout the vertebrates and most of the animals (McPartland et al., 2006b; Elphick, 2012). Beyond doubt, the eCB system is widely distributed phylogenetically and points to a fundamental modulatory role of eCBs in the control of many central and peripheral biological functions, and is a promising tool for its pharmacological manipulation and potential therapeutic exploitation (Di Marzo, 2009).

Main Role Players

The eCB system is composed of the ensemble of cannabinoid receptors (CB1R, CB2R), their endogenous ligands (AEA, 2-AG, N-arachidonoyl-dopamine (NADA), virodhamine (OAE), lysophosphatidylinositol (LPI)), enzymes of synthesis (N-acyl phosphatidylethanolamine-specific phospholipase D (NAPE-PLD), diacylglycerol lipase (DAGL), phospholipase C (PLC)), degradation (fatty acid amide hydrolase (FAAH), monoacylglycerol lipase (MAGL), cyclooxygenase-2 (COX-2)), and other proteins that regulate ligand concentrations (cannabinoid receptor interacting protein (CRIP1a)).

Endocannabinoids

Full endogenous agonists

2-Arachidonoylglycerol (2-AG)

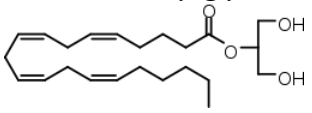

Highly present in CNS, 2-AG is an agonist of CB1R and CB2R. 2-AG is synthesized from arachidonic acid-containing diacylglycerol (DAG) mediated by Phospholipase C (PLC) and diacylglycerol lipase (DAGL). Monoacylglycerol lipase (MAGL), fatty acid amide

hydrolase (FAAH) degrade the 2-AG, immediately after release (Sugiura et al., 1995; Di Marzo, 2011).

Synthesis and degradation

Phospholipase C (PLC) facilitates the synthesis of DAG from the arachidonic acid present in the membrane phospholipids. DAG is then hydrolyzed by DAGL (Bisogno et al., 2003), localized in plasma membrane and stimulated by Ca^{2+}, to form 2-AG. The degradation procedure of the 2-AG is mediated by MAGL. MAGL is hydrolyzing the binding of arachidonic acid to glycerol (Pertwee, 2005). In more than 85% of the brain and CNS, 2-AG is inactivated by MAGL. The remained 15% is shared between two less characterized enzymes: β-hydrolase 6 (Abhd6) and α, β-hydrolase 12 (Abhd12) (Blankman et al., 2007).

DAGL

DAGL has two isoforms, α and β, with around 33% similarity in sequence level. It has been shown that the α isoform of DAGL is more abundant in the adult brain and β is more prevalent during development. There is a 80% decrease in 2-AG levels in the brain's of DAGLα knockout mice. This number is about 50% in DAGLβ knockouts. Thus, DAGLα is necessary and essential in the synthesis of the 2-AG and endocannabinod signaling in the rat brain (Gao et al., 2010).

MAGL

Monoacylglycerol lipase (MAGL) is a 33-kDa, membrane-associated serine hydrolase. MAGL is localized presynaptically with a nearly complementary expression pattern with FAAH (postsynaptic) in rat hippocampus, cerebellum and amygdala (Dinh et al., 2002).

Mechanism of action

Highly lipophilic eCB agonists, unlike the other water-soluble neurotransmitters, cannot be stored in the vesicles and are produced "on demand" (Piomelli, 2003). Cannabinoid receptors (CBRs) are subtypes of the cell membrane G-protein coupled receptors. As G-protein receptors, CBRs include seven transmembrane domains that activate a signal transduction pathway inside the cell by detecting a signal from the outside.

The presynaptic CBRs can reduce neurotransmitter release retrogradedly and mediating transient synaptic plasticity (short-term depression (STD) whether as depolarization-induced suppression of excitation (DSE)(Kreitzer and Regehr, 2001) or inhibition (DSI) (Ohno-Shosaku and Kano, 2014; Wilson and Nicoll, 2001). Additionally, eCB can mediate long-term depression (LTD) at both excitatory (Chevaleyre and Castillo, 2003; Marsicano et al., 2002) and inhibitory synapses (Gerdeman et al., 2002). Throughout the CNS, both LTD and STD regulate various types of GABAergic and glutamatergic synapses (Figure 1-5A). High levels of this system are found in cerebral regions that correspond to the pharmacological effects of THC. The disturbance of normal eCB activity may be associated with some diseases (Bluett et al., 2014; McPartland et al., 2014; Russo, 2008; Smith and Wagner, 2014). Some studies suggest that the modulation of eCB activity holds therapeutic promise for a broad range of diseases, including neurodegenerative, cardiovascular and inflammatory disorders (Robson, 2001).

2-AG in eCB-STD

The augmentation of the intracellular Ca^{2+} and/or activation of $G_{q/11}$ coupled receptors induce the release of 2-AG from postsynaptic neurons. 2-AG binds to presynaptic CB1R and inhibits the release of neurotransmitter. The retrograde signaling terminates when MAGL degrades 2-AG (Tanimura et al., 2012; Ohno-Shosaku and Kano, 2014) (Figure 1-5A).

2-AG in eCB-LTD

Utilizing a similar mechanism to eCB-STD (Ca^{2+} driven eCB release), eCB-LTD is induced mostly by repetitive stimulations that trigger the release of glutamate from excitatory presynaptic terminals. Glutamate activates the post-synaptic mGluRs and induces activation of CB1R via 2-AG release (Figure 1-5B). Generally 2-AG induces a fast, transient and point-to-point retrograde signal.

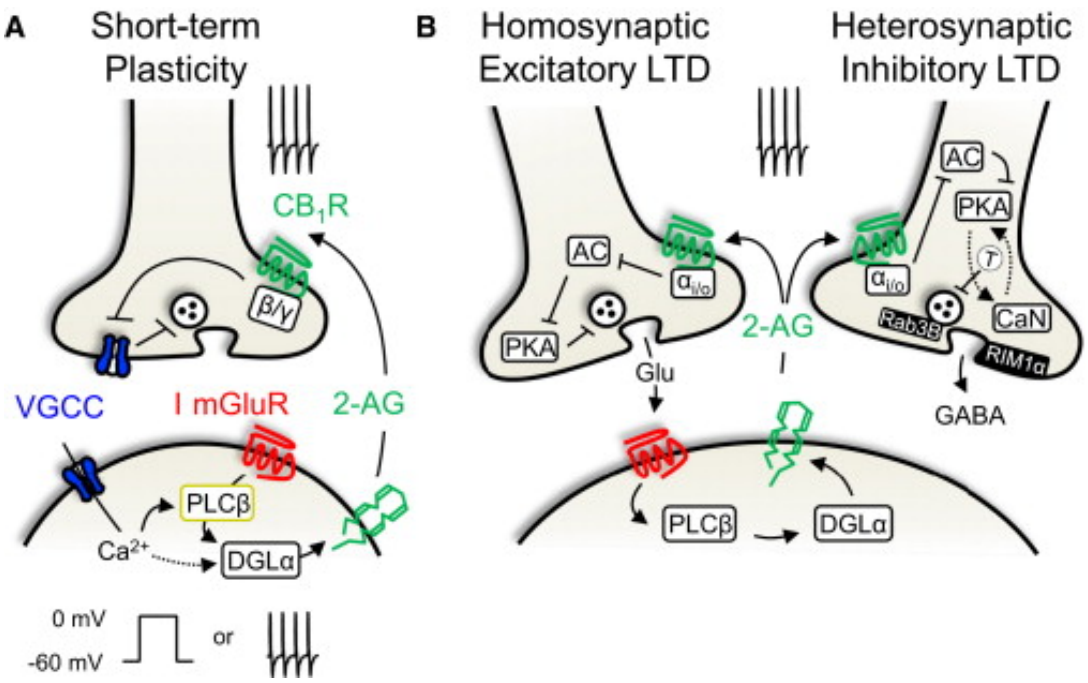

Figure 1-5 eCB and (A) STD: Influx of the Ca^{2+} from voltage gated Ca^{2+} channels (VGCCs) triggered by a postsynaptic activity. Ca^{2+} stimulates the production of eCB via DAGLα. The activation of the postsynaptic group I metabotropic glutamate receptors (mGluRs I) can also prompt the eCB mobilization via PLCβ. (B) Inhibitory and excitatory LTD via eCBs. eCB (2-AG) inhibits the postsynaptic mGluRs that has activated by glutamate released via reduction in adenylyl cyclase (AC) and protein kinase A (PKA) activity. On the other hand, in the inhibitory synapses, eCB reduces the GABA release via decreased PKA activity, in conjunction with activation of the Ca2+-sensitive phosphatase calcineurin (CaN)(Castillo et al., 2012)

Anandamide

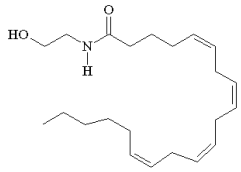

N-arachidonoylethanolamine (AEA) also known as anandamide is a CB1R and CB2R endogenous agonist. It is found in very low concentrations and has a short half-life. It can be found throughout the CNS and periphery. It may a play role in human behavior, such as eating and sleeping patterns, and pain relief (Di Marzo and Fontana, 1995; Wilson and Nicoll, 2001; Mouslech and Valla, 2009).

Synthesis and degradation

Di Marzo et al suggested a hypothesis for the synthesis of the AEA, for the first time. The neurons, which are stimulated with a membrane-depolarizing agent, produce anandamide in response to intracellular Ca^{2+} elevation (Di Marzo et al., 1994). The calcium dependent N-acyltransferase (NAT) synthesizes the immediate precursor of AEA, N-acyl-phosphatidylethanolamine (NAPE) from phospholipids. The phospholipase D enzyme, NAPE-PLD, produces the AEA from NAPE (Pertwee, 2005). The enzyme FAAH hydrolyzes the anandamide from its binding site and degrades it to arachidonic acid and ethanolamine rapidly (Figure 1-6A)(Pertwee, 2005; Wang and Ueda, 2009).

NAPE-PLD

This cell-membrane-associated enzyme composed of 396 (in mouse) and 393 (in human) highly homologous residues (90% similarity between rat and human) produce a 46 kDa protein. In rodents, NAPE-PLD is widely distributed with higher expression in the brain (specially thalamus) and testis (Okamoto et al., 2004; Morishita et al., 2005). Besides its role in eCB biosynthesis, many other physiological roles have been proposed for NAPE-PLD, such as anti-inflammatory (Lambert et al., 2002), anorexic (Rodriguez de Fonseca et al., 2001), and pro-apoptotic effects (Maccarrone et al., 2002).

FAAH

The catabolic enzyme, FAAH, is the principal integral membrane hydrolase for all fatty acid amides including; anandamide (eCB), oleamide (sleep inducing lipid), N-acyltaurines transient receptor potential (TRP) channels, etc. (Cravatt et al., 1996). FAAH is highly expressed in the cerebellum, hippocampus, neocortex, olfactory bulb, thalamus, mid brain, hind brain, entorhinal cortex, and amygdala. Comparing the pattern of expression of FAAH and CB1R, they show complementary, overlapping and unrelated distribution (Egertová et al., 2003).

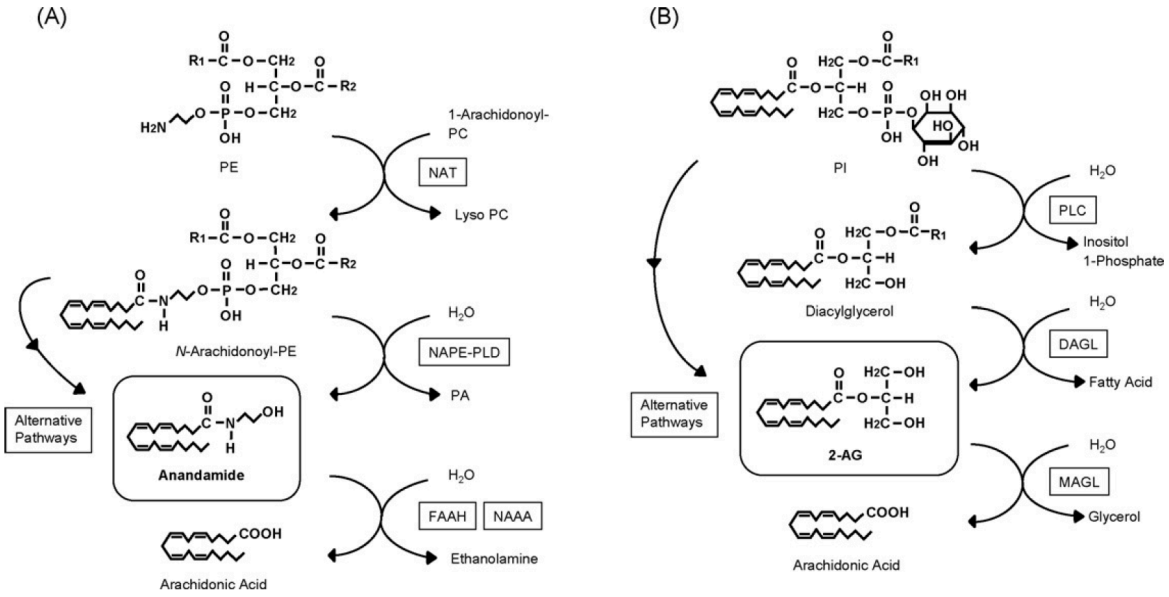

Figure 1-6 Endocannabinoid biosynthesis and degradation pathways for (A) anandamide and (B) 2-AG. NAAA, N-acylethanolamine-hydrolyzing acid amidase; PA, phosphatidic acid (Wang and Ueda, 2009).

Anandamide and eCB signaling

Anandamide mediates eCB-LTD with high-frequency stimulations. Anandamide's contribution to LTD is not limited to eCB receptors. Part of the LTD effect is induced via transient receptor potential vanilloid type 1 (TRPV1) and intracellular calcium (Lerner and Kreitzer, 2012). TRPV1, capsaicin receptor or the vanilloid receptor 1, is mainly responsible for regulation of body temperature and nociperception. The effect of the anandamide on TRPV1 depends on the species and tissue. Moreover, cannabinoid receptor activation via AEA, modulate TRPV1 responsiveness. In some cases, the coactivation of both receptors makes it difficult to distinguish the exact signaling pathway (Toth et al., 2009)

Anandamide, unlike 2-AG, contributes to homeostatic plasticity in the hippocampus by making an eCB tone (Figure 1-7) (Kim and Alger, 2010).

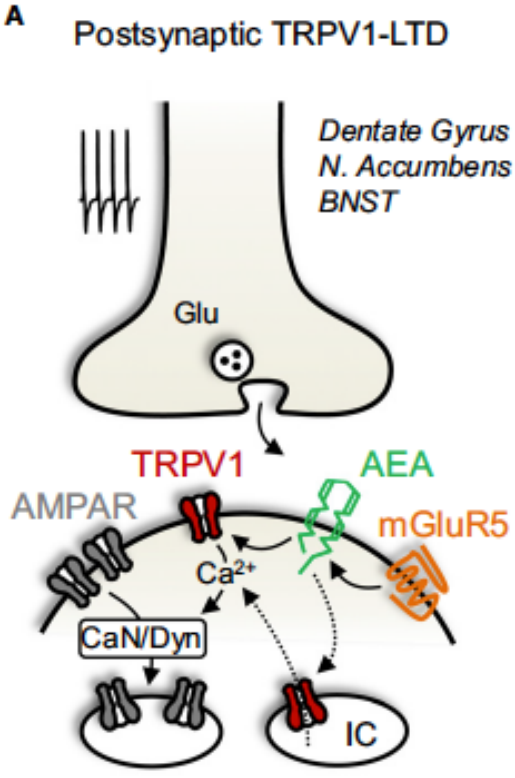

Figure 1-7 Function of anandamide in eCB and TRPV1 signal transmission

Receptors

Two leading receptors and a potential receptor have been introduced for the eCB system so far.

CB1R

Known as the primary receptor for the eCB system, CB1R is responsible for the main physiological and psychological actions of the cannabinoids; CB1R, a 472 amino acid protein, is the most abundant G-protein-coupled receptor in the brain. It is the first CB receptor that was cloned from the rat (Matsuda et al., 1990) and shows up to 98% similarity across species (Elphick and Egertová, 2001). Like all other G-protein-coupled receptors, CB1R contains seven transmembrane domains connected by three extracellular and three intracellular loops, an extracellular N-terminal tail, and an intracellular C-terminal tail (Figure 1-8). It couples to inhibitory G-proteins ($G_{i/o}$) implying that cannabinoid agonists inhibit adenylate cyclase (AC) and decrease the activity of PKA, decreasing the release of neurotransmitters. Activation of CB1R, coupling to $G_{i/o}$ proteins, decreases the intracellular cAMP concentration and augments the activity of MAP kinase. It can also activate the adenylate cyclase via G_s proteins (Pertwee, 2006). The modulation of cAMP will indirectly influence several ion channels and enzymes such as inwardly rectifying potassium channels, calcium channels, PKA, protein kinase C (PKC), Raf-1, ERK, JNK, p38, c-fos, c-jun, and others (Demuth and Molleman, 2006; Pagotto et al., 2006).

Expression

CB1R is the most abundant G-protein-coupled receptor in the brain, it is copious in the CNS as a pre-synaptic receptor at both glutamatergic and GABAergic interneurons (Elphick and Egertová, 2001). CB1R is primarily found in the hippocampus, the association cortices, cerebellum and basal ganglia (Herkenham et al., 1991; Tsou et al., 1998), peripheral nervous system (Egertová and Elphick, 2000), central and peripheral parts of the retina (Straiker et al., 1999; Yazulla et al., 1999; Bouskila et al., 2012) of rodent and primate. Its presence is also reported in certain populations of interneurons in somatosensory area, primary motor, thalamus, retinal and visual cortex of the rodent (Marsicano and Lutz, 1999; Zabouri et al., 2011a) and primates (Eggan and Lewis, 2007; Bouskila et al., 2012). It is also expressed in peripheral tissues such as lungs, testes, the uterus, the immune system, intestine, bladder, and retinal cells endothelial however at a lower concentration than in the CNS (Sugiura and Waku, 2002). Also, CB1R is expressed in human sperm and ovaries, oviducts myometrium, decidua, and placenta (Pagotto et al., 2006).

Known functions of CB1R

Activation of CB1R inhibits the release of excitatory or inhibitory neurotransmitters, such as acetylcholine, noradrenaline, dopamine, 5-HT, GABA, glutamate, D-aspartate, and cholecystokinin and acts as retrograde synaptic mediators (Pertwee, 2008). In some diseases such as in hepatocellular carcinoma and prostate cancer cells, the expression of CB1R is

amplified. It is proposed that this modulation of neurotransmitter release prevents pain and inflammation response (Pisanti et al., 2013).

The removal of the CB1R of GABAergic and glutamatergic neurons in *cnr1* knockout mouse results in opposite behavior changes. Exploration of objects, socialization, and open field movement increased in GABAergic *cnr1* knockout mice and decreased in glutamatergic *cnr1* knockouts (Haring et al., 2011).

As the main role player in psycho-effective symptoms of cannabis, CB1R principal behavioral effects include but are not limited to the disruption of psychomotor behavior (Pillay et al., 2004; Rodríguez de Fonseca et al., 2005), short-term memory impairment (Kanayama et al., 2004; Jager et al., 2006; Han et al., 2012) stimulation of appetite (Mattes et al., 1994), anti-nociceptive actions (Pini et al., 2012) and anti-emetic effects (Tramer et al., 2001). The eCB system has been shown to be prevalent in the development of the retina (Zabouri et al., 2011a; Zabouri et al., 2011b), development of CNS (Fernández-Ruiz et al., 2000), axon guidance (Argaw et al., 2011), and proper development of the rodent embryo (Pagotto et al., 2006).

Exogenous synthetic agonists

WIN 55,212-2

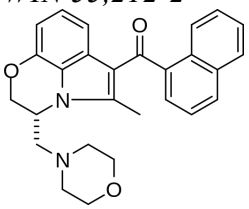

This synthetic agonist is an aminoalkylindole derivative that has a similar effect to THC with much higher affinity to CB1R with a completely different structure that is not similar to any classical and nonclassical eicosanoid cannabinoids.

CP 55,940

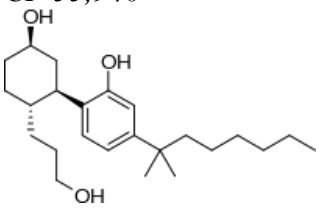

This is a synthetic full agonist for both CB1R and CB2R made by Pfizer. It is 45 times more potent than THC and acts as the antagonist of GPR55.

Antagonists:

Rimonabant

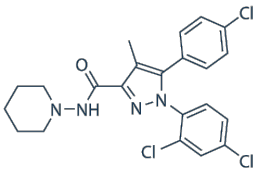

SR141716 or rimonabant was the first CB1R blocker that has been developed by Sanofi as an anorectic anti-obesity drug branded under the name of Acomplia. It has also been approved for smoking cessation in Europe. Mainly *in vitro* and at the molecular level, rimonabant is acting as an agonist, a neutral antagonist or an inverse agonist (Fong and Heymsfield, 2009). At physiological levels, rimonabant reduces food intake, liver lipid production, and fat mass but increases the energy expenditure (Addy et al., 2008).

In 2008, the European Medicines Agency's Committee for Medicinal Products for Human Use announced that due to the risk of serious psychiatric problems and suicidal thoughts, the risk of rimonabant outweighed its benefits.

AM251

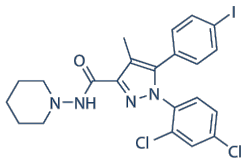

AM251 is another cannabinoid inverse agonist of CB1R. It has a very similar structure to rimonabant and a better binding affinity for the receptor (Lan et al., 1999).

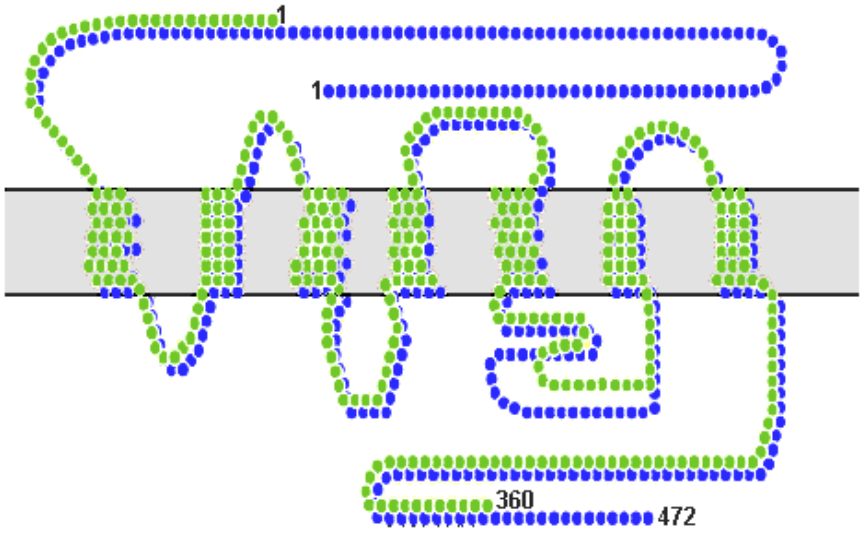

Figure 1-8 Structures of the CB1R (blue) and CB2R (green).

CB2R

Comprised of approximately 360 amino acids in human, with about 44% of similarity in sequence level and high likeliness in structure to CB1R, CB2R is another G-protein-coupled receptor of the eCB system. Rats and humans share up to 81% homology in their CB2R genes (Griffin et al., 2000). Due to its abundant expression in the immune system, it was first informally considered as the "peripheral" cannabinoid receptors (Munro et al., 1993). The

variations (mainly increase) in the expression level of CB2R in different diseases such as nerve injury, multiple sclerosis, amyotrophic lateral sclerosis, make it attractive as a therapeutic target (Wotherspoon et al., 2005; Yiangou et al., 2006). Later on, some other groups reported the expression of CB2R in brain and CNS (Cabral et al., 2008). 2-AG is considered as the principal agonist due to its higher efficacy to activate CB2R (Lynn and Herkenham, 1994). Anandamide, on the other hand, has a lower affinity for the receptor and is considered as a partial agonist for CB2R (Showalter et al., 1996). The exogenous agonist cannabinol has higher affinity towards CB2R (Felder et al., 1995).

Similar to CB1R, CB2R inhibits the adenylyl cyclase through the $G_{i/o}$ coupled G protein receptor (Shoemaker et al., 2005). Moreover, it has been proposed that CB2R can regulate a series of complex signal transduction via the MAPK-ERK pathway (Demuth and Molleman, 2006). Unlike CB1R, CB2R is not a proper modulator for calcium and inwardly rectifying potassium channels (Felder et al., 1995). Interestingly, the pharmacological responses of the CB2R vary from one species to another (Mukherjee et al., 2004).

Expression

As a "peripheral" eCB receptor, CB2R mRNA was found in immune cells such as monocytes, macrophages, B-cells, and T-cells, and immune/peripheral tissues such as the spleen, tonsils, and thymus gland 10-100 times more than CB1R (Galiègue et al., 1995). In the CNS, the expression of CB2R is reported in rodent cerebellum purkinje, granule cells and white matter (Skaper et al., 1996; Ashton et al., 2006). This expression in the cerebellum was not colocalized with astrocyte marker glial fibrillary acidic protein (GFAP) and were probably

microglial or neuronal (Ashton et al., 2006). The expression of CB2R has been reported in rodent brainstem's cochlear and vestibular nuclei (Baek et al., 2008), many areas of hippocampal formation (Onaivi, 2006; Onaivi et al., 2006), striatum and hypothalamus (Gong et al., 2006). The immunoreactivity of CB2R has been reported in many thalamic nuclei, olfactory bulbs, cortex and midbrain despite the nonappearance of the mRNA or protein expression (Gong et al., 2006; Onaivi, 2006). CB2R is present throughout the rodent retina and along the retino-thalamic pathway (Cecyre et al., 2013; Duff et al., 2013).

Known functions of CB2R

Due to the expression pattern of the CB2R, its role in immune system has been widely studied, particularly its effects on the immunological activity of leukocytes, immune suppression, induction of apoptosis, and induction of cell migration (Kaminski, 1998; Basu et al., 2011). Since the CB2R agonist inhibits T-cell receptor signaling by changing cAMP level, the possibility of applying the CB2R agonist as a treatment of inflammation and pain is under investigation (Cheng and Hitchcock, 2007). CB2R can play a noteworthy role in neurogenesis. For instance, JWH-015, a CB2R agonist, eliminates the beta-amyloid protein that impairs neural activity in Alzheimer patients (Tolon et al., 2009). The CB2R may play a modulatory role in axon guidance and participate in the retinothalamic pathway formation (Duff et al., 2013). It has been shown that in the rat brain and human neurons, the CB1R and CB2R form functional heteromers in which the activation of one resulted in a negative modulation of the other receptor (Callen et al., 2012). This heterodimerization may explain the co-expression of these receptors in some parts of the brain (Koch et al., 2008) as well as the negative cross talk between the CB1R antagonist and the CB2R agonist and inverse agonists.

Agonist

JWH-015

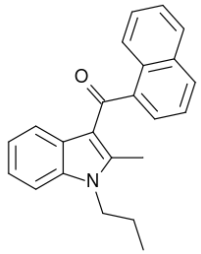

A synthetic agonist from naphthoylindole family that binds 28 times stronger to CB2R than CB1R. Despite of the selectivity of this agonist on CB2R, in some models it activates CB1R efficaciously. Due to some modulatory effects of this agonist, it is considered as a possible therapeutic candidate to treat pain and inflammation (Balter et al., 1993).

Antagonists

AM630

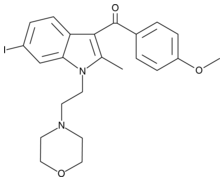

AM630 is a selective inverse agonist for CB2R and a partial agonist for CB1R. It is a derivative of indole and commonly used to investigate the CB2R signalization (Shoemaker et al., 2005; Pertwee, 2006).

SR144528

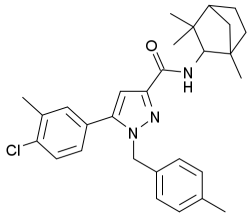

SR144528 is a highly selective inverse agonist of CB2R with a very low affinity for CB1R that binds 660 times stronger to CB2R than CB1R and used in research as a candidate to isolate the activity of CB2R (Rinaldi-Carmona et al., 1998).

Table 1-1 Comparison of the CB1R and CB2R agonists' efficacy

	CB_1Ra affinity (K_i)	Efficacy towards CB1R	CB_2R affinity (K_i)	Efficacy towards CB2R	Type
THC[1]	10 nM	Partial agonist	24 nM	Partial agonist	Phytogenic
2-AG[2]	58.3 nM	Full agonist	145 nM	Full agonist	Endogenous
AEA[3]	78 nM	Full agonist	370 nM	Partial agonist	Endogenous
JWH-015[4]	383 nM	Partial agonist	13.8 nM	Full agonist	Synthetic
JWH-133[1]	680 nM	Weak agonist	3.4nM	Full agonist	Synthetic
WIN 55,212-2[5]	62.3 nM	Agonist	3.3 nM	Agonist	Synthetic
ACEA[6]	1.4 nm	Agonist	3100nm	Weak agonist	Synthetic

1. PDSP Database – UNC. NIMH Psychoactive Drug Screening Program. 2013; 2. Sugiura et al., 1994; 3. Devane et al., 1992; 4. Aung et al 2000; 5-Felder et al., 1995; 6. Hillard et al., 1999.

GPR55

Human GPR55 is composed of 319 amino acids and shares only 13.5% similarity to CB1R and 14.4 % identity to CB2R, while it is very similar to rhodopsin family (Sharir and Abood, 2010). GPR55 is potentially activated by endogenous L-α-lysophosphatidylinositol (LPI) but also responds to AM251, rimonabant, THC, 2-AG, and anandamide. Despite all the controversies and disagreements, GPR55, as an orphan G-protein-coupled receptor, is considered as the third potential cannabinoid receptor (Ryberg et al., 2007). Interestingly, the strong CB1R and CB2R agonist, WIN 55,212-2, cannot activate the GPR55 despite its unique

structure (Johns et al., 2007). GPR55 activates the PLC and RhoA signal transduction pathways via G_q and $G_{12/13}$ and promotes the ERK1/2 signaling pathway (Oka et al., 2007).

Expression

The expression of the GPR55 mRNA reported, from the highest to lowest, in the adrenals, caudate, putamen, frontal cortex, striatum, jejunum, hypothalamus, brain stem, hippocampus, cerebellum, spleen, spinal cord, long, liver, uterus, bladder, stomach and kidney (Ryberg et al., 2007). GPR55 was also found in various cell types including, endothelial and Schwann cells (Daly et al., 2010), human and mouse oseteoclasts and osteoblasts (Whyte et al., 2009), murine insulin secreting β-cells (Romero-Zerbo et al., 2011), rat prostate and ovarian cells (Pineiro et al., 2011).

Known functions of GPR55

The physiological functions of GPR55 are poorly characterized. The *gpr55* knockout mice showed no specific phenotypes (Johns et al., 2007). Referring to the role of GPR55 in increasing the intracellular Ca^{2+} in large-diameter dorsal root ganglion neurons, a modulation of nociception was suggested after tissue damage and inflammation in nervous system (Gold and Gebhart, 2010). An increase in GPR55 mRNA and protein in patients with type-2 diabetes, visceral adiposity and higher level of circulating LPI in obese patients suggests its role in energetic metabolism (Maccarrone et al., 2010; Moreno-Navarrete et al., 2012). The abundance of the GPR55 and LPI in the brain also insinuates a modulatory role of the GPR55 in the CNS (Oka et al., 2009). Other studies suggest potential roles for GPR55 in bone

physiology and activity of osteoclasts (Whyte et al., 2009), cancer (Sutphen et al., 2004), and cell proliferation (Andradas et al., 2011).

Agonists

L-α-Lysophosphatidylinositol (LPI)

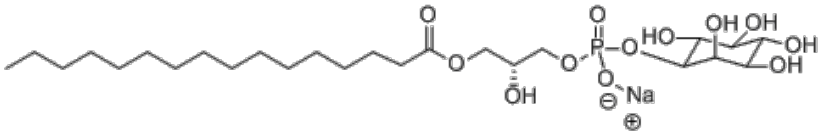

Found in sodium salt of soybeans and also made in human body, it induces phosphorylation of ERK and augmentation of intracellular Ca^{2+} via GPR55.

O-1602

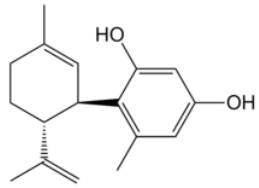

A synthetic agonist with a very low affinity towards the classical CB1R and CB2R but with a high affinity for GPR55 and some other orphan G-protein coupled receptors. O-1602 creates some of the well-known cannabinoid symptoms such as appetite stimulation, anti-inflammatory role and analgesic effect. Interestingly it doesn't trigger any psychoactive and pain relief symptoms of the common cannabinoid agonists.

Antagonists

CID-16020046

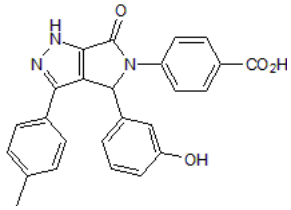

A synthetic selective antagonist that inhibits many effects of GPR55 activations such as restraint of the Ca2+ signaling prompted by LPI, phosphorylation of ERK1/2 and activation of the transcription factor mediated by GPR55.

O-1918

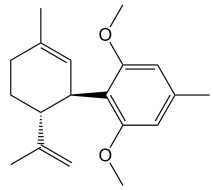

O-1918 is a synthetic cannabidiol related antagonist of GPR55 and GPR18 and used to study the non-CB1R non-CB2R related effect of cannabinoids.

PSB-SB-487

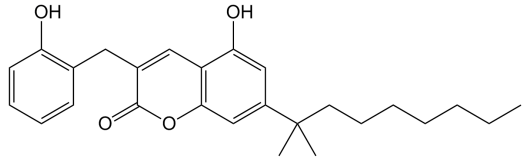

Selective antagonist of GPR55, that plays the role of a weak antagonist for CB1R and partial agonist for CB2R. As a derivative of coumarin, it is a weak antagonist of CB1R and a partial agonist of CB2R.

Cannabidiol

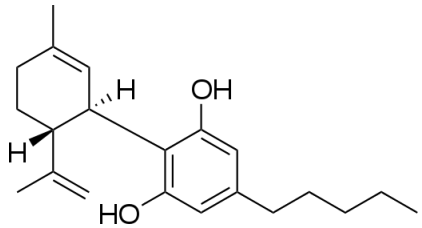

As one of the natural components found in cannabis that has no significant effect on CB1R and CB2R, cannabidiol is an antagonist of GPR55

The Visual System

The visual system of all vertebrates comprises three main constituents: the eye, as a capturing machine detects the light that converts optical data to electro-chemical neuronal messages; visual pathways, which transfer the neuronal message from the eye to the brain; and visual brain, that translates the neuronal messages to practical images.

Eye

The light reflected from surrounding objects is refracted through the clear cornea, passes through the pupillary opening in the middle of the beautiful iris to reach the lens. The lens focuses the light entering the eye on the retina. The retina transduces the optical stimuli into electrical impulses, which are transmitted to the brain. (Figure 9). The axons of the ganglion cells in the retina transfer the retinal electrical impulse via optic nerve to optic chiasm and via optic tract to the dorsal lateral geniculate nucleus (dLGN) and superior colliculus (SC). The dLGN relays the signal for a basic analysis to the occipital lobe of the brain where the visual cortex resides (Purves et al., 2012).

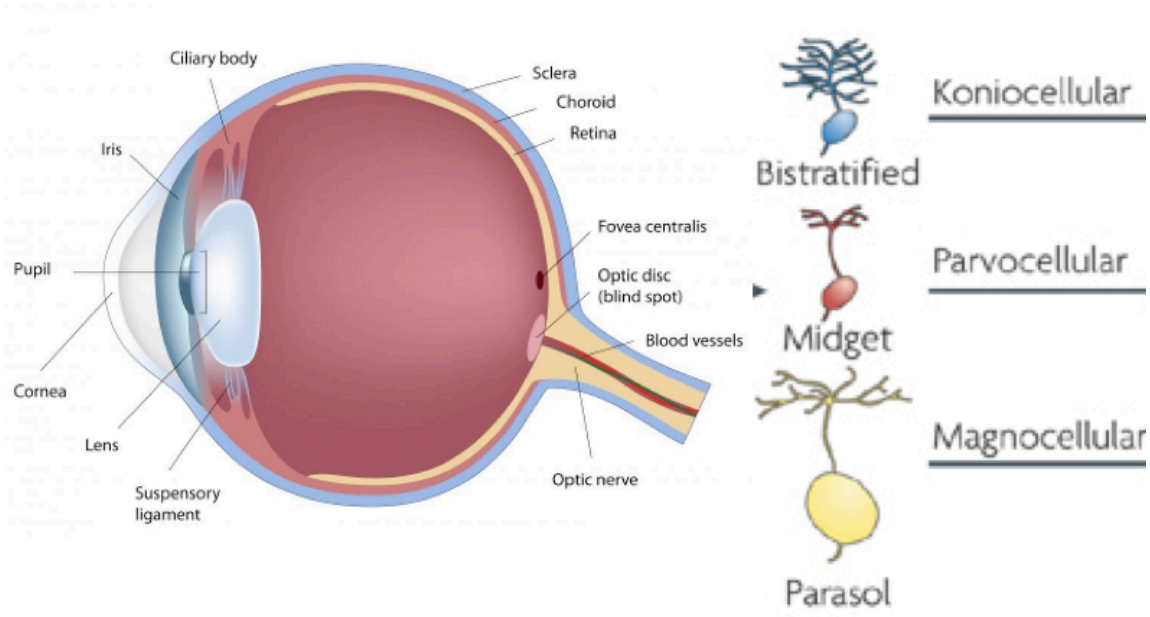

Figure 1-9 Anatomy of the primate eye (taken from Principles of Neural Science, Eric Kandel et al.)

The bulbus oculi (globe of the eye) that creates a cavity for the vitreous is composed of three layers. The outermost layer, sclera, is a series of opaque collagen and elastic fibers that support the wall of the eyeball. The choroid layer, in the middle, provides nutrition and oxygen to the eyes and reduces the light reflection inside the globe via its melanin-pigmented layers. The most inner layer is the retina (Figure 1-9).

Structure of the Retina

The light sensitive thin and fragile meshwork of the retina is considered as an extension of the brain that initiates the visual perception encountering the light. It is composed of three layers of nerve cells (inner nuclear layer (INL), outer nuclear layer (ONL), and ganglion cell layer (GCL)) and two layers of synapses (inner plexiform layer (IPL), outer plexiform layer (OPL)). INL contains the nuclei of horizontal cells, bipolar cells and amacrine

cells. ONL is composed the cell bodies of rods and cones. The ganglionic cell layer contains the ganglion cells and some displaced amacrine cells. In the plexiform layers, the IPL is the designation of the location where synapses between bipolar cells' axons and ganglion and amacrine cell dendrites connect to each other. The OPL is the crossroad of the rods and cones' synapses with the bipolar, amacrine and horizontal cells (Figure 1-10).

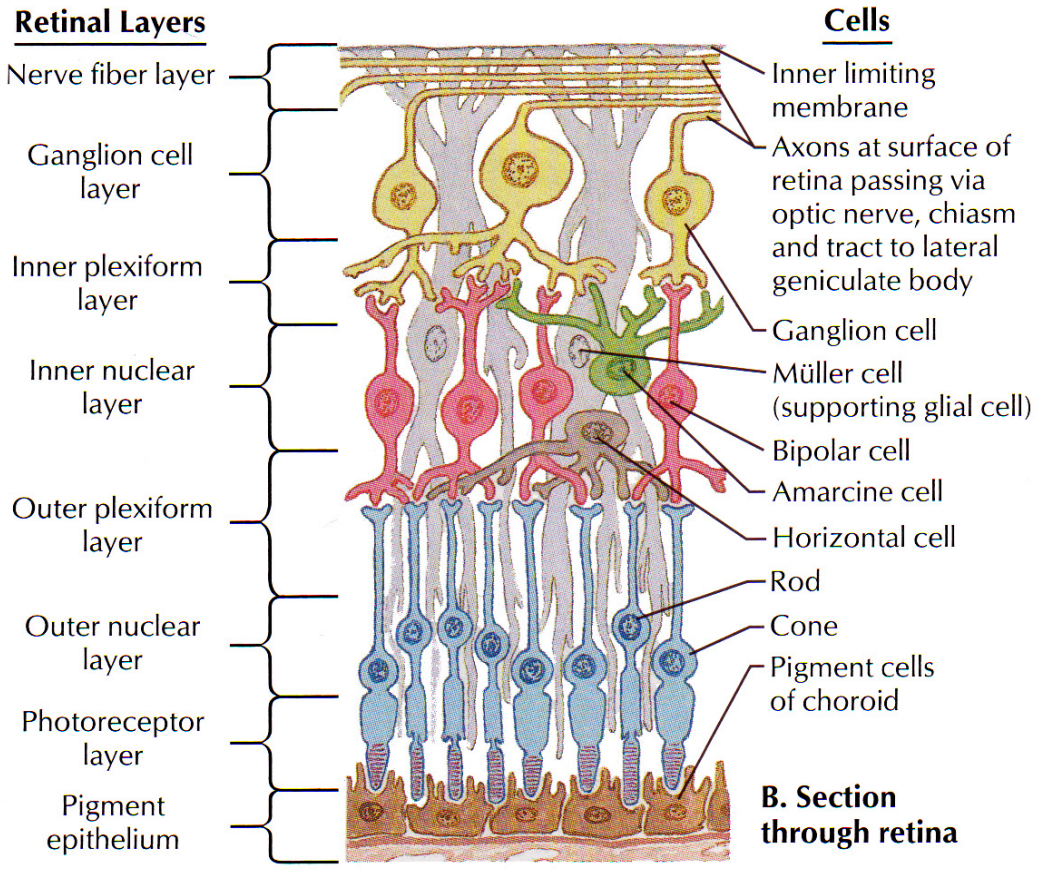

Figure 1-10 Structure of the primate retina (from ELSEVIER Netterimages.com)

The photoreceptors

Photoreceptor cells, found in the back of the eye adjacent to the pigment epithelium and behind all other retinal cells, trigger the potential change in the cell membrane by

absorbing light photons and initiating the visual processing. Light absorption isomerizes the visual pigment that hyperpolarizes the photoreceptor. Rods and cones are the two chief photoreceptors in the retina. They are in the depolarized state and release glutamate continuously before being stimulated. Cones are the main role player for the photopic vision, and rods mediate scotopic vision.

Cones

Cones are less responsive to light and highly sensitive to small changes, capable of detecting contrast, faster response and responsible for the color vision. In the retina of human and non-human primates, three types of cones are present. S cones that are absorbing the short wavelength light (blue, 420–440 nm), M cones for medium wavelength (green, 534–545 nm) and L cones that are reacting to the long wavelength (red, 564–580 nm) (Bowmaker and Dartnall, 1980) (Figure 1-11).

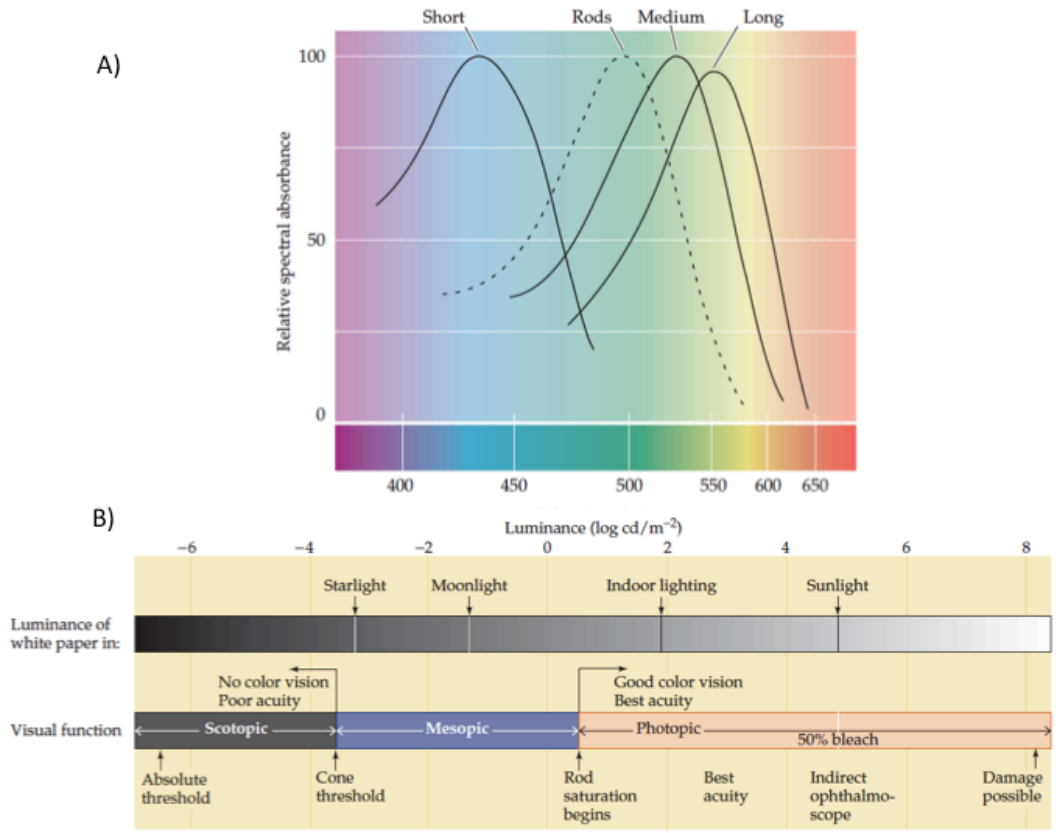

Figure 1-11 Rods and cones sensitivity spectra. A) Color visions and light absorption spectra for rods and cones. B) The luminance thresholds of the vision and each correspondent role player (taken from Purves et al., third edition).

Around five million cones can be found in human retinal with the highest density in the rod-free central fovea and macula. The quantity of cones is declined as one moves towards the peripheral retina (Curcio et al., 1990). Each cone is associated with two bipolar cells: ON and an OFF. Cones release glutamate neurotransmitter that inhibit (hyperpolarizes) ON bipolar and excites (depolarizes) the OFF cells. Lack of light and darkness depolarizes the cones so that they open the synaptic voltage-gated Ca^{2+} channels, increase the Ca^{2+} in terminals and release the glutamate. The release of glutamate inhibits the ON bipolar cells (Schiller, 1992). Inversely, the light closes the voltage-gated Ca^{2+} channels and reduces the influx of Ca^{2+} and consequently, decreases the release of glutamate that hyperpolarizes the OFF bipolar cells

(Figure12). Moreover, glutamate opens a form of cation channel in OFF cells that carries an inward Na^+ current into cells. Light exposure after a full dark adaptation causes a temporary saturation of the cones (Schiller, 1992).

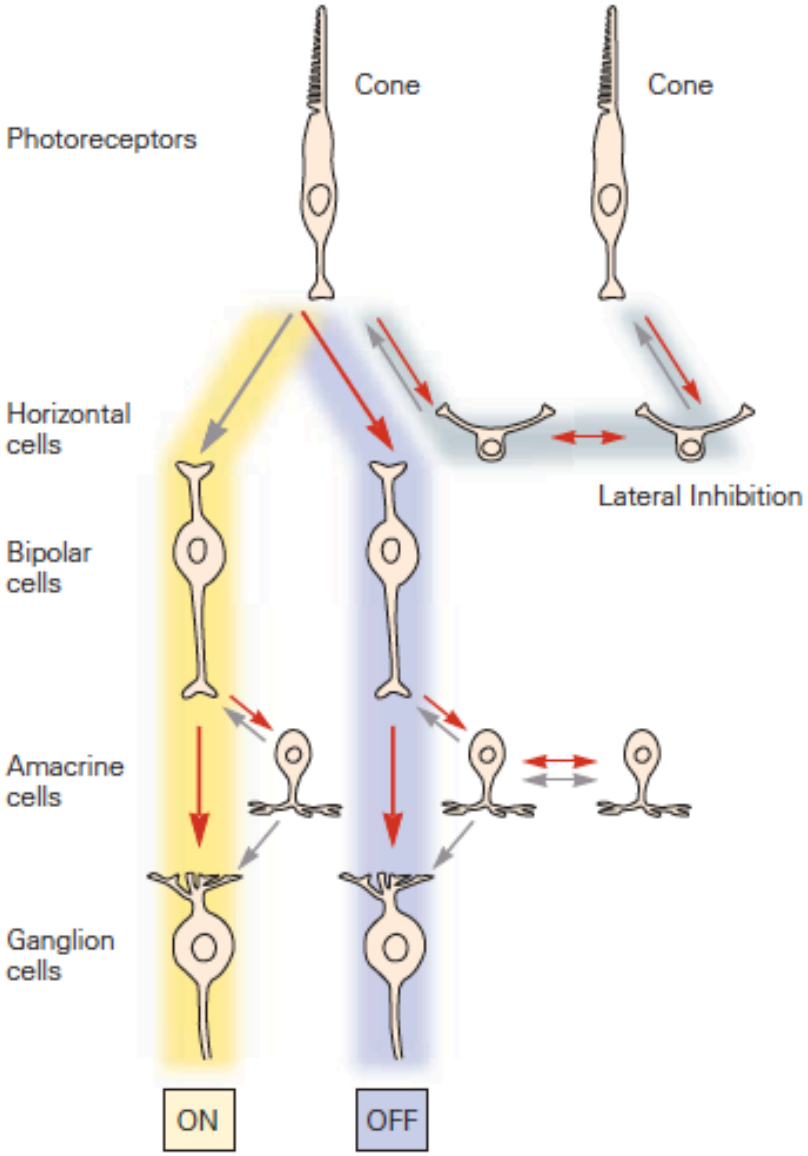

Figure 1-12 Conte retinal circuitry. Retinal connection to ON and OFF bipolar cells in light and dark. Red arrows indicate sign-preserving connections through electrical or glutamatergic synapses. Gray arrows represent sign-inverting connections through GABAergic, glycinergic, or glutamatergic synapses (Principles of Neural Science-Kandel 2013).

Rods

With higher concentration in the outer segments of the retina, rods play an important role in dim light and peripheral vision. Human retina possess approximately 125 million rods. Rods are more sensitive to light than cones due to their abundant photosensitive visual pigments. While about ten photons are required to evoke an electrical response in cones, one photon will be enough to evoke a similar response in a rod. Rods create a very convergent system with their bipolar neurons. Many rods can have synapses on the same bipolar cell as their target thus signals from rods are pooled and reinforce each other in the bipolar cells. Rods are connected to ON bipolar cells. In the dark, the depolarized rods release glutamate and hyperpolarize the bipolar cells. The rhodopsin in rods captures a photon and triggers a cascade of events that close the cyclic guanosine monophosphate (cGMP)-gated channels that are normally opened in darkness (Yee and Liebman, 1978; Burns and Baylor, 2001).

Table 1-2 Comparison of the photoreceptors: rods and cones (adapted from *Principles of Neural Science, Eric Kandel et al.*)

	Rods	Cones
Sensitivity to light	High: night vision	Low: day vision
Photopigments	More	Less
Light amplification	High: single photon detection	Low
Temporal resolution	Low: slow response, long integration time	High: fast response, short integration time
Sensitivity to	More scattered light	More direct axial rays
Acuity	Low; not in fovea, highly convergent retinal pathway	High; concentrated in fovea, dispersed retinal pathway
Chromaticity	Achromatic	Chromatic

Rod and Cone structure

Both rods and cones have a similar basic structure. Rods are more abundant and a little longer and leaner than the cones.

Photoreceptors have three major functional regions (Figure 1-13):

1- Outer segment; filled with photo-absorbing pigments, specialized for signal transduction. The outer segment of both photoreceptors contains a stack of membrane discs that resides in the photopigments.

2- Inner segment; include the nucleus and biosynthetic machinery.

3- Synaptic terminal; make contacts with the targets.

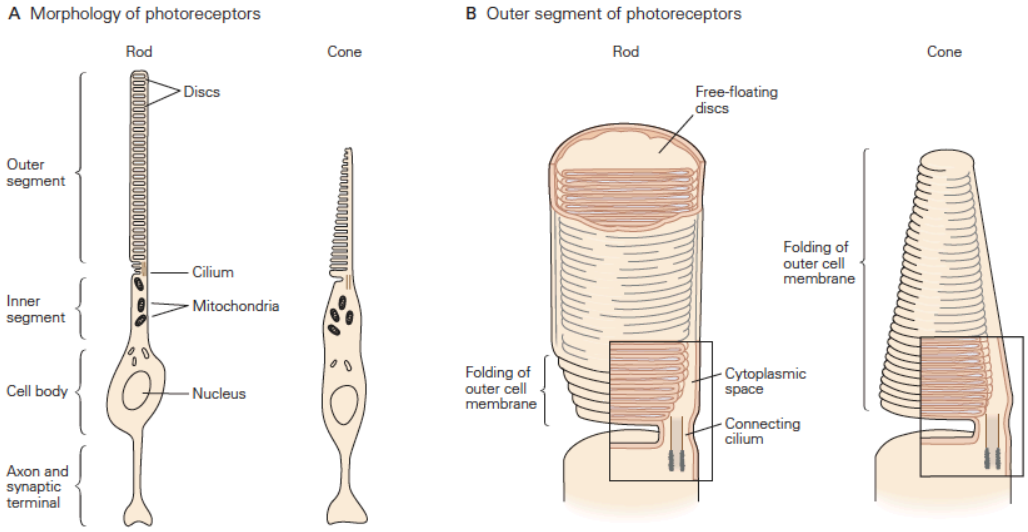

Figure 1-13 Similar structure of the photoreceptors, rods and cones. A) morphology B) outer segment of the photoreceptors (taken from Principles of Neural Science, Eric Kandel et al.)

Horizontal cells

In the INL of the vertebrate's retina, horizontal cells laterally connect the neural population of the retina. Most mammals have two types of horizontal cells (Figure 1-14) that

assist the regulation and modulation of the feedback onto both rods and cones and possibly to bipolar cells' dendrites and adjust the eye to see in dim light and bright light conditions (Muller and Peichl, 1993; Masland, 2012). The photoreceptors release of glutamate in scotopic conditions depolarizes horizontal cells and triggers the release of GABA. As an inhibitory neurotransmitter, GABA hyperpolarizes the adjacent photoreceptors. Inversely, illumination results in hyperpolarization of the horizontal cells and depolarization of the surrounding photoreceptors (Masland, 2012).

Bipolar cells

Found in the middle layer of the retina, bipolar cells transmit signals from either cones or rod to ganglion cells. Generally divided into two main categories of ON and OFF cells, bipolar cells have a diverse morphology (Figure 1-14). Based on the extent of the dendritic arbor, there are two types of bipolar cells in the primate retina; midget cells that contact a single cone and diffuse cells that contact multiple cones. Both rods and cones release glutamate in scotopic conditions that inhibit the ON (hyperpolarize) and excite the OFF (depolarize) bipolar cells. The glutamate hyperpolarizes ON bipolar cells through metabotropic receptors mGluR6 or glutamate transporter (Koyasu et al., 2008) while they depolarize OFF bipolar cells through ionotropic glutamate receptors (iGluR) (DeVries, 2000). Mainly the ON bipolar cells synapses in the inner layer of IPL and OFF bipolar cells terminate in the outer IPL. Rod bipolar cells do not directly contact the ganglion cells but synapse with all amacrine cells and consequently inhibit the cone OFF bipolar cells and excite cone ON bipolar cells (Stell et al., 1977; Schiller, 1992).

Amacrine cells

Amacrine cells, with more than 29 types (Figure 1-14), are the most variable neuronal cells in the retina. Main inputs of retinal ganglion cells from bipolar cells are transduced via amacrine cells. Residing adjacent to axon terminals of bipolar cells makes amacrine cells an apt regulator of the output signal of bipolar cells to ganglion cells (Masland, 2001). Amacrines make a heterogenous population that play an important role in analysis of the spatial and temporal parameters of visual information in the inner retina (MacNeil and Masland, 1998). In addition, they may orchestrate the ganglion cell firing. Inputs from an amacrine cell correlate several ganglion cells to fire simultaneously. This characteristic expands the capacity of the optic nerve to pass the visual information (Masland, 2001).

Ganglion cells

In vicinity of the INL, ganglion cells receive the visual information of the photoreceptors via the bipolar, horizontal and amacrine cells. They are the only neural cells that transfer action potentials from the eye to rest of the brain. Approximately 1.5 million ganglion cells receive visual input from about 125 million photoreceptors; every 100 photoreceptors give input to a ganglion cell (this ratio varies from the fovea to the periphery). Morphologically, about ten to fifteen types of retinal ganglion cells have been identified that are different in terms of size, connections, and responses to visual stimulation (Masland, 2001) but all of them have a long axon which originates in GCL passing through optic nerve, optic chiasm, and optic tract, and terminating in the brain.

Similar to bipolar cells, most ganglion cells have concentric (ON and OFF) receptive field organization, which receive input from ON and OFF bipolar cells respectively. Hence, in the middle of their receptive fields, ON ganglion cells are depolarized in light spot and OFF ganglion cells will respond to a dark spot.

Based on the projection and function, there are at least five main classes of retinal ganglion cells: parasol cell (magnocellular, M cells), midget cell (parvocellular, P cells) and non-M non-P cells including; bistratified cell (koniocellular, K cells), photosensitive ganglion cells, other ganglion cells projecting to the superior colliculus for eye movements (saccades).

Parasol cell

The ganglion M cells, with larger dendritic trees and cell body size and make up 5% of the retinal ganglion cells. They have larger receptive fields and receive the signal from many photoreceptors. M ganglion cells are faster in conducting the action potentials in the optic nerve and are more sensitive to low contrast. They transfer the retinal action potential to magnocellular layer of the dorsal lateral geniculate nucleus (dLGN).

Midget cell

The ganglion P cells, with small dendritic trees and cell body size, make up about 90% of the retinal ganglion cells. They have smaller receptive fields and receive the input from few photoreceptors. P ganglion cells are slower in conducting the action potentials to the optic nerve. They are more sensitive to colors and less responsive to feeble changes in contrast. They transfer the retinal action potential to parvocellular layer of the dLGN.

Bistratified cell

Despite their very large receptive fields, the small ganglion K cells make up only 5% of the ganglion cells and project to the koniocellular layer of the dLGN. They receive inputs from some rods and cones and have a moderate spatial resolution and contrast sensitivity. Their receptive fields contain only the center field and are constantly ON for blue and OFF for red and green cones (Bears et al 2007). Other non-M non-P cells like photosensitive retinal ganglion cells are less assessed. Some of their proposed roles include circadian rhythms, and pupillary control (Wong et al., 2005).

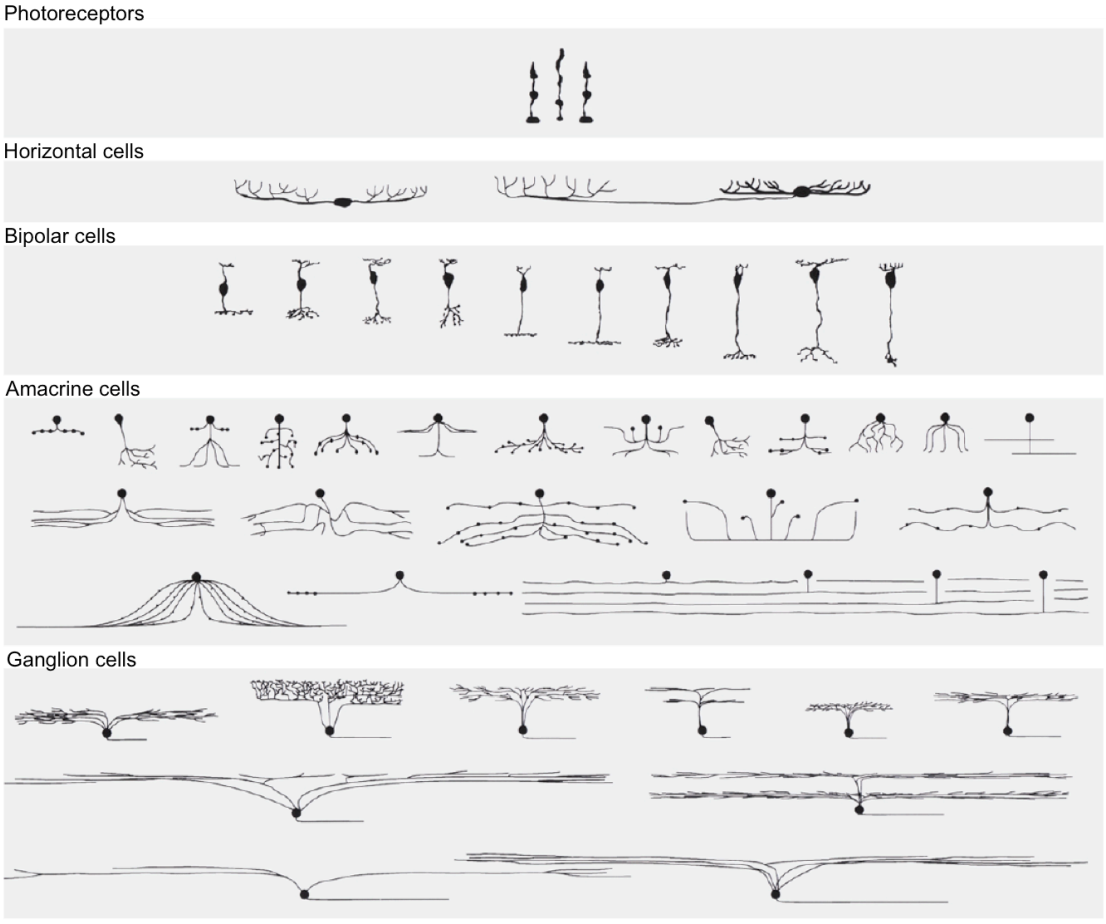

Figure 1-14 Major cells in the mammalian retina. Adapted from (Masland, 2001)

Retinal glial cells

In addition to several microglia in retina, Müller cells, found as main retinal macroglia in vertebrates, are responsible for homeostatic and metabolic support of retinal neurons across the retinal thickness, important elements for immune responses and disposal of the metabolic wastes (Newman and Reichenbach, 1996). Müller cells are produced from progenitor cells of retina and are in contact with all retinal neurons (Distler and Dreher, 1996). They are roughly 150 μm in length with a cylindrical, fiber-like shape. Glutamine synthetase (GS), which is uniquely present in Müller cells and glia, rapidly convert glutamate into glutamine. Müller cells release this glutamine that is mainly utilized by bipolar and ganglion cells as a precursor for glutamate and/or GABA (Bringmann et al., 2009). On other hand, Müller cells collect the neuronal GABA and glutamate and release metabolic substrate to prevent oxidative stress (Bringmann et al., 2009). They are so crucial for support of photoreceptor function, especially cones, that in transgenic mice that lack Müller cells the photoreceptors face apoptosis (Shen et al., 2012). Müller cells control the osmotic and ionic homeostasis of extracellular potassium level via passive current through Kir4.1 channels (Bringmann et al., 2009). Additionally, resembling a living optic fiber, Müller cells minimize the light scattering and direct the light towards the photoreceptors in inner layers of the retina (Franze et al., 2007). Astrocytes are produced in brain and migrate through the optic nerve fibers to the of ganglion cell layer (Huxlin et al., 1992).

Beyond The Retina

All the axons of the ganglion cells are packed together in optic disk and exit the retina towards the brain through a neuronal cable called the optic nerve. Lack of photoreceptors in the optic disk region makes it insensitive to light and cause the blind spot phenomena. Optic nerves cross at the base of the diencephalon at the optic chiasm. In primate, about 60% of the nerves cross over the opposite side of the brain while the remaining cells continue into the brain onto the ipsilateral side. The set of axons passing the optic chiasm to the ipsilateral dLGN is called optic tract (Figure 1-15).

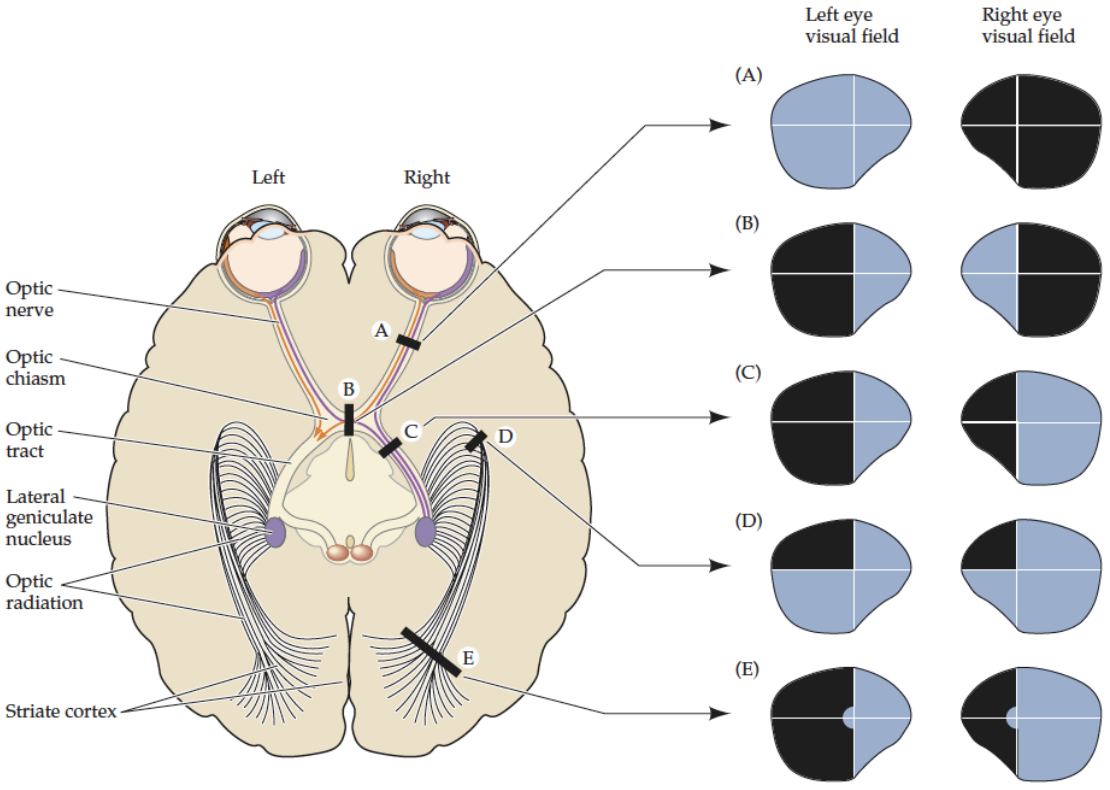

Figure 1-15 The primary visual pathway from the retina to the visual cortex. The resulted visual image in each eye after damages in different point along the pathway (taken from Purves et al., third edition).

Dorsal Lateral geniculate nucleus

Located in the dorsal thalamus, dLGN receives and analyzes the majority of the retinal visual information coming via the optic tract and relays them to the efferent visual cortex. A coronal section of the primate dLGN is similar to a laminar «Bicorne hat» consisting of 6 layers with 5 interlayers. This laminar structure shows that the specific elements of visual information should be treated differently at this level. The first two ventral laminae of the dLGN are magnocellular layers (an ipsilateral and a contralateral) that obtain their inputs from M ganglion cells. Each layer receives the visual information from one eye only. The four dorsal layers called parvocellular layers (two ipsilateral and two contralateral) receive inputs of P ganglion cells. The interlaminar layers, called the koniocellular layers, are the destination of the non-M and non-P ganglion cells (Figure 1-16). Similar to M ganglion cells, magnocellular layers have larger cells with a large receptive field and rapid axon conduction. The magnocellular pathway plays a role in coarse-grain information transmission and perception of movement. The magnocellular layers contribute to the ventral stream that is associated with object recognition and form representation. The dorsal stream, also known as the "where or how" pathway, is involved in the spatial awareness, guidance of action and analyzing the movements. On the other hand, the four parvocellular layers with small cell volume and receptive field, play a role in object recognition, form representation and highly selective for color vision. Including the majority of the dLGN cells, parvocellular layers contribute to ventral stream or "what" pathway. The koniocellular layers have the smallest relay cells that are stimulated by blue short-wavelength cones (Martin et al., 1997).

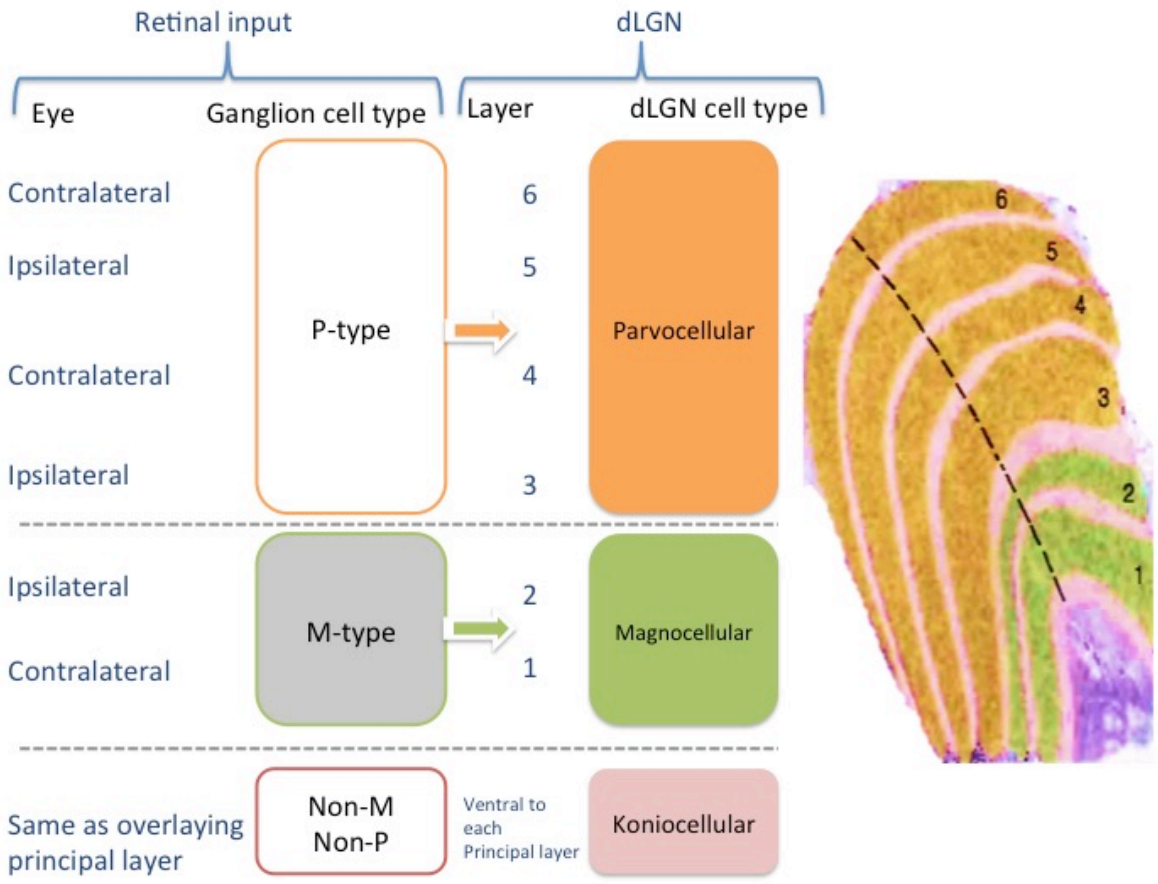

Figure 1-16 The dLGN Organization. Ganglion cells' projection to dLGN layers (adopted from Principles of Neural Science, Eric Kandel et al and studydroid.com).

Table 1-3 Comparison of the M, P and K pathways.

	Cell size	Source	Response	Functions
Magnocellular	Large	Rods	Fast	Motion perception, Depth, sensitive to brightness, nystagmus
Parvocellular	Small	Cones	Slow	Color and form
Koniocellular	Very small	Blue cones	In between	Yellow and blue color perception

Visual cortex

Via dLGN, the visual information is transferred to the visual cortex that consists of a multitude of areas in the occipital, parietal, and temporal lobes. The visual cortex is divided into striate cortex (includes primary visual cortex (V1)) and the extrastriate areas that contain the visual areas two (V2), three (V3), four (V4), and five (V5) (Figure 1-17).

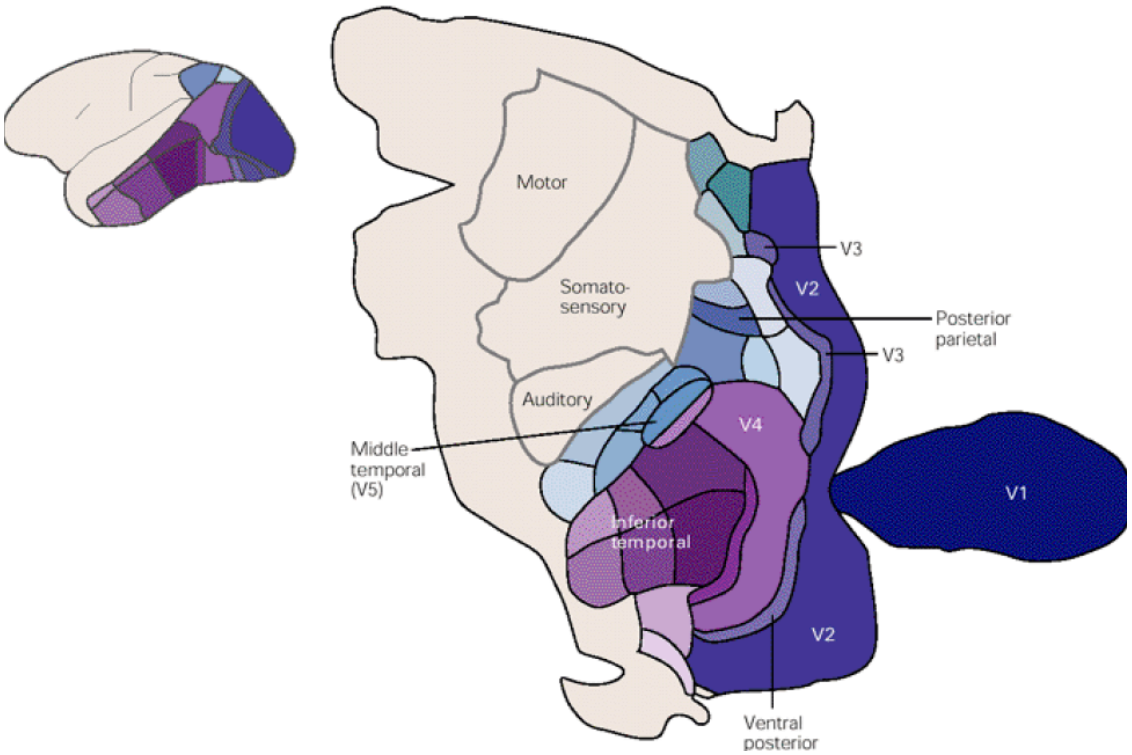

Figure 1-17 The visual cortex subdivisions in the macaque monkey (taken from Principles of Neural Science, Eric Kandel et al.)

V1 is the most studied part of the visual cortex. Located in the occipital lobe, V1 neurons are tuned for spatial frequency processing, pattern recognition, visual orientations, and color perception. Both dorsal and ventral streams initiate in V1 and pass to V2 project to V5 (MT), and posterior parietal cortex or to V4, and to the inferior temporal cortex, respectively.

The 2 mm thick visual cortex in primates is divided into six layers. The layer 4, which receives the majority of the dLGN projections, is subdivided into four sub-layers: 4A, 4B, 4Cα, and 4Cβ. Magnocellular layer cells are first projected into 4Cα, and then 4B (Figure 1-18). 4B cells are projected into middle temporal (MT) and a large stripe towards V2, from which cells project to MT. Parvocellular layers mainly target the 4Cβ with a thin strip towards V2 that may turn the project into V4. Collaterals of both project and receive robust corticogeniculate feedback to and from layer 6 (Van Horn et al., 2000).

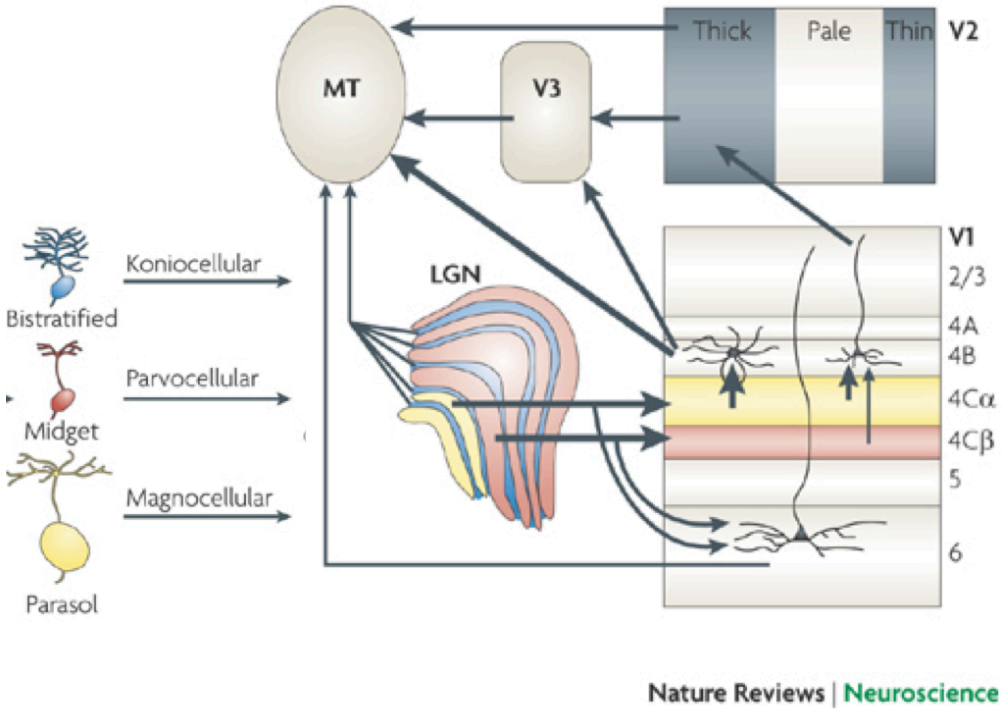

Figure 1-18 The geniculocortical and corticogeniculate pathway in the primate brain.

Prestriate cortex (V2) sends and receives robust connections from and to V1. It also sends connections to V3, V4, and V5. As V1, it plays a crucial role in perception of orientation of the objects, their color and horizontal disparity. V2 continues the analysis of the

contour (specially illusory contours) began in V1 and affects both dorsal and ventral stream. V4, placed anteriorly to V2, plays a role exclusively in color vision. Moreover, V4 also responds to a combination of color, form and orientation of the stimuli (Goddard et al., 2011). Area MT or V5 is the motion perception site of the visual cortex. MT receives inputs mainly from V1, V2 (Felleman and Van Essen, 1991), Magnocellular and Koniocellular layers of dLGN (Sincich et al., 2004). A lesion in MT and medial superior temporal area (MST) impairs motion perception and smooth-pursuit eye movement in primates (Dursteler et al., 1987; Newsome and Pare, 1988). The dorsomedial area or V6 is part of the dorsal stream and associated with self-motion perception (Cardin and Smith, 2010).

Cannabinoids and The visual system

Cannabinoid and The Ocular Tissues

The presence of the eCBs in ocular tissues has been demonstrated in the ciliary body, iris, choroid, trabecular meshwork and retina in rodent, porcine, bovine, monkey and human (Matsuda, 1997; Porcella et al., 1998; Porcella et al., 2000; Chen et al., 2005; Chang et al., 2007). In bovine retina, activation of the CB1R stimulates monoamine oxidase (Gawienowski et al., 1982). In guinea pig retina, same activation results in inhibition of the dopamine release (Schlicker et al., 1996). Cannabinoid agonists increase the cone response to light offset (Struik et al., 2006). The CB1R mRNA level is ten time more prevalent in the ciliary body compared to retina of rodent and human (Porcella et al., 1998; Porcella et al., 2000). Except for the lens, the eCBs AEA and 2-AG has been found in all ocular tissues of human (Chen et al., 2005).

The expression of CB1R, FAAH and CB2R was demonstrated during postnatal development of the rodent retina. FAAH is widely distributed in the retina of zebra fish and gold fish (Yazulla and Studholme, 2001; Glaser et al., 2005). In the adult rodents, the CB1R, FAAH and CB2R are expressed throughout the retina (Zabouri et al., 2011a; Zabouri et al., 2011b). The presence of eCBs in ocular tissues, including the ciliary body, iris, choroid and trabecular meshwork has been clearly showed by physiological and biochemical studies (Matsuda et al., 1990; Porcella et al., 1998; Porcella et al., 2000; Chen et al., 2005; Stumpff et al., 2005). Our lab reported that in non-human primate, the CB1R is expressed throughout the retina, from the foveal pit to the far periphery. CB1R is present in the photoreceptor, outer plexiform, inner nuclear, inner plexiform, and retinal ganglion cell layers (PRL, OPL, INL, IPL, and RGCL, respectively) (Bouskila et al., 2012). CB1R is also expressed in the visual cortex with higher expression in layer 6 and the lowest abundance in layer 4. Higher-order visual areas such as MT and MST show greater expression of CB1R in non-human primates (Eggan and Lewis, 2007). During development, CB1R mRNA was detected in the rat's embryo, in the ganglion cells from the embryonic day 15 and what appears to be the inner nuclear layer (INL) from day 20 (Buckley et al., 1998). In the developing rat retina, CB1R was found in all cell types except rod photoreceptors and Müller cells (Bouskila et al., 2012; Bouskila et al., 2013a; Zabouri et al., 2011a). Recently, the expression of the MAGL and DAGLα were studied in developing mice and show that DAGLα is highly expressed in mouse photoreceptor, horizontal, amacrine, and ganglion cells from the early stage of development but MAGL appears later during the development in amacrine and Müller cells (Cécyre et al., 2014b).

The variation of the content of eCBs in certain diseases suggests that they may play a crucial role in ocular homeostasis. In patients with glaucoma, a decrease in 2-AG level of ciliary bodies was reported (Chen et al., 2005). Unlike patients with diabetic retinopathy, in age-related macular degeneration (AMD) patients, 2-AG levels amplified in the iris and AEA increased in the retina (Matias et al., 2006). The same pattern of augmentation of AEA was observed in retina, choroid, ciliary body and cornea of the AMD patients (Matias et al., 2006).

Besides the well-known "red eye" effect (vasodilation) of marijuana and reduction of intraocular pressure (IOP) (Green, 1979; Porcella et al., 1998), the functional effect of cannabinoids on vision is still not well identified. Case studies interviewed high-potency heavy cannabis smokers and reported several categories of visual disturbances, including: visual distortions, distorted perception of distance, illusions of movement of stationary and moving objects, color intensification of objects, dimmed color, dimensional distortion and blending of patterns and objects (Levi and Miller, 1990; Lerner et al., 2011). The popular urban myth about dilated pupil and marijuana has not been supported by experimental data (Brown et al., 1977).

Cannabis causes impaired performance in tests that require fine psychomotor control such as tracking a moving point of light on a screen (Adams et al., 1975; Adams et al., 1978). THC increases the time course of glare recovery by several seconds (5-10%) only at low contrast (Adams et al., 1978). Higher doses of THC can produces side effects, including blurred vision (Noyes et al., 1975), double vision and vision dimness (Consroe et al., 1997). Numerous reports claim that smoking marijuana improves dim light vision (Dawson et al., 1977; Merzouki and Mesa, 2002; Russo et al., 2004). Acute consumption of marijuana reduces

the Vernier and Snellen acuity, alters color discrimination, increases photosensitivity and decreases dark adaptation (Kiplinger et al., 1971; Dawson et al., 1977; Russo et al., 2004). No significant effect has been observed on static visual acuity (Adams et al., 1975) after consumption of THC with alcohol. Although there was a marked reduction in acuity of moving targets when coordinated eye movements were required (Leweke et al., 1999). Binocular depth inversion is reduced in regular cannabis users while it does not affect the normal depth perception (Leweke et al., 1999; Semple et al., 2003). Dronabinol, a synthetic THC, impaired binocular depth inversion and the top-down processing of visual sensory data (Leweke et al., 1999).

Testing the visual functions by use of steady state visual evoked potential (SSVEP) and Electroencephalography (EEG) on occipital lobe suggests a disruption of later-stage visual processing in regular users (Skosnik et al., 2006). In rats, CB1R at the visual thalamic level plays a dynamic modulatory role in sending visual information into the visual cortex (Dasilva et al., 2012). Recently, Cécyre et al reported that the amplitude of the electroretinogram (ERG) a-wave is increased in *cnr2* knockout mice only and not *cnr1* (Cecyre et al., 2013). Yoneda and colleagues reported that the expression and localization of CB1R in the visual cortex of the mouse is regulated during the development and through visual experiences. In mouse, expression of CB1R in deep layers of V1 decreased after dark rearing from birth to P30. However, two days of monocular deprivation up-regulated the localization of CB1R in inhibitory nerve terminal in deep layers (Yoneda et al., 2013).

The Animal model; Vervet Monkeys (c*hlorocebus sabaeus)*

The extensive resemblance of the non-human primates to *homo sapiens* in various aspects, from genome sequence and molecular pathways to physiology and cognition, makes them the closest laboratory model to human that cannot be approximated by any other animal model. Among the monkeys, old world monkeys are the closest to the human physiology and behavior, after the apes. Old world monkeys show more inter-species brain anatomy similarity compared with human and apes (Jasinska et al., 2013). The animal model that was used in these studies, vervet monkey or green African monkey, is an old world monkey from the cercopithecidae family native to Africa that 23 million years ago diverged from the *hominoid* family (Figure 1-19) (Goodman et al., 1998). Like all the other old-world monkeys, vervets are medium to large size, have a tail with prehensile nerve ending and are omnivorous with preference to plant matters. The St-Kitts vervet monkeys were imported from Senegambia in the seventeenth century (Palmour et al., 1997). Vervet monkeys are progressively employed in biomedical research with a second citation record among the non-human primates after rhesus macaque (Jasinska et al., 2013). Vervets are very similar in physiology and behavior to macaque, but they are more accessible, disease-free with less health and safety risks.

From the visual point of view, old world monkeys have a foveal binocular vision with laminated retina with a high cone density that decreases with eccentricity, trichromatic color vision and a six-layered dLGN. In monkeys the organization of the retinal mosaic has an impact on visual functions; the center being largely involved in visual acuity, color-coding and photopic sensitivity (cone vision), whereas the periphery is more concerned with scotopic functions (rod vision) (Wässle et al., 1995; Jacobs, 2008).

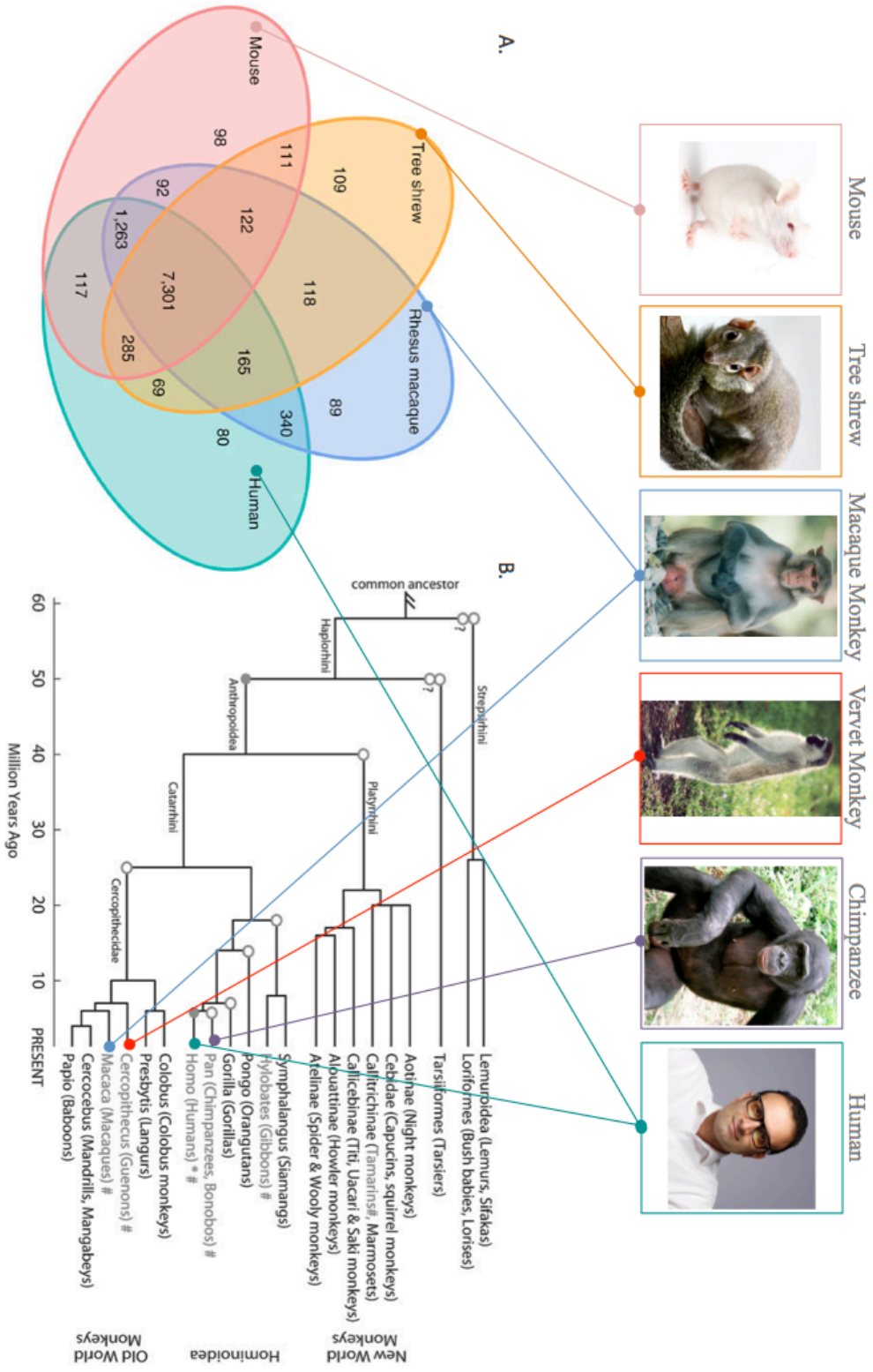

Figure 1-19 a) Venn diagram of comparison of monkeys with human, tree shrew and mouse gene families. Adopted from(Fan et al., 2013) b) Primate phylogenetic tree. Adapted from (Petkov and Jarvis, 2012)

Objectives & Hypothesis

The main objective of this doctoral thesis was to investigate the expression pattern and role of the eCB system in the monkey retinogeniculate pathway. The majority of the cannabinoid studies on vision have previously been done in rodents. Despite the high quality of those interesting researches, it was difficult to translate them to human models due to physiological differences in rodent visual systems. For this study, we used vervet monkeys as our model rather than rodents; their visual system is much closer to that of humans. This study was divided into three specific aims:

Firstly, we sought to investigate the hypothesis that the eCB system components would express in different patterns in the monkey retina. Based on our previous findings that CB2R expresses differently in monkeys than rodents, we predicted that the expression pattern of other eCB components would also vary among different species. By using classic immunohistochemistry, we visualized the eCB system throughout the retina of vervet monkeys and compared the expression patterns to three other species: mouse, tree shrew, and macaque. (We presume that the tree shrew, as a phylogenetic intermediary, expresses a pattern in between mouse and monkey.)

Secondly, due to the differential expression of CB1R and CB2R in retinal layers, we hypothesized that their blockade would affect the amplitude of the ERG waves. To test this, we blocked the CB1 or CB2 receptors in the normal monkey retina with specific antagonists (AM251 and AM630, respectively) and measured the alteration in electrical responses by electroretinography (ERG).

Thirdly, we expect that the eCB system should be present beyond the retina in the dLGN of vervets with a distinctive laminar pattern of expression. To examine this, we assessed the expression pattern of the main cannabinoid receptors in the dLGN of the vervet monkey by confocal microscopy.

CHAPTER 2: Müller cells express the cannabinoid CB2 receptor in the vervet monkey retina

Published in J Comp Neurol. 2013 Aug 1; 521(11): 2399-415. doi: 10.1002/cne.23333.

Müller cells express the cannabinoid CB2 receptor in the vervet monkey retina

Joseph Bouskila*[1, 2], Pasha Javadi*[1], Christian Casanova[1], Maurice Ptito[1, 3], and Jean-François Bouchard[1]

[1]School of Optometry, University of Montreal, Montreal, QC, Canada

[2]Biomedical Sciences, Faculty of Medicine, University of Montreal, Montreal, QC, Canada

[3]BRAINlab, Department of Neuroscience and Pharmacology, University of Copenhagen, Copenhagen, Denmark

* These authors contributed equally to this work.

Abbreviated title: CB2R expression in Müller cells

Associate Editor: Ian A. Meinertzhagen

Keywords: Endocannabinoids, CB1R, CB2R, Retinal Glia, Immunofluorescence, Confocal Microscopy

Correspondence should be addressed to:
Jean-François Bouchard, BPharm, PhD
School of Optometry, room 260-7
3744 Jean-Brillant,
University of Montreal,
Montreal, Quebec, Canada, H3T 1P1

Financial Support: The Natural Science and Engineering Research Council of Canada (311892-2010, JFB; 6362-2012, MP; 194670-2009, CC) and the Canadian Institutes of Health Research (MOP-86495, JFB) supported this work. JB holds a scholarship from "Fonds de

recherche du Québec - Santé (FRQS)". MP is Harland Sanders Chair professor in Visual Science. JFB is supported by a "Chercheur-Boursier Junior 2" from FRQS.

Abstract

The presence of the cannabinoid receptor type 1 (CB1R) has been largely documented in the rodent and primate retinas in recent years. There is however some controversy concerning the presence of the CB2 receptor (CB2R) within the central nervous system. Only recently, CB2R has been found in the rodent retina, but its presence in the primate retina has not yet been demonstrated. The aim of this study was twofold: 1) to characterize the distribution patterns of CB2R in the monkey retina and compare this distribution to that previously reported for CB1R and 2) to resolve the controversy on the presence of CB2R in the neural component of the retina. We therefore thoroughly examined the cellular localization of CB2R in the vervet monkey (*Chlorocebus sabeus*) retina, using confocal microscopy. Our results demonstrate that CB2R, like CB1R, is present throughout the retinal layers with however striking dissimilarities. Double labeling of CB2R and glutamine synthetase shows that CB2R is restricted to Müller cell processes, extending from the internal limiting membrane with very low staining, to the external limiting membrane with heavy labeling. We conclude that CB2R is indeed present in the retina but exclusively in the retinal glia whereas CB1R is only expressed in the neuro-retina. These results extend our knowledge on the expression and distribution of cannabinoid receptors in the monkey retina, although further experiments are still needed in order to clarify their role in retinal functions.

Introduction

Anandamide (AEA) and 2-arachidonoylglycerol (2-AG) are endocannabinoids (eCBs) that bind to cannabinoid receptors (CB1R and CB2R) to exert their physiological effects (Devane et al., 1992; Mechoulam et al., 1995; Sugiura et al., 1995; Piomelli, 2003). The eCBs are endogenous lipid messengers that are involved in the regulation of many physiological processes in mammals (Di Marzo et al., 2007). They are synthetized on demand and rapidly degraded by enzymes, particularly fatty acid amide hydrolase (FAAH), monoglycerol lipase (MAGL) and cyclooxygenase-2 (COX-2) (Cravatt et al., 1996; Dinh et al., 2002; Kozak et al., 2000). The activation of cannabinoid receptors by eCBs leads to cannabis-like effects and CB1R is considered to be the main element responsible of those properties. The eCB system present in the retina likely plays a role in the visual effects of cannabis (Yazulla, 2008 for review). The distribution of CB1R has been well characterized in the retina of rodents and primates (Yazulla et al., 1999; Straiker et al., 1999; Bouskila et al., 2012). It is present in cone pedicles and rod spherules, bipolar cells, amacrine cells, horizontal cells, and ganglion cells. This pattern is also observed in the central and peripheral parts of the monkey retina (Bouskila et al., 2012).

Concerning CB2R, its mRNA was first detected by reverse transcription polymerase chain reaction (RT-PCR) in the adult mouse retina and by *in situ* hybridization in the adult rat retina (Lu et al., 2000) but not in rat embryos (Buckley et al., 1998). Interestingly, using different transcripts, CB2 mRNA was not detected in rat and human retinas (Porcella et al., 1998, 2000). In agreement with (Lu et al., 2000), using immunohistochemistry, CB2R protein was localized in rat retinal pigment epithelium, inner photoreceptor segments, horizontal and

amacrine cells, cells localized in the ganglion cell layer, and in fibres of inner plexiform layer (López et al., 2011). However, this study did not proceed by double labeling with specific retinal cell markers. Instead, cell types were identified based on the position in the retinal layer and on the morphology of the cells. CB2R expression was found in the trabecular meshwork of the porcine eye, in which an injection of a CB2R agonist increased aqueous humour outflow (Zhong et al., 2005). The presence of both CB1R and CB2R has been reported in human retinal pigment epithelial cells in primary cultures and ARPE-19 cells (Wei et al., 2009). Recently, CB2R expression was found at mRNA levels by RT-PCR and protein by Western blot analysis in *in vitro* retinal explants and primary cultures of human Müller glia (Krishnan and Chatterjee, 2012).

The human CB2R was cloned first (Munro et al., 1993). Subsequent studies on CB2R expression patterns focused on the presence of CB2R in peripheral tissues of the immune system (Galiègue et al., 1995). Later on, CB2R was cloned in the mouse (Shire et al., 1996) and rat (Griffin et al., 2000). Unlike CB1R, which is highly conserved across mammalian species, sequences of the murine and human CB2R are divergent, raising the possibility of species-specific amino acid sequences. Indeed, CB2R has evolved far more rapidly (McPartland et al., 2007), such that there is only an 81% sequence homology at the amino acid level between the rat and human CB2R, increasing to 87% identity in the critical trans-membrane regions (Griffin et al., 2000). As a result, rodent models may not reliably predict the performance of a CB2R agonist for human CB2 receptors (Mackie, 2008). Consequently, accurate comparisons between human and rodent receptors are crucial considering that cannabinoids vary in their affinity to CB2R depending upon the species (Mukherjee et al.,

2004). Our study will fill an important gap in the knowledge of the expression patterns of CB2R in the retina.

The presence of CB2R in neurons has raised an important debate in the scientific community (Atwood and Mackie, 2010). While some are convinced that CB2R is not present in neurons, or at least at very low levels (Atwood and Mackie, 2010), others suggest otherwise (Onaivi et al., 2012). Nevertheless, all agree that CB2R is present in the CNS and could be expressed in its glial elements. Despite the extensive knowledge of the distribution of CB2R in the rodent brain, there are no published reports regarding its expression and localization in the human and monkey retinas. Given that eCBs are present in human ocular tissues especially the retina (Chen et al., 2005), it is reasonable to assume the presence of cannabinoid receptors therein. Therefore, the main objective of this study is to characterize the expression and localization patterns of CB2R throughout the *in vivo* monkey retina.

Materials and Methods

Choice of species. Monkey tissue, the experimental model for the current study, was chosen for several reasons. First monkey tissue allows us to generalize more easily to humans. The anatomical similarity between the monkey and human retina is remarkable. Primates are mammals that have a macular/foveal region and multiple cone types, which offers them high visual acuity and color vision. Finally, the high cross-reactivity between human and monkey antigens increases chances of success for targeting CB2R in monkeys using an anti-human CB2R antibody.

Animal Preparation. Three adult vervet monkeys (*Chlorocebus sabaeus*) were used for this study. Monkey tissues were kindly provided by Professor Roberta Palmour from McGill University, Montreal, Canada. The monkeys were part of Dr. Palmour's and Dr. Ptito's research project that was approved by the McGill University Animal Care and Use Committee. The animals were born and raised in enriched environments in the laboratories of the Behavioural Sciences Foundation (St-Kitts, West Indies) that is recognized by the Canadian Council on Animal Care (CCAC). The animals were fed with primate chow (Harlan Teklad High Protein Monkey Diet; Harlan Teklad, Madison, WI) and fresh local fruits, with water available *ad libitum*. The experimental protocol was reviewed and approved by the local Animal Care and Use Committee and the Institutional Review Board of the Behavioural Science Foundation. Each animal was sedated with ketamine (10 mg/kg, i.m.), deeply anaesthetized with sodium pentobarbital (25 mg/kg, i.v.) and perfused transcardially with phosphate buffer saline (PBS pH 7.4), followed by 4% paraformaldehyde.

Antibody characterization. All the primary antibodies used in this work, their sources and working dilutions, are summarized in Table 2-1. These antibodies were successfully used in previous studies and are well characterized in regards to the specific primate retinal cell type immunostaining, as described below for each antibody.

Table 2-1 Primary antibodies used in this study

Primary Antibodies Used in This Study

Antibody*	Immunogen	Source†	Working dilution
GS	Full protein purified from sheep brain	Chemicon, Temecula, CA; MAB302, mouse monoclonal, clone GS-6	H: 1:500
CB	Purified bovine kidney calbindin-D28K	Sigma, St. Louis, MO; C9848, mouse monoclonal, clone CB-955	H: 1:250
PKCα	Peptide mapping the aa 296–317 of human PKCα	Santa Cruz Biotechnology, Santa Cruz, CA; sc-8393, mouse monoclonal, clone H-7	H: 1:500
PV	Full protein purified from frog muscle	Sigma, St. Louis, MO; P3088, mouse monoclonal, clone PARV-19	H: 1:250
Syntaxin	Synaptosomal plasma fraction of rat hippocampus (Barnstable et al., 1985)	Sigma, St. Louis, MO; S0664, mouse monoclonal, clone HPC-1	H: 1:500
Brn3a	Fusion protein containing aa 186–224 of Brn3a protein	Chemicon, Temecula, CA; MAB1585, mouse monoclonal, clone 5A3.2	H: 1:100
CB1R	Fusion protein containing aa 1–77 of rat CB1R	Sigma, St. Louis, MO; C1233, rabbit polyclonal	H: 1:150
CB2R	Synthetic peptide corresponding to aa 20–33 of human CB2R	Cayman Chemical, Ann Arbor, MI; 101550, rabbit polyclonal	H: 1:150 W: 1:500
Kir4.1	Synthetic peptide corresponding to aa 352–368 of human Kir4.1	Osenses, Keswick, South Australia; OSP00134W, goat polyclonal	H: 1:500
GAPDH	Full-length rabbit muscle GAPDH protein	Sigma, St. Louis, MO; G8795, mouse monoclonal, clone GAPDH-71.1	W: 1:20,000

*GS, glutamine synthetase; CB, calbindin; PKCα, protein kinase C (α isoform); PV, parvalbumin; CB1R, cannabinoid receptor type 1; CB2R, cannabinoid receptor type 2; GAPDH, glyceraldehyde-3-phosphate dehydrogenase; aa, amino acids; H, immunohistochemistry; W, Western blot.
†The source column indicates the commercial company, catalog reference and origin. The clone designation is given for monoclonal antibodies.

GS. The mouse monoclonal (IgG2a) to glutamine synthetase (GS) was obtained from Chemicon International (Temecula, CA) and directed against GS purified from sheep brain. This antibody generates a single 45 kDa band in immunoblots of adult mammalian brain tissue (manufacturer's data sheet). This antibody labels Müller cells in rat (Riepe and Norenburg, 1977) and monkey retinas (Nishikawa and Tamai, 2001; Bouskila et al., 2012).

Calbindin. The mouse monoclonal (IgG1) to calbindin (CB) was obtained from Sigma (St. Louis, MO) and directed against purified bovine kidney Calbindin-D-28K. This antibody recognizes a 28 kDa band on Western Blots (manufacturer's data sheet). The calbindin antibody labels cones outside the foveal region, cone bipolar cells and a subset of horizontal cells in human and monkey retinas (Chiquet et al., 2002; Fischer et al., 2001; Kolb et al., 2002; Martínez-Navarrete et al., 2007; Martínez-Navarrete et al., 2008; Bouskila et al., 2012).

PKC. The mouse monoclonal (IgG2a) to protein kinase C (PKC) was developed by Santa Cruz Biotechnology (Santa Cruz, CA) by using as immunogen purified bovine PKC and its epitope is mapped to its hinge region (amino acids 296–317). It detects the PKCa isoform, a well-known specific marker for rod bipolar cells (Mills and Massey, 1999). As stated by the manufacturer, this antibody gives a single band of 80 kDa on Western blots of human cell lines, and has been previously used for immunohistochemistry on rodent (Zabouri et al., 2011a; Zabouri et al., 2011b) and monkey (Cuenca et al., 2005; Martínez-Navarrete et al., 2008; Bouskila et al., 2012) retinas.

PV. The mouse monoclonal (IgG1) to parvalbumin (PV) was obtained from Sigma (St. Louis, MO) by using as immunogen purified frog muscle PV. It recognizes a 12 kDa band from human, bovine, pig, canine, feline, rabbit, rat, and fish tissues (manufacturer's technical information). The pattern of labeling with this antibody was the same as reported previously (Kolb et al., 2002; Bordt et al., 2006). This small calcium-binding protein is expressed in the primate retina by horizontal cells (Wässle et al., 2000) and the antiserum has been used to visualize monkey thalamic nuclei (Qi et al., 2011).

Syntaxin. The mouse monoclonal (IgG1) to syntaxin (clone HPC-1) was developed by Barnstable et al. (1985) and is distributed by Sigma (St. Louis, MO). This antibody recognizes syntaxin-1, a 35 kDa protein, from hippocampal, retinal and cortical neurons (Inoue et al., 1992). This antibody labels horizontal cells and amacrine cells, in the developing and adult human retina (Nag and Wadhwa, 2001). The staining pattern obtained in the current study was similar to that found in human retina (Nag and Wadhwa, 2001). We have used this antibody to label monkey retinal amacrine and horizontal cells (Bouskila et al., 2012).

Brn3a. The mouse monoclonal (IgG1) to Brn3a was obtained from Chemicon International (Temecula, CA) and made against amino acids 186-224 of Brn3a fused to the T7 gene 10 protein. The Brn3a antibody shows no reactivity to Brn3b or Brn3c by western blot and no reactivity to Brn3a knockout mice (manufacturer's technical information). Its specificity for rodent (Nadal-Nicolás et al., 2009) and monkey (Xiang et al., 1995) retinal ganglion cells has been documented. We used the POU-domain transcription factor Brn3a to label the nuclei of retinal ganglion cells (Bouskila et al., 2012).

CB1R. The rabbit anti-CB1R was obtained from Sigma (St. Louis, MO). It was developed by using a highly purified fusion protein containing the first 77 amino acid residues of the rat CB1R as the immunogen. It recognizes a major band of 60 kDa and less intense bands of 23, 72, and 180 kDa (manufacturer's data sheet, C1233). This antibody targets the rat CB1R (Zabouri et al., 2011a) but specifically recognizes the CB1R (60 kDa) from many species (manufacturer's data sheet), including vervet monkey retinal tissue (Bouskila et al., 2012).

CB2R. The rabbit anti-CB2R was obtained from Cayman Chemical (Ann Arbor, MI). It was developed by using a synthetic peptide corresponding to the amino acids 20-33 (NPMKDYMILSGPQK) of the human CB2R sequence conjugated to KLH as immunogen. This antibody recognizes a band at 45 kDa and a band at 39-40 kDa (manufacturer's data sheet, 101550). This antibody was used in human nervous tissues (Ellert-Miklaszewska et al., 2007; Zurolo et al., 2010). Its specificity to CB2R was recently validated in CB2R knockout mice retinal tissue. CB2R immunohistochemistry signal present in CB2R wild-type mice was completely absent in their knockout littermates (Argaw et al., 2011).

GAPDH. The mouse monoclonal (IgM) to GAPDH (GlycerAldehyde-3-Phosphate DeHydrogenase, clone GAPDH-71.1) was obtained from Sigma (St. Louis, MO) by using as immunogen purified rabbit muscle GAPDH (whole molecule). As stated by the manufacturer, this antibody recognizes monkey GAPDH and gives a single band at about 37 kDa.

Kir4.1. The goat polyclonal anti-Kir4.1 antibody was purchased from Osenses (Keswick, South Australia). This antibody was raised against a synthetic peptide corresponding to amino acids 352-368 (PEKLKLEESLREQAEKE) of human KCNJ10 (Kir4.1) conjugated to an immunogenic carrier protein and gives a single band at about 37 kDa in Western Blot. The peptide is homologous in mouse and rat and was predicted to react in rat, mouse and human tissues (manufacturer's technical information, cat. #OSP00134W). It has been characterized by immunoblot and immunostaining of HEK cells transfected with Kir4.1 and used to target the Kir4.1 in mouse cortical astrocytes (Li et al., 2001).

CB2R blocking peptide. The CB2R blocking peptide containing the human CB2R amino acid sequence 20-33 (NPMKDYMILSGPQK; Cayman Chemical; catalog number 301550) was used in the present study for immunohistochemistry and western blot analysis. The specificity of the CB2R antibody was also tested by preincubation with the corresponding blocking peptide. For preadsorption, the primary antibody was diluted in PBS and incubated with a ratio 1:1 for 2 hours at room temperature with occasional inversion. Thereafter, the antibody-blocking peptide solution was added to the slices and subsequent immunohistochemistry followed the protocol as described further.

Tissue preparation. The eyes were extracted and the retina was dissected free from the eyecup in a PBS bath. The retina was laid flat so that the vitreous body could be removed by blotting with filter paper and gentle brushing (Burke et al., 2009). Samples of retina (4 mm^2) were taken from the center (radius of 4 mm around the fovea), middle (radius of 10 mm around the fovea) and periphery (radius of 20 mm around the fovea), along with the fovea. Each sample was cryoprotected in 30% sucrose overnight and embedded in Shandon embedding media at -65^{0}C. Retinal samples were sectioned in a cryostat (18 μm) and mounted onto gelatinized glass microscope slides, air-dried and stored at -20^{0}C.

Western blotting. In order to test the specificity of the CB2R antisera, Western blots were performed on monkey tissue. A fresh dissected sample of retina, visual cortex or cerebellum was homogenized by hand by using a sterile pestle in RIPA buffer (150 mM NaCl, 20 mM Tris, pH 8.0, 1%, NP-40 (USB Corp., Cleveland, OH, USA), 0.1% SDS, 1 mM EDTA), supplemented with a protease-inhibitor mixture (aprotinin (1:1,000), leupeptin (1:1,000),

pepstatin (1:1,000) and phenylmethylsulfonyl fluoride (0.2 mg/ml); Roche Applied Science, Laval, QC, Canada). Samples were centrifuged at 4°C for 10 minutes, and the supernatant was extracted and stored at -20°C until further processing. Protein content was equalized by using a Thermo Scientific Pierce BCA Protein Assay Kit (Fisher Scientific, Ottawa, ON, Canada). Thirty micrograms of protein/sample of the homogenate was resolved with 10% sodium dodecyl sulfate (SDS)-polyacrylamide gel electrophoresis, transferred onto a nitrocellulose membrane filter (BioTrace NT, Life Sciences, Pall, Pensacola, FL), blocked for 1 hour in 5% skim milk (Carnation, Markham, ON, Canada) in TBST (0.15 M NaCl, 25 mM Tris-HCl, 25 mM Tris, 0.5% Tween- 20), and incubated overnight with the primary antibody, namely, rabbit anti-CB2R (1:500) in blocking solution. The following day, the blot was exposed to a secondary antibody conjugated to horseradish peroxidase (1:5,000; Jackson ImmunoResearch, West Grove, PA) in blocking solution for 2 hours. Detection was carried out by using homemade ECL Western blotting detection reagents (final concentrations: 2.50 mM luminol, 0.4 mM p-coumaric acid, 0.1 M Tris-HCl pH 8.5, 0.018% H_2O_2). The membrane was then air-stripped, reblocked, and exposed to a second primary antibody, namely mouse anti-GAPDH (1:20,000), until all proteins of interest were tested. Densitometric analysis was performed by using ImageJ software (Version 1.45; http://rsb.info.nih.gov/ij/) on scanned films.

Immunohistochemistry. Single, double and triple labeling of the retina were performed according to previously published methods (Bouskila et al., 2012). Briefly, sections were postfixed for 5 minutes in 70% ethanol, rinsed 3 x 5 minutes in 0.1 M Tris buffer, pH 7.4/0.03% Triton and blocked for 90 minutes in 10% normal goat serum (NDS) in 0.1 M Tris buffer/0.5% Triton. Sections were incubated overnight at room temperature with primary

antibody in blocking solution. The CB2R antibody was used conjointly with a known retinal cell type marker: calbindin, PKCa, syntaxin, Brn3a, or glutamine synthetase (Table 2-1). The next day, sections were washed for 10 minutes and 2 x 5 minutes in 0.1 M Tris /0.03% Triton, blocked in 10% NDS, 0.1 M Tris /0.5% Triton for 30 minutes and incubated with secondary antibody for 1 hour: Alexa 488 donkey anti-mouse, Alexa 488 donkey anti-goat, Alexa 555 donkey anti-mouse or biotinylated donkey anti-rabbit followed by the addition of streptavidin-Alexa 647 (1:200), all in a blocking solution as described above. Sections were washed again in Tris buffer, counterstained with bisbenzimide (Hoechst 33258, Sigma, 2.5 μg/mL), a fluorescent nuclear marker, and coverslipped with Fluoromount-G™ Mounting Medium (SouthernBiotech, Birmingham, AL).

Sequential labeling of CB1R and CB2R. The CB1R and CB2R antibodies that we selected came from the same host, making the use of simultaneous double-labeling protocol not adequate. To circumvent this problem, we used a sequential protocol previously described by our research group (Zabouri et al., 2011a; Zabouri et al., 2011b; Bouskila et al., 2012). Briefly, the sections were labeled in a serial manner. The exposition to the first primary antibody was conducted as described above, followed by incubation of a goat anti-Fab fragment solution (Jackson ImmunoResearch Laboratories, West Grove, PA); Brandon, 1985). This allowed for the tagging of the first primary antibody as goat rather than rabbit. The sections were revealed with a secondary Alexa donkey anti-goat 488. Thereafter, they were exposed to a second primary antibody overnight and revealed the following day with an Alexa donkey anti-rabbit 647. The validity of the sequential staining was then verified for CB1R/CB2R co-labeling with the following two controls: (1) omission of the second primary antibody resulted in a strong

staining with the goat secondary 488 but no staining with rabbit secondary 647; (2) omission of the first secondary and second primary antibodies revealed faint signal for the goat secondary 488 and no signal for the rabbit secondary 647.

Confocal microscopy. Fluorescence was detected with a Leica TCS SP2 confocal laser-scanning microscope (Leica Microsystems, Exton, PA), using a 40X (n.a.: 1.25 – 0.75) or a 100X (n.a.: 1.40 – 0.7) objective. Images were obtained sequentially from the green and far-red channels on optical slices of less than 0.9 μm of thickness. Throughout the *Results* section, images taken from the green channel correspond to the retinal cell markers and from the far-red channel to CB2R. When co-expression of CB2R and retinal cell markers was ambiguous in some retinal layers, co-labeling or its absence was demonstrated by taking z-stacks with optimized steps. This allowed for visualization of the cells in the X-Y, X-Z and Y-Z axes, thereby confirming the presence or absence of CB2R in the cells. All photomicrograph adjustments, including size, color, brightness, and contrast were done with Adobe Photoshop (CS5, Adobe Systems, San Jose, CA) and then exported to Adobe InDesign (CS5, Adobe Systems, San Jose, CA), where the final figure layout was completed. The schematic panels of Figure 9 were created using Adobe Illustrator (CS5, Adobe Systems, San Jose, CA).

Results

CB2R antibody specificity. Immunoblots of CB2R antisera in homogenates of fresh vervet monkey retina, visual cortex, and cerebellum (Figure 2-1A) showed one intense band at 45 kDa for each homogenate. Pre-incubation with CB2R blocking peptide completely abolished antibody signal (Figure 2-1B). The same blot was reprobed using the GAPDH antibody (37 kDa) to ensure the proper equalization and loading of all samples (Figure 2-1A and 2-1B, lower panels). As an added control, the CB2R antibody was preadsorbed with its blocking peptide prior to incubation with retinal sections, resulting in an absence of staining signal in the section (Figure 2-1D, see CB2R blocking peptide paragraph in the Materials and Methods section). Furthermore, the CB2R knock out mice validated the specificity of anti-CB2R by elimination of the immunolabeling (Argaw et al., 2011). CB2R-immunoreactivity (IR) was present throughout the monkey retina, extending from the fovea centralis to the periphery and from the external limiting membrane to some cell bodies of the inner nuclear layer (Figure 2-1C). CB2R was densely expressed in the Henle Fiber layer (Figure 2-1C), comprising the cone photoreceptor oblique axons with accompanying Müller glial cell processes and forming a pale-staining fibrous-looking area not seen in the peripheral retina (Figure 2-3H).

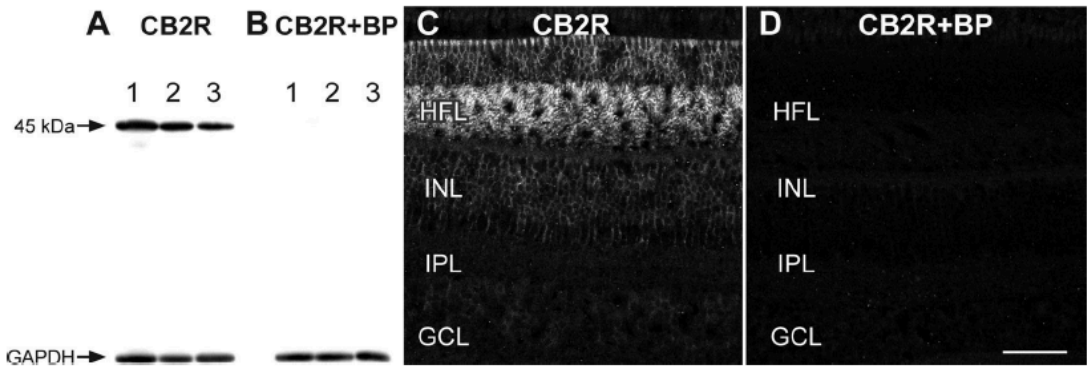

Figure 2-1 Characterization of CB2R antibody in the vervet monkey. Western blot analysis of total protein samples from retina (A – lane 1**), visual cortex (**A – lane 2**) and cerebellum (**A – lane 3**) showing detection of one heavy protein band at 45 kDa. The band was not detected when the antibody was pre-incubated with the corresponding CB2R blocking peptide (BP) (**B – lanes 1-3**). All lanes contained 10 µg of total protein. The lower blots for CB2R and CB2R-BP show the expression of the protein GAPDH and demonstrates loading in all lanes. Immunohistochemistry on vervet retinal tissue with the anti-CB2R antibody revealed a unique staining profile (**C**). When the CB2R antibody was pre-incubated with its BP, it revealed an absence of staining (**D**). HFL, Henle fiber layer; INL, inner nuclear layer; IPL, inner plexiform layer; GCL, ganglion cell layer. Scale bar = 75 µm.**

CB2R immunoreactivity throughout the monkey retina. The expression pattern of CB2R near the fovea and in the peripheral retina seems different on visual examination, but this is misleading, because Müller cells have different morphological characteristics in the central and peripheral retina (Distler and Dreher, 1996). If one looks at the pattern of Müller cell processes, CB2R distributions are rather similar. The strongest CB2R signal is localized in the Henle fiber layer with generally weaker signals in the inner retina (Figure 2-2).

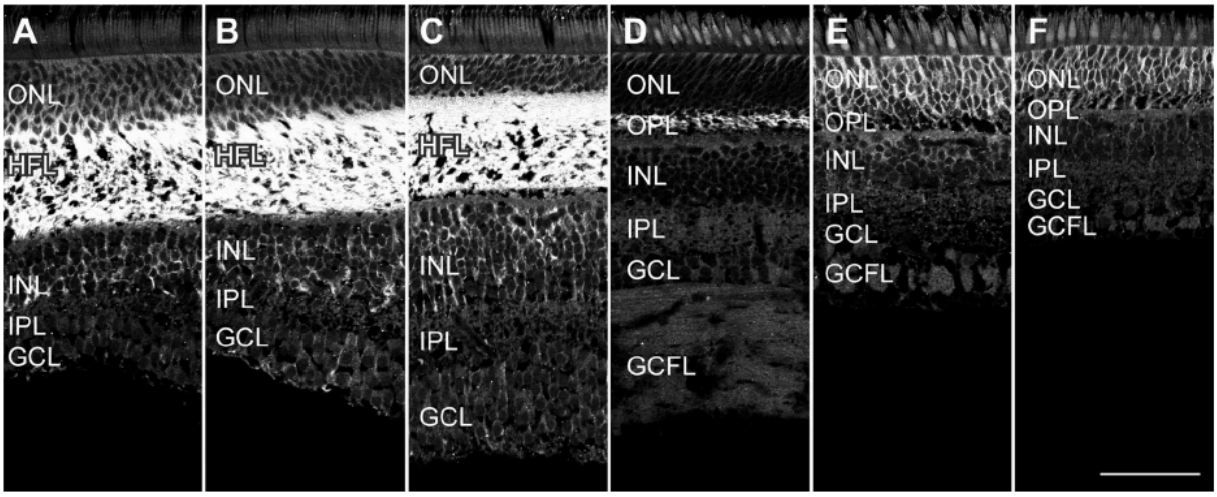

Figure 2-2 Labeling pattern of CB2R-IR throughout the monkey retina. Confocal micrographs taken from the fovea (A), and from 1 mm (B), 2 mm (C), 5 mm (D), 10 mm (E), 20 mm (F) of the fovea. Note that the most prominent staining of CB2R is located in the Henle fiber layer present in samples of central retina. ONL, outer nuclear layer; HFL, Henle fiber layer; OPL, outer plexiform layer; INL, inner nuclear layer; IPL, inner plexiform layer; GCL, ganglion cell layer; GCFL, ganglion cell fiber layer. Scale bar = 75 µm.

Double-label immunohistochemistry. In order to verify the retinal cell type expression, double immunostaining was carried out for CB2R and a specific molecular marker for primate retinal cells. A consistent staining pattern across all three monkey retinas was found for each double staining. Although labeling was located in all distal layers of the retina, from the photoreceptor to the inner nuclear layers, CB2R-IR was most prominent in the Henle Fiber layer within the central retina (Figures 2-3, 5, 6, 9).

Cellular distribution of CB2R

CB2R is present in Müller cells. The extensive CB2R-immunoreactive fibers along the external limiting membrane were suggestive of Müller cells (Figure 2-3A-C). This hypothesis was tested by double-labeling CB2R-IR with GS-IR, which labels Müller cells in the mammalian retina, including vervet monkey retina (Riepe and Norenburg, 1977; Bouskila et

al., 2012). All fibers that were GS-immunoreactive were also double labeled for CB2R-IR in the central retina (Figure 2-3D-F) and in the middle retina (Figure 2-3G-I). This included all the Müller cell fibers but not Müller cell bodies (Figure 2-3A-C). Most prominent staining was found in the distal retina with only faint staining in the proximal retina. On occasion, some GS-immunoreactive proximal fibers were not CB2R-immunoreactive. Villous processes extending beyond the external limiting membrane (arrows) did not co-localize with CB2R-IR.

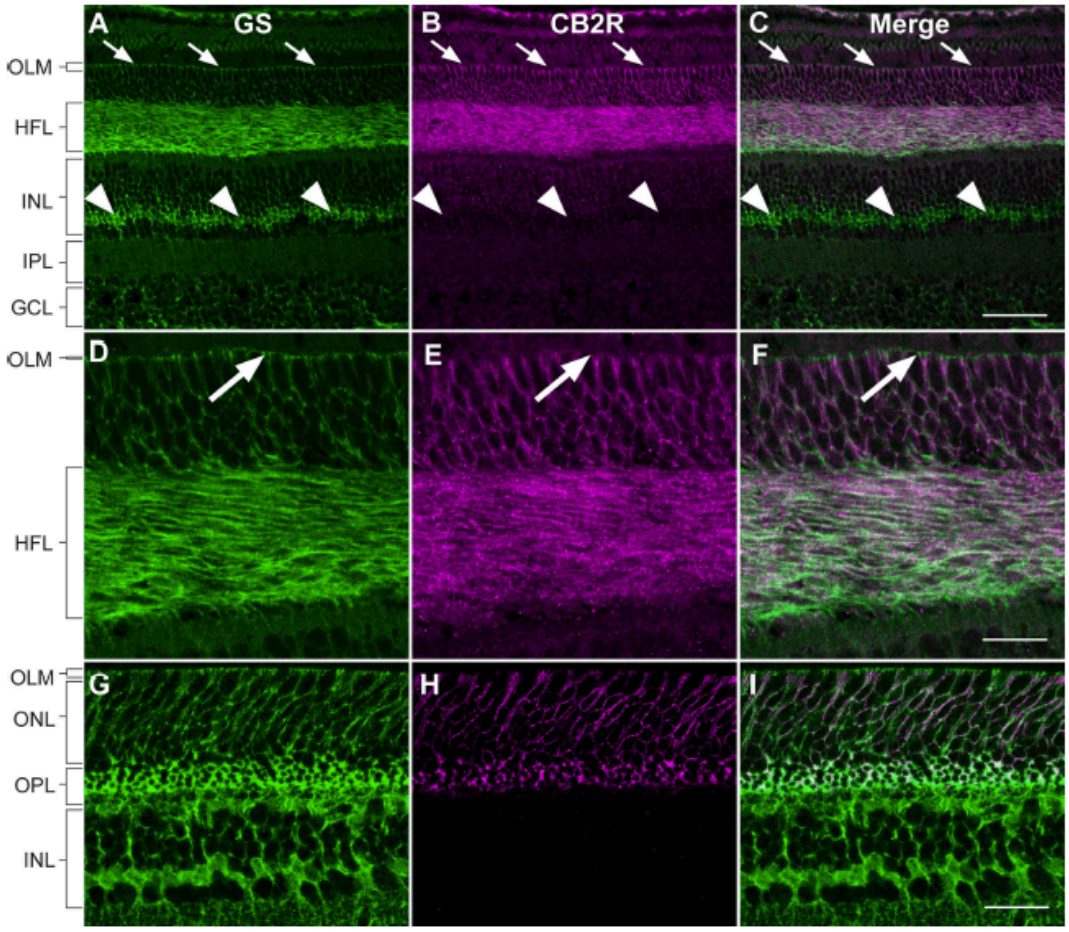

Figure 2-3 CB2R co-localizes extensively with glutamine synthetase-labeled Müller cells in the monkey retina. A-I**: Vertical sections taken near the fovea (**A-F**) and in the middle retina (**G-I**). Confocal micrographs of retinas co-immunolabeled for CB2R and glutamine synthetase (GS), a cell type specific marker for Müller cells. Each protein is presented alone in gray scale in the first columns. The merge image is presented in the last column (GS in green and CB2R in magenta). Arrows indicate the projections of the Müller cell membrane in the apical margin known as apical villi that lack CB2R. Arrowheads point at Müller cell bodies that do not express CB2R.** D-F**: Higher magnification views of the outer limiting membrane (OLM) demonstrate the absence CB2R/GS double labeling in the Müller cell villi. OLM, outer limiting membrane; HFL, Henle fiber layer; INL, inner nuclear layer; IPL, inner plexiform layer; GCL, ganglion cell layer. Scale bar = 75 µm for** A-C**, and 30 µm for** D-I**.**

No expression of CB2R in cones. Because the Henle fiber layer comprises densely packed oblique cone photoreceptor axons with accompanying Müller cell processes, CB2R and calbindin co-localization was needed to rule out the possibility that CB2R was present in cones. Given that CB labels cones outside the foveola, a central (Figure 2-4A-C) and middle (Figure 2-4D-F) retinal samples were taken to perform co-localization with CB2R and CB. Although the patterns of CB2R-IR throughout the ONL and OPL appeared very similar to those of GS-IR, it was not clear from an overlay projection presented in Figure 4 that CB2R-IR is truly adjacent to cone axons. A flattened Z-series indicated that CB2R-IR in the ONL was due exclusively to fibers of the Müller cells and do not include cone axons (Figure 2-4G). In order to further corroborate the localization of CB2R in GS-positive fibers, but not in CB-positive axons, confocal optical sections, were investigated in the X-Z and Y-Z projections. The X-Z and Y-Z images were drawn through the point of double-labeling between CB-IR and CB2R-IR, and the two orthogonal views clearly show no overlap (Figure 2-4H).

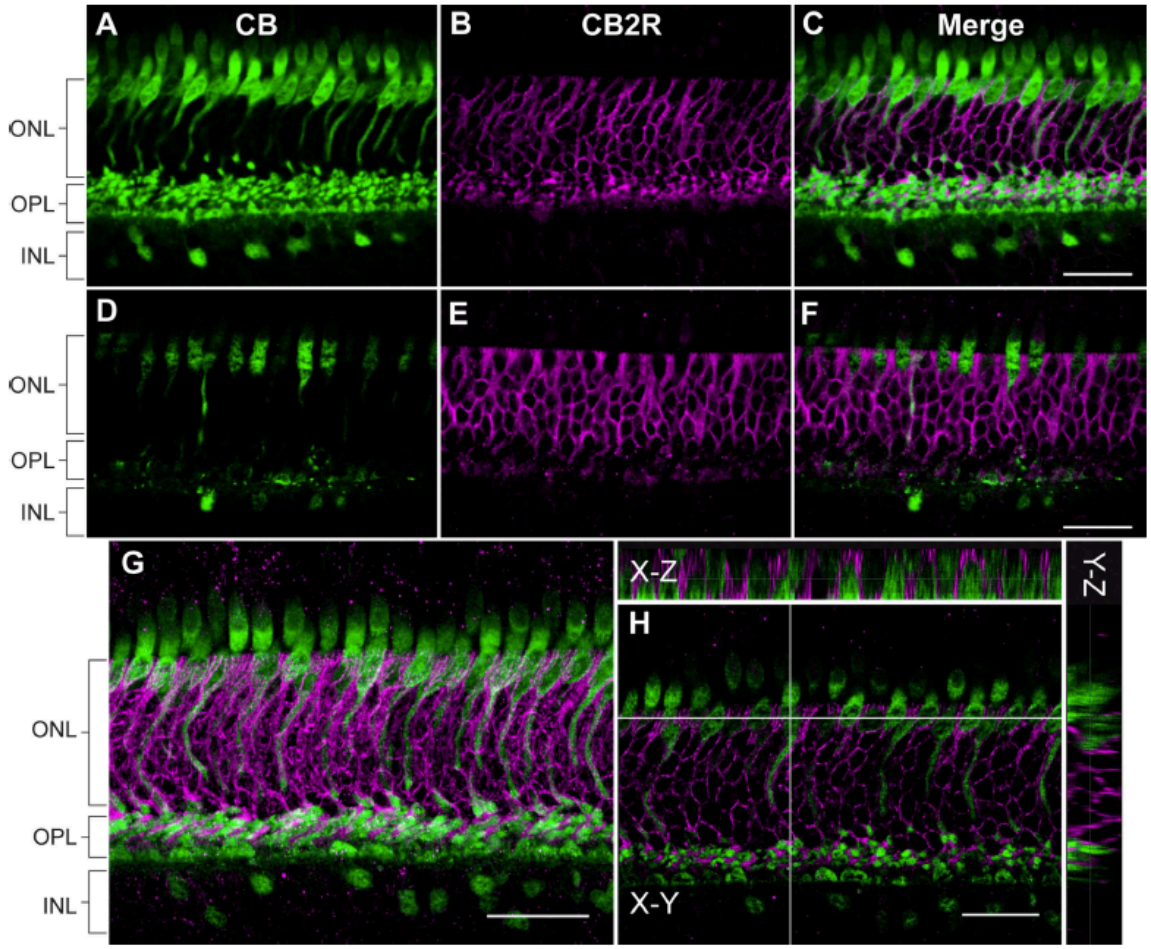

Figure 2-4 Double-label immunofluorescence illustrating localization of calbindin (CB) and CB2R. A-C**: Calbindin-IR labeled cone photoreceptors in the monkey central retina, and these were not CB2R immunoreactive. Note that CB2R-IR appears co-localized in the ONL, but a flattened Z-series (**G**) and a 3D reconstruction in the X-Z and Y-Z axes showed no co-localization (**H**). CB2R-IR was not present throughout cones outside of the central region, as illustrated in the overlay of the two micrographs (**D-F**). This overlay clearly shows that the CB2R-immunoreactive outer processes were neighboring to the CB-immunoreactive cone photoreceptors. ONL, outer nuclear layer; OPL, outer plexiform layer; INL, inner nuclear layer. Scale bar = 75 µm.**

CB2R is not present in rod bipolar cells. Occasionally, there were CB2R-immunoreactive cell fibers in the proximal INL that looked like PKC-immunoreactive rod bipolar cell axons in the central retina (Figure 2-5A-C) and peripheral retina (Figure 2-5D-F). No PKC-immunoreactive rod bipolar cell, including its cell body, axon and axon terminal, was co-localized with CB2R-IR, confirming that CB2R-IR was not present in rod bipolar cells.

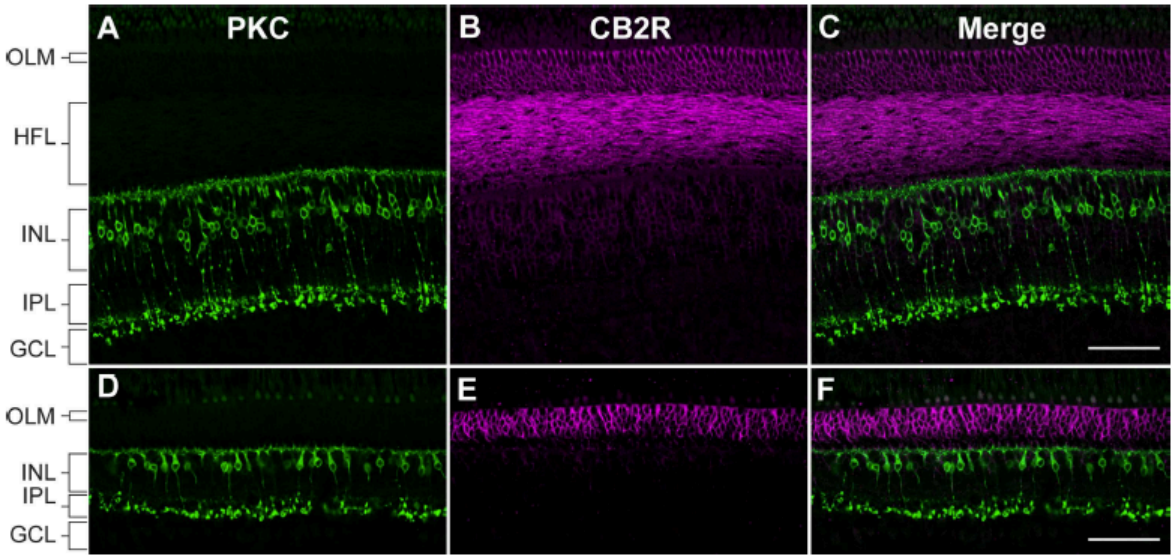

Figure 2-5 Double-label immunofluorescence illustrating the localization of PKC and CB2R. A-F: Vertical sections showing PKC-positive fibers representing rod bipolar cell axons that appear co-localized near the fovea (A-B) and in the middle retina (D-F). CB2R-IR followed the Müller cell processes insinuating themselves between cell bodies of the neurons in the inner nuclear layer. No PKC-immunoreactive cell was CB2R-immunoreactive. OLM, outer limiting membrane; HFL, Henle fiber layer; INL, inner nuclear layer; IPL, inner plexiform layer; GCL, ganglion cell layer. Scale bar = 75 µm.

Horizontal cells do not express CB2R. CB2R-IR did not co-localize with PV-IR in the central retina (Figure 2-6A-C) and peripheral retina (Figure 2-6D-F) indicating that horizontal cells were not CB2R-immunoreactive. The PV-IR is classically associated with equal staining of 2 morphological types of horizontal cells in the primate retina (arrows), H1 and H2 horizontal cells (Röhrenbeck et al., 1987), and no clear co-localization was found in any horizontal cells of the vervet monkey retina (Figure 2-6A-F).

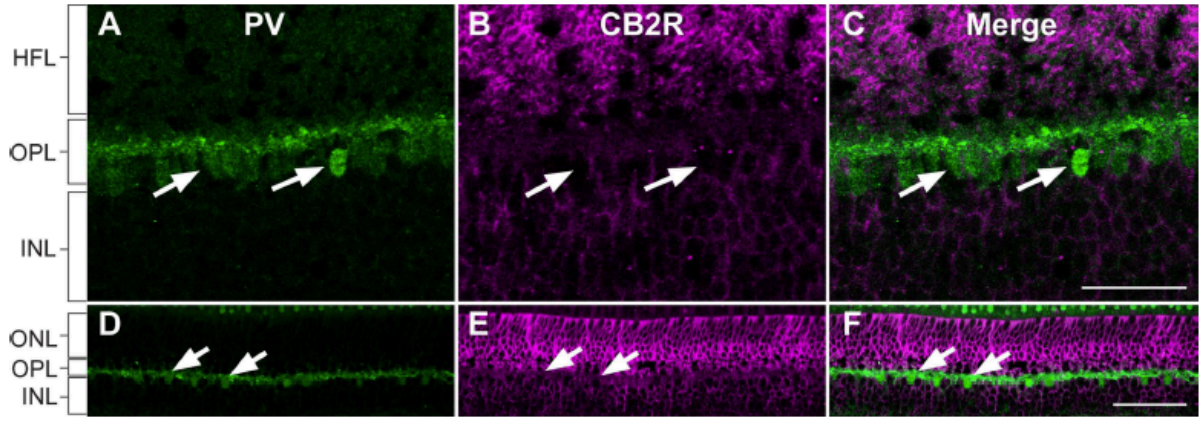

Figure 2-6 Localization of parvalbumin (PV) and CB2R within the central and peripheral retina. Note that the CB2R labeling (magenta) is not located within PV-immunoreactive horizontal cell somata and processes (green). High-magnification images of PV, CB2R, and merged views, respectively in the central retina (A-C**) and in the middle retina (**D-F**). Occasional CB2R-immunoreactive fibers in the OPL surround the horizontal cell somata (arrows). HFL, Henle fiber layer; ONL, outer nuclear layer; OPL, outer plexiform layer; INL, inner nuclear layer. Scale bar = 37.5 µm for** A-C **and 75 µm for** D-F**.**

CB2R is not present in amacrine cells. The monoclonal antibody HPC-1 that recognizes syntaxin in horizontal and amacrine cells was used to evaluate CB2R-IR expression in amacrine cells (Figure 2-7A-C). Despite variations in intensity of immunolabeling, virtually no amacrine cells showed expression of CB2R-IR in the central retina (Figure 2-7D-F) or the middle retina (Figure 2-7G-I). Although there was no visible expression of CB2R in horizontal cells (arrows) and amacrine cells (arrowheads), the staining found in the layers of horizontal and amacrine cells was limited to the Müller cell processes (Figure 2-7B and 2-7E).

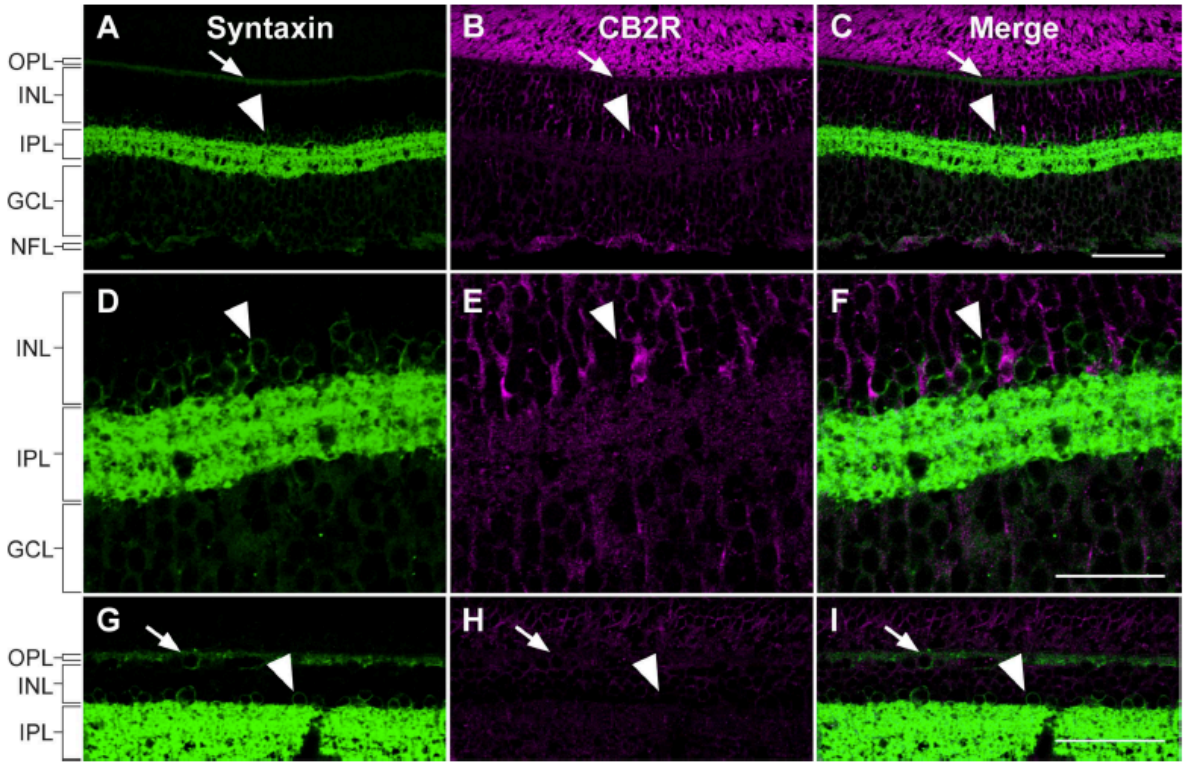

Figure 2-7 Double-label immunofluorescence illustrating the localization of syntaxin (green) and CB2R (magenta) in the monkey retina. A-C**: Syntaxin-immunoreactive horizontal (arrows) and amacrine cells (arrowheads) were clearly not labeled with CB2R in the central retina.** D-F**: Higher magnification of syntaxin-IR and CB2R-IR in the central retina.** G-I**: Syntaxin-IR and CB2R-IR in the middle retina. Syntaxin-IR labeled heavily the membrane of horizontal cells in the OPL but lightly their cytosol, and also labeled heavily the membrane of amacrine cells and IPL but lightly their cytosol. OPL, outer plexiform layer; INL, inner nuclear layer; IPL, inner plexiform layer; GCL, ganglion cell layer; NFL, nerve fiber layer. Scale bar = 75 µm for** A-C **and** G-I**, and 37.5 µm for** D-F**.**

CB2R is absent in ganglion cells. Brn3a immunoreactivity specifically labels retinal ganglion cell nuclei. CB2R-IR was not detected in ganglion cell bodies (arrowheads) either in the central (Figure 2-8A-C) or middle retina (Figure 2-8D-F). Displaced Brn3a-positive cells located in the IPL were not CB2R-immunoreactive (arrows). Double-labeling Brn3a/CB2R showed that CB2R was not expressed in ganglion cells.

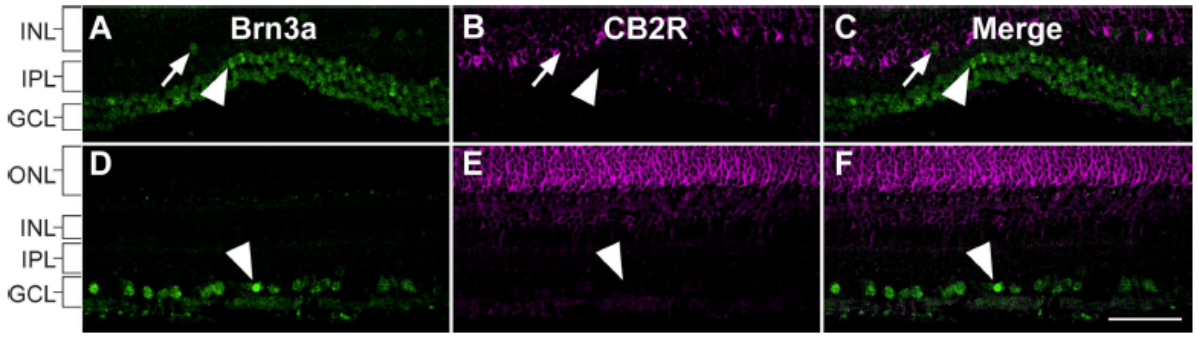

Figure 2-8 Double-label immunofluorescence illustrating localization of CB2R (magenta) and Brn3a (green) in the central retina (A-C) and in the middle retina (D-F). The antibody against Brn3a labels the nucleus of ganglion cells in the monkey retina and these cells were not CB2R immunoreactive. The occasional labeling of CB2R in the ganglion cell layer was localized in the Müller cells inner processes. Arrows point at Brn3a positive cell that is not localized in the GCL and arrowheads indicate Brn3a positive ganglion cells that are not CB2R-immunoreactive. ONL, outer nuclear layer; INL, inner nuclear layer; IPL, inner plexiform layer; GCL, ganglion cell layer. Scale bar = 75 µm.

Differential CB1R and CB2R labeling. Double-labeling of CB1R-IR and CB2R-IR was performed in a retinal sample of 2 mm eccentricity from the fovea (Figure 2-9A-C) and of 6 mm eccentricity from the fovea (Figure 2-9J-L) to differentiate the localization of these cannabinoid receptors. There was no large overlap in the expression of these two receptors in the ONL, INL, IPL, and GCL, but apparent overlap in the HFL. Detailed analysis of the expression of CB1R for each cell type has been previously characterized (Bouskila et al., 2012) and precise expression of CB2R is presented in Figures 3-8. Note that for the most part, CB1R expression is found throughout the retinal neurons of the monkey retina and CB2R in the retinal Müller cells. In order to distinguish CB1R-IR from CB2R-IR in the HFL, a 6 mm eccentricity sample of the monkey retina was taken, as the HFL is only present in the central retina close to the fovea. Figure 2-9A-C shows immunostaining for the complete protocol where strong signals for both CB1R (Figure 2-9A) and CB2R (Figure 2-9B) can be seen. Figure 2-9D-F illustrates the first control in which the second primary antibody was omitted: a

clear signal for CB1R (Figure 2-9D) whereas no staining for CB2R (Figure 2-9E). Figure 9G-I presents the results for the second control where the first secondary and second primary antibodies were omitted: no staining for CB1R (Figure 2-9G) and CB2R (Figure 2-9H). Figure 2-9J-L clearly shows no co-localization of CB1R (Figure 2-9J) and CB2R (Figure 2-9K) in the outer retina. Arrowheads follow a CB1R-positive cone cell body and axon; note that CB2R-positive Müller cell processes envelop this cone. These data are summarized in Figure 2-10A for all retinal cell types.

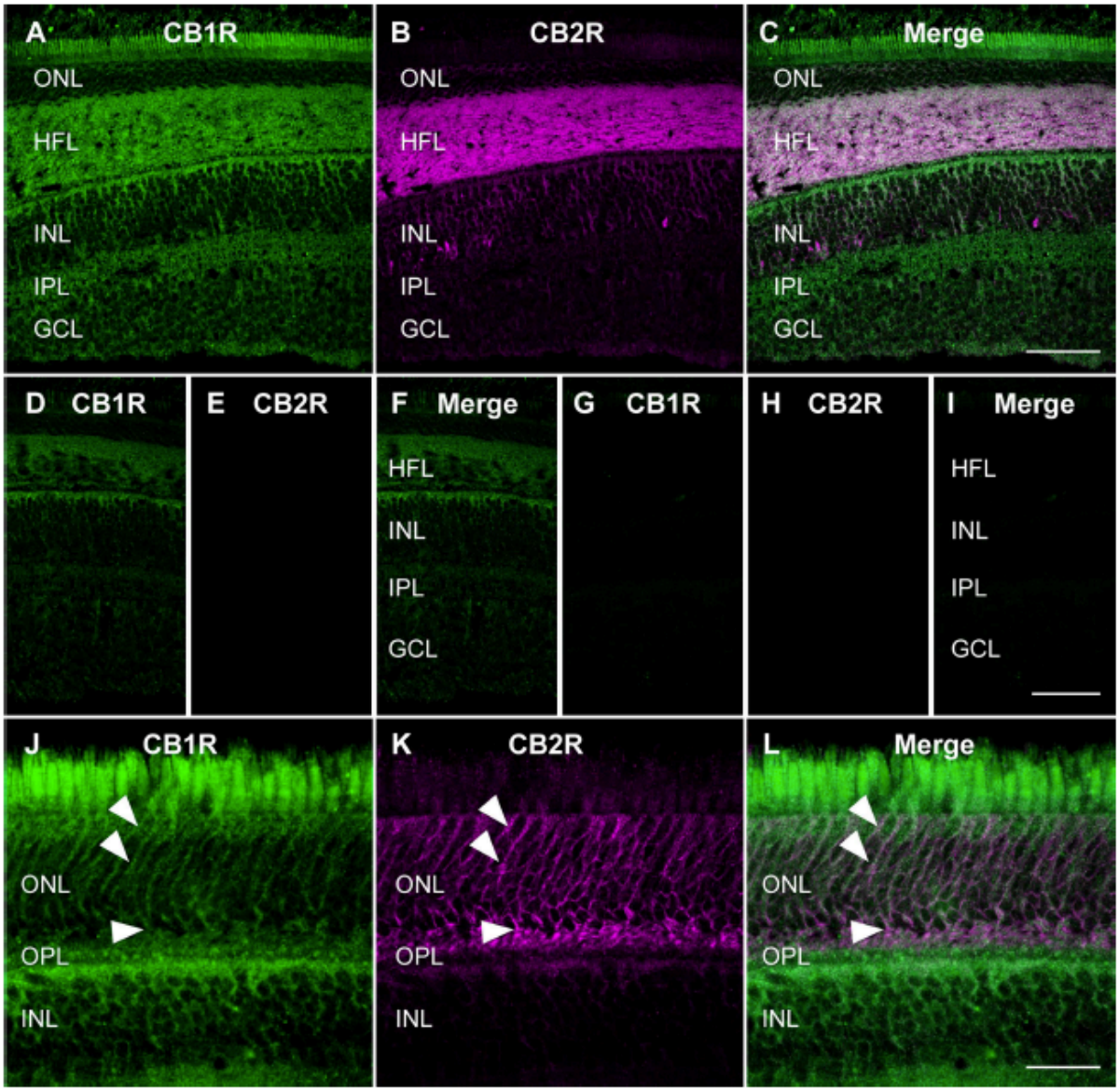

Figure 2-9 Comparison of CB1R and CB2R retinal expressions. Confocal micrographs of retinas co-immunolabeled for CB1R (green) and CB2R (magenta). CB1R (A, D, G, J**), CB2R (**B, E, H, K**) signals, and their overlay (**C, F, I, L**).** A-C**: Complete sequential protocol in the central retina.** D–F**: The second primary antibody was omitted.** G–I**: The first secondary and second primary antibodies were lacking.** J-L**: Localization of CB1R and CB2R in the outer retina. Arrowheads follow a CB1R-positive cone cell body and axon, and CB2R-positive Müller cells processes that enroll this cone. ONL, outer nuclear layer; HFL, Henle fiber layer; INL, inner nuclear layer; IPL, inner plexiform layer; GCL, ganglion cell layer. Scale bar = 75 µm.**

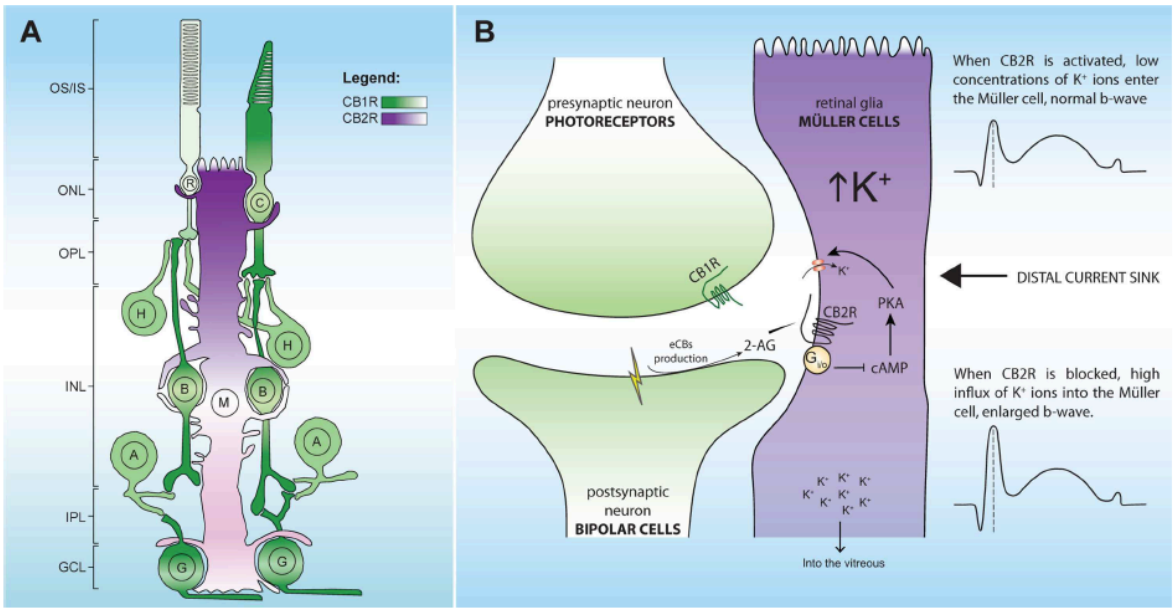

Figure 2-10 Schematic illustration representing the localization of the principal cannabinoid receptors (A) and a hypothetical function for CB2R (B) in the monkey retina. CB1R is localized in neural components and CB2R in glial components (Müller cells). Color bars in the legend indicate the intensity of CB1R (green) and CB2R (magenta) expressions. OS/IS, outer and inner segments of rods and cones; ONL, outer nuclear layer; OPL, outer plexiform layer; INL, inner nuclear layer; IPL, inner plexiform layer; GCL, ganglion cell layer; C, cones; R, rods; H, horizontal cells; B, bipolar cells; A, amacrine cells; G, retinal ganglion cells; M, Müller cells.

Triple labeling of CB2R, GS, and Kir4.1. Triple immunofluorescent labeling was performed in order to verify if potassium channels co-localize with CB2R in Müller cells. Expression of Kir4.1 was found in CB2R positive and GS positive Müller cells of the central retina. Co-expression of CB2R and Kir4.1 was found in the HFL but scarcely in the proximal parts of Müller cells (Figure 2-11A-D). There was a large overlap in the expression of GS and Kir4.1 in the INL, IPL, and GCL (Figure 2-11E-L).

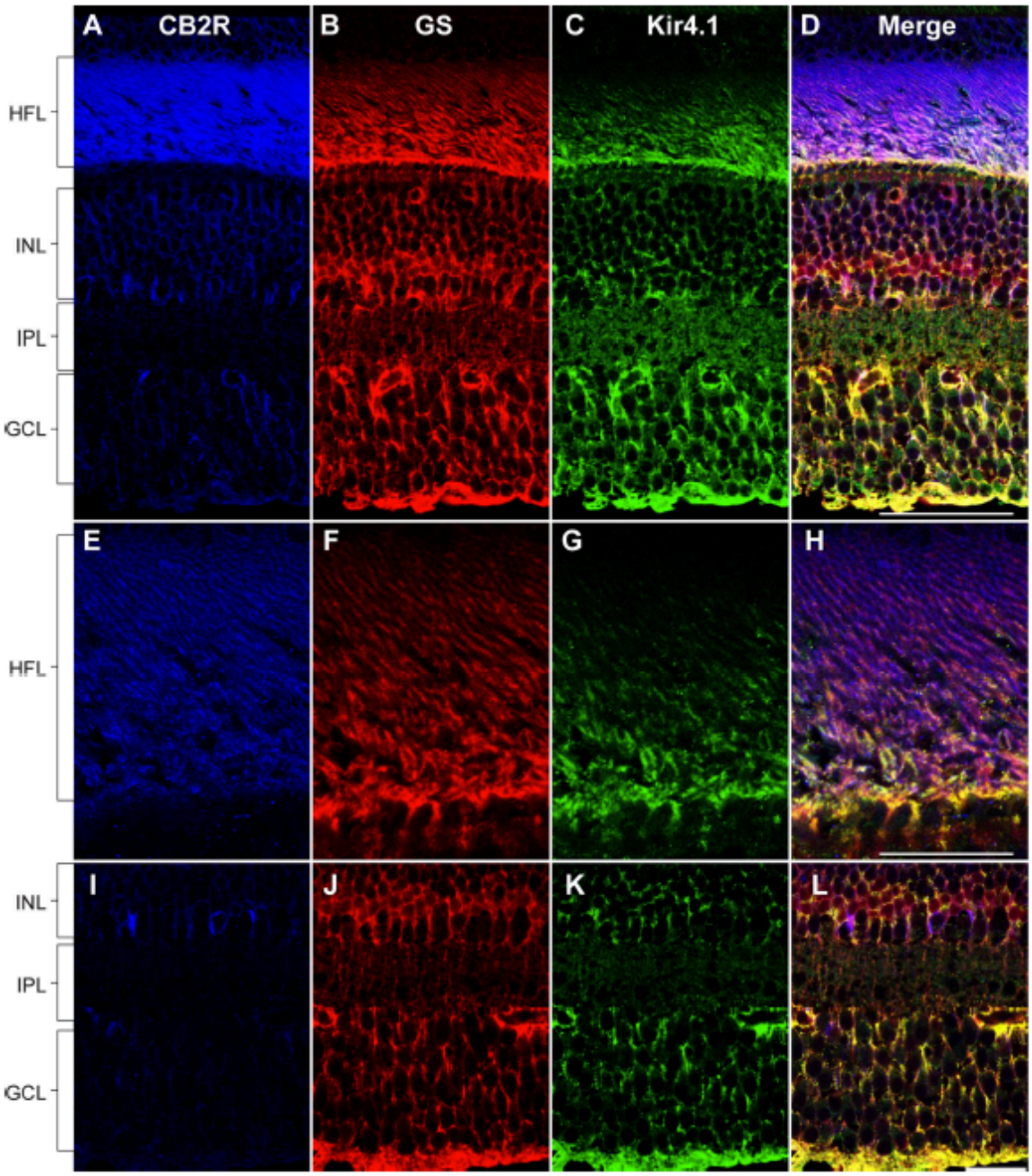

Figure 2-11 Triple immunofluorescent labeling of CB2R, glutamine synthetase (GS), and the potassium ion channel Kir4.1 in the monkey central retina. Each protein is presented alone in gray scale in the first columns. The merge image is presented in the last column (CB2R in blue, GS in red, and Kir4.1 in green). A-D: Low magnification images showing Kir4.1 and CB2R expression in GS positive Müller cells. E-H: High magnification images of Kir4.1, CB2R, and GS immunoreactivity in the distal retina showing co-localization of CB2R and Kir4.1 in Müller cell fibers of the Henle fiber layer. I-L: High magnification images of Kir4.1 expression in the proximal retina. HFL, Henle fiber layer; INL, inner nuclear layer; IPL, inner plexiform layer; GCL, ganglion cell layer. Scale bar = 75 µm for A-D and 30 µm for E-L.

Discussion

This study reports the presence of cannabinoid CB2 receptor (CB2R) in Müller cells of the vervet monkey retina. These findings are important because, although the presence of CB1R in the monkey retina is well established (Straiker et al., 1999; Bouskila et al., 2012), we are still far from identifying the exact role of eCB signaling in the monkey retina. Furthermore, CB2R has been previously ascribed a critical role in CNS glial function (Cabral et al., 2008) and its visual function remains elusive. Our aim was to characterize further the retinal localization of cannabinoid receptors, especially by comparing CB2R expression profile with CB1R localization. We demonstrate here that CB2R is present in the retina of the vervet monkey and specifically in retinal Müller cells. These data, in agreement with CB2R glial expression in the CNS, suggest that the CB2 receptor plays a role in retinal functions.

There are 3 types of glial cells in the primate retina: Müller cells, astrocytes and microglia. Müller cells are the principal glial cells of the retina and are radially oriented across the thickness of the retina, analogous to CB2R expression profile in the distal retina. Their processes extend from the outer limiting membrane to the inner limiting membrane. Given that the expression of the CB2R followed the same pattern, with a higher polarization towards the outer retina, we suggest that CB2R is localized in these glial cells, verified by the co-localization of CB2R-IR with GS-IR. Müller cell processes surround neuronal cell bodies in the nuclear layers and envelop groups of neural processes in the plexiform layers. A 3D visualization was therefore needed in order to determine whether or not CB2R-IR was present in neurons. The outer limiting membrane, which represents the outer border of CB2R expression, is composed of junctions among Müller cells, and photoreceptor cells. However,

CB2R-IR was not detected in the apical villi of Müller cells that extend distally from the OLM. The inner limiting membrane, formed by the conical endfeet of Müller cells, appeared devoid of CB2R-IR. Müller cells also form endfeet on the large retinal blood vessels at the inner surface of the retina. Given the apparent absence of CB2R-IR in the most proximal retina, CB2R may not have a role in the regulation of inner retinal blood vessels.

The presence of CB2R in Müller cells and CB1R in the retinal neuronal cells, points towards a complementary relationship between neurons and glia regarding eCB function. CB2R in Müller cells could protect neurons from exposure to excess neurotransmitters such as L-glutamate (Placzek et al., 2008). Generally, CB2R activation leads to sequences of activities of a protective nature (Pacher and Mechoulam, 2011 for review). Stimulation of CB2R increases microglial cell proliferation (Carrier et al., 2004) and reduces the release of harmful factors, including tumor necrosis factor (TNF) and free radicals (Eljaschewitsch et al., 2006; Ramírez et al., 2005; See Stella, 2009 for review). In fact, exposure to eCBs in activated primary human Müller glia inhibited the production of several proinflammatory cytokines (Krishnan and Chatterjee, 2012). CB2R in Müller cells might therefore be an important player in inflammation, neurotoxicity and neuroprotection. The localization of CB1R in the photoreceptor layer already suggested that the transduction of light (Yazulla, 2008) occurring at this stage could also be modulated by the CB2R expressed in distal Müller cells fibers. Perhaps, the whole eCB system participates in the modulation of light transduction, where CB1R is neuronal and CB2R glial. The expression of CB1R in bipolar cells, shown by double-labeling with CHX10 and PKC retinal cell type markers, suggested that the eCB system acts as an autoregulation system that modulates the signal received by the photoreceptors in order

to transmit it to ganglion cells (Yazulla et al., 1999; Yazulla, 2008; Bouskila et al., 2012). Similarly, this could also occur in horizontal and amacrine cells that show little expression of CB1R (Bouskila et al., 2012). Finally, it is possible that the results of Lu et al. (2000) who demonstrated the expression of CB2R in the ganglion cell layer of the adult rat retina using *in situ* hybridization and RT-PCR did include CB2R-immunoreactive Müller cell processes. In agreement with the latter study, using immunohistochemistry and cell morphology, López et al. (2011) suggested that CB2R was localized in photoreceptors, horizontal cells, amacrine cells and cells localized in the GCL of the adult rat retina. These studies differ with ours not only regarding the animal model (rat versus monkey) but the choice of the antibody used. While we used an antibody targeted against the 20-33 amino acids of the human CB2R, López et al., (2011) used an antibody against residues 326–342 of the rat CB2R. Moreover, double-labeling of CB2R with a retinal cell marker was not performed and given that Müller cells envelop the cell bodies in the GCL it could be CB2R positive cells. In addition, CB1R-IR in the Henle fiber layer and ganglion cell layer of the monkey retina has the most prominent staining found throughout the retinal layers (Bouskila et al., 2012), as opposed to only the Henle fiber layer that has the highest CB2R signal. Recently, Krishnan and Chatterjee (2012) showed that CB2R protein was expressed in homogenates of 12-18 days *ex vivo* retinal explants and 18 days *in vitro* primary Müller glia from human retina by Western blotting. We provide here direct evidence for the *in vivo* expression pattern of CB2R in monkey Müller cells by immunohistochemistry.

Hypothetical functional consequences

Activation of photoreceptors by light evokes an increase of K^+ ions in the retinal extracellular space (Newman and Reichenbach, 1996). In order to maintain an electrolytic balance, Müller cell inwardly rectifying K^+ channels (K_{IR}) release the excess K^+ ions into the vitreous. This spatial buffering mechanism is termed K^+ siphoning (Newman et al., 1984). Immunoreactivity to the $K_{IR}4.1$ channel in rat retina was densely distributed around photoreceptor cells in ONL, where the distal ends of Müller cells surround PR cells, and in a scattered manner around ganglion cells in GCL in rat retina (Ishii et al., 1997). Interestingly, $K_{IR}4.1$-IR as reported by Ishii et al., (1997) for the rodent retina is similar to CB2R expression found in Müller cells in the present study in the monkey central retina (Figure 2-11). The cellular origin of the b-wave component of the ERG is attributed to an interaction between ON-bipolar cells and Müller cells (Stockton and Slaughter, 1989; Wen and Oakley, 1990). The b-wave of the ERG reflects the K^+ mediated spatial buffering currents of Müller cells (Miller and Dowling, 1970; Kline et al., 1985). Moreover, blocking K^+ channels in Müller cells reduces the ERG b-wave (Wen and Oakley, 1990). Given that activation of CB2R leads to a reduction of cAMP and PKA levels due to coupling via $G_{i/o}$ (Howlett et al., 2002 for review Bolognini et al., 2010) and that PKA increases the activity of $K_{IR}4.1$ channels in Müller cells (MacGregor et al., 1998), it is reasonable to propose that CB2R plays a role in the generation of the b-wave. CB2R could act therefore as a negative modulator of K^+ channels. Conversely, blocking CB2R activates K^+ channels (because of the constitutive activity of CB2R) that in turn produce a constant influx of K^+ ions into the Müller cell and an enlarged b-wave (Figure 2-10B). Further experiments are however still needed in order to verify this retinal CB2R putative function.

Other acknowledgments

We thank Sophie Charron and Florence Dotigny for excellent technical assistance. We are grateful to

References

Argaw A, Duff G, Cherif H, Cécyre B, Tea N, and Bouchard J-F. 2011. Cannabinoid receptor CB2 modulates axon guidance. Abstract #B045, 8th IBRO World Congress on Neuroscience, Firenze, Italy.

Atwood BK, Mackie K. 2010. CB2: a cannabinoid receptor with an identity crisis. Br J Pharmacol 160(3):467-479.

Barnstable CJ, Hofstein R, Akagawa K. 1985. A marker of early amacrine cell development in rat retina. Brain Res 352(2):286-290.

Bolognini D, Costa B, Maione S, Comelli F, Marini P, Di Marzo V, Parolaro D, Ross RA, Gauson LA, Cascio MG, Pertwee RG. 2010. The plant cannabinoid Delta9-tetrahydrocannabivarin can decrease signs of inflammation and inflammatory pain in mice. Br J Pharmacol 160(3):677-687.

Bordt A, Hoshi H, Yamada E, Perryman Stout W, Marshak D. 2006. Synaptic input to OFF parasol ganglion cells in macaque retina. J Comp Neurol 498(1):46-57.

Bouskila J, Burke MW, Zabouri N, Casanova C, Ptito M, Bouchard JF. 2012. Expression and localization of the cannabinoid receptor type 1 and the enzyme fatty acid amide hydrolase in the retina of vervet monkeys. Neuroscience 202(0):117-130.

Brandon C. 1985. Improved immunocytochemical staining through the use of Fab fragments of primary antibody, Fab-specific second antibody, and Fab-horseradish peroxidase. The journal of histochemistry and cytochemistry 33(7):715-719.

Buckley NE, Hansson S, Harta G, Mezey E. 1998. Expression of the CB1 and CB2 receptor messenger RNAs during embryonic development in the rat. Neuroscience 82(4):1131-1149.

Burke M, Zangenehpour S, Bouskila J, Boire D, Ptito M. 2009. The gateway to the brain: dissecting the primate eye. J Vis Exp(27):e1261.

Cabral GA, Raborn ES, Griffin L, Dennis J, Marciano-Cabral F. 2008. CB2 receptors in the brain: role in central immune function. Br J Pharmacol 153(2):240-251.

Carrier EJ, Kearn CS, Barkmeier AJ, Breese NM, Yang W, Nithipatikom K, Pfister SL, Campbell WB, Hillard CJ. 2004. Cultured rat microglial cells synthesize the endocannabinoid 2-arachidonylglycerol, which increases proliferation via a CB2 receptor-dependent mechanism. Molecular Pharmacology 65(4):999-1007.

Chang ML, Wu CH, Jiang-Shieh YF, Shieh JY, Wen CY. 2007. Reactive changes of retinal astrocytes and Müller glial cells in kainate-induced neuroexcitotoxicity. J Anat 210(1):54-65.

Chen J, Matias I, Dinh T, Lu T, Venezia S, Nieves A, Woodward DF, Di Marzo V. 2005. Finding of endocannabinoids in human eye tissues: implications for glaucoma. Biochem Biophys Res Commun 330(4):1062-1067.

Chiquet C, Dkhissi-Benyahya O, Chounlamountri N, Szel A, Degrip WJ, Cooper HM. 2002. Characterization of calbindin-positive cones in primates. Neuroscience 115(4):1323-1333.

Cravatt BF, Giang DK, Mayfield SP, Boger DL, Lerner RA, Gilula NB. 1996. Molecular characterization of an enzyme that degrades neuromodulatory fatty-acid amides. Nature 384:83–87.

Cuenca N, Herrero MT, Angulo A, de Juan E, Martínez-Navarrete GC, López S, Barcia C, Martín-Nieto J. 2005. Morphological impairments in retinal neurons of the scotopic

visual pathway in a monkey model of Parkinson's disease. J Comp Neurol 493(2):261-273.

Devane WA, Hanus L, Breuer A, Pertwee RG, Stevenson LA, Griffin G, Gibson D, Mandelbaum A, Etinger A, Mechoulam R. 1992. Isolation and structure of a brain constituent that binds to the cannabinoid receptor. Science 258(5090):1946-1949.

Di Marzo V, Bisogno T, De Petrocellis L. 2007. Endocannabinoids and related compounds: walking back and forth between plant natural products and animal physiology. Chemistry & Biology 14(7):741-756.

Dinh TP, Carpenter D, Leslie FM, Freund TF, Katona I, Sensi SL, Kathuria S, Piomelli D. 2002. Brain monoglyceride lipase participating in endocannabinoid inactivation. Proc Natl Acad Sci U S A 99:10819–10824.

Distler C, Dreher Z. 1996. Glia cells of the monkey retina—II. Müller cells. Vision Research 36(16):2381-2394.

Eljaschewitsch E, Witting A, Mawrin C, Lee T, Schmidt P, Wolf S, Hoertnagl H, Raine C, Schneider Stock R, Nitsch R, Ullrich O. 2006. The endocannabinoid anandamide protects neurons during CNS inflammation by induction of MKP-1 in microglial cells. Neuron 49(1):67-79.

Ellert-Miklaszewska A, Grajkowska W, Gabrusiewicz K, Kaminska B, Konarska L. 2007. Distinctive pattern of cannabinoid receptor type II (CB2) expression in adult and pediatric brain tumors. Brain Research 1137(0):161-169.

Fischer AJ, Hendrickson A, Reh TA. 2001. Immunocytochemical characterization of cysts in the peripheral retina and pars plana of the adult primate. Invest Ophthalmol Vis Sci 42(13):3256-3263.

Galiègue S, Mary S, Marchand J, Dussossoy D, Carrière D, Carayon P, Bouaboula M, Shire D, Le Fur G, Casellas P. 1995. Expression of central and peripheral cannabinoid receptors in human immune tissues and leukocyte subpopulations. European Journal of Biochemistry 232(1):54-61.

Galve Roperh I, Aguado T, Palazuelos J, Guzmán M. 2008. Mechanisms of control of neuron survival by the endocannabinoid system. Current pharmaceutical design 14(23):2279-2288.

Griffin G, Tao Q, Abood ME. 2000. Cloning and pharmacological characterization of the rat CB(2) cannabinoid receptor. J Pharmacol Exp Ther 292(3):886-894.

Howlett AC, Barth F, Bonner TI, Cabral G, Casellas P, Devane WA, Felder CC, Herkenham M, Mackie K, Martin BR, Mechoulam R, Pertwee RG. 2002. International Union of Pharmacology. XXVII. Classification of cannabinoid receptors. Pharmacol Rev 54(2):161-202.

Inoue A, Obata K, Akagawa K. 1992. Cloning and sequence analysis of cDNA for a neuronal cell membrane antigen, HPC-1. J Biol Chem 267(15):10613-10619.

Ishii M, Horio Y, Tada Y, Hibino H, Inanobe A, Ito M, Yamada M, Gotow T, Uchiyama Y, Kurachi Y. 1997. Expression and clustered distribution of an inwardly rectifying potassium channel, KAB-2/Kir4.1, on mammalian retinal Müller cell membrane: their regulation by insulin and laminin signals. J Neurosci 17(20):7725-7735.

Kline RP, Ripps H, Dowling JE. 1985. Light-induced potassium fluxes in the skate retina. Neuroscience 14(1):225-235.

Kolb H, Zhang L, Dekorver L, Cuenca N. 2002. A new look at calretinin-immunoreactive amacrine cell types in the monkey retina. J Comp Neurol 453(2):168-184.

Kozak KR, Rowlinson SW, Marnett LJ. 2000. Oxygenation of the endocannabinoid, 2-arachidonylglycerol, to glyceryl prostaglandins by cyclooxygenase-2. J Biol Chem 275:33744–33749.

Krishnan G, Chatterjee N. 2012. Endocannabinoids alleviate proinflammatory conditions by modulating innate immune response in Müller glia during inflammation. Glia 60(11):1629-1645.

Li L, Head V, Timpe LC. 2001. Identification of an inward rectifier potassium channel gene expressed in mouse cortical astrocytes. Glia 33(1):57-71.

López EM, Tagliaferro P, Onaivi ES, López-Costa JJ. 2011. Distribution of CB2 cannabinoid receptor in adult rat retina. Synapse 65(5):388-392.

Lu Q, Straiker A, Maguire G. 2000. Expression of CB2 cannabinoid receptor mRNA in adult rat retina. Vis Neurosci 17(1):91-95.

MacGregor GG, Xu JZ, McNicholas CM, Giebisch G, Hebert SC. 1998. Partially active channels produced by PKA site mutation of the cloned renal K+ channel, ROMK2 (kir1.2). Am J Physiol 275(3 Pt 2):F415-422.

Mackie K. 2008. Cannabinoid receptors: where they are and what they do. J Neuroendocrinol 20 Suppl 1:10-14.

Martínez-Navarrete GC, Angulo A, Martín-Nieto J, Cuenca N. 2008. Gradual morphogenesis of retinal neurons in the peripheral retinal margin of adult monkeys and humans. J Comp Neurol 511(4):557-580.

Martínez-Navarrete GC, Martín-Nieto J, Esteve-Rudd J, Angulo A, Cuenca N. 2007. Alpha synuclein gene expression profile in the retina of vertebrates. Mol Vis 13:949-961.

McPartland JM, Norris RW, Kilpatrick CW. 2007. Coevolution between cannabinoid receptors and endocannabinoid ligands. Gene 397(1-2):126-135.

Mechoulam R, Ben Shabat S, Hanus L, Ligumsky M, Kaminski NE, Schatz AR, Gopher A, Almog S, Martin BR, Compton DR. 1995. Identification of an endogenous 2-monoglyceride, present in canine gut, that binds to cannabinoid receptors. Biochemical pharmacology 50(1):83-90.

Miller RF, Dowling JE. 1970. Intracellular responses of the Müller (glial) cells of mudpuppy retina: their relation to b-wave of the electroretinogram. J Neurophysiol 33(3):323-341.

Mills SL, Massey SC. 1999. AII amacrine cells limit scotopic acuity in central macaque retina: a confocal analysis of calretinin labeling. J Comp Neurol 411(1):19-34.

Mukherjee S, Adams M, Whiteaker K, Daza A, Kage K, Cassar S, Meyer M, Yao BB. 2004. Species comparison and pharmacological characterization of rat and human CB2 cannabinoid receptors. Eur J Pharmacol 505(1-3):1-9.

Munro S, Thomas KL, Abu-Shaar M. 1993. Molecular characterization of a peripheral receptor for cannabinoids. Nature 365(6441):61-65.

Nadal-Nicolás FM, Jiménez-López M, Sobrado-Calvo P, Nieto-López L, Cánovas-Martínez I, Salinas-Navarro M, Vidal-Sanz M, Agudo M. 2009. Brn3a as a marker of retinal ganglion cells: qualitative and quantitative time course studies in naïve and optic nerve–injured retinas. Investigative Ophthalmology & Visual Science 50(8):3860-3868.

Nag TC, Wadhwa S. 2001. Differential expression of syntaxin-1 and synaptophysin in the developing and adult human retina. J Biosci 26(2):179-191.

Newman E, Reichenbach A. 1996. The Müller cell: a functional element of the retina. Trends Neurosci 19(8):307-312.

Newman EA, Frambach DA, Odette LL. 1984. Control of extracellular potassium levels by retinal glial cell K+ siphoning. Science 225(4667):1174-1175.

Nishikawa S, Tamai M. 2001. Müller cells in the human foveal region. Curr Eye Res 22(1):34-41.

Onaivi E, Ishiguro H, Gu S, Liu Q-R. 2012. CNS effects of CB2 cannabinoid receptors: beyond neuro-immuno-cannabinoid activity. Journal of psychopharmacology 26(1):92-103.

Pacher P, Mechoulam R. 2011. Is lipid signaling through cannabinoid 2 receptors part of a protective system? Progress in lipid research 50(2):193-211.

Piomelli D. 2003. The molecular logic of endocannabinoid signalling. Nat Rev Neurosci 4(11):873-884.

Placzek EA, Okamoto Y, Ueda N, Barker EL. 2008. Mechanisms for recycling and biosynthesis of endogenous cannabinoids anandamide and 2-arachidonylglycerol. J Neurochem 107(4):987-1000.

Porcella A, Casellas P, Gessa GL, Pani L. 1998. Cannabinoid receptor CB1 mRNA is highly expressed in the rat ciliary body: implications for the antiglaucoma properties of marihuana. Molecular Brain Research 58(1-2):240-245.

Porcella A, Maxia C, Gessa GL, Pani L. 2000. The human eye expresses high levels of CB1 cannabinoid receptor mRNA and protein. European journal of neuroscience 12(3):1123-1127.

Qi H-X, Gharbawie OA, Wong P, Kaas JH. 2011. Cell-poor septa separate representations of digits in the ventroposterior nucleus of the thalamus in monkeys and prosimian galagos. J Comp Neurol 519(4):738-758.

Ramírez BG, Blázquez C, del Pulgar TG, Guzmán M, de Ceballos ML. 2005. Prevention of Alzheimer's disease pathology by cannabinoids: neuroprotection mediated by blockade of microglial activation. J Neurosci 25(8):1904-1913.

Riepe RE, Norenburg MD. 1977. Müller cell localisation of glutamine synthetase in rat retina. Nature 268(5621):654-655.

Röhrenbeck J, Wässle H, Heizmann CW. 1987. Immunocytochemical labelling of horizontal cells in mammalian retina using antibodies against calcium-binding proteins. Neurosci Lett 77(3):255-260.

Shire D, Calandra B, Rinaldi-Carmona M, Oustric D, Pessègue B, Bonnin-Cabanne O, Le Fur G, Caput D, Ferrara P. 1996. Molecular cloning, expression and function of the murine CB2 peripheral cannabinoid receptor. Biochim Biophys Acta 1307(2):132-136.

Stella N. 2009. Endocannabinoid signaling in microglial cells. Neuropharmacology 56 Suppl 1:244-253.

Stockton RA, Slaughter MM. 1989. B-wave of the electroretinogram. A reflection of ON bipolar cell activity. J Gen Physiol 93(1):101-122.

Straiker A, Stella N, Piomelli D, Mackie K, Karten HJ, Maguire G. 1999. Cannabinoid CB1 receptors and ligands in vertebrate retina: localization and function of an endogenous signaling system. Proc Natl Acad Sci U S A 96(25):14565-14570.

Sugiura T, Kondo S, Sukagawa A, Nakane S, Shinoda A, Itoh K, Yamashita A, Waku K. 1995. 2-Arachidonoylglycerol: a possible endogenous cannabinoid receptor ligand in brain. Biochemical and biophysical research communications 215(1):89-97.

Wässle H, Dacey DM, Haun T, Haverkamp S, Grunert U, Boycott BB. 2000. The mosaic of horizontal cells in the macaque monkey retina: with a comment on biplexiform ganglion cells. Vis Neurosci 17(4):591-608.

Wei Y, Wang X, Wang L. 2009. Presence and regulation of cannabinoid receptors in human retinal pigment epithelial cells. Molecular vision 15:1243-1251.

Wen R, Oakley B, 2nd. 1990. K(+)-evoked Müller cell depolarization generates b-wave of electroretinogram in toad retina. Proc Natl Acad Sci U S A 87(6):2117-2121.

Xiang M, Zhou L, Macke JP, Yoshioka T, Hendry SH, Eddy RL, Shows TB, Nathans J. 1995. The Brn-3 family of POU-domain factors: primary structure, binding specificity, and expression in subsets of retinal ganglion cells and somatosensory neurons. J Neurosci 15(7 Pt 1):4762-4785.

Yazulla S. 2008. Endocannabinoids in the retina: from marijuana to neuroprotection. Prog Retin Eye Res 27(5):501-526.

Yazulla S, Studholme KM, McIntosh HH, Deutsch DG. 1999. Immunocytochemical localization of cannabinoid CB1 receptor and fatty acid amide hydrolase in rat retina. J Comp Neurol 415(1):80-90.

Zabouri N, Bouchard JF, Casanova C. 2011a. Cannabinoid receptor type 1 expression during postnatal development of the rat retina. J Comp Neurol 519(7):1258-1280.

Zabouri N, Ptito M, Casanova C, Bouchard JF. 2011b. Fatty acid amide hydrolase expression during retinal postnatal development in rats. Neuroscience 195:145-165.

Zhong L, Geng L, Njie Y, Feng W, Song Z-H. 2005. CB2 cannabinoid receptors in trabecular meshwork cells mediate JWH015-induced enhancement of aqueous humor outflow facility. Investigative Ophthalmology & Visual Science 46(6):1988-1992.

Zurolo E, Iyer AM, Spliet WGM, Van Rijen PC, Troost D, Gorter JA, Aronica E. 2010. CB1 and CB2 cannabinoid receptor expression during development and in epileptogenic developmental pathologies. Neuroscience 170(1):28-41.

Chapter 3: The endocannabinoid system is differently expressed in the retina of mice, tree shrews and monkeys

Under review in Frontier in Neuroanatomy (December 2014)

The endocannabinoid system is differently expressed in the retina of mice, tree shrews and monkeys

Pasha Javadi[1], Joseph Bouskila[1, 2], Laurent Elkrief[1, 3], Christian Casanova[1], Jean-François Bouchard[1] and Maurice Ptito[1, 4, 5]

[1]School of Optometry, University of Montreal, Montreal, QC, Canada
[2]Biomedical Sciences, Faculty of Medicine, University of Montreal, Montreal, QC, Canada
[3]Faculty of Science, McGill University, Montreal, QC, Canada
[4]BRAINlab, Department of Neuroscience and Pharmacology, University of Copenhagen, Copenhagen, Denmark
[5]Laboratory of Neuropsychiatry, Psychiatric Centre Copenhagen and Department of Neuroscience and Pharmacology, University of Copenhagen, DK-2100 Copenhagen, Denmark

Abbreviated title: The retinal endocannabinoid system in mammals

Keywords: CB1, CB2, endocannabinoids, mammals, retina, comparative

Correspondence should be addressed to:
Maurice Ptito, PhD
School of Optometry, room 260-7
3744 Jean-Brillant Street,
University of Montreal,
Montreal, Quebec, Canada, H3T 1P1

Abstract

The endocannabinoid (eCB) system comprises the cannabinoid receptors, the endogenous cannabinoid ligands (eCBs), and the enzymes regulating the levels of eCBs. This system is widely expressed in various parts of the central nervous system, including the retina. The localization of the key eCB receptors, particularly CB1R and CB2R, has been recently reported in rodent and primate retinas with striking interspecies differences. However, little is known about the enzymes involved in the synthesis and degradation of these eCBs. We therefore examined the expression and localization of the main components of the eCB system in the retina of three vertebrates: mice, tree shrews and monkeys. We found that the CB1R and FAAH distributions are well preserved among these species. The NAPE-PLD expression in monkeys is however circumscribed to the photoreceptor layer, unlike mice and tree shrews. In contrast, the CB2R expression is variable across these species; in mice, CB2R is found in the retinal neurons; in tree shrews, it is expressed in the Müller cell processes of the outer retina and in the retinal neurons of the inner retina. In monkeys, CB2R is restricted to the Müller cells that span the entire retinal thickness. The expression patterns of MAGL and DAGLα are juxtaposed in the inner retinal layers. Overall, these results provide the evidence that the eCB system is differently expressed in the retina of these mammals and suggest a distinctive role of endocannabinoids in visual processing.

Introduction

Marijuana contains over 70 cannabinoids that mimic the endogenous ligands called endocannabinoids (eCBs) and cause global psychoactive and physiological effects. The eCB system is mainly made up of the G-protein-coupled receptors CB1 and CB2 (CB1R and CB2R) and the eCBs anandamide (AEA) and 2-arachidonoyl glycerol (2-AG). It also contains the enzymes of synthesis: N-acyl phosphatidylethanolamine-specific phospholipase D (NAPE-PLD) and diacylglycerol lipase a (DAGLα); the degradation enzymes: fatty acid amide hydrolase (FAAH) and monoacylglycerol lipase (MAGL) that regulate the levels of the eCBs. The cannabinoid receptors are found in many mammals, as well as in various classes of vertebrates and invertebrates, in all major subdivisions of bilaterians, urochordates and cephalochordates, but not in the nonchordate invertebrate phyla like insects (McPartland et al., 2006a; McPartland et al., 2007; Cottone et al., 2013). The cannabinoid receptors may have evolved in the last common ancestor of the bilaterians with a secondary loss in the insects and other clades (McPartland et al., 2006a). The enzymes responsible for the biosynthesis and the degradation of the eCBs are present throughout the animal kingdom (McPartland et al., 2006b; Elphick, 2012). For example, in the rat hippocampus, cerebellum and amygdala, the distribution of the cytosolic enzyme MAGL is nearly complementary to the FAAH, with a presynaptic localization similar to DAGLα rather than postsynaptic (Dinh et al., 2002). The eCB system appears widely distributed in the central nervous system and points to a fundamental modulatory role of the eCBs in the control of many central and peripheral biological functions (Di Marzo, 2009). A number of specific roles have been ascribed to the eCB system in biological functions, such as neuroprotection, neurogenesis, axon guidance,

synaptic plasticity, nociception, motor activity, and memory (Harkany et al., 2007; Harkany et al., 2008; Argaw et al., 2011; Duff et al., 2013; Xu and Chen, 2014). Disturbances of normal eCB activity may therefore be associated with various brain disorders (Russo, 2008; Bluett et al., 2014; McPartland et al., 2014; Smith and Wagner, 2014).

The eCB system is also found in the retina of various mammalian species (Yazulla, 2008) albeit noticeable differences in its anatomical organization. Compared to rodents, the retina of tree shrews is more similar to primates (Fan et al., 2013). Mice have a rod-dominated retina that is specialized for scotopic conditions (Jeon et al., 1998) with a low visual resolution (Prusky and Douglas, 2004). Mouse and tree shrew retinas have no fovea compared to primates. However, tree shrews have a well-developed binocular visual system, with a cone-dominated retina (Muller and Peichl, 1993). Interestingly, the highest density of both cones and rods are in the inferior retina, not in the central area (Muller and Peichl, 1989). Monkeys, on the other hand, have a fovea with a high cone density that decreases with eccentricity (Herbin et al., 1997). Comparative studies on the organization of the retina of different animal species led to the conclusion that ancestral mammals may have already developed cone photopigments (Jacobs, 2008). These cone pigments are still present in many contemporary representatives from four of the major vertebrate groups (fishes, birds, amphibians, and reptiles); thus, many vertebrates maintained the capacity for elaborate color vision over their histories (Imamoto and Shichida, 2014).

Concerning the retina, the expression of the cannabinoid receptors is well preserved in many species including mice, rats, chicks, larval tiger salamanders, goldfish, and rhesus monkeys (Straiker et al., 1999). CB1R and CB2R are present in various retinal cell types

(cones, bipolar, ganglion, horizontal, and amacrine cells) with however some differences (Yazulla, 2008; Zabouri et al., 2011a; Zabouri et al., 2011b; Bouskila et al., 2012; Bouskila et al., 2013; Cécyre et al., 2014a). For example, CB2R is expressed throughout the mouse retina (Cécyre et al., 2014a) but it is present exclusively in the Müller cells of the vervet monkey (Bouskila et al., 2013). While DAGLα is widely distributed throughout the IPL in the mouse retina, MAGL is only present in rod spherules, cone pedicles in OPL, but also the IPL (Hu et al., 2010). Both MAGL and DAGLα have been found in an overlapping pattern with CB1R and CB2R in the rat retina. In rats, DAGLα is expressed from the early stages of development in photoreceptors, horizontal, amacrine, and ganglion cells and MAGL later during development mainly in amacrine and Müller cells. (Cécyre et al., 2014b). The expression and distribution of the major components of the eCB system, notably the metabolizing enzymes (NAPE-PLD, DAGLα, FAAH, MAGL), in the retina of different mammals have not been studied in depth. It is therefore our aim to analyze the expression of several components of the endocannabinoid system and to characterize their distribution pattern in the distinct retinal layers and cell types of three different mammalian species: mice, tree shrews and monkeys (vervets and macaques).

Materials and Methods

Biological material. Eyes from three adult mice (C57BL/6), two tree shrews (*Tupaia belangeri*), three vervet monkeys (*Chlorocebus sabeus*), and two rhesus monkeys (*Macaca mulatta*) were used in this study. The animals were part of ongoing research projects that were approved by the University of Montreal and McGill University Animal Care and Use Committees. For all species, anterior segment of the eye and vitreous were cut away. The eyecups were bathed in 4% paraformaldehyde made in 0.1 M sodium phosphate buffer at pH 7.4. After the fixation, the eyecups were kept in a 30% sucrose solution in the phosphate buffer for at least two days before being frozen in an OCT embedding medium.

Immunohistochemistry. Single-, double-, and triple-labelings of the retina were performed according to previously published methods (Bouskila et al., 2012; Bouskila et al., 2013a, b). Briefly, the sections were post-fixed for 5 minutes in 70% ethanol, rinsed 3 x 5 minutes in 0.1 M Tris buffer, pH 7.4/0.03% Triton and blocked for 90 minutes in 10% normal goat serum (NDS) in 0.1 M Tris buffer/0.5% Triton. Sections were incubated overnight at room temperature with primary antibodies prepared in blocking solution. The cannabinoid-related antibodies (CB1R, FAAH, NAPE-PLD, CB2R, DAGLα, MAGL) were also used conjointly with a known specific retinal cell type marker such as rhodopsin, calbindin, glutamine synthetase, and Brn3a (Table 1). The next day, sections were washed for 10 minutes and 2 x 5 minutes in 0.1 M Tris /0.03% Triton, blocked in 10% NDS, 0.1 M Tris /0.5% Triton for 60 minutes and incubated with secondary antibody for one hour: Alexa 488 donkey anti-mouse, and biotinylated donkey anti-rabbit followed by the addition of streptavidin-Alexa 647

(1:200), all in a blocking solution as described above. Sections were washed again in Tris buffer, counterstained with bisbenzimide (Hoechst 33258, Sigma, 2.5 μg/mL), a fluorescent nuclear marker, and coverslipped with Fluoromount-G™ Mounting Medium (SouthernBiotech, Birmingham, AL).

Antibody characterization. The source and the working dilution of all primary antibodies used in this study are summarized in Table 3-1.

Brn3a. The mouse monoclonal (IgG1) to Brn3a was acquired from Chemicon and directed against amino acids 186–224 of Brn3a fused to the T7 gene 10 protein. The antibody has no reactivity with Brn3b or Brn3c in Western blots. Its specificity for rodent (Nadal-Nicolás et al., 2009) and monkey (Bouskila et al., 2013) retinal ganglion cells has been already documented. This antibody has been used to label the nuclei of retinal ganglion cells (Bouskila et al., 2012).

Calbindin. The mouse monoclonal (IgG1) to calbindin (CB) was purchased from Sigma (St. Louis, MO) and directed against purified bovine kidney calbindin-D-28K. This antibody produces a 28 kDa band on Western blots (manufacturer's data sheet). The CB antibody labels cones outside the foveal region, cone bipolar cells, and a subset of horizontal cells in human and monkey retinae (Bouskila et al., 2012).

CB1R. The rabbit anti-CB1R was purchased from Calbiochem (Gibbstown, NJ, USA) and was developed by using a highly purified fusion protein with the first 77 amino acid residues of the rat CB1R. According to the manufacturer's data sheet, it recognizes a major band of

60 kDa with also less intense bands of 23, 72, and 180 kDa. This antibody was shown to be specific using *cnr1* knockout mouse retinal tissue (Zabouri et al., 2011). It recognizes the CB1R (60 kDa) from many species, including the vervet monkey tissues (Bouskila et al., 2012).

CB2R. The rabbit anti-CB2R was purchased from Cayman Chemical (Ann Arbor, MI) and was developed by using a synthetic peptide corresponding to the amino acids 20-33 (NPMKDYMILSGPQK) of the human CB2R sequence conjugated to keyhole limpet hemocyanin (KLH) as immunogen. This antibody recognizes a band at 45 kDa and a band at 39-40 kDa (manufacturer's data sheet; 101550). Its specificity to CB2R was validated in *cnr2* knockout mouse (Cécyre et al., 2014) and monkey (Bouskila et al., 2013) retinal tissue.

DAGLα. The goat anti-DAGLα (Diacylglycerol lipase α) antibody was purchased from Novus Biologicals (Littleton, CO, USA) and was developed by using the synthetic peptide corresponding to PAKQDELVISAR of the C-terminus of human DAGLα. This sequence has a 100% identity homology with old world monkeys, 92% with marmoset, and 83% identity with mouse, rat, hamster, and tree shrews.

FAAH. The rabbit anti-FAAH (Fatty acid amide hydrolase) was purchased from Cayman Chemical (Ann Arbor, MI, USA) and developed by using a synthetic peptide corresponding to amino acids 561-579 (ELCLRFMREVEQLMTPQKQPS) of the rat FAAH conjugated to KLH. As expected, it recognizes a dense band at about 66 kDa and a very light one below

37 kDa. The specificity of this antibody has been demonstrated in rat (Suárez et al., 2008; Zabouri et al., 2011) and vervet monkey (Bouskila et al., 2012) tissues.

GS. The mouse monoclonal (IgG2a) to glutamine synthetase (GS) was obtained from Chemicon (Temecula, CA, USA) and directed against the GS purified from sheep brain (manufacturer's data sheet). This antibody generates a single 45 kDa band in immunoblots. This antibody labels Müller cells in the rodent (Elphick and Egertova, 2005; Riepe and Norenburg, 1977) and monkey retinae (Bouskila et al., 2012).

MAGL. The rabbit anti-MAGL (Monoacylglycerol lipase) was obtained from Cayman Chemical (Ann Arbour, MI) and was developed by using a synthetic peptide from amino acids 1-14 (MPEESSPRRTPQSI) of the human MAGL. It has a high identity protein sequence between human, mouse and tree shrews and has a molecular weight of approximately 33 kDa on western blot.

NAPE-PLD. The rabbit anti-NAPE-PLD (N-acyl phosphatidylethanolamine-specific phospholipase D) was obtained from Cayman Chemical (Ann Arbor, MI, USA) and developed by using a synthetic peptide from human NAPE-PLD amino acids 159-172 (YMGPKRFRRSPCTI). Its cross reactivity has been tested in many species, and it recognizes an intense band at 46 kD on a western blot of the human cerebellum (manufacturer's data sheet).

Rhodopsin. The mouse monoclonal (IGg1) anti-rhodopsin (clone Rho 4D2) was purchased from Abcam (Toronto, ON, Canada) and developed by using as immunogen the bovine rhodopsin. This antibody recognizes a 39 kDa band on Western Blots and is predicted to react with human retinal tissues (manufacturer's data sheet). It has been proven effective to specifically label rods in the rodent (Ozawa et al., 2008) and the monkey (Bouskila et al., 2013b) retina.

Protein kinase C. The mouse monoclonal (IgG2a) to protein kinase C (PKC) was obtained from Santa Cruz Biotechnology (Santa Cruz, CA) and developed by using as immunogen purified bovine PKC, and its epitope is mapped to its hinge region (amino acids 296–317). In western blot this antibody gives a single band of 80-kDa on human cell lines and has been previously used in vervet monkeys and rodent (Zabouri et al., 2011; Bouskila et al., 2012).

Table 3- 2 List of antibodies used in this study

Antibody	Immunogen	Source†	Working dilution
Brn3a	Fusion protein containing aa 186–224 of Brn3a protein	Chemicon, Temecula, CA; MAB1585, mouse monoclonal, clone 5A3.2	1:100
CB	Purified bovine kidney calbindin-D28K	Sigma, St. Louis, MO; C9848, mouse monoclonal, clone CB0955	1:250
CB1R	Fusion protein containing aa 1–77 of rat CB1R	Sigma, St. Louis, MO; C1233, rabbit polyclonal	1:150
CB2R	Synthetic peptide corresponding to aa 20–33 of human CB2R	Cayman Chemical, Ann Arbour, MI; 101550, rabbit polyclonal	1:150
DAGLα	Peptide with sequence CPAKQDELVISAR, from the C Terminus of the protein sequence	Novus, Littleton, CO; NBP2-31856, rabbit polyclonal	1:100
FAAH	Synthetic peptide aa 561–579 of rat FAAH	Cayman Chemical, Ann Arbour, MI; 101600, rabbit polyclonal	1:150
GS	Full protein purified from sheep brain	Chemicon, Temecula, CA; MAB302, mouse monoclonal, clone GS-6	1:500
MAGL	Human MAGL aa 1-14	Cayman Chemical, Ann Arbour, MI; 100035, rabbit polyclonal	1:150
NAPE-PLD	Purified protein corresponding to aa 159-172 NAPE-PLD human	Cayman Chemical, Ann Arbour, MI; 10305, rabbit polyclonal	1:200
Rhodopsin	Bovine rhodopsin	Abcam, Toronto, ON; ab98887, mouse monoclonal, clone Rho 4D2	1:500
PKCα	Peptide mapping the aa 296–317 of human PKCα	Santa Cruz Biotechnology, Santa Cruz, CA; sc-8393, mouse monoclonal, clone H-7	1:500

Confocal microscopy. Fluorescence was detected with a Leica TCS SP2 confocal laser-scanning microscope (Leica Microsystems, Exton, PA), using a 40X (n.a.: 1.25 – 0.75) or a 100X (n.a: 1.40 – 0.7) objective. Images were obtained sequentially from the green, blue and far-red channels on optical slices of less than 0.9 µm of thickness. All photomicrograph adjustments, including size, color, brightness, and contrast were done with Adobe Photoshop (CS5, Adobe Systems, San Jose, CA) and then exported to Adobe InDesign (CS5, Adobe Systems, San Jose, CA), where the final figure layout was completed.

Results

Single-label immunocytochemistry

CB1R is present throughout the retina of all three species. A fairly consistent retinal distribution pattern of CB1R across all six retinal layers was observed in mice, tree shrews, vervet and rhesus monkeys, as illustrated in immunolabeled retinal sections (Figure 3-1**A-D**).

FAAH expression is found throughout the retina of all three species. FAAH, like CB1R, is expressed in all five retinal layers and in the photoreceptor layer of the three species (Figure 3-1**E-H**). In mice and tree shrews, there is an increased protein expression in the IPL (see arrow in Figure 3-1**E,F**) compared to primates (Figure 3-1**G,H**). There is a high expression of FAAH in NFL of all species (arrowhead in Figure 3-1**E-H**).

NAPE-PLD distribution is dissimilar between the species. NAPE-PLD is abundantly expressed in the GCL and NFL (arrowheads Figure 3-1**I,J**) of mice and tree shrews, and in lower concentration in the ONL for all three species (Figure 3-1**I-L**). In mice, NAPE-PLD is distributed in all layers, especially the GCL and NFL, except the ONL. In tree shrews, NAPE-PLD is found in all five retinal layers, but mostly in the OPL (arrow in Figure 3-1**J**) and NFL (arrow Figure 3-1**J**). Inversely, in both vervet and macaque monkeys, NAPE-PLD is located in the outer retina, mainly in photoreceptors, ONL and OPL (arrows in Figure 3-1**K-L**).

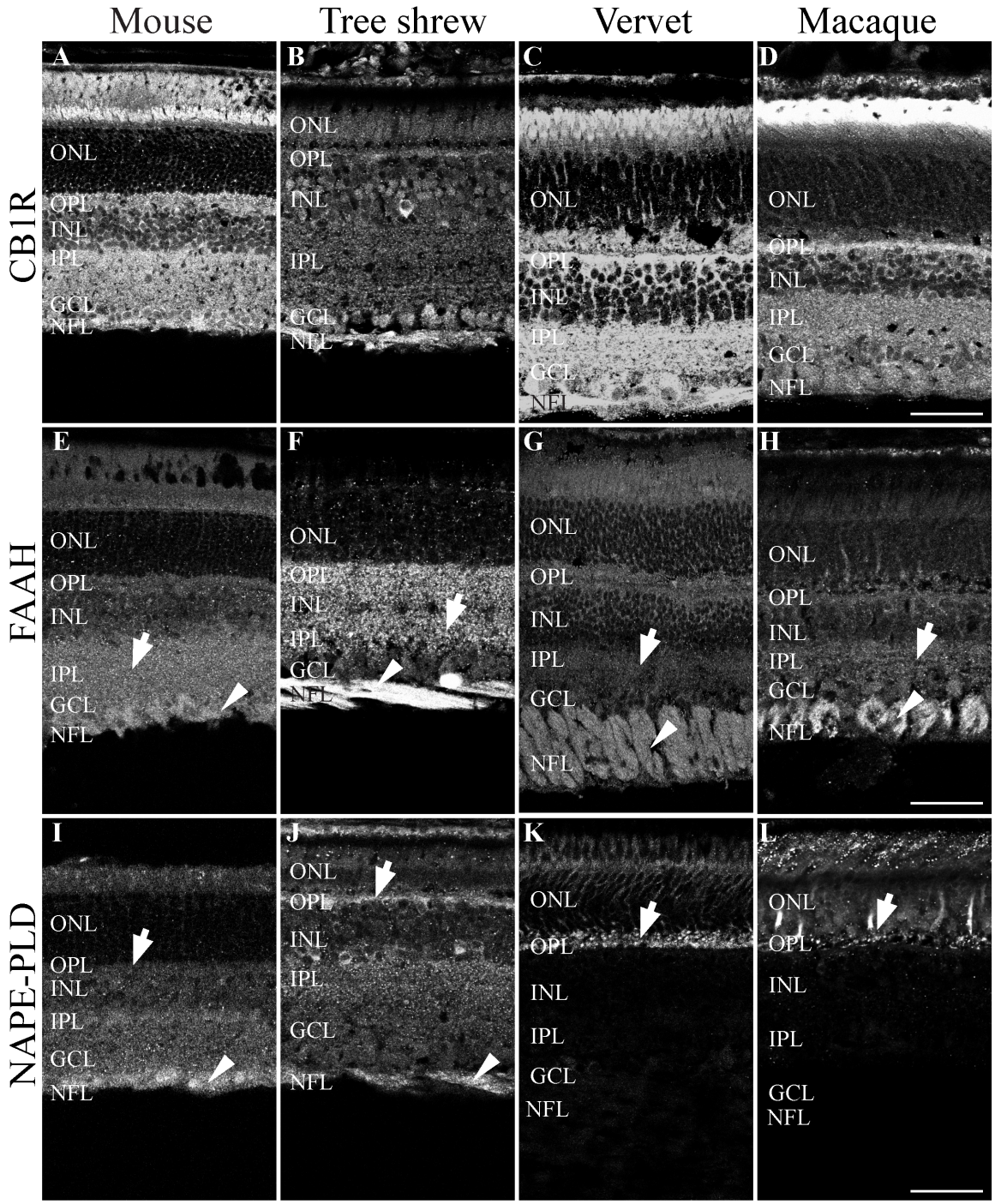

Figure 3- 1 CB1R system immunoreactivity pattern in the retina. Shown are the retinal sections immunolabeled for the CB1R (A-D), FAAH (E-H), and NAPE-PLD (I-L) in mouse, tree shrew, vervet and macaque monkeys. Arrows and arrowheads point out areas of different levels of expression between retinal segments. ONL, outer nuclear layer; OPL, outer plexiform layer; INL, inner nuclear layer; IPL, inner plexiform layer; GCL, ganglion cell layer. Scale bar = 75 µm

CB2R expression is restricted to Müller cells in monkeys. Unlike CB1R, the immunolabeling pattern of CB2R is not consistent in the 3 species. In mice, CB2R is not detectable in ONL and very little in INL but strongly expressed in OPL (arrow Figure 3-2**A)**, IPL, GCL, and NFL (arrowhead Figure 3-2**A**). In tree shrews, CB2R is expressed throughout all five retinal cell layers with more emphasis (contrary to the mouse) in the external layers (ONL and OPL) (arrow Figure 3-2**B)** and INL (arrow Figure 3-2**B**). In both vervets and macaques, CB2R expression is more abundant in ONL (arrows Figure 3-2**C-D**).

Localization of MAGL. In mice, the MAGL is expressed in the OPL, INL, IPL, GCL and NFL with the most prominent staining towards the bottom two layers (Figure 3-2**E**). The two bands that are strongly seen in the IPL of the mouse retina probably represent an accumulation of MAGL in the dendrites and synaptic layers (arrows in Figure 3-2**E**). In tree shrews, MAGL is expressed in all five layers and most strongly in the GCL (arrow) and IPL (arrowhead Figure 3-2**F**). In vervets and macaques, the MAGL is expressed mainly in the OPL (arrows Figure 3-2**G,H**). It is also found in the GCL (arrowheads Figure 3-2**G, H**).

Expression of the DAGLα. In mice, DAGLα is expressed weakly in ONL and OPL (Figure 3-2**I**) but more strongly in IPL (arrowhead in Figure 3-2**I**), GCL and NFL (arrows in Figure 3-2**I**). In tree shrews, the DAGLα is strongly expressed in a band of the upper GCL (arrow in Figure 3-2**J)**. In vervets and macaques, DAGLα is weakly expressed in the ONL, INL and IPL. There is a high expression in the OPL (arrows) and GCL (arrowheads Figure 3-2**K,L**).

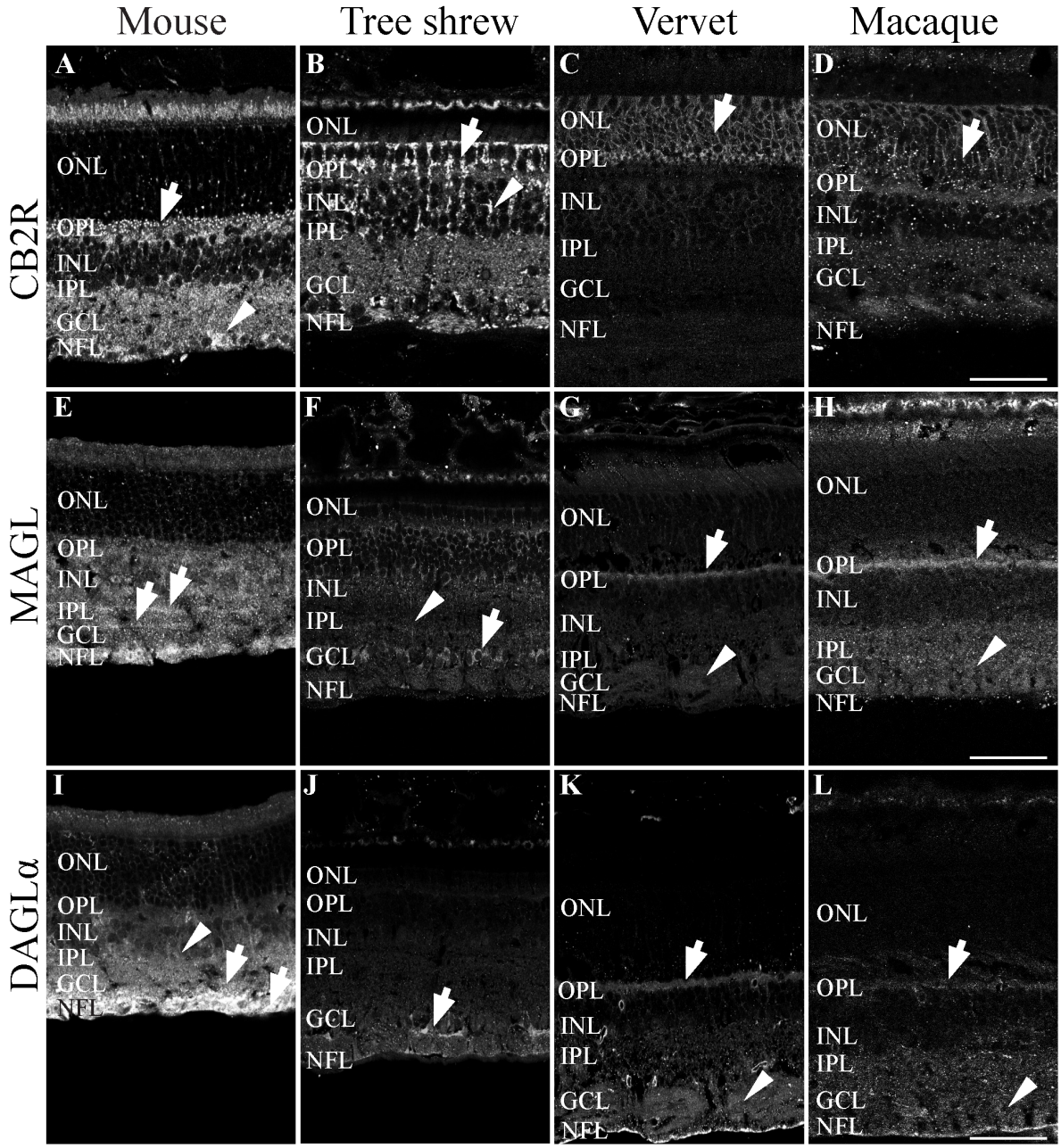

Figure 3- 2 CB2R system immunoreactivity pattern in the retina. The retinal sections immunolabeled for CB2R (A-D**), MAGL (**E-H**), and DAGLα (**I-L**) in mouse, tree shrew, vervet and macaque monkeys. Arrows and arrowheads point out areas of different levels of expression between retinal segments. ONL, outer nuclear layer; OPL, outer plexiform layer; INL, inner nuclear layer; IPL, inner plexiform layer; GCL, ganglion cell layer. Scale bar = 75 µm.**

Double-label immunocytochemistry

CB1R in INL. The PKC labels the rod bipolar cells and a subset of amacrine cells, were colocalized with the CB1R at INL (arrows) and IPL in all the species (arrowheads Figure 3 **A-D**). The cone-dominant retina of the tree shrew has much less rod bipolar cells.

CB2R and Müller cells. To label Müller cells, glutamine synthetase (GS) was used. This antibody has proved to be efficient to label Müller cells in the rat (Riepe and Norenburg, 1977), mouse (Cécyre et al 2013), and monkey retinas (Nishikawa and Tamai, 2001; Bouskila et al., 2012; Bouskila et al., 2013). In mice, the CB2R is weakly expressed in the ONL (arrow Figure 3-3**E**) although intense expression was found in the inner layers. In tree shrews, CB2R and GS were both expressed in the photoreceptor layer and ONL (arrow Figure 3**F**). CB2R is co-localized with GS and on other cases was differentially expressed. In both vervet and macaque monkeys, the CB2R was expressed throughout the photoreceptor layer (arrow Figure 3-3**G-H)** and also is well co-localized with GS in OPL (arrowhead Figure 3-3**G-H**). These results indicate that the expression of CB2R in Müller cells is an exclusive feature of primates.

MAGL and DAGLα. The expression of MAGL and DAGLα were assessed (Figure 3-3 **I-L**). MAGL and DAGLα are complementarily expressed in the inner retinal layers of mice, tree shrews, vervets, and macaques especially in the GCL (arrows in Figure 3-3**I-L**). To label the nuclei of retinal ganglion cells, Brn3a was utilized. MAGL. The colocalization of MAGL with ganglion cells is more apparent in macaque and vervet monkeys (arrows Figure 3-3 **M-P**)

NAPE-PLD, cones and rods. Calbindin (CB) is a marker of cones outside the foveal region, cone bipolar cells, and a subset of horizontal cells (Bouskila et al., 2012; Fischer et al., 2001).

CB is strongly expressed in the mouse OPL alongside with NAPE-PLD, but none of them were present in ONL (Figure 3-3**Q**). In tree shrews, CB is highly co-expressed with NAPE-PLD in the OPL (arrowhead in Figure 3-3R) and ONL (arrow in Figure 3-3**R**). CB is expressed in the ONL of the monkey retina where NAPE-PLD is not very abundant (arrows in Figure 3-3**S-T**) and highly co-expressed in OPL (arrowhead Figure 3-3**S**). The rhodopsin antibody was used to label rods in the retina. In the mouse, NAPE-PLD was not co-expressed with rods (arrow in Figure 3-3**U**). However, in the cone-dominant retina of the tree shrew with only very few rods, NAPE-PLD is slightly co-localized with rods (arrow Figure 3-3**V**). In monkeys, NAPE-PLD is abundantly expressed in rods (arrow in Figure 3-3**W-X**). Interestingly, comparing the two synthesis enzymes, NAPE-PLD and DAGLα in different species, revealed that in mice, the expression pattern of both enzymes is similar throughout the retina.

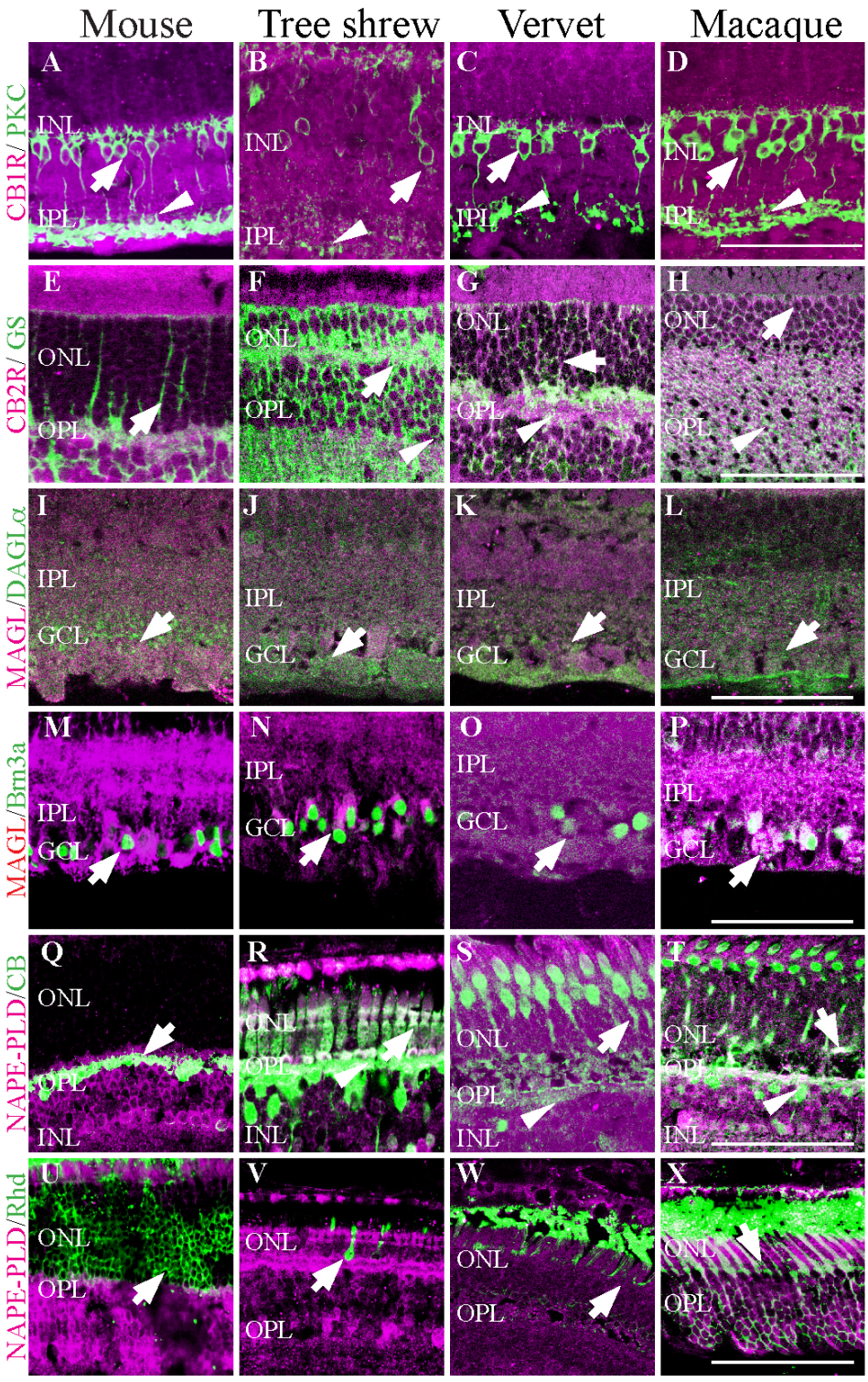

Figure 3- 3 Double-labeling of components of the eCB system with retinal cell specific markers. High magnification double-labeling of the retinal sections in the mouse, tree shrew, macaque and vervet monkey. A-D **are stained for CB1R (magenta) and rod bipolar cells (green) labeled by PKC** E-H **are stained for GS-positive Müller cells (green) and CB2R (magenta) in ONL and OPL.** I-L **double labeling of MAGL (magenta) and DAGLα (green)** M-P **are labeled for**

Brn3a-positive ganglion cells (green) and MAGL (magenta) in IPL and GCL. Q-T **are marked for calbindin-positive cones (green) and NAPE-PLD (magenta) in ONL, OPL and INL.** U-X **are stained for rhodopsin-positive rods (green) and NAPE-PLD (magenta) in ONL and OPL. Arrows and arrowheads point out areas of different levels of expression between segments. ONL, outer nuclear layer; OPL, outer plexiform layer; INL, inner nuclear layer; IPL, inner plexiform layer; GCL, ganglion cell layer. Scale bar = 75 µm.**

Discussion

In this study, we compared the localization of two cannabinoid receptors (CB1R, CB2R), two endocannabinoid synthesizing enzymes (NAPE-PLD and DAGLα), and two endocannabinoid degrading enzymes (FAAH and MAGL) in the retina of mice, tree shrews, and monkeys. This is the first study that shows the expression pattern of all the above-mentioned eCB components in the tree shrew retina as well as the localization of the NAPE-PLD, MAGL and DAGLα in the monkey retina. These phylogenetically related species were chosen due to the specialization of their visual systems; from the primitive monocular, rod-dominated visual system in mice with a low visual resolution to the well-developed visual system (Sirotin and Das, 2010) in monkeys that is similar to humans (Jacobs, 2008). Tree shrews are a species with binocular cone-dominated vision that is phylogenetically between mice and monkeys (Muller and Peichl, 1989; Muller and Peichl, 1993). We also compared two phylogenetically close primate models: the vervet and the macaque, to demonstrate that their visual systems are similar enough to use either in vision research.

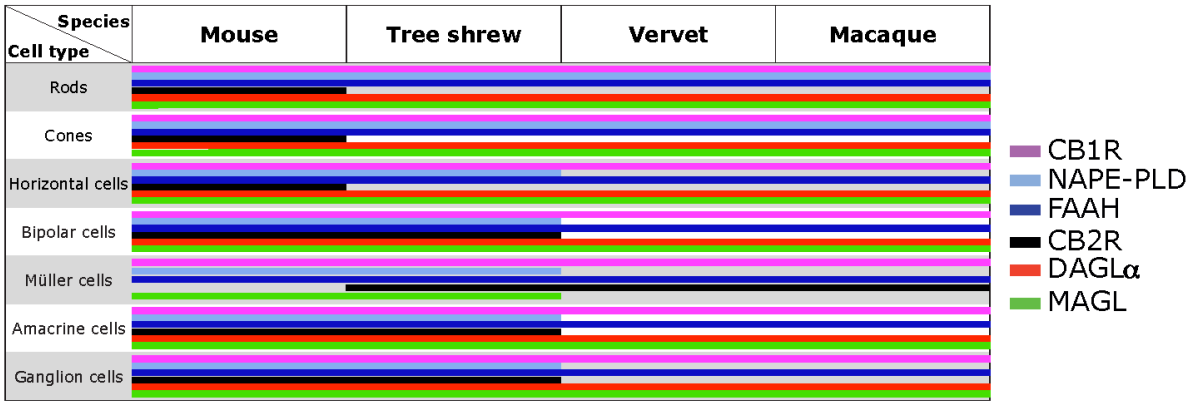

Figure 3- 4 Comparison of the expression patterns of CB1R (magenta), NAPE-PLD (light-blue), FAAH (dark-blue), CB2R (black), DAGLα (red) and MAGL (green) in the retina of mice, tree shrews, vervets and macaques.

The cannabinoid receptors: localization vs function

We recently reported that the distribution of the CB2R in the primate retina (Bouskila et al., 2013) is different than the rodent retina (Cécyre et al., 2014). While the CB2R is expressed in the rodent retinal neuronal cells (Cécyre et al., 2014), it is only expressed in the primate retinal glia, the Müller cells (Bouskila et al., 2013a). This finding prompted us to look into the retinal eCB system expression profiles across species. Interestingly, we show that only some components of the eCB system are preserved across the three animal species studied here while others are strikingly different. Notably, as reported by Elphick in his thought-provoking review (Elphick, 2012), CB1R and CB2R are unique to chordates, but the enzymes involved in the biosynthesis and the inactivation of the eCBs like NAPE-PLD and FAAH are found throughout the animal kingdom (McPartland 2006b). These proteins may have therefore evolved as presynaptic or postsynaptic receptors for eCBs. This is fascinating because although the expression and the localization of the evolutionary preserved receptor CB1R, and the enzyme FAAH, seem to be similar in mice, tree shrews, and primates, it is not comparable for CB2R, NAPE-PLD, MAGL and DAGLα.

There are many controversies on the neuronal and/or peripheral expression of CB2R. Our results show that the expression pattern of the CB2R differs from the mouse to the monkey. Similar to CB1R, CB2R shows a general expression in the neuro-retina: photoreceptors, horizontal cells, amacrine cells, and cells localized in the GCL of rodents (Cécyre et al., 2013; Lopez et al., 2011). In the mouse, CB2R expressed in the photoreceptor layer, was mostly found in cones and some rods (Cécyre et al., 2013). Similar to its position in the phylogeny tree, the tree shrew has an in-between position showing expressions in all

layers, as in rodents, and in Müller cells, as in primates (Figure 3-2**B**). In agreement with the CB2R glial expression in the CNS, the primate retina expresses CB2R mainly in Müller cells, with a higher polarization towards the outer retina (Bouskila et al., 2013a). The Müller cells, with their unique anatomy, span the entire thickness of the retina and contact with the majority of the retinal neurons (Reichenbach et al., 1995). It is known that the activation of CB2R leads to a series of neuro-protective properties such as cell proliferation (Carrier et al., 2004), reduction of tumor necrosis factors and free radicals (Stella, 2009). The emergence of the CB2R in the Müller cells in well developed visual systems may be related to the specialization of the vision protective system in higher animals and can therefore play a role in neuroprotection. This complementary expression pattern of CB1R and CB2R in the primate retina reveals thus a reciprocal relationship between retinal neurons and glia regarding their function via the eCB system. The ubiquitous CB1R system may play a more general role in the light transduction in all three species, as previously suggested (Yazulla, 2008).

The function of the cannabinoid receptors in the retina has been highlighted in recent ERG studies in adult mice (Cécyre et al., 2013) and vervet monkeys (Bouskila et al., 2014; Ptito et al. 2014). Cécyre et al., (2013) demonstrated a significant change in the a-wave amplitude of scotopic ERG in CB2R knockout mouse. However they did not find the same meaningful difference in *cnr1* knockout. They concluded that CB2R is likely to play a greater role in mouse retinal processing than CB1R. In monkeys we have recently reported a significant increase in the b-wave component of the photopic ERG after blockade of both CB1R and CB2R with their specific antagonists (Ptito et al. 2014). This variation can be due to the different pattern of expression and specialization of the eCB system in the monkey.

Numerous anecdotal reports claim that smoking marijuana improves dim light vision in humans (Merzouki and Mesa, 2002; Russo et al., 2004). Acute consumption of marijuana reduces the Vernier and Snellen acuities, alters color discrimination, increases photosensitivity, glare recovery and decreases dark adaptation (Kiplinger et al., 1971; Dawson et al., 1977). These data indicate that the eCBs are more likely to be involved in shaping retinal responses to light and suggest a more crucial role for this system in visual processing.

Significance of the distribution pattern of enzymes and cannabinoid receptors

The expression pattern of CB1R and FAAH has been reported in the CNS as complementary, overlapping or unrelated distributions (Egertová et al., 2003; Yazulla, 2008). Here, we report an overlapping distribution; CB1R expressing neurons also express FAAH. In this case, the degrading enzyme may remotely influence the CB1R (Egertová et al., 2003). During development of the mouse retina, CB1R and FAAH expression patterns are present in the deepest neuroblast layers at birth, and spread-out throughout the retina in adulthood (Zabouri et al., 2011a; Zabouri et al., 2011b). In our three species, the FAAH expression overlaps the CB1R distribution pattern not only in the photoreceptor layers but also in the ganglion cells (Figure 3-1**A-D** and **I-L**). This suggests that cannabinoids act not only on photoreceptors (Yazulla, 2008) but also directly on ganglion cell. This expression pattern has been reported not only in the retina of the vervet monkey (Bouskila et al., 2012), but also in the optic nerve, the dorsal lateral geniculate nucleus (Javadi et al., 2015) and the visual cortex of Rhesus monkeys (Eggan and Lewis, 2007).

Anandamide (an endogenous agonist of the CB1R) and other N-acylethanolamines (NAEs) are biosynthesized from phospholipids of the cell membrane assisted by NAPE-PLD hydrolysis. In this study, we report a variation in the expression of this membrane associated synthesis enzyme, NAPE-PLD, despite its well-preserved sequence from rodents to humans (Okamoto et al., 2004). In the mouse, NAPE-PLD follows the same pattern of expression as CB1R and FAAH. Moreover, unlike the mouse but like the primate, the tree shrew has a high expression of NAPE-PLD in ONL and OPL. We show here for the first time that NAPE-PLD expression in monkeys is exclusively restricted to the photoreceptor layer. Unlike CB1R, NAPE-PLD is ubiquitously expressed in the rat brain with the highest level in the thalamus (Morishita et al., 2005). Besides its role in the eCB biosynthesis, many other physiological roles have been linked to NAPE-PLD such as, anti-inflammatory effect (Lambert et al., 2002), anorexic effect (Rodriguez de Fonseca et al., 2001), and pro-apoptotic effect (Maccarrone et al., 2002). Moreover, the NAE products in axons suggest a role in the regulation of postsynaptic neuron activity as anterograde synaptic signaling molecules (Egertová et al., 2008). This pattern of expression also suggests another direct role of NAEs in primate photo-transduction.

Given that the lipophilic eCBs are released and degraded close to their action site, it would be reasonable to assume that the DAGLα and MAGL expressions are in the vicinity of CB2R. In the mouse retina, the DAGLα and MAGL expressions are often near or in the same cell types as CB1R and CB2R. CB1R is present in cones, horizontal, bipolar, amacrine and ganglion cells in the rat retina (Zabouri et al., 2011a; Zabouri et al., 2011b). CB2R is present in cone and rod photoreceptors, horizontal, bipolar, amacrine and ganglion cells in the adult

mouse retina (Cécyre et al., 2013). This distribution pattern may suggest that, in the mouse retina, eCBs such as 2-AG are faithfully expressed adjacent to the cannabinoid receptors and could be involved in their retinal function (Cécyre et al 2014). But the primates and the tree shrews have followed a complementary distribution pattern, and may have adopted a more complex and specific strategy to regulate their visual activity via the eCB system. The eCB expression pattern in the mouse rod-dominated retina with monocular vision, the tree shrew cone-dominated retina with binocular vision, and the monkey duplex retina with binocular vision proposed that the retinal eCB system plays a fundamental role in the mammal visual processing.

Acknowledgements

The Natural Science and Engineering Research Council of Canada (311892-2010, JFB; 6362-2012, MP; 194670-2014, CC) and the Canadian Institutes of Health Research (CIHR) (MOP-86495, JFB, MOP-301710, JFB and CC) supported this work. JB received support from a Frederick Banting and Charles Best Canada Graduate Scholarship Doctoral Award from CIHR. MP is Harland Sanders Chair professor in Visual Science. JFB is supported by a "Chercheur-Boursier Senior" from Fonds de Recherche du Québec – Santé (FRQ-S). We are grateful to Dr Frank Ervin and Dr Roberta Palmour of St.-Kitts, West Indies, for supplying the vervet monkey eyes. We would like to thank Dr Amir Shmuel from the Montreal Neurological Institute for donating the macaque eyes. We also would like to thank Reza Abbas Farishta for graciously preparing the tree shrew eyes.

Conflict of interest

The authors declare no conflict of interest.

Role of the authors

All authors had full access to all the data collected in the study and take responsibility for the integrity of these data and the accuracy of the analysis. Study concept and design: PJ, JB, MP, J-FB. Acquisition of data: PJ, JB, LE. Analysis and interpretation of data: PJ and JB. Drafting of the manuscript: PJ. Critical revision of the manuscript for important intellectual content: MP, J-FB, CC. Obtained funding: CC, MP, and J-FB. Administrative, technical, and material support: CC, MP and J-FB. Study supervision: MP and J-FB.

References

Argaw A, Duff G, Zabouri N, Cécyre B, Chaine N, Cherif H, Tea N, Lutz B, Ptito M, Bouchard JF. 2011. Concerted action of CB1 cannabinoid receptor and deleted in colorectal cancer in axon guidance. J Neurosci 31(4): 1489-1499.

Bluett RJ, Gamble-George JC, Hermanson DJ, Hartley ND, Marnett LJ, Patel S. 2014. Central anandamide deficiency predicts stress-induced anxiety: behavioral reversal through endocannabinoid augmentation. Transl Psychiatry 4:e408.

Bouskila J, Burke MW, Zabouri N, Casanova C, Ptito M, Bouchard JF. 2012. Expression and localization of the cannabinoid receptor type 1 and the enzyme fatty acid amide hydrolase in the retina of vervet monkeys. Neuroscience 202:117-130.

Bouskila J, Javadi P, Casanova C, Ptito M, Bouchard JF. 2013a. Müller cells express the cannabinoid CB2 receptor in the vervet monkey retina. J Comp Neurol. 521(11): 2399-415.

Bouskila J, Javadi P, Casanova C, Ptito M, Bouchard JF. 2013b. Rod photoreceptors express GPR55 in the adult vervet monkey retina. PLoS One. 8(11):e81080.

Carrier EJ, Kearn CS, Barkmeier AJ, Breese NM, Yang W, Nithipatikom K, Pfister SL, Campbell WB, Hillard CJ. 2004. Cultured Rat Microglial Cells Synthesize the Endocannabinoid 2-Arachidonylglycerol, Which Increases Proliferation via a CB2 Receptor-Dependent Mechanism. Mol Pharmacol 65(4): 999-1007.

Cécyre B, Zabouri N, Huppé-Gourgues F, Bouchard JF, Casanova C. 2013. Roles of cannabinoid receptors type 1 and 2 on the retinal function of adult mice. Invest Ophthalmol Vis Sci. 54(13):8079-90.

Cécyre B, Thomas S, Ptito M, Casanova C, Bouchard JF. 2014a. Evaluation of the specificity of antibodies raised against cannabinoid receptor type 2 in the mouse retina. Naunyn Schmiedebergs Arch Pharmacol. 387(2): 175-184.

Cécyre B, Monette M , Beudjekian L, Casanova C and Bouchard JF. 2014b. Localization of diacylglycerol lipase alpha and monoacylglycerol lipase during postnatal development of the rat retina. 150 (8): 1-17.

Cottone E, Pomatto V, Cerri F, Campantico E, Mackie K, Delpero M, Guastalla A, Dati C, Bovolin P, Franzoni MF. 2013. Cannabinoid receptors are widely expressed in goldfish: molecular cloning of a CB2-like receptor and evaluation of CB1 and CB2 mRNA expression profiles in different organs. Fish Physiol Biochem 39(5): 1287-1296.

Dasilva MA, Grieve KL, Cudeiro J, Rivadulla C. 2012. Endocannabinoid CB1 receptors modulate visual output from the thalamus. Psychopharmacology (Berl) 219(3): 835-845.

Dawson WW, Jimenez-Antillon CF, Perez JM, Zeskind JA. 1977. Marijuana and vision--after ten years' use in Costa Rica. Invest Ophthalmol Vis Sci 16(8): 689-699.

Di Marzo V. 2009. The endocannabinoid system: its general strategy of action, tools for its pharmacological manipulation and potential therapeutic exploitation. Pharmacol Res 60(2): 77-84.

Dinh TP, Carpenter D, Leslie FM, Freund TF, Katona I, Sensi SL, Kathuria S, Piomelli D. 2002. Brain monoglyceride lipase participating in endocannabinoid inactivation. Proc Natl Acad Sci U S A 99(16): 10819-10824.

Duff G, Argaw A, Cécyre B, Cherif H, Tea N, Zabouri N, Casanova C, Ptito M, Bouchard JF. 2013. Cannabinoid Receptor CB2 Modulates Axon Guidance. PLoS One 8(8): e70849.
Egertová M, Cravatt BF, Elphick MR. 2003. Comparative analysis of fatty acid amide hydrolase and cb(1) cannabinoid receptor expression in the mouse brain: evidence of a widespread role for fatty acid amide hydrolase in regulation of endocannabinoid signaling. Neuroscience 119(2): 481-496.
Egertová M, Simon GM, Cravatt BF, Elphick MR. 2008. Localization of N-acyl phosphatidylethanolamine phospholipase D (NAPE-PLD) expression in mouse brain: A new perspective on N-acylethanolamines as neural signaling molecules. J Comp Neurol 506(4): 604-615.
Eggan SM, Lewis DA. 2007. Immunocytochemical distribution of the cannabinoid CB1 receptor in the primate neocortex: a regional and laminar analysis. Cereb Cortex 17(1): 175-191.
Elphick MR. 2012. The evolution and comparative neurobiology of endocannabinoid signalling. Philos Trans R Soc Lond B Biol Sci 367(1607): 3201-3215.
Elphick MR, Egertova M. 2005. The phylogenetic distribution and evolutionary origins of endocannabinoid signalling. Handb Exp Pharmacol (168): 283-297.
Fan Y, Huang ZY, Cao CC, Chen CS, Chen YX, Fan DD, He J, Hou HL, Hu L, Hu XT, Jiang XT, Lai R, Lang YS, Liang B, Liao SG, Mu D, Ma YY, Niu YY, Sun XQ, Xia JQ, Xiao J, Xiong ZQ, Xu L, Yang L, Zhang Y, Zhao W, Zhao XD, Zheng YT, Zhou JM, Zhu YB, Zhang GJ, Wang J, Yao YG. 2013. Genome of the Chinese tree shrew. Nat Commun.4: 1426.
Fischer AJ, Hendrickson A, Reh TA. 2001. Immunocytochemical characterization of cysts in the peripheral retina and pars plana of the adult primate. Invest Ophthalmol Vis Sci 42(13): 3256-3263.
Harkany T, Guzman M, Galve-Roperh I, Berghuis P, Devi LA, Mackie K. 2007. The emerging functions of endocannabinoid signaling during CNS development. Trends Pharmacol Sci 28(2): 83-92.
Harkany T, Keimpema E, Barabas K, Mulder J. 2008. Endocannabinoid functions controlling neuronal specification during brain development. Mol Cell Endocrinol 286(1-2 Suppl 1): S84-90.
Herbin M, Boire D, Ptito M. 1997. Size and distribution of retinal ganglion cells in the St. Kitts green monkey (Cercopithecus aethiops sabeus). J Comp Neurol 383(4): 459-72.
Hu SS, Arnold A, Hutchens JM, Radicke J, Cravatt BF, Wager-Miller J, Mackie K, Straiker A. 2010. Architecture of cannabinoid signaling in mouse retina. J Comp Neurol 518(18): 3848-3866.
Imamoto Y, Shichida Y. 2014. Cone visual pigments. Biochim Biophys Acta 1837(5): 664-673.
Jacobs GH. 2008. Primate color vision: A comparative perspective. Vis Neurosci 25(5-6):619-633.
Javadi P, Bouskila J, Bouchard JF, Ptito M. 2015. The endocannabinoid system within the dorsal lateral geniculate nucleus of the vervet monkey. Neuroscience, (In Press).
Jeon CJ, Strettoi E, Masland RH. 1998. The major cell populations of the mouse retina. J Neurosci 18(21): 8936-8946.
Kiplinger GF, Manno JE, Rodda BE, Forney RB. 1971. Dose-response analysis of the effects of tetrahydrocannabinol in man. Clin Pharmacol Ther 12(4): 650-657.

Lambert DM, Vandevoorde S, Jonsson KO, Fowler CJ. 2002. The palmitoylethanolamide family: a new class of anti-inflammatory agents? Curr Med Chem 9(6): 663-674.
Lopez EM, Tagliaferro P, Onaivi ES, Lopez-Costa JJ. 2011. Distribution of CB2 cannabinoid receptor in adult rat retina. Synapse 65(5):388-392.
Maccarrone M, Pauselli R, Di Rienzo M, Finazzi-Agro A. 2002. Binding, degradation and apoptotic activity of stearoylethanolamide in rat C6 glioma cells. Biochem J 366(Pt 1): 137-144.
McPartland JM, Agraval J, Gleeson D, Heasman K, Glass M. 2006a. Cannabinoid receptors in invertebrates. Journal of evolutionary biology 19(2): 366-373.
McPartland JM, Guy GW, Di Marzo V. 2014. Care and feeding of the endocannabinoid system: a systematic review of potential clinical interventions that upregulate the endocannabinoid system. PLoS One 9(3): e89566.
McPartland JM, Matias I, Di Marzo V, Glass M. 2006b. Evolutionary origins of the endocannabinoid system. Gene 370:64-74.
McPartland JM, Norris RW, Kilpatrick CW. 2007. Coevolution between cannabinoid receptors and endocannabinoid ligands. Gene 397(1-2): 126-135.
Merzouki A, Mesa JM. 2002. Concerning kif, a Cannabis sativa L. preparation smoked in the Rif mountains of northern Morocco. J Ethnopharmacol.81(3): 403-406.
Morishita J, Okamoto Y, Tsuboi K, Ueno M, Sakamoto H, Maekawa N, Ueda N. 2005. Regional distribution and age-dependent expression of N-acylphosphatidylethanolamine-hydrolyzing phospholipase D in rat brain. J Neurochem 94(3): 753-762.
Muller B, Peichl L. 1989. Topography of cones and rods in the tree shrew retina. J Comp Neurol 282(4): 581-594.
Muller B, Peichl L. 1993. Horizontal cells in the cone-dominated tree shrew retina: morphology, photoreceptor contacts, and topographical distribution. J Neurosci 13(8): 3628-3646.
Nag TC, Wadhwa S. 2001. Differential expression of syntaxin-1 and synaptophysin in the developing and adult human retina. J Biosci 26(2): 179-191.
Nishikawa S, Tamai M. 2001. Müller cells in the human foveal region. Curr Eye Res 22(1): 34-41.
Ohiorhenuan IE, Mechler F, Purpura KP, Schmid AM, Hu Q, Victor JD. 2014. Cannabinoid neuromodulation in the adult early visual cortex. PLoS One 9(2): e87362.
Okamoto Y, Morishita J, Tsuboi K, Tonai T, Ueda N. 2004. Molecular characterization of a phospholipase D generating anandamide and its congeners. J Biol Chem 279(7): 5298-5305.
Ozawa Y, Nakao K, Kurihara T, Shimazaki T, Shimmura S, Ishida S, Yoshimura A, Tsubota K, Okano H. 2008. Roles of STAT3/SOCS3 pathway in regulating the visual function and ubiquitin-proteasome-dependent degradation of rhodopsin during retinal inflammation. J Biol Chem 283(36): 24561-24570.
Prusky GT, Douglas RM. 2004. Characterization of mouse cortical spatial vision. Vision Res 44(28): 3411-3418.
Ptito M, Javadi, P, Bouskila J, Casanova C, Bouchard JF (2014), Role of retinal cannabinoid receptors
CB1 and CB2, and GPR55 defined by electroretinography in vervet monkeys. FENS - 0297-D021

Reichenbach A, Fromter C, Engelmann R, Wolburg H, Kasper M, Schnitzer J. 1995. Muller glial cells of the tree shrew retina. J Comp Neurol 360(2): 257-270.
Riepe RE, Norenburg MD. 1977. Müller cell localisation of glutamine synthetase in rat retina. Nature 268(5621): 654-655.
Rodriguez de Fonseca F, Navarro M, Gomez R, Escuredo L, Nava F, Fu J, Murillo-Rodriguez E, Giuffrida A, LoVerme J, Gaetani S, Kathuria S, Gall C, Piomelli D. 2001. An anorexic lipid mediator regulated by feeding. Nature 414(6860): 209-212.
Russo EB. 2008. Clinical endocannabinoid deficiency (CECD): can this concept explain therapeutic benefits of cannabis in migraine, fibromyalgia, irritable bowel syndrome and other treatment-resistant conditions? Neuro Endocrinol Lett 29(2): 192-200.
Russo EB, Merzouki A, Mesa JM, Frey KA, Bach PJ. 2004. Cannabis improves night vision: a case study of dark adaptometry and scotopic sensitivity in kif smokers of the Rif mountains of northern Morocco. J Ethnopharmacol. 93(1):99-104.
Sirotin YB, Das A. 2010. Zooming in on mouse vision. Nat Neurosci 13(9): 1045-1046.
Smith SC, Wagner MS. 2014. Clinical endocannabinoid deficiency (CECD) revisited: Can this concept explain the therapeutic benefits of cannabis in migraine, fibromyalgia, irritable bowel syndrome and other treatment-resistant conditions? Neuro Endocrinol Lett 35(3): 198-201.
Stella N. 2009. Endocannabinoid signaling in microglial cells. Neuropharmacology 56 Suppl 1:244-253.
Straiker A, Stella N, Piomelli D, Mackie K, Karten HJ, Maguire G. 1999. Cannabinoid CB1 receptors and ligands in vertebrate retina: localization and function of an endogenous signaling system. Proc Natl Acad Sci U S A 96(25): 14565-14570.
Xu JY, Chen C. 2014. Endocannabinoids in Synaptic Plasticity and Neuroprotection. Neuroscientist. 1073858414524632.
Yazulla S. 2008. Endocannabinoids in the retina: from marijuana to neuroprotection. Prog Retin Eye Res 27(5): 501-526.
Zabouri N, Bouchard JF, Casanova C. 2011a. Cannabinoid receptor type 1 expression during postnatal development of the rat retina. J Comp Neurol 519(7): 1258-1280.
Zabouri N, Ptito M, Casanova C, Bouchard JF. 2011b. Fatty acid amide hydrolase expression during retinal postnatal development in rats. Neuroscience 195:145-165.

CHAPTER 4: Standardized full-field electroretinography in the Green Monkey (*Chlorocebus sabaeus*)

Published in PLoS One. 2014 Oct 31;9(10):e111569. doi: 10.1371/journal.pone.0111569. eCollection 2014.

Standardized full-field electroretinography in the Green Monkey (*Chlorocebus sabaeus*)

Joseph Bouskila*[1, 2], Pasha Javadi*[1], Roberta M. Palmour[3, 4], Jean-François Bouchard[1] and Maurice Ptito[1, 5]

[1]School of Optometry, University of Montreal, Montreal, Quebec, Canada
[2]Biomedical Sciences, Faculty of Medicine, University of Montreal, Montreal, Quebec, Canada
[3]Behavioral Science Foundation, Basseterre, St. Kitts, West Indies
[4]Departments of Psychiatry and Human Genetics, McGill University, Montreal, Quebec, Canada
[5]BRAINlab and Neuropsychiatry Laboratory, Department of Neuroscience and Pharmacology, University of Copenhagen, Copenhagen, Denmark

* These authors contributed equally to this work.

Keywords: electroretinogram, dark adaptation, scotopic ERG, photopic ERG, oscillatory potentials, flicker ERG.

Correspondence should be addressed to:
Maurice Ptito, Ph.D.
School of Optometry, room 260-7
3744 Jean-Brillant,
University of Montreal,
Montreal, Quebec, Canada, H3T 1P1

Abstract

Full-field electroretinography is an objective measure of retinal function, serving as an important diagnostic clinical tool in ophthalmology for evaluating the integrity of the retina. Given the similarity between the anatomy and physiology of the human and Green Monkey eyes, this species has increasingly become a favorable non-human primate model for assessing ocular defects in humans. To test this model, we obtained full-field electroretinographic recordings (ERG) and normal values for standard responses required by the International Society for Clinical Electrophysiology of Vision (ISCEV). Photopic and scotopic ERG recordings were obtained by full-field stimulation over a range of 6 log units of intensity in dark-adapted or light-adapted eyes of adult Green Monkeys (*Chlorocebus sabaeus*). Intensity, duration, and interval of light stimuli were varied separately. Reproducible values of amplitude and latency were obtained for the a- and b-waves, under well-controlled adaptation and stimulus conditions; the i-wave was also easily identifiable and separated from the a-b-wave complex in the photopic ERG. The recordings obtained in the healthy Green Monkey matched very well with those in humans and other non-human primate species (*Macaca mulatta* and *Macaca fascicularis*). These results validate the Green Monkey as an excellent non-human primate model, with potential to serve for testing retinal function following various manipulations such as visual deprivation or drug evaluation.

Introduction

The retina is a complex and well-organized neuronal structure that is vulnerable to internal influences such as retinopathies and ocular pathologies, and is furthermore sensitive to external factors such as drugs and alcohol toxicity. Full-field electroretinography represents a useful diagnostic clinical tool in ophthalmology and is widely used as a measure of retinal function. Electroretinogram (ERG) recordings are generated through different summation of currents evoked in distinct populations of retinal cells, including photoreceptors (cones and rods), neurons (horizontal cells, bipolar cells, amacrine cells, and ganglion cells), glial cells (Müller cells), and epithelial cells [1]. Accordingly, the influence of environmental manipulations on the function of retinal cells can be assessed objectively in the ERG. Whereas the full-field ERG reflects the response of the entire retina to stimulus, it is possible to differentiate between responses of various retinal structures to light [2]; in fact, the positive and negative waves of the ERG emerge from different levels of retinal processing, and the response of particular retinal cell populations and circuits is targeted by the choice of stimulus and recording environment. Research on the origins of pathophysiological conditions displayed in human electroretinography is mostly carried out in animal models, with non-human primates remaining particularly important in visual neuroscience research, due to their superior emulation of human retinal function [3]. Indeed, the non-human primate ERG plays an important role in studies of visual abnormalities and potentially therapeutic pharmacological effects in the retina. The International Society for Clinical Electrophysiology of Vision (ISCEV) proposes a minimum of five types of measurements in order to obtain standardization for investigations in humans [4], all of which can be obtained in non-human primates.

Green Monkeys have become important non-human primate species for visual neuroscience research. The genome of Green Monkeys has 90% parity with the human genome, which lends support to its use to model a range of behavioral and non-behavioral pathologic disorders in human [5], [6]. In fact, Green Monkeys are used as a model organism for the study of diabetes, cardiovascular disease, HIV/AIDS, Parkinson's disease, substance abuse, attention deficit disorder, alcoholism, reproduction, tissue regeneration and other conditions [5], [7], [8], [9]. The Green Monkey has been utilized in visual neuroscience for many years [7], [10], [11], [12], [13], [14], [15], [16], [17], [18], [19], leading to a thorough anatomical description of the visual pathways and the publication of anatomical brain atlases [20], [21], [22]. Their large brain and ocular size relative to the 3.5 kg bodyweight of adult Green Monkeys is particularly advantageous in the electrophysiological study of visual abnormalities arising in the retina and optic nerve. The organization of the retina of the green monkey is similar to that of other Old World species such as Macaques, for example. The retina contains several layers and different cell populations: photoreceptors, bipolar cells, ganglion cells, amacrines and horizontal cells. There is a monotonic decrease in the number of cones from the fovea centralis (containing mainly cones) to the periphery made out of rods [17], [23]. This developed fovea is well suited for high visual acuity, color vision and photopic sensitivity whereas the peripheral retina is responsible for scotopic vision (nocturnal) [24]. From the study of Herbin et al. (1997), the only one available on the green monkey retina, the retinal ganglion cells (RGCs) number derived from retinal wholemounts was estimated at 1 228 646. The topographical distribution of RGCs shows a strong centro-peripheral gradient, with the majority of small cells (P cells) in the fovea, the larger ones being encountered in the

periphery (M cells). The axons of the ganglion cells form the optic nerve and their counts derived from semi-thin sections (1 220 000) are close to the estimated number of RGCs for the vervet monkey and are in the range with those reported for *Macaca Mulatta* (1 468 000 RGCs) [25].

However, little is known about the electrophysiology of the Green Monkey retina, since most of such studies have been conducted in the rhesus monkey, for which a standardized procedure for electroretinographic examination has been published [26]. Due to the lack of corresponding data in Green Monkeys despite their growing importance in visual neuroscience, a standardized electroretinography protocol is needed. We therefore present here full-field ERG data for Green Monkeys, including the five standard responses recommended by the ISCEV.

Table 4-1 Subject profile of animals used in this study

	Animal ID	Sex	Weight (Kg)	IOP (mm Hg)	Pupil dilatation (mm)
1	05011-5	Male	3.950	OD 10 / OS 9	OD 9 / OS 9
2	05010-6	Male	3.725	OD 7 / OS 7	OD 8 / OS 8
3	09093-1-3-1	Female	3.050	OD 9 / OS 9	OD 9 / OS 9
4	08274	Female	2.800	OD 10 / OS 11	OD 9 / OS 9
5	08275	Female	2.925	OD 8 / OS 6	OD 8.5 / OS 8.5
6	07862	Female	2.875	OD 15 / OS15	OD 8.5 / OS 8.5
7	08297	Female	2.750	OD 6 / OS 6	OD 9 / OS 9
8	07866	Female	2.950	OD 12 / OS 12	OD 9 / OS 9
9	01336-7-1-3	Female	2.950	OD 12 / OS 13	OD 9 / OS 9
10	08315	Female	2.775	OD 10 / OS 11	OD 9 / OS 9
11	07868	Female	2.825	OD 8 / OS8	OD 8.5 / OS 8.5
12	08375	Female	2.900	OD 11 / OS 12	OD 9 / OS 9
13	08376	Female	2.850	OD 6/ OS 6	OD 9 / OS 9
14	08336	Female	2.925	OD 14 / OS 15	OD 9 / OS 9
15	08377	Female	2.852	OD 9 / OS 10	OD 9 / OS 9

Materials and Methods

Animals

A total of 15 adult male and female Green Monkeys (*Chlorocebus sabaeus*), aged 3 to 4 years and weighing 3.01 ± 0.35 Kg, were used for this study (Table 4-1). The animals were born and raised in enriched environments in the laboratories of the Behavioral Science Foundation (St-Kitts, West Indies). As adults, the animals were fed with primate chow (Harlan Teklad High Protein Monkey Diet; Harlan Teklad, Madison, WI) and fresh local fruits, with water available *ad libitum*. Infant Green Monkeys are born into an outdoor social group comprising several females, one male and other offspring of the same general age. Infants live with their parents until about 8 months of age, at which time they move to a playpen with 5 other age-mates. The natal cage is equipped with swings, perches, hiding places and jungle gyms. We do put in toys, but the animals are so busy playing with one another that they ignore the toys. In the smaller playpens, there are also swings, perches and climbing spots, as well as puzzle feeders and foraging boards. At about 18 months of age, youngsters graduate to a large, outdoor peer group of about 16 animals (like-ages, both sexes) where there are tunnels, swings, ladders, jungle-gyms and a variety of manipulanda (more complex puzzle feeders; natural forage opportunities, such as brush and vines; foraging boards). Plastic chain and baited balls are popular toys, but vervets of this age are uninterested in most other commercially available toys. All experiments were performed according to the guidelines of the Canadian Council on Animal Care (CCAC) and the Association for Research in Vision and Ophthalmology (ARVO) Statement for the Use of Animals in Ophthalmic and Vision Research. The experimental protocol was also reviewed and approved by the local Animal Care and Use Committee (University of Montreal, protocol # 14-007) and the Institutional Review Board of

the Behavioral Science Foundation that is recognized by the CCAC. None of the animals were sacrificed for this study.

Animal preparation for ERG recording

The following procedure describes a typical recording session in Green Monkeys, including successively a 30 minutes of animal preparation, 30 minutes of dark adaptation, 15 minutes of scotopic recordings, 2 minutes of light adaptation, 15 minutes of photopic recordings, and 2 minutes of flicker recordings (Figure 4-1). The values of dark and light adaptation were chosen based on data obtained in cynomologus monkeys [27]. The animals were sedated with an intramuscular injection of a mixture of ketamine (10 mg/kg; Troy Laboratories, Glendenning, New South Wales, Australia) and xylazine (1 mg/kg; Lloyd Laboratories, Shenandoah, IA). In this condition, the pupils were fully dilated to approximately 9 mm in diameter and the accommodation reflex was paralyzed with topical application of 1% tropicamide (Mydriacyl) and 2.5% phenylephrine hydrochloride (Mydfrin) (Alcon Laboratories, Fort Worth, TX). Intraocular pressures (IOP) were also monitored before and after the recording session by applanation tonometry (TonoPen XL; Mentor, Norwell, MA, USA). There were no significant IOP and pupil size differences noted between the beginning and the end of the ERG procedure. The eyes were treated with 0.5% proparacaine hydrochloride (Alcaine; Alcon Laboratories, Fort Worth, TX, USA) to anesthetize the cornea and then protected by application of 2.5% methylcellulose (Gonak; Akorn, Inc., Buffalo Grove, IL, USA) to prevent corneal drying. Body temperature was maintained between 36.5°C and 38°C with a heating pad. Recording sessions lasted approximately two hours for each

animal, after which they were allowed to recover and returned to their prior naturalistic setting.

Visual Stimulation

Full-field stimulation was produced with an UTAS BigShot Ganzfeld light source (UTAS E-3000 electrophysiology equipment; LKC Technologies, Inc., Gaithersburg, MD, USA) that was placed in front of the animal's face. Both eyes were simultaneously recorded and averaged as detailed below. The ERGs were evoked by white flashes of light of intensities ranging from 0.00025 cd.sec.m^{-2} to 1000 cd.sec.m^{-2} delivered in full-field conditions. During the course of dark adaptation, ERGs were recorded at 3 minutes intervals over 30 minutes of dark adaptation with a constant stimulus of approximately 0.025 cd.s.m^{-2}. LED flash luminance of 0.00025 to 6 cd.sec.m^{-2} (-50 dB to 4 dB in LKC units) was used for scotopic stimulation. Responses were averaged for each of the 14 time-integrated flash luminance levels presented (ranging from -3.6 to 2.9 log cd.s.m^{-2} in approximately 0.3 log-unit steps; flash duration, 20 μs; inter-stimulus interval, 5 sec for -3.6 to 0.4 log cd.s.m^{-2} and 15 sec for 0.6 to 2.9 log cd.s.m^{-2}) and xenon flash luminance of 2.5 to 800 cd.sec.m^{-2} (0 dB to 25 dB in LKC units) for photopic stimulation (ranging from -2.2 to 2.9 log cd.s.m^{-2} in approximately 0.3 log-unit steps; flash duration, 20 μs; inter-stimulus interval, 2 sec for all intensities). For light-adapted ERGs a steady white background-adapting field (30 cd/m^2) was presented inside the Ganzfeld to saturate the rod system. Flash intensities and background luminance were calibrated using a research radiometer (IL1700 Photometer; International Light Inc., Newburyport, MA, USA) with a SED033 detector placed at 36 cm from the source.

ERG recording and analysis

All experimental protocols followed the guidelines of the ISCEV [4], specifying the 5 standard responses: (1) a dark-adapted response (rod response), (2) a dark-adapted maximal response (combined rod–cone response), (3) a dark-adapted oscillatory potentials response, (4) a light-adapted response (cone response), and (5) a light-adapted response to a rapidly repeated stimulus (30 Hz flicker). ERG recordings and signal processing were recorded with contact lens electrodes lying across the center of the cornea of each eye moistened with 1% carboxymethylcellulose sodium (Refresh Celluvisc, Allergan Inc., Markham, ON, Canada). The corneal contact lens electrode (Jet electrodes; Diagnosys LLC, Lowell, MA, USA) was equipped with four small posts on the convex surface in order to keep the eyelids open. Reference and ground gold disc electrodes (model F-E5GH; Grass Technologies, Astro-Med, Inc., West Warwick, RI, USA) were kept in place with adhesive paste (Ten20 conductive EEG paste; Kappa Medical, Prescott, AZ, USA) at the external canthi and forehead, respectively. Responses were amplified 10,000 times and filtered with a band pass from 1 to 500 Hz except for the oscillatory potentials, which were extracted with the LKC software with a band pass from 75 to 500 Hz. Each tracing included a 20 ms pre-stimulus baseline. Depending on the measured stimulus, up to 10 waveforms were averaged to reduce variability and background noise. Based on literature focusing on the origins of ERG waves in a primate model (macaque monkey) whose retina is very similar to that of humans [2], the origins of the waveforms are described. For the waveform analysis, the amplitude of the a-wave, which mainly reflects the function of photoreceptors, was measured from the baseline to the peak of the a-wave for the combined rod-cone response and the single-flash cone response. The amplitude of the b-wave, which reflects the activity of the inner nuclear layer, was measured from the peak of the a-

wave to the peak of the b-wave for all responses. The peak latency was defined from the onset of the flash to the peak. In the case of the oscillatory potentials, the latency to the second peak was usually determined, where the amplitude was defined as peak to trough amplitude from the peak of the second wave to the following trough. The amplitude of the i-wave was measured from the trough of the b-wave to the peak of the i-wave and its respective peak time was also measured from flash onset. The exact origin of the i-wave is still controversial. Some have suggested that this component is generated at the inner retinal level [28], and others that it origins at a more distal location [29]. The latter point is highlighted in ocular pathology studies. For example, the i-wave in glaucoma patients [30] and in glaucoma animal models [29] is increased, suggesting that it does indeed originate in the distal retina. In the 30 Hz flicker ERG, the second peak was evaluated in relation to the preceding trough. Retinal response diagrams were drawn using Adobe Illustrator and processed in Adobe InDesign (Adobe Systems, software version CS5; San Jose, CA, USA). The ERG procedure is summarized schematically in Figure 4-1.

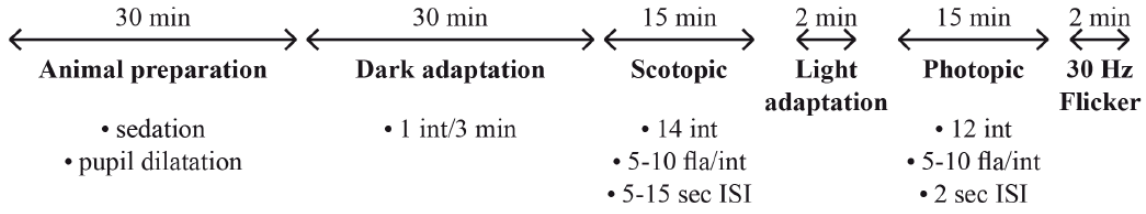

Figure 4-1 Summarized schematic procedure describing a typical electroretinography recording session in a Green Monkey (*Chlorocebus sabaeus*). Int, intensity; Fla, flashes; ISI, inter stimulus interval.

Results

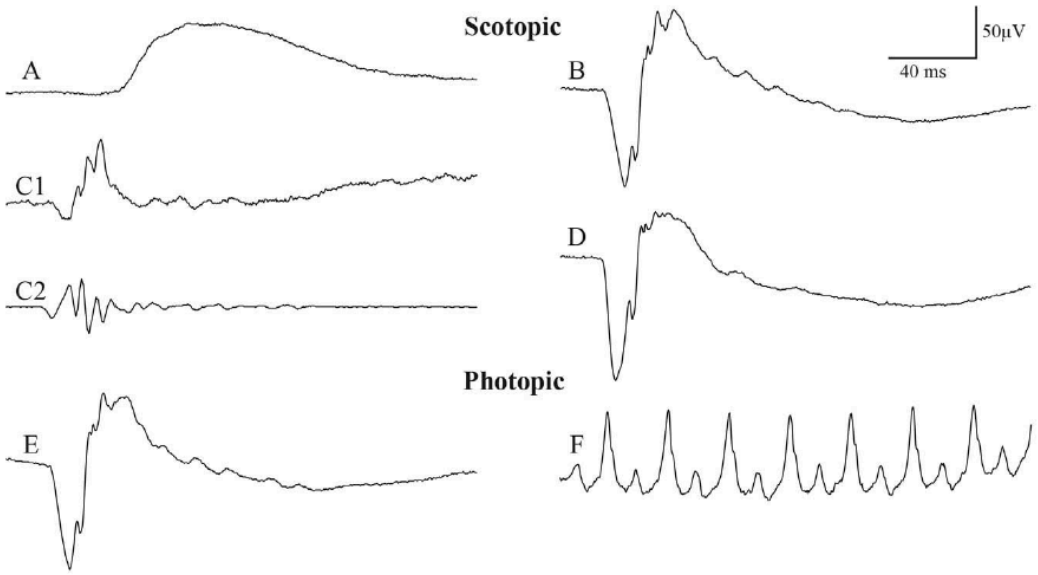

Figure 4-2 Standard responses for full-field electroretinography in a representative Green Monkey (*Chlorocebus sabaeus*), including the 5 standard responses: a rod response, a combined rod–cone response, oscillatory potentials, a cone response, and a flicker response. (A**) Rod response elicited at -2.2 log cd.s.m^{-2} (0.0064 cd.s.m^{-2}) after 30 minutes of dark adaptation. (**B**) Maximal response elicited at 0.4 log cd.s.m^{-2} (2.57 cd.s.m^{-2}, standard flash) in the dark-adapted eye. (**C1**) Broadband scotopic ERG waveform and (**C2**) the corresponding software-filtered oscillatory potentials elicited at 0.6 log cd.s.m^{-2} (4.4 cd.s.m^{-2}) in the dark-adapted eye. (**D**) The recommended additional stronger flash ERG elicited at 10.0 cd.s.m^{-2} in the dark-adapted eye. (**E**) White flash cone response elicited at 0.4 log cd.s.m^{-2} in the light adapted eye with a background illumination of 30 cd.m^{-2}. (**F**) Flicker response (30 Hz) elicited at 0.4 log cd.s.m^{-2} after five minutes of light adaptation with a background illumination of 30 cd.m^{-2}. Tracings (**A, B, C1, D, E**) included a 20 ms pre-stimulus baseline. Horizontal calibration, 40 ms; vertical calibration, 50 µV.**

The five standard responses

All 15 Green Monkeys displayed very well detectable and easily reproducible ERG recordings, using the protocol described in the Experimental Procedure section (Figure 4-1). As indicated by the ISCEV, the five standard responses and the recommended additional stronger scotopic flash ERG are illustrated in Figure 4-2 for a representative Green Monkey. The typical scotopic ERG signal is formed, as expected, by an initial negative wave (the a-wave) and followed by a larger positive wave (the b-wave). Faster components of lower amplitude, known as the oscillatory potentials (OPs), are seen in the ascending limb of the

scotopic b-wave. These OPs were as prominent as those obtained in humans. Given uncertainty of how best to quantify OPs, we chose to measure the amplitude from the peak of the second wave to the following trough, as described in the Experimental Procedure section. Thus, the chronological sequence of electrical events in a typical photopic ERG response observed in the Green Monkey, as in humans, is the a-wave, b-wave, and i-wave. During 30 Hz flicker stimulation, double peaks were often detectable in the b-waves. In these cases, both the amplitudes and implicit times were measured at the first peak. The signal-to-noise ratio was high for all categories, and no extra filter such as a notch filter had to be used, even in single sweep curves. Our mean results obtained in 15 Green Monkeys are summarized in Table 4-2; the mean amplitudes and latencies of the five standard ISCEV responses are specific to a flash intensity and light adaptation status.

Table 4-2 Responses to standardized electroretinography in Green Monkeys, Data are reported as mean ± SEM (Standard error of the mean).

Standard response (ISCEV)	a-wave amplitude (μV)	a-wave peak latency (ms)	b-wave amplitude (μV)	b-wave peak latency (ms)	Flash intensity ($cd.s.m^{-2}$)	Adaptation status
Rod response	-	-	88.9 ± 26.6	79.9 ± 6.1	0.0064	Dark
Maximal response	115.1 ± 40.2	14.8 ± 0.7	203.7 ± 52.6	36.7 ± 3.8	2.5	Dark
Oscillatory potential	-	-	60.2 ± 15.5	20.3 ± 0.9	4.4	Dark
Strong flash response	174.9 ± 27.2	9.8 ± 0.4	230.7 ± 40.6	30.8 ± 3.6	10.0	Dark
White flash cone response	22.1 ± 4.5	12.3 ± 1.2	81.5 ± 19.4	27.7 ± 1.5	2.5	Light
30 Hz flicker	-	-	88.9 ± 20.2	24.3 ± 1.0	2.5	Light

ERG responses throughout dark-adaptation

ERGs were recorded during the course of dark-adaptation at 3 min intervals over 30 min with a constant stimulus intensity of approximately 0.006 $cd.s.m^{-2}$ (Figure 4-3). We have not pursued the recordings over 30 minutes based on the human [4] and monkey literature [27]. For example, Bee (2001) reported that in cynomologus monkeys (*Macaca fascicularis*), plateau was reached around 20 minutes.

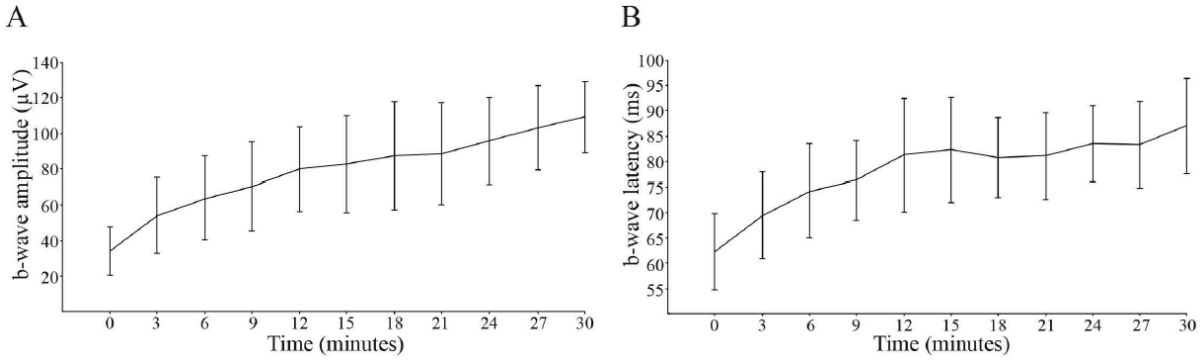

Figure 4-3 Response versus time functions of b-wave amplitude (A) and latency (B) throughout dark-adaptation elicited at -2.2 log cd.s.m^{-2} (0.0064 cd.s.m^{-2}). Each data point indicates average (± SEM) of all 15 monkeys.

Intensity–response function of scotopic and photopic ERG

Beyond the ordinary requirements of the ISCEV, ERG responses to stimuli of increasing flash intensity in dark-adapted (Figure 4-4A) and light-adapted conditions (Figure 4-4B) were also recorded. Both intensity response series were obtained from the same monkey, and in the same recording session. It can be seen in the figure that the two recording conditions yield ERG responses of different amplitude, timing and morphology. The distribution of full-field ERG amplitudes and implicit times are often asymmetrical, even in large groups of normal monkeys, such that use of statistics based on a normal distribution can be misrepresentative [27]. We used a log transformation of the data to reduce variance. Figure 4-5 shows the results of the scotopic a-wave and b-wave amplitudes and latency versus log flash intensity (cd.s.m^{-2}) functions. It is worthwhile to note a sigmoid curve characterizes the amplitudes as well as the latencies functions in the Green Monkey. Moreover, the b-wave amplitude decreased at the highest intensity of 2.9 log cd.s.m^{-2} with an inter-stimulus interval of 15 seconds (Figure 4-5A and 4-5C). The photopic functions are shown in Figure 6. The values given at 0.4 log cd.s.m^{-2} (standard flash) represent the white flash cone response as recommended by the ISCEV. These results are also known from studies on non-human and human primate retinal functions [27],

[31].

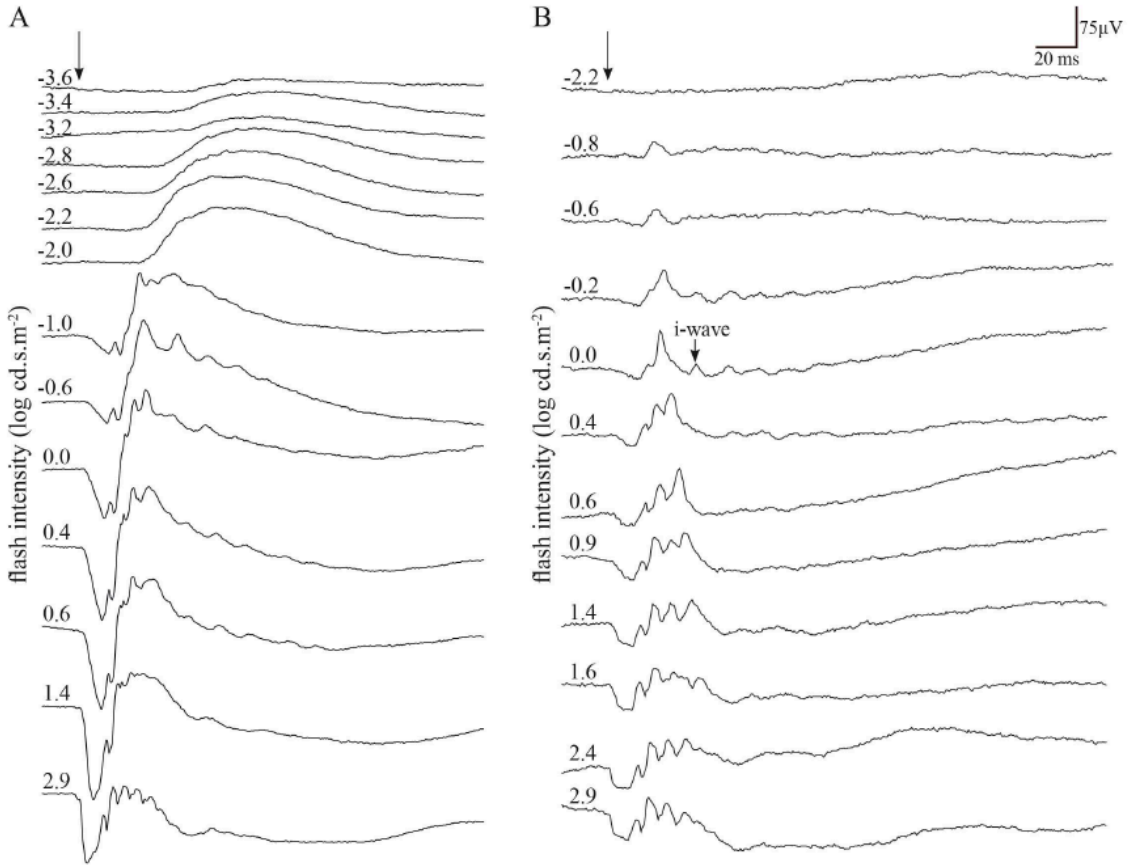

Figure 4-4 ERG responses to stimuli of increasing flash intensity, from top to bottom, in the dark-adapted eye (A) and in the light-adapted eye (B) of a representative Green Monkey (*Chlorocebus sabaeus*). Vertical arrow indicates flash onset. Horizontal calibration, 20 ms; vertical calibration, 75 µV.

The photopic hill effect

In the recordings of light-adapted eyes, the amplitude of the a-wave augments regularly with the gradual increase in intensity of the stimulus, while amplitude of the b-wave first increases to a maximum (V_{max}), and finally decreases with presentation of progressively brighter stimuli. This effect has been well demonstrated in humans [32]. The photopic flash ERG of the Green Monkey includes a post b-wave component identified as the i-wave that is

best seen using the standard flash (0.0 log cd.s.m^{-2}) after light adaptation (Figure 4-4).

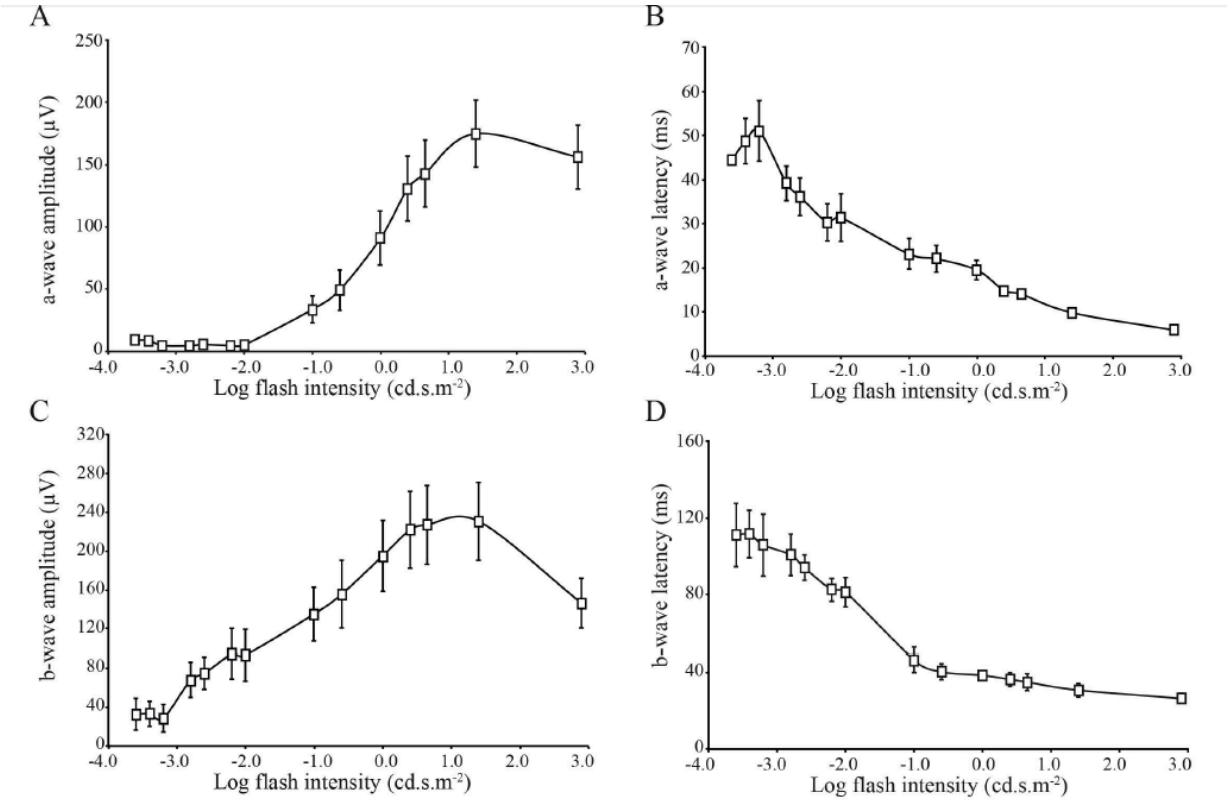

Figure 4-5 Response versus intensity function for the a-wave amplitude (A), a-wave latency (B), b-wave amplitude (C), and b-wave latency (D) of the scotopic ERG. Each data point indicates average (± SEM) of all 15 monkeys.

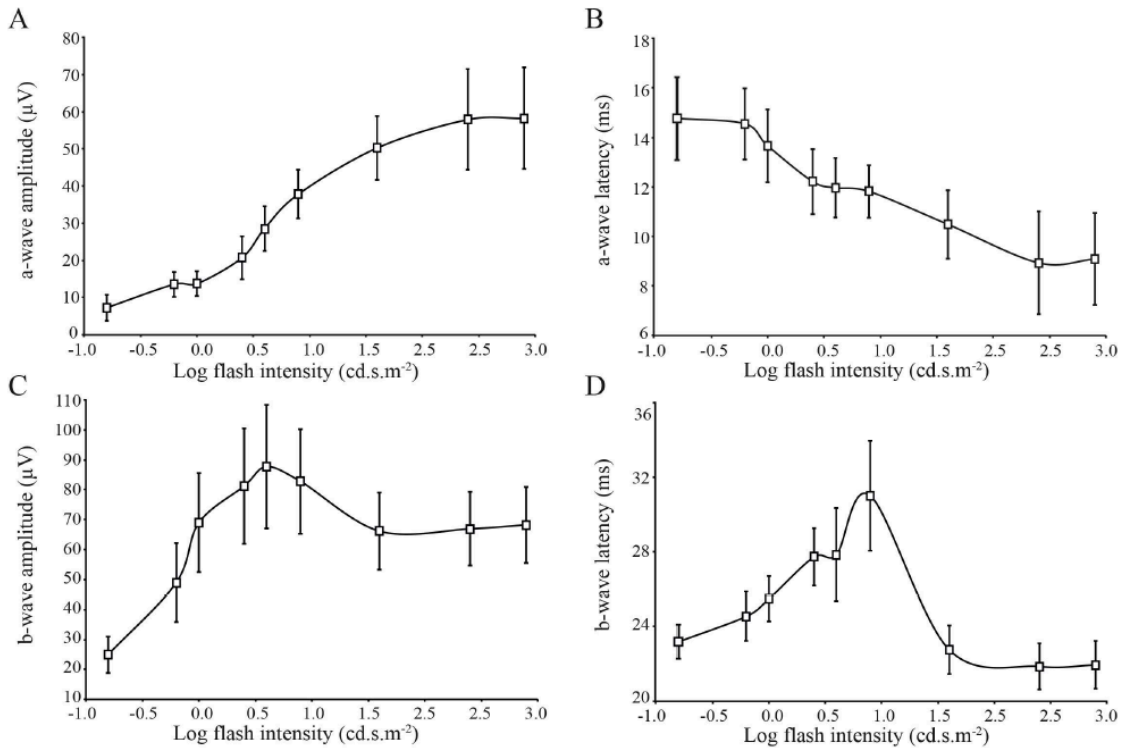

Figure 4-6 Response versus intensity function for the a-wave amplitude (A), a-wave latency (B), b-wave amplitude (C), and b-wave latency (D) of the photopic ERG under rod-suppressing background illumination (30 cd.m^{-2}). Each data point indicates average (± SEM) of all 15 monkeys.

Discussion

These results provide normative values for the standard ERG protocol in Green Monkeys, with the general finding that full field flash ERG responses in these monkeys are similar to those in humans. We report the 5 responses in Green Monkeys as recommended by ISCEV, which are the standard protocols for ERG in humans [4] and cynomolgus monkeys [27]. The ISCEV consensus standard provides the basis for stable comparison between research laboratories and clinical ERG recordings. However, information about additional stimuli is often necessary for specific applications, such as in considering the higher retinal illuminances for rod responses in human neonates [33], and dark-adapted flicker in retinitis pigmentosa [34]. Throughout the present study, particular attention was paid to IOP and pupil

dilatation, with an aim to reduce variability (Table 1). Human and non-human primates are mammals that share similar vascular anatomy of the eyes, and have a macular/foveal region and multiple cone types that offer them high visual acuity and color vision. It is notable that our values of amplitude and latency in Green Monkeys are closer to those in humans [4], relative to corresponding results in cynomolgus monkeys [27], [35], and it may be that the differences are as much attributable to laboratories they are to species differences.

The ERG responses to the standard tests in Green Monkeys were similar to the responses in humans even though the axial length of Green Monkey eyes is a bit lower than humans, i.e. 18 mm in the Green Monkey and 24 mm in humans [36]. In particular, the shape and latency of the curves are highly comparable. We can safely assume that the higher amplitudes found in man [31] are due to the large diameter and larger retinal surface area of the human eye, which have a direct relation with the net electric field and thus on the measured responses. Accordingly, differences in amplitude but not latency have been observed in human subjects with high myopia or small refractive error, as expected due to differences in axial length [37]. In the present study, slight differences in amplitude were occasionally noticed in the other eye, but were in every case within the 10% inter-ocular amplitude differences in normal human subjects [38]. Furthermore, the standard amplitude of OPs was a bit larger than the range in cynomolgus monkeys [27], but lower than those of humans [39]. The implicit times of OPs were within the same range for monkeys and humans.

Full-field stimulation, as employed presently, is the most effective way of eliciting an ERG representative of the entire population of cones and rods in the primate retina [40].

Replicable peak amplitudes and implicit times can therefore be obtained with full-field ERG recordings. Recordings of photopic ERGs are used to assess the functioning of the cone system in humans and animals. As defined above, in response to progressively brighter stimuli, the b-wave of the photopic ERG gradually increases in amplitude, attains a plateau (the maximal b-wave amplitude which is reached for a narrow range of intensities, V_{max}), and then rapidly decreases with further increments in the luminance of the flash. This unique luminance–response function was originally termed "the photopic hill" [41]. The photopic hill in the primate ERG results mainly from two factors: the reduction of the ON-component amplitude at higher intensities and the delay in the positive peak of the OFF-component at higher intensities [42]. Scotopic ERGs, on the other hand, are used to evaluate the integrity of the rod system in humans and animals [2], [43].

At about 20 ms after a typical human photopic b-wave, a second positive signal is seen, the i-wave [44]. This feature is common to the photopic ERG of many species except mice and rats [28]. The i-wave amplitudes and latencies in Green Monkeys were similar to those reported previously for most mammals [28]. It is interesting to note that in humans, the amplitude of the i-wave saturates at a dimmer flash intensity than that needed to evoke a b-wave of maximal amplitude [45].

In general, it is important to consider how best to interpret a finding of altered electroretinogram in the clinic and in animal models. Normal scotopic and photopic a-waves indicate normal functioning of rod and cone outer segments. In particular, it has been proposed that the scotopic ERG b-wave is the result of depolarization of ON-bipolar cells [46], [47].

Consequently, a pathological or pharmacological decrease in amplitude of the b-wave of the rod ERG and of the scotopic standard combined ERG might both result from a postsynaptic abnormality in the rod ON-pathway, plausibly due to a postsynaptic abnormality in the cone ON-pathway because it generates this response [46], [48]. The ON-pathway is often considered to influence contrast sensitivity [49], [50]. For instance, impairments of contrast sensitivity are reported clinically in disorders with ON-pathway dysfunction [51], such as melanoma-associated retinopathy [52], congenital stationary night blindness [53].

Specific values for amplitude and b-wave implicit time will necessarily differ between laboratories due to minor variations in recording electrodes, equipment, and protocol, not to mention species differences. Among the various technical factors potentially impacting the ERG amplitudes include contact lens placement, the structural integrity of the corneal surface, pupil size, and even IOP. It is important to consider these factors when interpreting the results. Nevertheless, in order to control for these technical and biological influences, we collected the physiological relevant data before and after the ERG recordings for each monkey, so as to provide a stable basis for comparison in future studies of pharmacology and disease models in the Green Monkey. The present results entailing recordings performed in accordance with the ISCEV, and with the ERG encompassing 30 minutes of dark adaptation correspond very well with similar results obtained in humans. Thus, the Green Monkey promises to serve as an excellent animal model for retinal function testing, for example in toxicity evaluation.

Acknowledgements

We would like to thank Dr. Pierre Lachapelle (McGill University, Montreal, Quebec) for his constructive comments. We also thank Ms. Anna Polosa, M.Sc. for her assistance in carrying out the calibration of the LKC apparatus and developing the protocol. We are very grateful to Dr. Amy Beierschmitt and Mr. Maurice Matthew, M.Sc. of the Behavioral Science Foundation Laboratories of St-Kitts for their expert technical assistance in handling the monkeys. We acknowledge Inglewood Biomedical Editing (www.inglewoodbiomedediting.com) for expert revision and editing of the manuscript.

References

1. Steinberg RH, Linsenmeier RA, Griff ER (1985) Chapter 2 Retinal pigment epithelial cell contributions to the electroretinogram and electrooculogram. Prog Retin Res 4: 33-66.

2. Frishman LJ (2006) Origins of the electroretinogram. In: Heckenlively JR, Arden GB, editors. Principles and Practice of Clinical Electrophysiology of Vision. The MIT Press: Cambridge, MA, pp 139–183.

3. Curcio C, Sloan K, Packer O, Hendrickson A, Kalina R (1987) Distribution of cones in human and monkey retina: individual variability and radial asymmetry. Science 236: 579-582.

4. Marmor MF, Fulton AB, Holder GE, Miyake Y, Brigell M, et al. (2009) ISCEV Standard for full-field clinical electroretinography (2008 update). Doc Ophthalmol 118: 69-77.

5. Palmour RM, Mulligan J, Howbert JJ, Ervin F (1997) Of monkeys and men: vervets and the genetics of human-like behaviors. Am J Hum Genet 61: 481-488.

6. Jasinska AJ, Service S, Levinson M, Slaten E, Lee O, et al. (2007) A genetic linkage map of the vervet monkey (Chlorocebus aethiops sabaeus). Mamm Genome 18: 347-360.

7. Ptito M, Herbin M, Boire D, Ptito A (1996) Neural bases of residual vision in hemicorticectomized monkeys. Prog Brain Res 112: 385-404.

8. Papia MF, Burke MW, Zangenehpour S, Palmour RM, Ervin FR, et al. (2010) Reduced soma size of the M-neurons in the lateral geniculate nucleus following foetal alcohol exposure in non-human primates. Exp Brain Res 205: 263-271.

9. Burke MW, Kupers R, Ptito M (2012) Adaptive neuroplastic responses in early and late hemispherectomized monkeys. Neural Plast 2012: 852423.

10. Herbin M, Boire D, Ptito M (1997) Size and distribution of retinal ganglion cells in the St. Kitts green monkey (Cercopithecus aethiops sabeus). J Comp Neurol 383: 459-472.

11. Theoret H, Boire D, Ptito M (2000) Retinal projections to the pregeniculate nucleus in the hemispherectomized monkey. Brain Res Bull 53: 239-243.

12. Boire D, Theoret H, Ptito M (2001) Visual pathways following cerebral hemispherectomy. Prog Brain Res 134: 379-397.

13. Theoret H, Boire D, Herbin M, Ptito M (2001) Anatomical sparing in the superior colliculus of hemispherectomized monkeys. Brain Res 894: 274-280.

14. Boire D, Theoret H, Ptito M (2002) Stereological evaluation of neurons and glia in the monkey dorsal lateral geniculate nucleus following an early cerebral hemispherectomy. Exp Brain Res 142: 208-220.

15. Burke MW, Palmour RM, Ervin FR, Ptito M (2009) Neuronal reduction in frontal cortex of primates after prenatal alcohol exposure. Neuroreport 20: 13-17.

16. Burke M, Zangenehpour S, Bouskila J, Boire D, Ptito M (2009) The gateway to the brain: dissecting the primate eye. J Vis Exp: e1261.

17. Bouskila J, Burke MW, Zabouri N, Casanova C, Ptito M, et al. (2012) Expression and localization of the cannabinoid receptor type 1 and the enzyme fatty acid amide hydrolase in the retina of vervet monkeys. Neuroscience 202: 117-130.

18. Bouskila J, Javadi P, Casanova C, Ptito M, Bouchard JF (2013) Muller cells express the cannabinoid CB2 receptor in the vervet monkey retina. J Comp Neurol 521: 2399-2415.

19. Bouskila J, Javadi P, Casanova C, Ptito M, Bouchard JF (2013) Rod photoreceptors express GPR55 in the adult vervet monkey retina. PLoS One 8: e81080.

20. Mikula S, Trotts I, Stone JM, Jones EG (2007) Internet-enabled high-resolution brain mapping and virtual microscopy. NeuroImage 35: 9-15.

21. Mikula S, Stone JM, Jones EG (2008) BrainMaps.org - Interactive High-Resolution Digital Brain Atlases and Virtual Microscopy. Brains Minds Media 3: bmm1426.

22. Woods RP, Fears SC, Jorgensen MJ, Fairbanks LA, Toga AW, et al. (2011) A web-based brain atlas of the vervet monkey, Chlorocebus aethiops. NeuroImage 54: 1872-1880.

23. Osterberg G (1935) Topography of the layer of rods and cones in the human retina. Actaophthal suppi 6: 11-97.

24. Jacobs GH (2008) Primate color vision: a comparative perspective. Vis Neurosci 25: 619-633.

25. Finlay BL, Franco EC, Yamada ES, Crowley JC, Parsons M, et al. (2008) Number and topography of cones, rods and optic nerve axons in New and Old World primates. Vis Neurosci 25: 289-299.

26. Buist DP, Heywood R (1982) A standardized procedure for electroretinographic examination of rhesus monkeys (Macaca mulatta). Lab Anim Sci 32: 91-93.

27. Bee WH (2001) Standardized electroretinography in primates: a non-invasive preclinical tool for predicting ocular side effects in humans. Curr Opin Drug Di De 4: 81-91.

28. Rosolen SG, Rigaudiere F, LeGargasson JF, Chalier C, Rufiange M, et al. (2004) Comparing the photopic ERG i-wave in different species. Vet Ophthalmol 7: 189-192.

29. Rangaswamy N, Frishman L, Dorotheo EU, Schiffman J, Bahrani H, et al. (2004) Photopic ERGs in patients with optic neuropathies: comparison with primate ERGs after pharmacologic blockade of inner retina. Invest Ophthalmol Vis Sci 45: 3827-3837.

30. Viswanathan S, Frishman LJ, Robson JG, Walters JW (2001) The photopic negative response of the flash electroretinogram in primary open angle glaucoma. Invest Ophthalmol Vis Sci 42: 514-522.

31. Jacobi PC, Miliczek KD, Zrenner E (1993) Experiences with the international standard for clinical electroretinography: normative values for clinical practice, interindividual and intraindividual variations and possible extensions. Doc Ophthalmol 85: 95-114.

32. Rufiange M, Dassa J, Dembinska O, Koenekoop RK, Little JM, et al. (2003) The photopic ERG luminance-response function (photopic hill): method of analysis and clinical application. Vision Res 43: 1405-1412.

33. Birch DG, Birch EE, Hoffman DR, Uauy RD (1992) Retinal development in very-low-birth-weight infants fed diets differing in omega-3 fatty acids. Invest Ophthalmol Vis Sci 33: 2365-2376.

34. Berson EL, Gouras P, Hoff M (1969) Temporal aspects of the electroretinogram. Arch Ophthalmol 81: 207-214.

35. Bee WH, Korte R, Vogel F (1995) Electroretinography in the non-human primate as a standardized method in toxicology. In: Weisse I, Hockwin O, Green K, Tripathi R, editors. Ocular Toxicology. Springer US. pp. 53-61.

36. Howland HC, Merola S, Basarab JR (2004) The allometry and scaling of the size of vertebrate eyes. Vision Res 44: 2043-2065.

37. Westall CA, Dhaliwal HS, Panton CM, Sigesmun D, Levin AV, et al. (2001) Values of electroretinogram responses according to axial length. Doc Ophthalmol 102: 115-130.

38. Rotenstreich Y, Fishman GA, Anderson RJ, Birch DG (2003) Interocular amplitude differences of the full field electroretinogram in normal subjects. Br J Ophthalmol 87: 1268-1271.

39. Birch DG, Anderson JL (1992) Standardized full-field electroretinography. Normal values and their variation with age. Arch Ophthalmol 110: 1571-1576.

40. Weleber RG (1981) The effect of age on human cone and rod ganzfeld electroretinograms. Invest Ophthalmol Vis Sci 20: 392-399.

41. Wali N, Leguire LE (1992) The photopic hill: a new phenomenon of the light adapted electroretinogram. Doc Ophthalmol 80: 335-345.

42. Ueno S, Kondo M, Niwa Y, Terasaki H, Miyake Y (2004) Luminance dependence of neural components that underlies the primate photopic electroretinogram. Invest Ophthalmol Vis Sci 45: 1033-1040.

43. Holopigian K, Seiple W, Greenstein VC, Hood DC, Carr RE (2001) Local cone and rod system function in patients with retinitis pigmentosa. Invest Ophthalmol Vis Sci 42: 779-788.

44. Freund PR, Watson J, Gilmour GS, Gaillard F, Sauve Y (2011) Differential changes in retina function with normal aging in humans. Doc Ophthalmol 122: 177-190.

45. Rufiange M, Rousseau S, Dembinska O, Lachapelle P (2002) Cone-dominated ERG luminance-response function: the Photopic Hill revisited. Doc Ophthalmol 104: 231-248.

46. Tian N, Slaughter MM (1995) Correlation of dynamic responses in the ON bipolar neuron and the b-wave of the electroretinogram. Vision Res 35: 1359-1364.

47. Robson JG, Frishman LJ (1995) Response linearity and kinetics of the cat retina: the bipolar cell component of the dark-adapted electroretinogram. Vis Neurosci 12: 837-850.

48. Stockton RA, Slaughter MM (1989) B-wave of the electroretinogram. A reflection of ON bipolar cell activity. J Gen Physiol 93: 101-122.

49. Knapp AG, Ariel M, Robinson FR (1988) Analysis of vertebrate eye movements following intravitreal drug injections. I. Blockade of retinal ON-cells by 2-amino-4-phosphonobutyrate eliminates optokinetic nystagmus. J Neurophysiol 60: 1010-1021.

50. Sieving PA (1993) Photopic ON- and OFF-pathway abnormalities in retinal dystrophies. Trans Am Ophthalmol Soc 91: 701-773.

51. Iwakabe H, Katsuura G, Ishibashi C, Nakanishi S (1997) Impairment of pupillary responses and optokinetic nystagmus in the mGluR6-deficient mouse. Neuropharmacology 36: 135-143.

52. Wolf JE, Arden GB (1996) Selective magnocellular damage in melanoma-associated retinopathy: comparison with congenital stationary nightblindness. Vision Res 36: 2369-2379.

53. Barnes CS, Alexander KR, Fishman GA (2002) A distinctive form of congenital stationary night blindness with cone ON-pathway dysfunction. Ophthalmology 109: 575-583.

Chapter 5: Cannabinoid receptors CB1 and CB2 modulate the electroretinographic waves in vervet monkeys

To be submitted to IOVS (January 2015)

Cannabinoid receptors CB1 and CB2 modulate the electroretinographic waves in vervet monkeys

Pasha Javadi[1], Joseph Bouskila[1, 2], Vanessa Harrar[1], Amy Beierschmitt[3], Roberta Palmour[4], Christian Casanova[1], Jean-François Bouchard[1], and Maurice Ptito[1, 5]

[1]School of Optometry, University of Montreal, Montreal, QC, Canada
[2]Biomedical Sciences, Faculty of Medicine, University of Montreal, Montreal, QC, Canada
[3]St-Kitts Behavioral Science Foundations, St-Kitts and Nevis, West Indies
[4]Department of Human Genetics, McGill University, Montreal, QC, Canada
[5]Laboratory of Neuropsychiatry, Psychiatric Centre Copenhagen and BRAINLab, Department of Neuroscience and Pharmacology, University of Copenhagen, Copenhagen, Denmark.

Keywords: CB1R, CB2R, ERG, a-wave, b-wave, monkey.

Correspondence should be addressed to:
Maurice Ptito, PhD
School of Optometry, room 260-7
3744 Jean-Brillant Street,
University of Montreal,
Montreal, Quebec, Canada, H3T 1P1

Running title: Role of CB1R and CB2R in the monkey retina

Financial Support: The Natural Science and Engineering Research Council of Canada (6362-2012, MP; 311892-2010, JFB; 194670-2014, CC) and the Canadian Institutes of Health Research (CIHR) (MOP-86495, JFB, MOP-301710, JFB and CC) supported this work. JB received support from a Frederick Banting and Charles Best Canada Graduate Scholarship Doctoral Award from CIHR. MP is Harland Sanders Chair professor in Visual Science. JFB is supported by a "Chercheur-Boursier Senior" from Fonds de Recherche du Québec – Santé (FRQ-S).

Abstract

The expression patterns of the endocannabinoid (eCB) receptors and related metabolic components are well documented in rodents and primates. While the cannabinoid receptor 1 (CB1R) is mainly expressed throughout the central retina, the cannabinoid receptor 2 (CB2R) is exclusively found in the retinal glia (Müller cells) of vervet monkeys. However, in primates, the role of these receptors in retinal function remains elusive. To study the retinal neural correlates that accompany the disruption of eCB signaling, we recorded the neural activity of the retina in adult vervet monkeys. We evaluated scotopic and photopic electroretinogram (ERG) response changes before and after blockade of the main cannabinoid receptors CB1R and CB2R by intravitreal administration of their specific antagonist (AM251 and AM630, respectively). Our results showed different effects of CB1R and CB2R on the ERG in photopic conditions: at low flash intensities, only the blockade of CB1R decreased the amplitude of the a -and b-waves, while at high flash intensities, blockade of CB2R increased the amplitude of both a- and b-waves. Moreover, blocking CB1R and CB2R resulted in an increase in the latency of the a- and b-waves of the ERG. In scotopic conditions, following dark-adaptation, blockade of CB1R and CB2R reduced the amplitude of the a-wave at high intensities only and decreased the b-wave at low intensities. Significant increases in latency were also observed by blocking cannabinoid receptors. Our results suggest an interaction between these retinal eCB receptors in the genesis and modulation of the ERG in normal vervet monkeys.

Introduction

The eCB system is mainly composed of cannabinoid receptor 1 (CB1R), cannabinoid receptor 2 (CB2R), their endogenous ligands (anandamide, 2-arachidonoylglycerol), and metabolizing enzymes. The physiological and psychological effects of cannabinoids can be detected almost everywhere in the body due to the abundance of their specific receptors. Expression patterns of CB1R and CB2R are well documented in the retina of numerous species such as rodents and primates (Straiker et al., 1999; Yazulla et al., 1999; Lopez et al., 2011; Cécyre et al., 2013), including vervet monkeys (Bouskila et al., 2012; Bouskila et al., 2013a). In rodents, CB1R and CB2R are expressed in many retinal cell types, particularly cone and rod photoreceptors, horizontal cells, amacrine cells, bipolar and ganglion cells (Zabouri et al., 2011; Cécyre et al., 2013). In vervet monkeys, CB1R is mainly found in cones of the central retina, in rod spherules with very low expression, horizontal cells, bipolar cells, amacrine and ganglion cells. CB2R, on the other hand, is strictly expressed in glial Müller cells (Bouskila et al., 2012; Bouskila et al., 2013a, b). Beyond the retina, the expression pattern of CB1R is also well documented in the dorsal lateral geniculate nucleus (Javadi et al., 2015) and primary visual cortex (Eggan and Lewis, 2007) of primates.

Most of our knowledge on the role of cannabinoids in human vision comes from reports, anecdotes and studies on cannabis consumers (for review see Schwitzer et al., 2014). Besides the well-known "red eye" effect (vasodilation) of marijuana and reduction of intraocular pressure (Flom et al., 1975; Green, 1979; Porcella et al., 1998), the functional effects of eCBs on the visual system are still not completely defined. Nevertheless, the administration of cannabinoids produces some alterations in the human visual system. Indeed, case studies suggested the existence of cannabis-mediated visual effects in humans,

particularly an increase in glare recovery at low contrast (Adams et al., 1978), a reduction in Vernier and Snellen acuities (Kiplinger et al., 1971; Adams et al., 1975), an increase dim light vision (Dawson et al., 1977; Merzouki and Mesa, 2002; Russo et al., 2004), a blurred vision (Noyes et al., 1975), changes in color discrimination, and an increase in photosensitivity (Dawson et al., 1977). Most of the latter effects have a retinal component. These various behavioral effects might be due to neurochemical changes induced by retinal eCB system. Indeed, a variety of physiological effects of cannabinoids have been reported for every retinal cell type in bovines, guinea pigs, rodents, and fishes (for review see Yazulla, 2008; Schwitzer et al., 2014). In the bovine retina, the activation of CB1R increases monoamine oxidase (Gawienowski et al., 1982). In the guinea pig retina, stimulation of CB1R results in the inhibition of dopamine release (Schlicker et al., 1996). In the rat retina, activation of cannabinoid receptors modulates [35S]GTPγ S-binding and voltage-dependent membrane currents in photoreceptors, bipolar cells and ganglion cells (Fan and Yazulla, 1999; Straiker et al., 1999; Yazulla et al., 2000; Fan and Yazulla, 2003; Straiker and Sullivan, 2003). Cannabinoid agonists increase the cone response to light offset in the goldfish retina (Struik et al., 2006).

The electroretinogram (ERG) is a useful tool for assessing retinal function by measuring the electrical responses of all populations of retinal cells principally photoreceptors (cones and rods), bipolar cells, and Müller cells (Steinberg et al., 1985). The ERG waves include two main components: the negative amplitude (a-wave) and the positive one (b-wave). The a-wave mainly reflects the response of the outer photoreceptor layer (rods and cones) to light (Armington et al., 1952). The generation of the b-wave, the major component of the ERG, is attributed to the inner retina, mainly the depolarization of bipolar and Müller cells

(Miller and Dowling, 1970; Stockton and Slaughter, 1989; Wen and Oakley, 1990). Specific stimuli and recording environments are selected to separate the component of the ERG and target particular populations of retinal cells; for instance, the function of the rods assessed in dark-adapted eyes under scotopic conditions (Robson et al., 2003). Inversely, the optimal setting to gauge the cone responses is the use of high-intensity flashes with a more elevated frequency in photopic conditions (Robson et al., 2003). However, it is worth stressing that it is impossible to register a pure response from either photoreceptor and the resulting response to light comes from both cones and rods (Rosolen et al., 2008).

The abundance of the CB1R and CB2R in the visual system, especially in the retina, indicates that they should play a role in vision. To the best of our knowledge, there is only one recent study that focused on the detailed function and morphology of the retina by using CB1R (*cnr1*$^{-/-}$) and CB2R (*cnr2*$^{-/-}$) knockout mice (Cécyre et al., 2013). Using ERG to measure the global evoked potential of various cells of the retina, the authors showed that no significant effect was observed in *cnr1*$^{-/-}$ mice under photopic and scotopic conditions. However, in *cnr2*$^{-/-}$ mice, the b-wave amplitude required more light adaptation time to reach stable values under photopic conditions and the a-wave amplitude increased in scotopic conditions (Cécyre et al., 2013). Based on the expression pattern of CB2R, mainly in Müller cells of the monkey retina, we have recently proposed that CB2R must play a role in the generation of the b-wave (Bouskila et al 2013a).

Given the paucity of studies on the putative role of the retinal eCB system in vision, we investigated the changes in retinal function as measured by ERG in adult vervet monkeys after acute blockade of CB1R and CB2R by their antagonists AM251 and AM630, respectively.

Material and Methods

Choice of species. Vervet monkeys are progressively employed in biomedical research with a second citation record among the non-human primates after the rhesus macaque (Jasinska et al., 2013). Vervets are very similar in physiology and behavior to macaque, and they are more accessible, disease-free with less health and safety risks. Vervet monkeys have a foveal binocular vision with a high cone density that decreases with eccentricity, trichromatic color vision and a six-layered dorsal lateral geniculate nucleus (Herbin et al., 1997; Boire et al., 2001). Recently, we have standardized a non-invasive, painless ERG method for vervet monkeys (Bouskila et al., 2014) that showed recordings highly comparable to macaques (Bee, 2001) and humans (McCulloch et al., 2014).

Subjects. Seventeen vervet monkeys (*Chlorocebus sabaeus*) were tested before and after the intravitreal administration of the cannabinoid receptor antagonists. Six of those monkeys were injected with AM251, and another 6 were injected with AM630. An additional 5 monkeys were injected with the vehicle (DMSO) in order to provide post-injection control values (Table 1). The animals were fed with primate chow (Harlan Teklad High Protein Monkey Diet; Harlan Teklad, Madison, WI) and fresh local fruits, with water available *ad libitum.* Infant Green Monkeys are born into an outdoor social group comprising several females, one male and other offspring of the same general age. Infants live with their parents until about 8 months of age, at which time they move to a playpen with 5 other age-mates. The natal cage is equipped with swings, perches, hiding places and jungle gyms. We do put in toys, but the animals are so busy playing with one another that they ignore the toys. In the smaller playpens, there are also swings, perches and climbing spots, as well as puzzle feeders and

foraging boards. At about 18 months of age, youngsters graduate to a large, outdoor peer group of about 16 animals (like-ages, both sexes) where there are tunnels, swings, ladders, jungle-gyms and a variety of manipulanda (more complex puzzle feeders; natural forage opportunities, such as brush and vines; foraging boards). Plastic chain and baited balls are popular toys, but vervets of this age are uninterested in most other commercially available toys. All experiments were performed according to the guidelines of the Canadian Council on Animal Care (CCAC) and the Association for Research in Vision and Ophthalmology (ARVO) Statement for the Use of Animals in Ophthalmic and Vision Research. The experimental protocol was also reviewed and approved by the local Animal Care and Use Committee (University of Montreal, protocol # 14-007) and the Institutional Review Board of the Behavioral Science Foundation that is recognized by the CCAC. None of the animals were sacrificed for this study.

Table 5- 2 Profile of the animals used in this study

	Animal ID	Sex	Weight (Kg)	Injection	Concentration
1	08275	Female	2.92	DMSO	100%/100 µl
2	07862	Female	2.87	DMSO	100%/100 µl
3	08376	Female	2.85	DMSO	100%/100 µl
4	08456	Male	3.55	DMSO	100%/100 µl
5	08560	Female	3.32	DMSO	100%/100 µl
6	08297	Female	2.75	AM251	1 mg/100 µl
7	07866	Female	2.95	AM251	1 mg/100 µl
8	01336-7-1-3	Female	2.95	AM251	1 mg/100 µl
9,10	08336	Female	2.92	AM251	0.3 mg/100 µl
11,12	08377	Female	2.85	AM630-AM251	0.3 -1 mg/100 µl
13	05010-6	Male	3.72	AM630-AM251	0.3 -1 mg/100 µl
14	09093-1-3-1	Female	3.05	AM630	0.3 mg/100 µl
15	05322-6	Female	3.25	AM630	0.3 mg/100 µl
16	08498	Female	2.86	AM630	0.3 mg/100 µl
17	08590	Female	2.94	AM630	0.3 mg/100 µl

Animal preparation for ERG recordings. All procedures were in accordance with the standard protocol of electroretinography in vervet monkeys (Bouskila et al., 2014). Briefly, all animals were sedated with ketamine (10 mg/kg; Troy Laboratories, Glendenning, New South Wales, Australia) and xylazine (1 mg/kg; Lloyd Laboratories, Shenandoah, IA, USA) intramuscular injection to maintain an adequate level that prevents the animals from moving and blinking. The sedation mixture shows no effect on ERG results (Nair et al., 2011). With 1% tropicamide (Mydriacyl®) and 2.5% phenylephrine hydrochloride (Mydfrin®) (Alcon Laboratories, Fort Worth, TX, USA), the pupils were fully dilated (approximately 9 mm in diameter), and the accommodation paralyzed. The cornea was anesthetized with 0.5% proparacaine hydrochloride (Alcaine®; Alcon Laboratories, Fort Worth, TX, USA) treatment. To prevent corneal drying, the eyes were moisturized frequently with 2.5% methylcellulose (Gonak; Akorn, Inc., Buffalo Grove, IL, USA). Body temperature was maintained between 36.5°C and 38°C with a heating pad. After a recording session of about two hours, animals were sent back to their prior natural settings after a period of isolated recovery.

Intravitreal Injection. The selective CB1R antagonist AM251 was purchased from Cayman Chemicals (Ann Arbor, MI, USA). The selective CB2R antagonist AM630 was purchased from Tocris (Tocris Bioscience, Ellisville, USA). Both antagonists were diluted in DMSO under sterile condition. Assuming no leakage, the final concentration was 0.01 mg/µl for AM251 and 0.003 mg/µl for AM630. After inspection and examination of the eyes, the cornea was cleaned with 5% povidone-iodine solution for 45 seconds. A topical anesthetic was also applied over the injection site using pilocarpine proparacaine. The conjunctival and corneal

surfaces were then moistened with methylcellulose (Gonak; Akorn, Inc., Buffalo Grove, IL, USA). The eye was covered with sterile coatings and a Barraquer eye speculum (1.75 inches, 10 mm wide small blades) was placed. In a 1 mL syringe with a 25G needle, 100 µL drug solution was injected 2 mm posterior to the corneal limbus into the vitreous cavity. The injection site was compressed for a minute using a sterile cotton swab to avoid reflux on removal of the needle. The back of the eyes was inspected using an ophthalmoscope before and after the intravitreal injection to determine the integrity of the retina. No substantial difference in intraocular pressure was observed before and ten minutes after the intravitreal administration. As a follow up, the animal eyes were checked every day for seven days and the topical antibiotic ointment was administered.

Visual Stimulation. Full-field stimulation was produced with a Ganzfeld light source (UTAS E-3000 electrophysiology equipment; LKC Technologies, Inc., Gaithersburg, MD, USA) that was placed in front of the animal's face. The ERG was acquired from both injected and non-injected eyes simultaneously. The ERGs were evoked by flashes of light of intensity ranging from 0.00025 cd.sec.m^{-2} to 1000 cd.sec.m^{-2} (duration <5 ms) delivered in full-field conditions. During the 30-minute dark adaptation period, every 3 minutes, ERGs were recorded using a constant stimulus of approximately 0.025 cd.s.m^{-2}. Xenon flash luminance of 2.5 to 800 cd.sec.m^{-2} (0 dB to 20 dB in LKC units) was used for photopic ERGs and LED flash luminance of $2.5x10^{-5}$ to 6 cd.sec.m^{-2} (-40 dB to 4 dB in LKC units) for scotopic ERGs. For light-adapted ERGs, a steady background-adapting field (30 cd.m^{-2}) was presented inside the Ganzfeld to saturate the rod system. Flash intensities and background luminance were

calibrated using a research radiometer (IL1700 Photometer, International Light Inc., Newburyport, MA, USA) with a SED033 detector placed at 36 cm from the source. Stimulus-intervals of at least 20 seconds were used at high intensities in the dark-adapted eyes.

ERG recording. All ERG procedures followed the ISCEV guidelines and recently published standardized ERG in vervet monkeys (Bouskila et al., 2014). Briefly, ERGs were recorded using corneal contact lens electrodes (Jet electrodes, Diagnosys LLC, Lowell, Massachusetts, USA) lying across the center of the cornea of each eye, moistened with 1% carboxymethylcellulose sodium (Refresh Celluvisc, Allergan Inc., Markham, ON, Canada). The jet electrodes were equipped with four small posts on the convex surface in order to keep the eyelids open. Reference and ground gold disc electrodes (model F-E5GH; Grass Technologies, Astro-Med, Inc., West Warwick, RI, USA) were respectively stick to the external canthi and forehead with adhesive paste (Ten20 conductive EEG paste; Kappa Medical, Prescott, AZ, USA). For the analysis of the waveforms, the a-wave amplitude, that mainly reflects the function of photoreceptors, was measured from the baseline to the peak of the a-wave for the combined rod-cone response and the single-flash cone response. As a measure of activity in the inner nuclear layer, the amplitude of the b-wave was measured from the trough of the a-wave to the peak of the b-wave for all responses. The peak latency was defined from the onset of the flash to the peak. Retinal response diagrams were drawn using Adobe Illustrator and processed in Adobe InDesign (Adobe Systems, software version CS5; San Jose, CA, USA). The recording procedure is summarized in Figure 5-1.

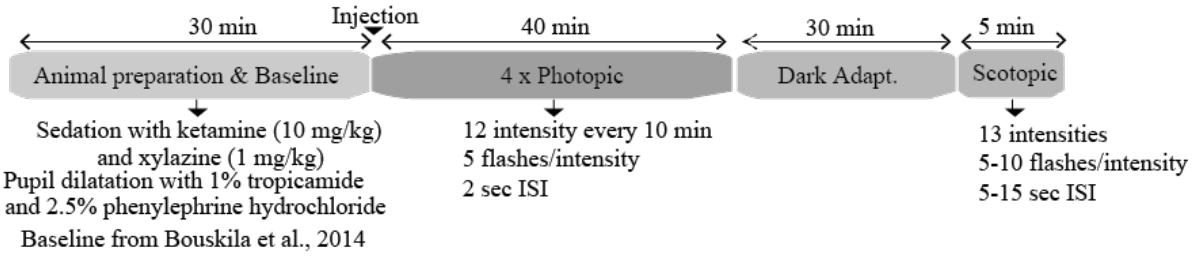

Figure 5- 1 Illustration of a typical ERG recording session after an intravitreal injection (modified from Bouskila et al., 2014).

Statistical analysis. The absolute trough (a-wave) and peak (b-wave) of the ERG curves were detected for each intensity. When no wave was detected, an amplitude and latency of 0 were recorded for that specific stimulus intensity. Outliers (±2 IQR) and blank values were replaced with a within-subject average obtained from stimuli with an intensity similar to the one being replaced. Additionally, when the ERG curve for weak stimulus intensities (<-2 log cd.sec/m^2) did not return to baseline 350 ms after the stimulus, the amplitude of the a- and b-waves were corrected to account for the shift. To determine the effect of injecting AM251 and AM630 in the eye, the standardized amplitude and latency post-injection values were calculated and then subtracted from the standardized baseline values (pre-injection, calculated individually for each monkey) and from the post-injection values obtained from the control group (DMSO-injected).

Results

Retinal Function in Photopic Conditions

To assess the effect of the blockade of CB1R and CB2R on the light-adapted retina, ERGs responses were registered before and 40 minutes after administration of DMSO, AM251 or AM630 in photopic conditions. The representative responses for stimuli of increasing intensity in different treatments (AM251 and AM630) are compared with the control vehicle (DMSO) (Figure 5-2). Latencies and amplitudes of a-waves and b-waves obtained during full-light conditions were submitted to a 12 (intensities levels) for 2 antagonists (AM251, AM630) mixed model ANOVA to demonstrate that the effect of the antagonist is modulated by the intensity of the flash ($p \leq 0.009$). A tendency of augmentation in amplitude of both a- and b-waves in higher intensities can be observed in both treatment groups AM251 and AM630 (Figure 5-2).

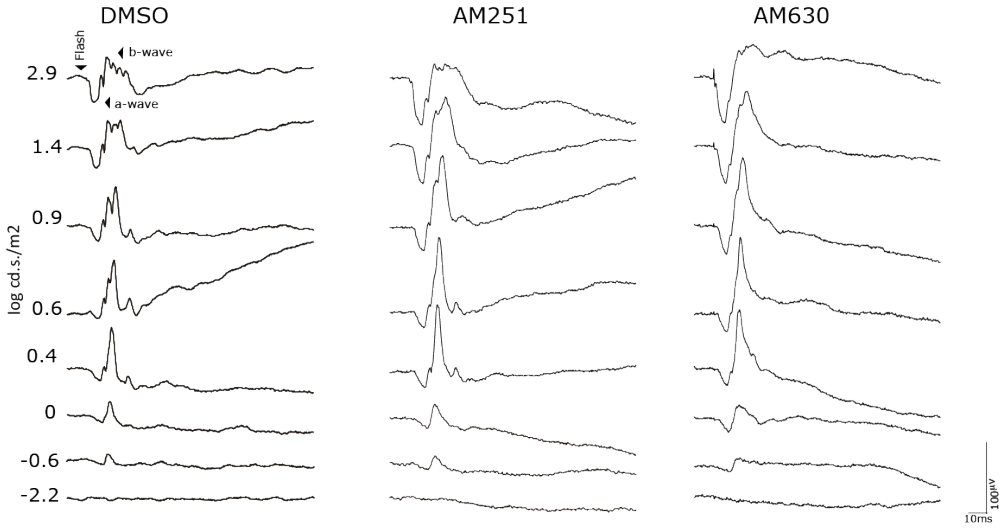

Figure 5- 2 Representative photopic ERGs recorded in animals that received the vehicle only (DMSO) as the baseline compared with the responses after injection of the CB1R antagonist AM251 (middle column) and the CB2R antagonist AM630 (right column). ERG recordings of each treated animal were established by presenting progressively brighter flashes indicated to the left of the traces as the log luminance (cd.s/m^2). Horizontal calibration, 10 ms; vertical calibration, 100 µV.

The Effect of Blockade of Cannabinoid Receptor in Photopic Conditions

To verify if the observed tendencies in Figure 5-2 are significant, the latencies and amplitudes of a- and b-waves obtained in a photopic condition with 12 intensity levels were calculated in different treatments using t-test for each stimulus intensity. At low flash intensities (0 log cd.sec/m^2 ≥), AM251 significantly decreases the amplitude of the a-wave and b-wave compare with DMSO (Figure 3, left column). Inversely, blockade of CB2R by AM630 increases the amplitude of both a- and b-waves in high flash intensities (Figure 5-3, left column). Moreover, blockade of CB1R, only increases the latency of a-wave in lower flash intensity. Both antagonists significantly delayed the time to peak time for b-wave in higher intensities (Figure 5-3, right column).

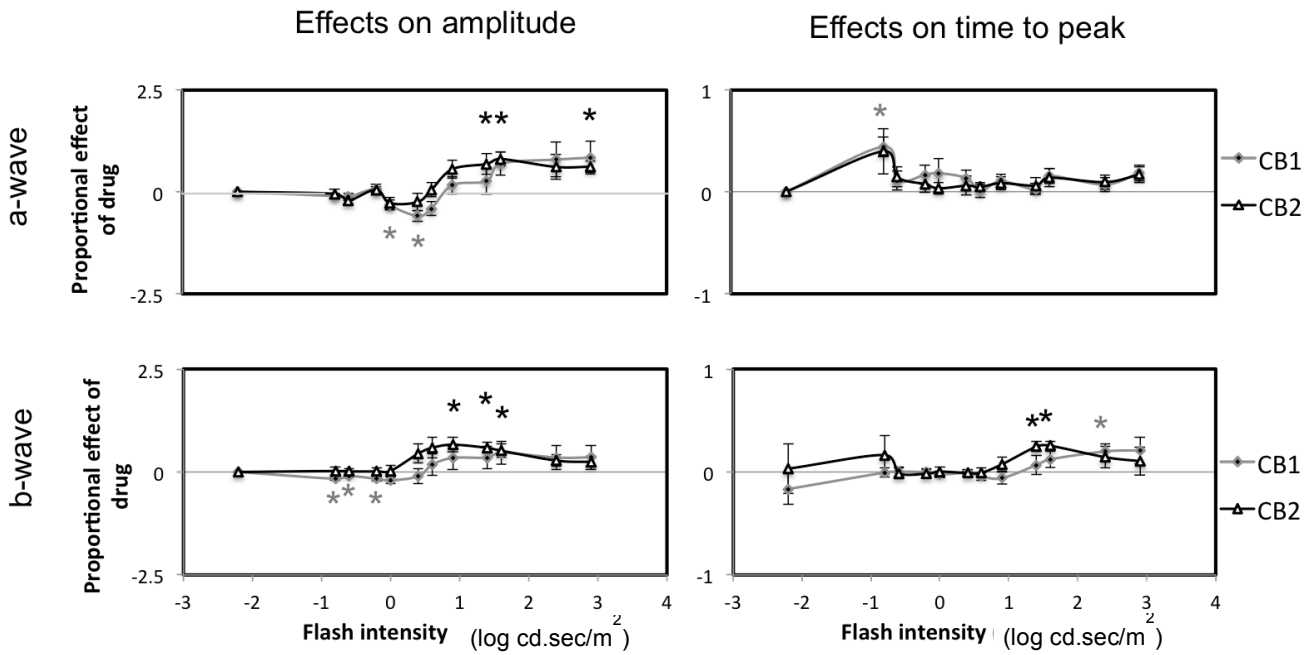

Figure 5- 3 The Effect of Blockade of Cannabinoid Receptor in Photopic Conditions. Amplitude (left) and latency (right) of a-wave (upper) and b-wave (lower) are plotted as a function of flash intensities presented in photopic conditions. Intensities at which the proportional differences are significantly different from DMSO control are identified with a * (indicating p<0.05 on a two-directional, one-sample t-test); Grey stars indicate that the CB1R is different from DMSO, and black stars indicate CB2R is different from DMSO. Values above zero indicate larger amplitudes or latencies following injection (relative to DMSO). Error bars represent standard error of the mean (SEM).

Retinal Function in Scotopic Condition

To assess the effect of the cannabinoid receptor antagonists on dark-adapted retina, ERGs responses were registered before and about 80 minutes after administration of DMSO, AM251 or AM630 in scotopic conditions. The representative responses for stimuli of increasing intensity in different treatments (AM251 and AM630) are compared with control (DMSO) (Figure 5-4). Latency and amplitude of the a-wave and b-wave obtained following dark adaptation were submitted to a 13 (intensities levels) for 2 antagonists (AM251, AM630) mixed model ANOVA to demonstrate that the effect of the drugs is modulated by the intensity of the flash ($p \leq 0.05$). A tendency of augmentation in amplitude of both a- and b-waves at higher intensities (0 log cd.sec/m^2 $\leq$) can be observed in both treatment groups (Figure 5-4).

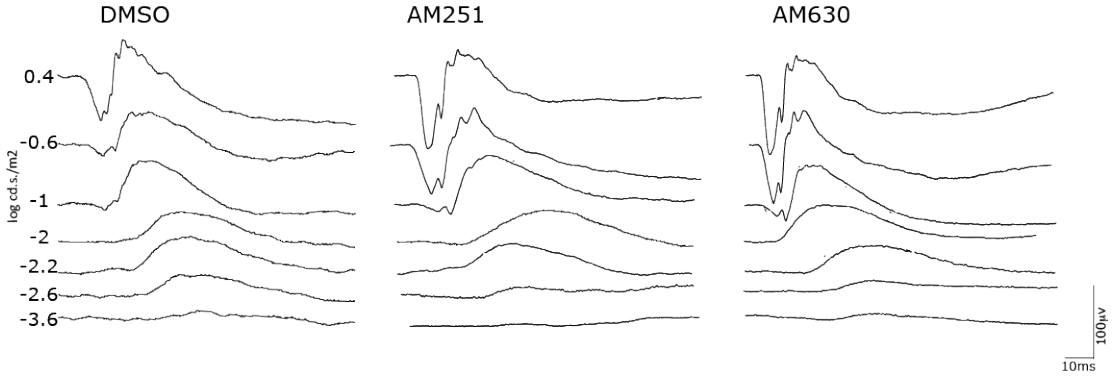

Figure 5- 4 Representative scotopic ERGs recorded in monkeys that received the vehicle only (DMSO) as the baseline compared with the responses after injection of AM251 (middle column) and AM630 (right column). The amplitude of the ERG responses seems to increase. Horizontal calibration, 10 ms; vertical calibration, 100 µV. The left column is the control injected with DMSO.

The Effect of Blockade of Cannabinoid Receptors in Scotopic Conditions

To verify if the observed tendencies in Figure 4 are meaningful, the amplitudes and latencies of a- and b-waves obtained in a scotopic condition with 13 intensity levels were calculated in different treatments using t-test for each stimulus intensity. At low flash intensities, AM251 and AM630 decrease significantly the amplitude of the b-wave (Figure 5-5, left column). Blockade of CB2R increases the amplitude of both a- and b-waves in high flash intensities (Figure 5-5, left column). At higher intensities, both treatments significantly reduce the amplitude of the a-wave. Both antagonists significantly delayed the time to peak for a- and b-wave in higher intensities (Figure 5-5, right column).

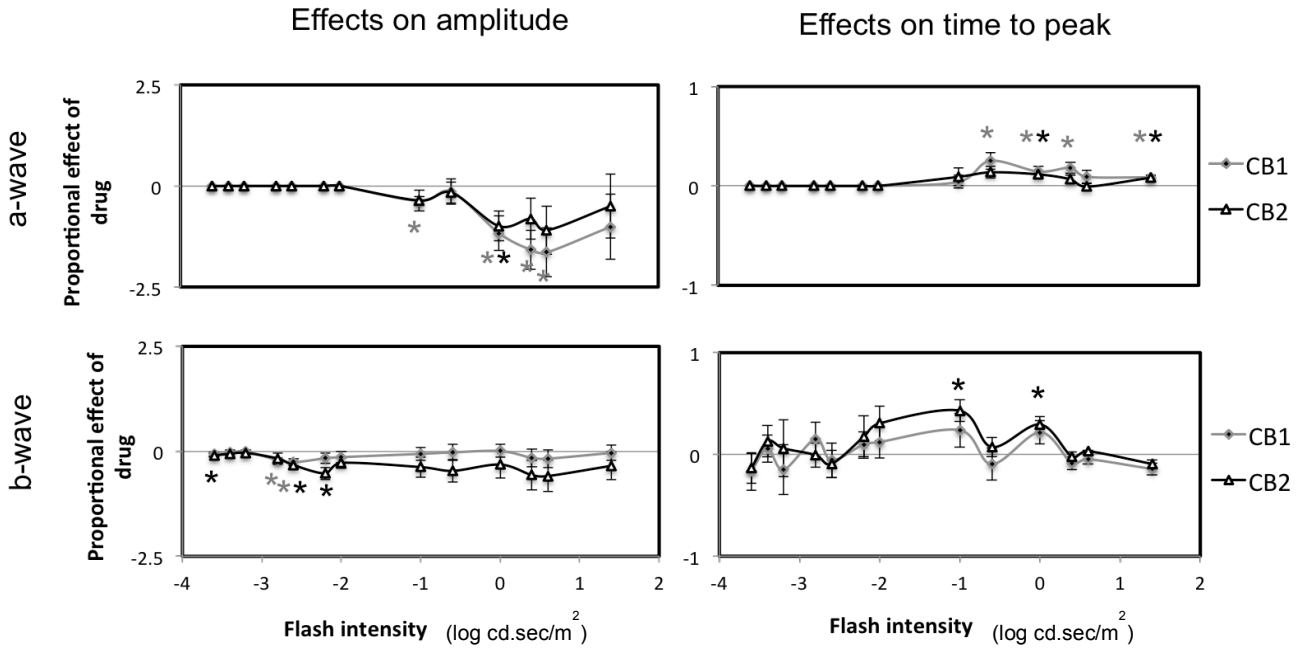

Figure 5- 5 The Effect of Blockade of Cannabinoid Receptors in Scotopic Conditions. Amplitude (left) and latency (right) of a-wave (upper) and b-wave (lower) are plotted as a function of flash intensities presented after dark adaptation in scotopic viewing conditions. Intensities at which the proportional differences are significantly different from DMSO are identified with a * (indicating $p<0.05$ on a two-directional, one-sample t-test); Grey stars indicate CB1R is different from DMSO, and black stars indicate CB2R is different from DMSO. Values above zero indicate larger amplitudes or latencies following injection (relative to baseline/control). Error bars represent SEM.

Discussion

The purpose of this study was to explore the role of eCB receptor CB1 and CB2 in visual processing in the monkey retina. To do so, we compare photopic and scotopic ERG responses before and after blocking these receptors with specific antagonists. Here, for the first time, we demonstrate that, in photopic conditions, blockade of retinal CB1R decreases the amplitude of the a-and b-waves at low flash intensities; blocking CB2R increases the amplitude of a-and b-waves in response to high flash intensities. In scotopic conditions, blockade of CB1R or CB2R decreases the a-wave amplitude at higher flash intensities and decreases the b-wave at lower intensities. Some significant increases in latency were observed in both cases following blockade of these eCB receptors. The summary of the ERG responses can be found in Table 5-3.

Table 5- 3 Summary of the ERG components after blockade of the CB1R and CB2R.

		Photopic				Scotopic			
		CB1R		CB2R		CB1R		CB2R	
		Amplitude	Latency	Amplitude	Latency	Amplitude	Latency	Amplitude	Latency
a-wave	Low intensity	↓	↑	NS	NS	NS	NS	NS	NS
	High Intensity	NS	NS	↑	NS	↓	↑	↓	↑
b-wave	Low intensity	↓	NS	NS	NS	↓	NS	↓	NS
	High Intensity	NS	↑	↑	↑	NS	NS	NS	↑

NS = non-significant, arrows $p<0.05$

Photopic Condition

CB1R decreases the amplitude of both a- and b-wave at low flash intensities

The amplitude of the a-wave in the photopic ERG originates from the activity of the photoreceptor layer mainly the cones (Hood and Birch, 1993, 1996). The activation of CB1R with WIN 55212-2 increases calcium current in rods and decreases it in large single cones. This agonist also suppresses the potassium current in both rods and cones (Straiker and Sullivan, 2003). Light-mediated hyperpolarization of the photoreceptors decreases the calcium current and reduces neurotransmitter release. The CB1R activation differentially modulates the calcium and potassium currents in rods and cones of the goldfish and salamander (Fan and Yazulla, 2003; Straiker and Sullivan, 2003; Fan and Yazulla, 2007). However, this effect was not observed in *cnr1*$^{-/-}$ mice, probably because the modulation of the ion currents was too weak to be detected by ERG (Cécyre et al., 2013). CB1R is mainly concentrated in the cone pedicles but is also slightly expressed in rod spherules (Bouskila et al., 2012) that may change the balance of differential modulation of CB1R in rods and cones. One of the visual side effects of cannabis consumption is an increase in photosensitivity (Dawson et al., 1977; Yazulla, 2008). Reduction of the a-wave amplitude after blockade of CB1R at lower intensities supports the idea that CB1R plays a role in the retinal photoreceptor responses and photosensitivity. Since there is little CB1R in rods (Bouskila et al., 2012), the effect might also be due to the presynaptic modulation of CB1R in cone photoreceptors. Indeed, higher photosensitivity might be the result of a decrease in neurotransmitter release and inhibition of the calcium current following CB1R activation (Straiker and Sullivan, 2003).

CB2R increases the amplitude of both a- and b-wave in higher intensities

The amplitude of the other main component of the ERG, the b-wave, is attributed to the interaction between the ON-bipolar cells and the Müller glial cells (Stockton and Slaughter, 1989; Wen and Oakley, 1990). In the vervet monkey, CB1R is expressed in the neuroretina cells and CB2R exclusively in the Müller cells leading to a complementary relationship between neurons and glia regarding eCB action (Bouskila et al., 2013a). Our results revealed an increase in the photopic b-wave amplitude following blockade of CB2R. The light-induced potassium increase in outer and inner plexiform cells that are depolarized by light (Dick et al., 1985), changes the Müller cell membrane potential and generates electrical responses. Müller cells, through siphoning of the excess potassium ions into the vitreous (Newman et al., 1984) controls the light-mediated potassium increase in retinal extracellular space (Newman and Reichenbach, 1996). The potassium channel responsible for the buffering of the Müller cells is reflected in the b-wave of the ERG (Miller and Dowling, 1970) so that the blockade of these potassium channels results in the decrease of the ERG b-wave (Wen and Oakley, 1990). Bouskila et al., (2013) recently proposed a model whereby CB2R in Müller cells uses potassium channel, $K_{IR}4.1$ to modulate the ERG. In summary, given that CB2R coupling via $G_{i/o}$ decreases cAMP and PKA levels (Howlett et al., 2002) and that PKA increases the activity of $K_{IR}4.1$ channels in the Müller cells, it is reasonable to propose that the blockade of the CB2R will therefore activate the potassium channels and increase the amplitude of the b-wave (Bouskila et al., 2013a). Our results support this model and explain the significant increase in the photopic amplitude of b-wave at high intensities.

Scotopic Condition

CB1R or CB2R blockade decreases the a-wave at higher intensities and the b-wave at lower intensities

In the dark-adapted retina, blockade of the CB1R significantly decreases the amplitude of the a-wave at high intensity values where the cones (mainly expressing CB1R) are responsive. A reduction in the amplitude of the b-wave was also observed following blockade of CB1R or CB2R at lower intensities where the rods are mostly responsive. The expression pattern of these receptors in the vervet retina may explain this reduction. The b-wave originates from bipolar and Müller cells. CB1Rs are mainly expressed in bipolar cells and suggest that this decrease can be due to their blockade. The fact that CB2R is mainly found in Müller cells, the potassium-buffering role of Müller cells (explained before) can proposed the reason for this reduction. At intensities from -3.6 to -0.6, the b-wave response represents the activation of the rod photoreceptors. Here we show that the blockade of the cannabinoid receptors in lower flash intensities decreases the amplitude of the b-wave. Our result is in line with the claim that activation of the cannabinoid receptors may cause an increase in rod responses through bipolar cells and/or Müller cells (Straiker and Sullivan, 2003) that can also explain the reports on the role of cannabis in improving the night vision (West, 1991, Merzouki and Mesa, 2002, Russo et al., 2004).

Cannabinoid receptors blockade increases the time to peak of a- and b-waves

In scotopic conditions, blockade of CB2R increases the latency of both a- and b-waves in higher intensity flashes. Blockade of CB1R only delays the a-wave amplitude with high intensity stimuli. However, in photopic conditions, high intensity stimuli only increase

the latency of the b- wave after blockade of either CB2R or CB1R. CB1R antagonist also increases the latency of a-wave in response to low intensity flashes. All other latencies do not show significant changes. The temporal component of the ERG waves is the implicit time that is the time required for each wave to get into their peak. The implicit time, similar to amplitude, is affected by light intensity, but there is little information in the literature on the meaning of this latency. It has been reported that the a-wave latency represents the optic nerve activity (Adrian and Matthews, 1927, Crampton and Boggs, 1959). Since CB1R was detected in the vervet monkey optic nerve (Javadi et al., 2013), the decrease in the a-wave latency can be due to the blockade of the CB1R modulators in the ganglion cells whose axons form the optic nerve. We also know that the time course of light adaptation after intense light exposure is significantly delayed by marijuana at low contrasts (Adams et al., 1978). The increase in the latency of the b-wave in the photopic condition, and both a- and b-wave in the scotopic condition suggests that cannabinoid receptors play a modulatory role in glare recovery.

Diseases and functions

Non-human primates and especially the vervet monkey have an ocular structure, retinal anatomy and ERG pattern very similar to humans (Bouskila et al., 2014) that make this species an ideal model for visual neuroscience research. The role of the eCB antagonists in the modification of the ERG waves may open new doors as a target for treatment of retinal intoxications (Hennekes, 1982; Duncker and Bredehorn, 1996) and diseases (Nilsson, 1971) where a general decrease in ERG amplitude is observed.

References

Adams AJ, Brown B, Flom MC, Jones RT, Jampolsky A (1975) Alcohol and marijuana effects on static visual acuity. Am J Optom Physiol Opt 52:729-735.

Adams AJ, Brown B, Haegerstrom-Portnoy G, Flom MC, Jones RT (1978) Marijuana, alcohol, and combined drug effects on the time course of glare recovery. Psychopharmacology (Berl) 56:81-86.

Adrian ED, Matthews R (1927) The action of light on the eye: Part I. The discharge of impulses in the optic nerve and its relation to the electric changes in the retina. J Physiol 63:378-414.

Armington JC, Johnson EP, Riggs LA (1952) The scotopic A-wave in the electrical response of the human retina. J Physiol 118:289-298.

Boire D, Théoret H, Ptito M. (2001) Visual pathways following cerebral hemispherectomy. Prog Brain Res 134:379-97.

Bouskila J, Burke MW, Zabouri N, Casanova C, Ptito M, Bouchard JF (2012) Expression and localization of the cannabinoid receptor type 1 and the enzyme fatty acid amide hydrolase in the retina of vervet monkeys. Neuroscience 202:117-130.

Bouskila J, Javadi P, Casanova C, Ptito M, Bouchard JF (2013a) Müller cells express the cannabinoid CB2 receptor in the vervet monkey retina. J Comp Neurol. 2013 Aug 1;521(11):2399-415.

Bouskila J, Javadi P, Casanova C, Ptito M, Bouchard JF (2013b) Rod photoreceptors express GPR55 in the adult vervet monkey retina. PLoS One 8:e81080.

Bouskila J, Javadi P, Palmour RM, Bouchard JF, Ptito M (2014) Standardized Full-Field Electroretinography in the Green Monkey (Chlorocebus sabaeus). PLoS One 9:e111569.

Cécyre B, Zabouri N, Huppe-Gourgues F, Bouchard JF, Casanova C (2013) Roles of cannabinoid receptors type 1 and 2 on the retinal function of adult mice. Invest Ophthalmol Vis Sci 54:8079-8090.

Chabre O, Conklin BR, Brandon S, Bourne HR, Limbird LE (1994) Coupling of the alpha 2A-adrenergic receptor to multiple G-proteins. A simple approach for estimating receptor-G-protein coupling efficiency in a transient expression system. J Biol Chem 269:5730-5734.

Crampton GH, Boggs N (1959) Latencies of the electroretinogram and optic tectum evoked potentials in the chicken. Am J Physiol 196:1067-1070.

Dawson WW, Jimenez-Antillon CF, Perez JM, Zeskind JA (1977) Marijuana and vision--after ten years' use in Costa Rica. Invest Ophthalmol Vis Sci 16:689-699.

Dick E, Miller RF, Bloomfield S (1985) Extracellular K+ activity changes related to electroretinogram components. II. Rabbit (E-type) retinas. J Gen Physiol 85:911-931.

Duncker G, Bredehorn T (1996) Chloroquine-induced lipidosis in the rat retina: functional and morphological changes after withdrawal of the drug. Graefes Arch Clin Exp Ophthalmol 234:378-381.

Eggan SM, Lewis DA (2007) Immunocytochemical distribution of the cannabinoid CB1 receptor in the primate neocortex: a regional and laminar analysis. Cereb Cortex 17:175-191.

Fan SF, Yazulla S (1999) Suppression of voltage-dependent K+ currents in retinal bipolar cells by ascorbate. Vis Neurosci 16:141-148

Fan SF, Yazulla S (2003) Biphasic modulation of voltage-dependent currents of retinal cones by cannabinoid CB1 receptor agonist WIN 55212-2. Vis Neurosci 20:177-188.

Fan SF, Yazulla S (2007) Retrograde endocannabinoid inhibition of goldfish retinal cones is mediated by 2-arachidonoyl glycerol. Vis Neurosci 24:257-267.

Flom MC, Adams AJ, Jones RT (1975) Marijuana smoking and reduced pressure in human eyes: drug action or epiphenomenon? Invest ophthalmol 14:52-55.

Gawienowski AM, Chatterjee D, Anderson PJ, Epstein DL, Grant WM (1982) Effect of delta 9-tetrahydrocannabinol on monoamine oxidase activity in bovine eye tissues, in vitro. Invest Ophthalmol Vis Sci 22:482-485.

Green K (1979) The ocular effects of cannabinoids. Curr Top Eye Res 1:175-215.

Hennekes R (1982) Clinical ERG findings in ethambutol intoxication. Graefes Arch Clin Exp Ophthalmol 218:319-321.

Henstridge CM, Balenga NA, Schroder R, Kargl JK, Platzer W, Martini L, Arthur S, Penman J, Whistler JL, Kostenis E, Waldhoer M, Irving AJ (2010) GPR55 ligands promote receptor coupling to multiple signalling pathways. Br J Pharmacol 160:604-614.

Hood DC, Birch DG (1993) Human cone receptor activity: the leading edge of the a-wave and models of receptor activity. Vis Neurosci 10:857-871.

Hood DC, Birch DG (1996) Assessing abnormal rod photoreceptor activity with the a-wave of the electroretinogram: applications and methods. Doc Ophthalmol 92:253-267.

Jasinska AJ, Schmitt CA, Service SK, Cantor RM, Dewar K, Jentsch JD, Kaplan JR, Turner TR, Warren WC, Weinstock GM, Woods RP, Freimer NB (2013) Systems biology of the vervet monkey. ILAR J 54:122-143.

Javadi P, Bouskila J, Casanova C, Bouchard JF, Ptito M (2013). Distribution pattern of the endocannabinoid system throughout the dorsal lateral geniculate nucleus of non-human primates. 8th Canadian Optometry Schools Research Conference Poster #35.

Kiplinger GF, Manno JE, Rodda BE, Forney RB (1971) Dose-response analysis of the effects of tetrahydrocannabinol in man. Clin Pharmacol Ther 12:650-657.

Laprevote V, Schwitzer T, Giersch A, Schwan R (2015) Flash electroretinogram and addictive disorders. Prog Neuropsychopharmacol Biol Psychiatry 56:264.

Lopez EM, Tagliaferro P, Onaivi ES, Lopez-Costa JJ (2011) Distribution of CB2 cannabinoid receptor in adult rat retina. Synapse 65:388-392.

McCulloch DL, Marmor MF, Brigell MG, Hamilton R, Holder GE, Tzekov R, Bach M (2014) ISCEV Standard for full-field clinical electroretinography (2015 update). Doc Ophthalmol 1-12.

Merzouki A, Mesa JM (2002) Concerning kif, a Cannabis sativa L. preparation smoked in the Rif mountains of northern Morocco. J Ethnopharmacol 81:403-406.

Miller RF, Dowling JE (1970) Intracellular responses of the Muller (glial) cells of mudpuppy retina: their relation to b-wave of the electroretinogram. J Neurophysiol 33:323-341.

Nair G, Kim M, Nagaoka T, Olson DE, Thule PM, Pardue MT, Duong TQ (2011) Effects of common anesthetics on eye movement and electroretinogram. Doca Ophthalmol 122:163-176.

Newman E, Reichenbach A (1996) The Müller cell: a functional element of the retina. Trends Neurosci 19:307-312.

Newman EA, Frambach DA, Odette LL (1984) Control of extracellular potassium levels by retinal glial cell K+ siphoning. Science 225:1174-1175.

Nilsson SE (1971) Human retinal vascular obstructions. A quantitative correlation of angiographic and electroretinographic findings. Acta Ophthalmol (Copenh) 49:111-133.

Noyes R, Jr., Brunk SF, Avery DA, Canter AC (1975) The analgesic properties of delta-9-tetrahydrocannabinol and codeine. Clin Pharmacol Ther 18:84-89.

Porcella A, Casellas P, Gessa GL, Pani L (1998) Cannabinoid receptor CB1 mRNA is highly expressed in the rat ciliary body: implications for the antiglaucoma properties of marihuana. Brain Res Mol Brain Res 58:240-245.

Robson JG, Frishman LJ (2014) The rod-driven a-wave of the dark-adapted mammalian electroretinogram. Prog Retin Eye Res 39:1-22.

Rosolen SG, Kolomiets B, Varela O, Picaud S (2008) Retinal electrophysiology for toxicology studies: applications and limits of ERG in animals and ex vivo recordings. Exp Toxicol Pathol 60:17-32.

Russo EB, Merzouki A, Mesa JM, Frey KA, Bach PJ (2004) Cannabis improves night vision: a case study of dark adaptometry and scotopic sensitivity in kif smokers of the Rif mountains of northern Morocco. J Ethnopharmacol 93:99-104.

Schlicker E, Timm J, Gothert M (1996) Cannabinoid receptor-mediated inhibition of dopamine release in the retina. Naunyn Schmiedebergs Arch Pharmacol 354:791-795.

Schwitzer T, Schwan R, Angioi-Duprez K, Ingster-Moati I, Lalanne L, Giersch A, Laprevote V (2014) The cannabinoid system and visual processing: A review on experimental findings and clinical presumptions. Eur Neuropsychopharmacol, in press.

Steinberg R, Linsenmeier R, Griff E (1985) Retinal pigment epithelial cell contributions to the electroretinogram and electrooculogram. Prog Ret Res 4:33-66.

Stockton RA, Slaughter MM (1989) B-wave of the electroretinogram. A reflection of ON bipolar cell activity. J Gen Physiol 93:101-122.

Straiker A, Stella N, Piomelli D, Mackie K, Karten HJ, Maguire G (1999) Cannabinoid CB1 receptors and ligands in vertebrate retina: localization and function of an endogenous signaling system. Proc Natl Acad Sci U S A 96:14565-14570.

Straiker A, Sullivan JM (2003) Cannabinoid receptor activation differentially modulates ion channels in photoreceptors of the tiger salamander. J Neurophysiol 89:2647-2654.

Struik ML, Yazulla S, Kamermans M (2006) Cannabinoid agonist WIN 55212-2 speeds up the cone response to light offset in goldfish retina. Vis Neurosci 23:285-293.

Sulcova E, Mechoulam R, Fride E (1998) Biphasic effects of anandamide. Pharmacol Biochem Behav 59:347-352.

Wen R, Oakley B, 2nd (1990) K(+)-evoked Muller cell depolarization generates b-wave of electroretinogram in toad retina. Proc Natl Acad Sci U S A 87:2117-2121.

West ME (1991) Cannabis and night vision. Nature 351:703-704.

Yazulla S, Studholme KM, McIntosh HH, Deutsch DG (1999) Immunocytochemical localization of cannabinoid CB1 receptor and fatty acid amide hydrolase in rat retina. J Comp Neurol 415:80-90.

Yazulla S, Studholme KM, McIntosh HH, Fan SF (2000) Cannabinoid receptors on goldfish retinal bipolar cells: electron-microscope immunocytochemistry and whole-cell recordings. Vis Neurosci 17:391-401.

Yazulla S (2008) Endocannabinoids in the retina: from marijuana to neuroprotection. Prog Retin Eye Res 27:501-526.

Zabouri N, Bouchard JF, Casanova C (2011) Cannabinoid receptor type 1 expression during postnatal development of the rat retina. J Comp Neurol 519:1258-1280.

CHAPTER 6: The endocannabinoid system within the dorsal lateral geniculate nucleus of the vervet monkey

In press in Neuroscience (Available online January 6, 2015)

The endocannabinoid system within the dorsal lateral geniculate nucleus of the vervet monkey

Pasha Javadi[1], Joseph Bouskila[1, 2], Jean-François Bouchard[1], and Maurice Ptito[1, 3, 4]

[1]School of Optometry, University of Montreal, Montreal, QC, Canada

[2]Biomedical Sciences, Faculty of Medicine, University of Montreal, Montreal, QC, Canada

[3]BRAINlab, Department of Neuroscience and Pharmacology, University of Copenhagen, Copenhagen, Denmark

[4]Laboratory of Neuropsychiatry, Psychiatric Centre Copenhagen and Department of Neuroscience and Pharmacology, University of Copenhagen, DK-2100 Copenhagen, Denmark

Running title: eCB system expression in the monkey dLGN

Correspondence should be addressed to:
Maurice Ptito, PhD
School of Optometry, room 260-7
3744 Jean-Brillant Street,
University of Montreal,
Montreal, Quebec, Canada, H3T 1P1

Abbreviation**:** AEA, anandamide; CB1R, cannabinoid receptor CB1; DAB, 3,3'-Diaminobenzidine; DAGL, diacylglycerol lipase enzyme; dLGN, dorsal lateral geniculate nucleus; eCB, endocannabinoid; ERG, electroretinogram; FAAH, fatty acid amide hydrolase; GABA, GABAergic cell; GFAP, glial fibrillary acidic protein; IR, immunoreactivity; MAGL, monoglycerol lipase; MT, middle temporal; MST, medial superior temporal; NAE, N-acylethanolamines; NAPE, N-acyl-phosphatidylethanolamine; NAPE-PLD, N-acyl-phosphatidylethanolamine phospholipase D; NDS, normal donkey serum ; PBS, phosphate-buffered saline; SEM*, standard error* of the mean; SC, superior colliculus; VGLUT1, vesicular glutamate transporter 1; 2-AG, 2-arachidonoylglycerol.

Abstract

The endocannabinoid system mainly consists of cannabinoid receptors type 1 (CB1R) and type 2 (CB2R), their endogenous ligands termed endocannabinoids (eCBs), and the enzymes responsible for the synthesis and degradation of eCBs. These cannabinoid receptors have been well characterized in rodent and monkey retinae. Here, we investigated the expression and localization of the eCB system beyond the retina, namely the first thalamic relay, the dorsal lateral geniculate nucleus (dLGN), of vervet monkeys using immunohistochemistry methods. Our results show that CB1R is expressed throughout the dLGN with more prominent labeling in the magnocellular layers. The same pattern is observed for the degradation enzyme, fatty acid amide hydrolase (FAAH). However, the synthesizing enzyme N-acyl-phosphatidylethanolamine phospholipase D (NAPE-PLD) is expressed homogenously throughout the dLGN with no preference for any of the layers. These proteins are weakly expressed in the koniocellular layers. These results suggest that the presence of the eCB system throughout the layers of the dLGN may represent a novel site of neuromodulatory action in normal vision. The larger amount of CB1R in the dLGN magnocellular layers may explain some of the behavioral effects of cannabinoids associated with the integrity of the dorsal visual pathway that plays a role in visual-spatial localization and motion perception.

Keywords: CB1R, FAAH, NAPE-PLD, dLGN, Monkey, Cannabinoid receptors.

Introduction

The physiological and psychological effects of phytocannabinoids, the active components of the cannabis plant, can be detected almost everywhere in the body due to their actions on specific receptors: mainly the cannabinoid receptors type 1 (CB1R) and type 2 (CB2R). Cannabinoid receptors are membrane receptors principally coupled to inhibitory G-proteins that modulate the release of neurotransmitters (Piomelli 2003; Gómez-Ruiz et al, 2007). They mediate biological functions not only via the exogenous cannabinoids, but also via endocannabinoids (eCBs) such as N-arachidonoylethanolamide (anandamide or AEA) and 2-arachidonoylglycerol (2-AG). Unlike the classical neurotransmitters, eCBs are synthesized "on demand" by catalyzing the release of N-acylethanolamines (NAEs) from N-acyl-phosphatidylethanolamine (NAPE) by specific enzyme, like N-acyl-phosphatidylethanolamine phospholipase D (NAPE-PLD) or from arachidonic acid via diacylglycerol lipase enzyme (DAGL). The eCBs are not accumulated into synaptic vesicles and are rather degraded rapidly by specific enzymes like fatty acid amid hydrolase (FAAH) and monoglycerol lipase (MAGL) (for review, see Deutsch and Chin 1993).

The localization and function of the molecular components of the eCB system in the central nervous system have been the subject of recent research. In fact, the role of the eCB system in learning, memory, neuroprotection and visual processing is essentially due to the modulation of neurotransmitter release by the presynaptic location of CB1R (Di Marzo et al., 1998; Straiker et al., 1999a). CB1R expression is found in the hippocampus, prefrontal cortex, cerebellum and basal ganglia of rodents (Herkenham et al., 1991) and primates (Eggan and Lewis 2007). It is expressed in glutamatergic and GABAergic neurons throughout the central

and peripheral nervous systems (Egertová and Elphick 2000). In the visual system, CB1R and FAAH have been localized in cone photoreceptors, horizontal, amacrine, bipolar, and retinal ganglion cells in the central and peripheral retina of vervet monkeys (Bouskila et al., 2012). CB1R is also found in the human retina (Straiker et al., 1999b).

Earlier studies reported that cannabis could affect several visual functions, such as photosensitivity (Adams et al., 1978), visual acuity (Moskowitz et al., 1972; Adams and Brown 1975), color vision (Dawson et al., 1977), ocular tracking (Flom et al., 1976), binocular depth inversion, and stereoscopic vision (Emrich et al., 1991; Leweke et al., 1999; Semple et al., 2003). Some case studies later claimed other visual effects of cannabis such as visual distortions, altered perception of distance, illusions of movement in stationary and moving objects, color intensification of objects, dimensional distortion and blending of patterns and objects (Levi and Miller 1990; Lerner et al., 2011). Given the localization of CB1R in the central retina, from cones to ganglion cells, it is reasonable to assume its implication in these visual manifestations.

In homogenates of rodent thalamus, high levels of AEA (Felder et al., 1996) and FAAH (Egertová et al., 2003), as well as an elevated cannabinoid receptor/G-protein amplification ratio (Breivogel et al., 1997) have been found. Also, using immunohistochemistry, moderate to low levels of CB1R expressions have been found both in thalamus of rats (Egertová et al., 1998; Tsou et al., 1998; Moldrich and Wenger 2000), non-human primates (Ong and Mackie 1999) and humans (Glass et al., 1997) without focusing on dLGN. However, there is no study, to our knowledge, that has thoroughly studied the

expression of the eCB system in this retino-recipient primary thalamic relay of the primate. Similar to apes and humans, the dLGN of vervet monkeys consists of six layers. The first two ventral layers, the magnocellular layers, receive input from large ganglion cells (rod signals) and are necessary for the perception of movement, depth and small difference in brightness. The four dorsal layers, parvocellular layers, receive input from small ganglion cells of the retina (cone signals) and play a role in color and form perception. These layers are well separated by an inter-laminar zone called koniocellular layers that contribute to short-wavelength "blue" cones (Xu et al., 2001). Given the expression and localization of CB1R in the retinal mosaic, we expect to find this receptor in the optic nerve and the dLGN layers.

Experimental procedures

Animals. Monkey tissues were obtained from 4 adult vervet monkeys (*Chlorocebus sabaeus*). The monkeys were part of Dr Ptito's and Dr Palmour's research project that was approved by McGill University Animal Care and Use Committee. The animals were born and raised under an enriched natural environment in the laboratories of the Behavioral Sciences Foundation (St-Kitts, West Indies), a facility recognized by the Canadian Council on Animal Care (CCAC). The experimental protocol was reviewed and approved by the local Animal Care and Use Committee (University of Montreal) and the Institutional Review Board of the Behavioral Science Foundation.

Tissue preparation. Each animal was sedated with ketamine hydrochloride (10 mg/kg, i.m.) and euthanized by an overdose of intravenously administered sodium pentobarbital (25 mg/kg), followed by transcardial perfusion of 0.1 M PBS (pH 7.4). The brains were then removed, blocked and flash-frozen in an isopentane bath cooled in a dry ice chamber and maintained at −80˚C. The blocks were cut along the coronal plane in 20 µm sections at −18˚C on a Leica CM3050S cryostat and mounted onto gelatinized subbed glass slides. The slide-mounted tissue sections were stored at −80˚C until further histological processing.

Immunohistochemistry (DAB). At least one slide-mounted 20 µm fresh-frozen tissue section per animal was selected from A6 to A9, at a level where the lamination of the dLGN is the clearest and thawed at room temperature. A hydrophobic barrier was created surrounding the slides, using PAP pen (Vector, Burlingame, CA, USA) to keep staining reagents localized on the tissue section. Sections were fixed with 70% ethanol solution for 15 minutes, followed by

two 5-min rinses with 0.1 M Tris buffer, pH 7.4/0.03% Triton X-100. To block the endogenous peroxidase activity, sections were washed with 0.3% hydrogen peroxide in PBS for 15 minutes. Following three times 5-min PBS-triton rinse, sections were blocked for 60 minutes with a solution of 10% normal donkey serum (NDS) and 0.1 M Tris buffer/0.5% Triton. Each section was incubated overnight at room temperature with primary antibodies (Table 1) diluted in the blocking solution. The next day, sections underwent three 10-min PBS-triton washes, followed by incubation in a secondary antibody solution (biotinylated donkey anti-rabbit antibody diluted 1:200 in blocking solution) for 2 hours. After three consecutive 10-min washes with PBS-triton, the sections were incubated for 1 hour in an avidin-biotin-conjugated horseradish peroxidase (Vectastain ABC kit, Burlingame, CA, USA) solution (1:500). Following three subsequent 10-min washes in PBS-triton, the sections were treated with a 3,3-diaminobenzidine (DAB) substrate. After rinsing in PBS-triton three times for 5 minutes each, sections underwent dehydration in graded ethanol steps, cleared in xylene, and cover-slipped with Permount mounting media (Fisher Scientific; Pittsburgh, PA, USA). Sections were examined on a Leica DMRB under bright field illumination.

Immunofluorescence. Double and triple labeling of the brain tissues were performed according to previously published methods on the vervet monkey retina (Bouskila et al., 2012; Bouskila et al., 2013a, b). Briefly, sections were post-fixed for 15 minutes in 70% ethanol, rinsed two times 5-min in 0.1 M Tris buffer, pH 7.4/0.03% Triton and blocked for 90 minutes in 10% NDS and 0.1 M Tris buffer/0.5% Triton. Sections were incubated overnight at room temperature with primary antibodies in blocking solution. The antibodies directed against molecular eCB components all raised in rabbit were used conjointly with a known cell marker:

glial fibrillary acidic protein (GFAP) (astrocytes marker), VGLUT1 (glutamatergic cell marker) and GABA (GABAergic cell marker) (Table 6-1). The next day, sections were washed for 10-min and two times 5-min in 0.1 M Tris /0.03% Triton and incubated with biotinylated donkey anti-rabbit diluted 1:200 in blocking solution for 2 hours for the eCB targets to amplify the signals. Sections were then incubated for another 2 hours with streptavidin 647 in order to amplify the signal and alexa 555 or 488 secondary antibodies when necessary. Sections were cover-slipped with Fluoromount-G^{TM} Mounting Medium (SouthernBiotech, Birmingham, AL) after 3x 10 min washes with 0.1 M Tris buffer. In the case of the GABA antibody, the sections had to fixed in PFA 4% and gluteraldehyde 1%. The GABA signals were amplified with biotinylated donkey anti-mouse and the cannabinoid signals with donkey anti rabbit HRP and alexa fluor tyramide (Invitrogen, Eugene, Oregon).

Antibody characterization. The source and working dilution of all primary antibodies used in this study are summarized in Table 6-1. The antibodies with the exception of NAPE-PLD were successfully used in previous studies and were well characterized in the vervet monkey (Bouskila et al., 2012).

CB1R. The rabbit anti-CB1R (Calbiochem, Gibbstown, NJ, USA) was developed using a highly purified fusion protein with the first 77 amino acid residues of rat CB1R. According to the manufacturer's data sheet, it recognizes a major band of 60 kDa with also less intense bands of 23, 72, and 180 kDa. This antibody was shown to be specific using CB1R knockout mouse retinal tissue (Zabouri et al., 2011). It recognizes the CB1R (60 kDa) from many species, including the vervet monkey tissues (Bouskila et al., 2012).

GFAP. The mouse anti-glial fibrillary acidic protein (GFAP, Clone G-A-5, Sigma-Aldrich, St. Louis, MO, USA) was produced using purified GFAP isolated from the pig spinal cord. This antibody recognizes the GFAP protein of 50 kDa in Western blots (manufacturer's data sheet). GFAP stains cells with the morphology and distribution expected for astrocytes in monkey dLGN (Takahata et al., 2010).

FAAH. The rabbit anti-fatty acid amide hydrolase (FAAH, Cayman Chemical, Ann Arbor, MI, USA) was developed using a synthetic peptide from rat FAAH amino acids 561-579 (CLRFMREVEQLMTPQKQPS) conjugated to KLH. As expected, it recognizes a dense band at about 66 kDa and a very light one below 37 kDa. The specificity of this antibody has been demonstrated in rat (Suárez et al., 2008; Zabouri et al., 2011) and vervet monkey (Bouskila et al., 2012) tissues.

NAPE-PLD. The rabbit anti-N-acyl phosphatidylethanolamine-specific phospholipase D (NAPE-PLD, Cayman Chemical, Ann Arbor, MI, USA) was developed using a synthetic peptide from human NAPE-PLD amino acids 159-172 (YMGPKRFRRSPCTI). Its cross reactivity has been tested in many species, and it recognizes an intense band at 46 kD on Western blot of the human cerebellum (manufacturer's data sheet).

NAPE-PLD blocking peptide. The NAPE-PLD blocking peptide containing the human NAPE-PLD amino acid sequence 159-172 (YMGPKRFRRSPCTI; Cayman Chemical, Ann Arbor, MI, USA) was used in the present study for Western blot analysis. The specificity of

the NAPE-PLD antibody was tested by pre-incubation with the corresponding blocking peptide. For pre-adsorption, the primary antibody was diluted in PBS and incubated with a ratio 1:5 for 2 hours at room temperature, with occasional inversion. Thereafter, the antibody-blocking peptide solution was added to the blot and subsequent Western blotting followed the protocol as described further.

VGLUT1. The mouse anti-vesicular glutamate transporter 1 (VGLUT1, Synaptic System, Goettingen

Germany) was raised against the aa 456-560 of the rat VGLUT1 protein. It is used as a glutamatergic neuron marker and its specificity has been verified in *vglut1* KO mouse tissue (Wojcik et al., 2004) as well as using the corresponding blocking peptide (Zhou et al., 2007).

GABA. The mouse anti-gamma aminobutyric acid antibody (GABA, Millipore, MA, USA) was synthesized coupling to BSA with gluteraldehyde. It is used as a marker of GABAergic neurons. Thus, for the GABA antibody, sections were fixed for 20 min in 1% gluteraldehyde, 4% PFA in PBS. The antibody has been frequently used in different animals, and its specificity has been verified in monkey (Jongen-Relo et al., 1999).

Table 6-1 Primary antibodies used in this study

Antibody	Immunogen	Source	Working dilution
CB1R	Fusion protein containing aa 1–77 of rat CB1R	Sigma, St. Louis, MO, C1233, Rabbit polyclonal	H: 1:200
FAAH	Synthetic peptide aa 561–579 of rat FAAH	Cayman Chemical, Ann Arbor, MI, 101600, rabbit polyclonal	H: 1:200
NAPE-PLD	Synthetic peptide aa 159-172 of human NAPE-PLD	Cayman Chemical, Ann Arbor, MI, 10305, rabbit, polyclonal	H: 1:200
GFAP	Purified protein isolated from pig spinal cord	Sigma-Aldrich, St. Louis, MO, G3893, mouse, G-A-5, monoclonal	H: 1:200
VGLUT1	Fusion protein containing aa 456 – 560 of rat VGLUT1	Synaptic System, Goettingen, Germany,135 311, mouse, 317D5 monoclonal	H: 1:200
GABA	Fusion Protein coupling to BSA with gluteraldehyde	Millipore, MA, MAB316, Monoclonal	H: 1:200

Microscopy. To detect the fluorescence signals, a Leica TCS SP2 confocal laser-scanning microscope (Leica Microsystems, Exton, PA) with 40x (n.a. 1.25–0.75) and 100x (n.a. 1.40–0.7) objectives was used. Subsequently, images were acquired from the green and far-red channels on optical slices of less than 0.9 μm. Adobe Photoshop (CS5; Adobe Systems, San Jose, CA) was used for all photomicrographic adjustments on size, color and shape before exporting them to Adobe InDesign (CS5; Adobe Systems), where the final figure layout was completed. For DAB staining, all photomicrographs were captured with a Leica DMR photomicroscope equipped with a Retiga 1300 video camera system (Q Imaging) using the QCapture software with a Leica 2.5x (0.07) objective.

Quantification. In order to enhance the visualization of CB1R spatial distribution throughout the dLGN layers, photomicrographs demonstrating the entire structure were generated in an 8-

bit gray scale. Using a MatLab code, the minimum and maximum thresholds of the gray values in the image were measured. The gray spectrum values were then eventually distributed within the RGB spectral subdivision in which the maximum threshold gray values were presented in red and the minimum in blue. Moreover, the average contrast intensity of each layers were calculated using the FIJI program (v. 1.48t, Wayn Rasband, NIH, USA). The program was calibrated using a calibration grid slide. The RGB images inverted to 8-bit with a linearly gray scaling from a minimum to a maximum pixel intensity (arbitrary value 0-255). The mean intensity of 4 sections (per condition) in their whole magno-, parvo- and koniocellular layers (±SEM) was reported after subtracting the average background intensity.

Results

Spatial expression of the endocannabinoid system in dLGN

To examine the laminar expression of the endocannabinoid system profile in dLGN, tissues were labeled with specific antibodies against CB1R, FAAH, and NAPE-PLD. Their expression pattern in the brain was quantified using heatmap analysis. Immunolabeled sections for CB1R were found throughout the magnocellular and parvocellular layers of the dLGN with a higher intensity in the magnocellular layers (Figure 6-1 a, d, g). The koniocellular layers had the lowest expression of CB1R (Figure 6-1 a, d, g). Similar patterns of expression were observed for FAAH (Figure 6-1 b, e, g). NAPE-PLD was expressed homogenously with no preferences for the magnocellular or parvocellular layers. The koniocellular layers still showed very low expression of the synthesizing enzyme (Figure 6-1 c, f, g). A consistent staining pattern across all 4 monkeys dLGN was found. Interestingly, all these three proteins were also highly expressed in the optic nerve (data not shown).

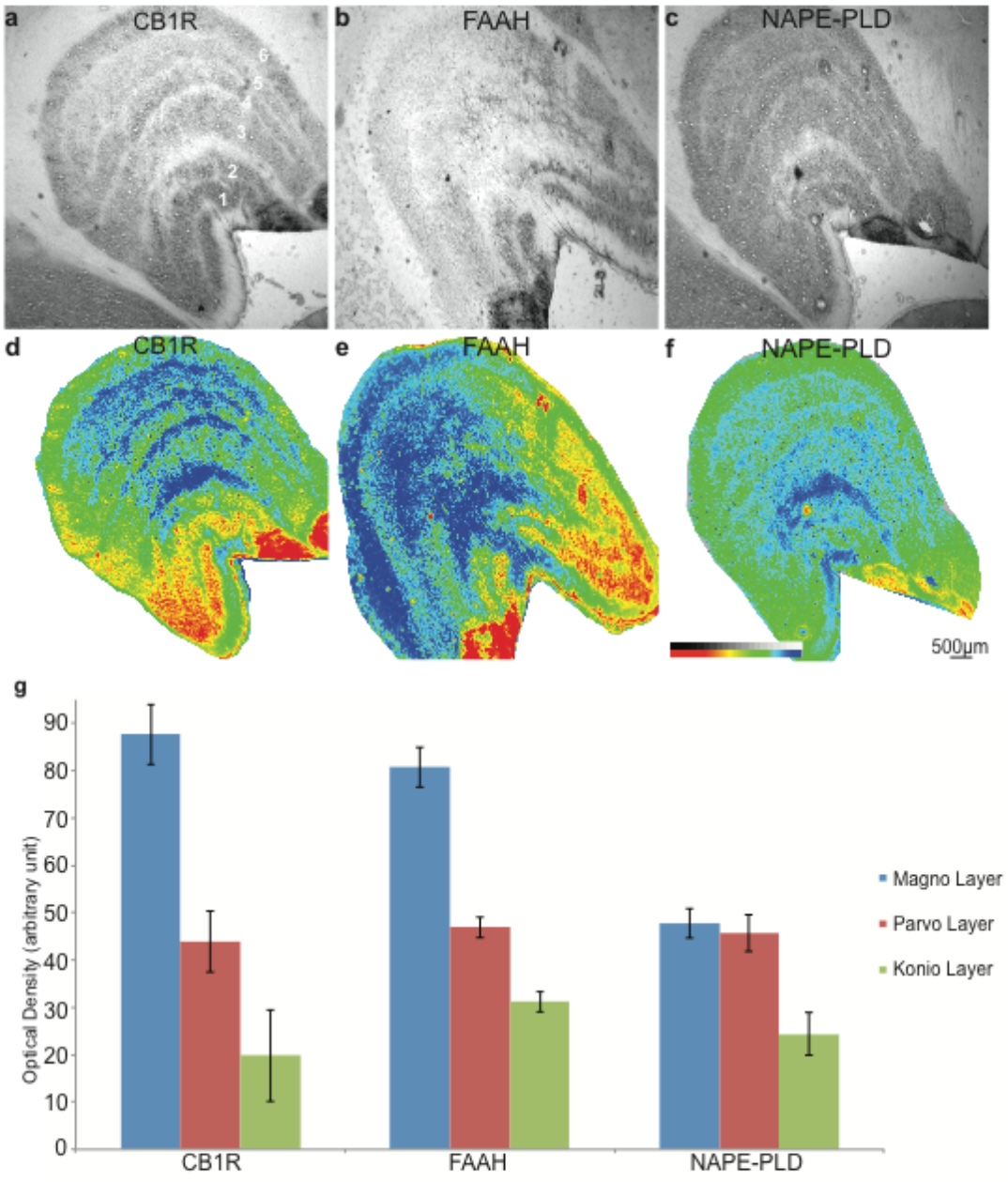

Figure 6-1 Spatial distribution of CB1R, FAAH, and NAPE-PLD throughout the dLGN (a-c) of vervet monkeys. The RGB heat map was used to enhance the display of the abundance of the CB1R (d), FAAH (e) and NAPE-PLD (f) in the dLGN. The gray spectrum was distributed within the RGB spectral subdivision in which the maximum threshold gray values were expressed as red and the minimum as blue. CB1R is more expressed within the first two layers of dLGN. FAAH expression pattern is similar to CB1R. The NAPE-PLD expression is similarly distributed throughout the magno and parvo cellular layers. Scale bars = 500 µm. (g) Quantification of the mean contrast intensity of CB1R, FAAH and NAPE-PLD-IR in magno-, parvo- and koniocellular layer. The bars indicate the standard error.

CB1R, FAAH and NAPE-PLD are not present in LGN astrocytes

The double immunostaining was carried out with molecular markers to examine the eCB system expression at the cellular level. Cytosolic spread expression of CB1R is not co-localized with GFAP positive glial cells (Figure 6-2 a-f). There is an apparent higher expression of CB1R in the magnocellular layers (Figure 6-2 a-c) compare to the parvocellular layers (Figure 6-2 d-f). The very weak expression of this receptor in the koniocellular layers is also evident (Figure 6-1 g-h). Similarly, FAAH-IR is not detected in astrocytes of magnocellular layer (Figure 6-2 j-l).

In contrast to the difference in the pattern of expression of NAPE-PLD, the cellular expression of this synthesizing enzyme is similar to that of CB1R and FAAH. NAPE-PLD is also absent in astrocytes; however, it is abundant in the cytosol of both magnocellular (Figure 6-2 m-o) and parvocellular (data not shown) dLGN neurons.

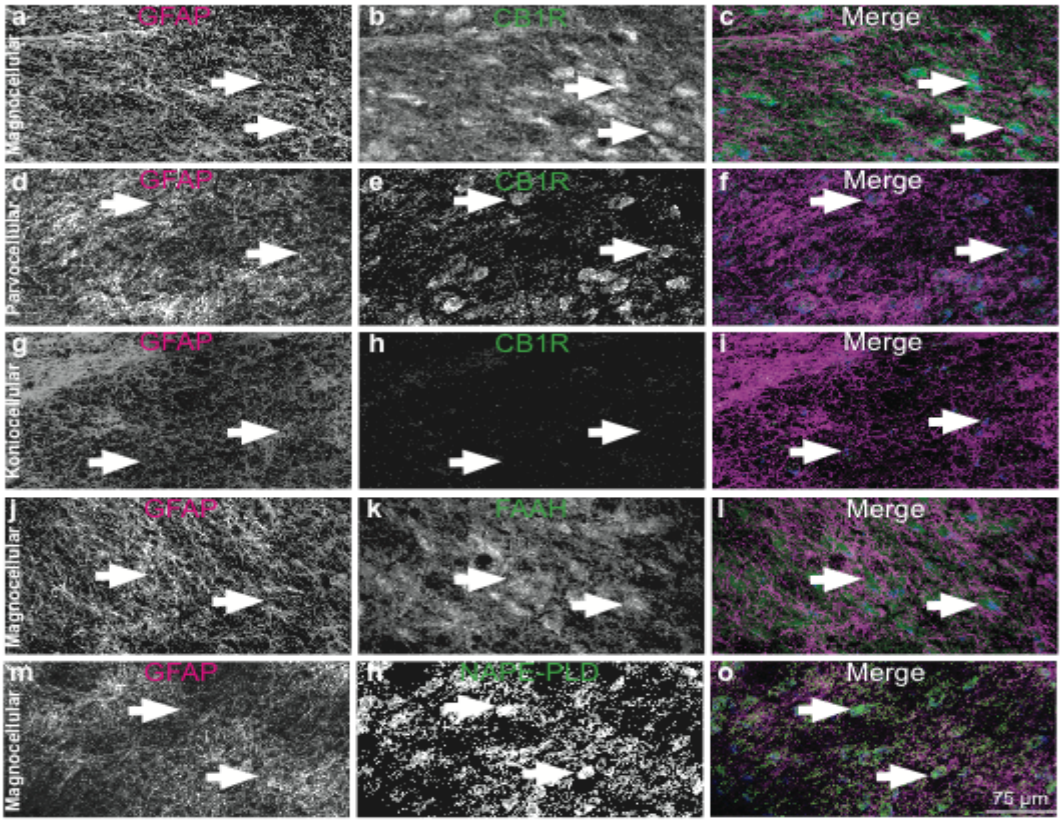

Figure 6-2 Triple-label immunofluorescence of the CB1R (magenta) and GFAP (green) expression with nucleic acid stain Sytox (blue), respectively in magnocellular (a-c), parvocellular (d-f) and koniocellular layers (g-i). The absence of GFAP with FAAH (j-l) and NAPE-PLD (m-o) co-localizations in the magnocellular layers of the monkey dLGN are shown. Each immunostaining is presented alone in gray scale in the first two columns (1st column: GFAP and 2nd column: CB) following their merged image in the third column. Arrows point at GFAP cell bodies with no expression of CB. Scale bars = 75 µm.

CB1R, FAAH and NAPE-PLD are expressed in glutamatergic and GABAergic neurons

As previously reported in rat brain, CB1R is expressed in both GABAergic and glutamatergic cells (Egertová and Elphick 2000). Our results validate the expression of CB1R within the GABAergic (Figure 6-3 a-c) and glutamatergic cells in the magnocellular layers (Figure 6-3 d-f). Furthermore, we report the same pattern of expression for FAAH and NAPE-

PLD in both GABAergic (Figure 6-3 g-i and m-o) and glutamatergic neurons (Figure 6-3 j-l and p-r) without any preferences for any of them.

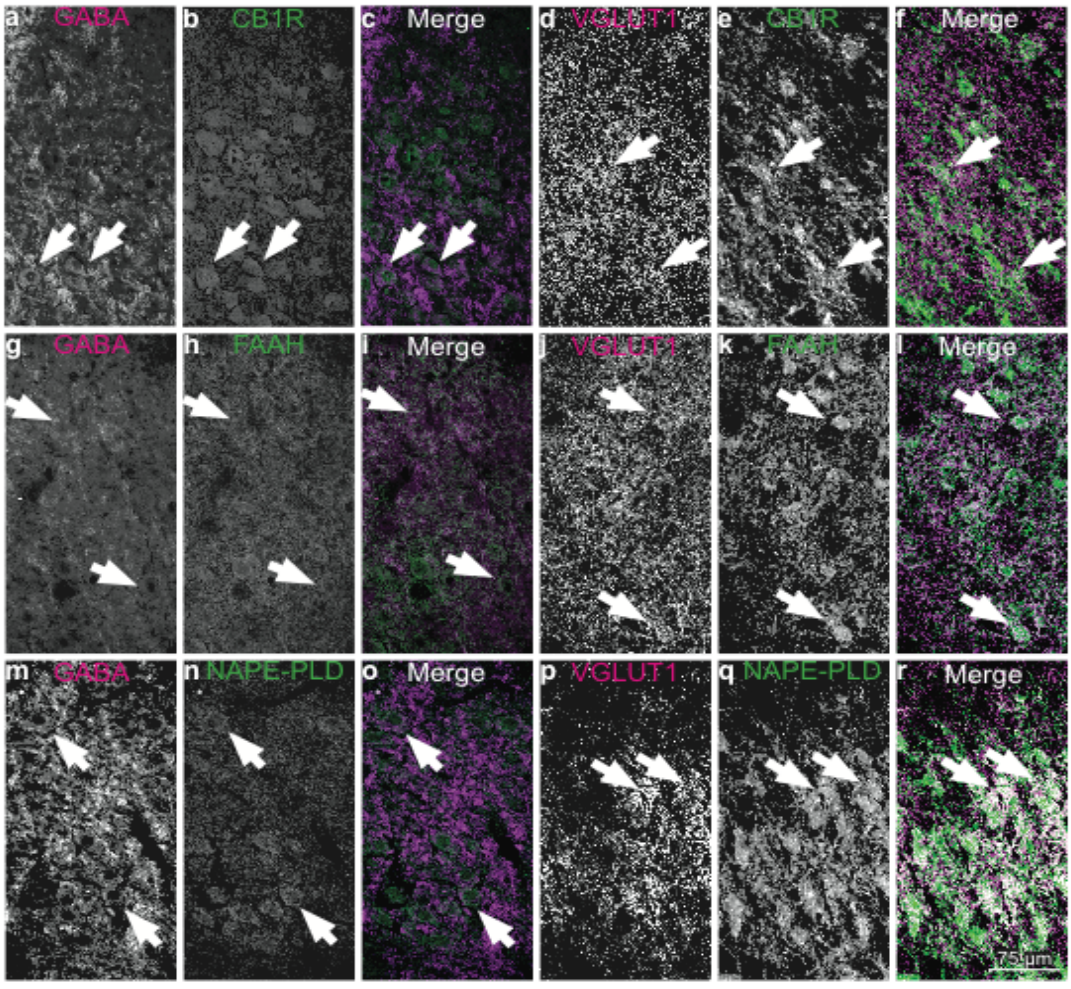

Figure 6-3 Immunofluorescence labeling illustrating the co-localization of CB1R (a-f), FAAH (g-l) and NAPE-PLD (m-r) with GABAergic (three left columns) and glutamatergic (three right columns) neurons in the magnocellular layer 1 of the dLGN. Each immunostaining is presented alone in gray scale in the first two columns following their merged image in the third column. Arrows point to the co-localization of eCB components with GABA and VGLUT1. Scale bar = 75 µm.

Discussion

To our knowledge, this is the first study reporting the spatial distribution of CB1R and the enzymes regulating the levels of its ligands, namely FAAH and NAPE-PLD in the dLGN of primates. Given that CB1R, FAAH and NAPE-PLD are expressed in an overlapping pattern in the dLGN (Figure 6-1), it might play a role in the auto-feedback control of neurotransmitter release, as proposed for the retina of the same species (Bouskila et al., 2012). This means that the same neurons that produce endocannabinoids may also respond to its ligands in order to control the release of neurotransmitters.

CB1R: from the retina to the dLGN

There are studies that assessed CB1R expression in the whole brain and reported its expression in the thalamus. The dorsal thalamus was found to slightly express CB1Rs in rats (Tsou et al., 1998), not at all (Eggan and Lewis 2007) or moderately (Ong and Mackie 1999) in primates and humans (Glass et al., 1997), without any focus on the dLGN. To date, we have found only one study looking specifically at the rodent dLGN and reporting CB1R expression (Argaw et al., 2011). These results are however difficult to generalize to the monkey and human dLGN given the major anatomical differences in its organization as well as its cortical projections. Moreover, while the vast majority of retinal inputs projects to the dLGN in primates, only a limited number of retinal ganglion cells axons converge to the basic dLGN of rodents (Dacey et al., 2003; Huberman and Niell 2011).

Retinal ganglion cells receive their input from rods and cones and transfer the visual information via parasol and midget cells to the magnocellular layers and the parvocellular

layers of dLGN, respectively. Magnocellular and parvocellular layers target layer 4 of area V1 (4Cα and 4Cβ respectively). Both the M and P pathways also project to layer 6 of the primary visual cortex and receive a robust corticogeniculate feedback from the same layer that is mainly excitatory and glutamatergic (McCormick and von Krosigk 1992; Fitzpatrick et al., 1994). The LGN is not just a passive relay; about 90% of its inputs are coming from sites other than retina, and about 30% of them are feedback inputs from V1 (Van Horn et al., 2000). Recent studies revealed that a close relationship in feedforward and feedback parallel streams instigates the functional influence of the LGN in visual processing. The magnocellular pathway is more sensitive to low spatial frequencies, low luminance contrasts, and responsible for the perception of motion and luminance, but it is chromatically non-opponent. On the other hand, parvocellular neurons (8 times more numerous than magno cells) convey chromatic and form information and are less sensitive to luminance contrasts (Briggs and Usrey 2011). Additionally, the middle temporal visual area (MT) and medial superior temporal area (MST), motion detection centers, mainly receive the magnocellular layers primary inputs (Maunsell et al., 1990; Merigan et al., 1991). In human and non-human primates, low to moderate density of CB1R has been reported in several cortical areas like the primary visual cortex (V1), specially layer 5 and 6, in higher-order visual areas (V2, V3, V4) with more density in MT and MST (Eggan and Lewis 2007). In V1, layers 5 and 6 contained the highest expression of CB1R (Eggan and Lewis 2007). Interestingly, the higher density of CB1R in magnocellular layers of LGN in our study concurs with well-defined thalamo-recipient cortical areas. Thus, expression of eCB components in the visual cortex of rodent and primate brains (Eggan and Lewis 2007; Jiang et al., 2010) indicates that the whole visual pathway, from retina to cortex, can be influenced by cannabinoids.

CB1R and FAAH are highly co-expressed throughout the retinal layers of the same species (Bouskila et al., 2012). Here, we show that both CB1R and FAAH are present in the dLGN mainly in the magnocellular layers. Previous studies showed a similar overlapping distribution of FAAH and CB1R in pyramidal cells of the mouse hippocampus, amygdala and entorhinal cortex (Marsicano and Lutz 1999) and the rat cortex (Hill et al., 2007).

NAPE-PLD: a dissimilar pattern of expression

NAPE-PLD is widely expressed in the mouse thalamus (Egertová et al., 2008). Furthermore, the presence of NAPE-PLD in the rat brain has been reported, with an increased expression in the thalamus (Morishita et al., 2005). Unlike CB1R and FAAH, the synthesizing enzyme, NAPE-PLD, is expressed homogenously throughout the magnocellular and parvocellular layers of the dLGN without any laminar preference (Figure 6-1c, f, g). Besides synthesizing the endocannabinoid anandamide, NAPE-PLD also generates NAEs that are major substrates for mediating various motivational functions (Viveros et al., 2008). Interestingly, the degrading enzyme FAAH can metabolize NAEs into cellular membrane components (Cravatt et al., 1996; Cravatt et al., 2001). Even though both FAAH and NAPE-PLD are expressed in rodent thalamic nuclei neuronal cells, FAAH is only present in neuronal somata (Egertová et al., 2003). Given that these proteins are targeted to the axons, axon terminals and cytosol of neurons suggest a putative role of the eCB system as a mediator of anterograde signaling at thalamic synapses. Our results show that FAAH and NAPE-PLD are also co-expressed in the monkey dLGN (Figure 6-1b, c). They support previously reported

results that NAE could serve as an autocrine synaptic signaling molecules regulating the release of neurotransmitters (Egertová et al., 2008).

CB1R, FAAH and NAPE-PLD are not present in LGN astrocytes

The presence of CB1R in astrocytes is controversial. While some studies have failed to show any expression of CB1R in astrocytes (reviewed in Stella 2004), others have detected it in the caudate, putamen (Rodriguez et al., 2001) and hippocampal astrocytes (Navarrete and Araque 2008). In the hippocampus, astrocyte activation of CB1R leads to phospholipase C-dependent Ca^{2+} mobilization from the store and mediation of the eCBs communication with the neurons. This intermediation might play a role in the physiology of CB addiction (Navarrete and Araque 2008). Our results show no co-expression between CB1R, FAAH and NAPE-PLD with GFAP in the LGN.

Functional significance

The geniculo-cortical distribution of CB1R (Figure 6-1) sheds light into the putative functions of the eCB system in vision. Indeed, cannabis at the retinal level could affect the upstream visual pathways namely the ventral and dorsal visual streams. The higher expression of CB1R and FAAH in the magnocellular layers could have a functional value for the dorsal visual system involved in motion processing and object location ("how/where" pathway) (Goodale and Milner 1992; Kupers and Ptito 2014). The abundance of the CB1R in the magnocellular layers of dLGN, areas MT and MST supports a role of eCB system in motion perception. In agreement with our findings, case studies on high-potency heavy cannabis smokers reported visual disturbances and impairment in motion perception (Levi and Miller

1990). Likewise, cannabis causes impaired performance in tests that require fine psychomotor control such as tracking a moving point of light on a screen (Adams et al., 1975; Adams et al., 1978). Magnocellular neurons are also more sensitive to low luminance contrasts (Tootell et al., 1988) and relatively unresponsive to chromatic contrasts (Croner and Kaplan 1995). Higher expression of CB1R in the magnocellular pathway prompts a role of the endocannabinoid system in the night vision. In agreement with this speculation, numerous reports claim that smoking marijuana improves dim light vision and photosensitivity (Dawson et al., 1977; Merzouki and Mesa 2002; Russo et al., 2004). Besides, the neurons in the magnocellular pathway are also sensitive to flickering stimuli (Lee et al., 1989) and lesions to the magnocellular layers of the dLGN can cause deficits in critical flicker fusion (Merigan and Maunsell 1990) and flicker detection (Schiller et al., 1990).

Even though the expression of the CB1R and FAAH is more abundant in magnocellular layers, they are nonetheless present in the parvocellular layers of the dLGN. If the eCB system plays any role in color perception, it should be through chromatic properties of parvo cells and retinal cones. Both of these components of the visual system express CB1R. Conjointly, one of the most frequently reported effects of cannabis is more intense and brighter colours (Green et al., 2003; Lerner et al., 2011). Although the eCB system is considered as a good candidate for modulation of the dynamics of the cortical networks (Robbe et al., 2006), there are few electrophysiological studies on the role of cannabinoids in the visual system. Recently, in primary and secondary visual cortices, it has been reported that the CB1R and CB2R full agonist, CP55940, decreases electroencephalogram and local field potential power in V1 and V2 in macaque monkeys. Moreover, it delayed the individual

neuronal response by almost 10 ms, although they referred to the low level of CB1R in the thalamus (Ong and Mackie, 1999) and linked this activity at the retinal level (Ohiorhenuan et al., 2014). To the best of our knowledge, there is only one study that has characterized the physiological effects of CB1R-mediated activity in the rat visual thalamus (Dasilva et al., 2012). Using single-unit extracellular recordings, the authors showed that, at the level of thalamus, CB1R activation revealed two cellular populations, one exhibiting excitatory effects (28%) and the other inhibitory ones (72%). These actions were blocked using AM251, a specific inverse agonist of CB1R. This suggests that CB1R in the rat thalamus acts as a dynamic modulator of visual information funneled to the cortex. The modulatory role of CB1R in the thalamus of monkeys and especially the dLGN could have a higher impact on visual processing due to its complex laminar structure and increased retinal inputs. Our results are in accordance with these electrophysiological findings and revealed that this neuromodulation of CB1R receptors may be due to their expression in the dLGN.

The expression pattern of these eCB components has been also well characterized in the primate retinal cells (Bouskila et al., 2012; Bouskila et al., 2013a, b) that project to the dLGN through the optic nerve. The importance of CB1R has been highlighted in a recent electroretinographic study (ERG) that showed the implication of this cannabinoid receptor in the generation of the ERG responses (Ptito et al., 2014). Indeed, blocking CB1R induces an increase in the b-wave component of the ERG. This increase is possibly reflecting the gating of calcium (Ca^{2+}) and potassium (K^{+}) ionic channels (Bouskila et al., 2013a). The change in neuronal membrane permeability to Ca^{2+} ions and activity of adenylyl cyclase may affect

neurotransmitter release and action (Di Marzo et al., 1998) not only at the retinal level, but also probably at the dLGN level.

The data presented here provide the first insight into the neuroanatomy of CB1R, FAAH, and NAPE-PLD expression in the primate dLGN and a new perspective of the neural function of this system. In other words, the presence of the endocannabinoid system in the dLGN and especially in the magnocellular pathway suggests a putative neuromodulatory action that affects the functions of the dorsal visual pathway involved in motion perception, object localization and action-oriented behaviors that depend on the perception of space.

Acknowledgments

The Natural Science and Engineering Research Council of Canada (6362-2012, MP; 311892-2010, JFB) and the Canadian Institutes of Health Research (MOP-86495, JFB) supported this project financially. J.F.B. holds a *Chercheur Boursier Senior* from the *Fonds de Recherche du Québec-Santé (FRQ-S)*. M.P is Harland Sanders Char Professor in Visual Science. We are also grateful to Dr Frank Ervin and Dr Roberta Palmour of St.-Kitts, West Indies, for supplying the vervet monkey tissues. We would like to thank Dr Mohammad Jabbari Hagh for writing the MATLAB codes for heat map.

Conflict of interest

The authors declare that they have no conflict of interest.

Cover Illustration Triple-label immunofluorescence of the cannabinoid receptor 1 (CB1R, magenta), glial fibrillary acidic protein (GFAP, green) and the nucleic acid stain SYTOX (blue), expression in the magnocellular layers of the monkey dLGN.

References

Adams AJ, Brown B (1975) Alcohol prolongs time course of glare recovery. Nature 257 (5526):481-483

Adams AJ, Brown B, Flom MC, Jones RT, Jampolsky A (1975) Alcohol and marijuana effects on static visual acuity. Am J Optom Physiol Opt 52 (11):729-735

Adams AJ, Brown B, Haegerstrom-Portnoy G, Flom MC, Jones RT (1978) Marijuana, alcohol, and combined drug effects on the time course of glare recovery. Psychopharmacology (Berl) 56 (1):81-86

Argaw A, Duff G, Zabouri N, Cecyre B, Chaine N, Cherif H, Tea N, Lutz B, Ptito M, Bouchard JF (2011) Concerted action of CB1 cannabinoid receptor and deleted in colorectal cancer in axon guidance. J Neurosci 31 (4):1489-1499

Bouskila J, Burke MW, Zabouri N, Casanova C, Ptito M, Bouchard JF (2012) Expression and localization of the cannabinoid receptor type 1 and the enzyme fatty acid amide hydrolase in the retina of vervet monkeys. Neuroscience 202:117-130

Bouskila J, Javadi P, Casanova C, Ptito M, Bouchard JF (2013a) Muller cells express the cannabinoid CB2 receptor in the vervet monkey retina. J Comp Neurol 521: 2399-2415

Bouskila J, Javadi P, Casanova C, Ptito M, Bouchard JF (2013b) Rod photoreceptors express GPR55 in the adult vervet monkey retina. PLoS One 8 (11):e81080

Breivogel CS, Sim LJ, Childers SR (1997) Regional differences in cannabinoid receptor/G-protein coupling in rat brain. J Pharmacol Exp Ther 282 (3):1632-1642

Briggs F, Usrey WM (2011) Corticogeniculate feedback and visual processing in the primate. J Physiol 589 (Pt 1):33-40

Cravatt BF, Demarest K, Patricelli MP, Bracey MH, Giang DK, Martin BR, Lichtman AH (2001) Supersensitivity to anandamide and enhanced endogenous cannabinoid signaling in mice lacking fatty acid amide hydrolase. Proc Natl Acad Sci U S A 98 (16):9371-9376

Cravatt BF, Giang DK, Mayfield SP, Boger DL, Lerner RA, Gilula NB (1996) Molecular characterization of an enzyme that degrades neuromodulatory fatty-acid amides. Nature 384 (6604):83-87

Croner LJ, Kaplan E (1995) Receptive fields of P and M ganglion cells across the primate retina. Vision Res 35 (1):7-24

Dacey DM, Peterson BB, Robinson FR, Gamlin PD (2003) Fireworks in the primate retina: in vitro photodynamics reveals diverse LGN-projecting ganglion cell types. Neuron 37 (1):15-27

Dasilva MA, Grieve KL, Cudeiro J, Rivadulla C (2012) Endocannabinoid CB1 receptors modulate visual output from the thalamus. Psychopharmacology (Berl) 219 (3):835-845

Dawson WW, Jimenez-Antillon CF, Perez JM, Zeskind JA (1977) Marijuana and vision--after ten years' use in Costa Rica. Invest Ophthalmol Vis Sci 16 (8):689-699

Deutsch DG, Chin SA (1993) Enzymatic synthesis and degradation of anandamide, a cannabinoid receptor agonist. Biochem Pharmacol 46 (5):791-796

Di Marzo V, Melck D, Bisogno T, De Petrocellis L (1998) Endocannabinoids: endogenous cannabinoid receptor ligands with neuromodulatory action. Trends Neurosci 21 (12):521-528

Egertová M, Cravatt BF, Elphick MR (2003) Comparative analysis of fatty acid amide hydrolase and cb(1) cannabinoid receptor expression in the mouse brain: evidence of a widespread role for fatty acid amide hydrolase in regulation of endocannabinoid signaling. Neuroscience 119 (2):481-496

Egertová M, Elphick MR (2000) Localisation of cannabinoid receptors in the rat brain using antibodies to the intracellular C-terminal tail of CB. J Comp Neurol 422 (2):159-171

Egertová M, Giang DK, Cravatt BF, Elphick MR (1998) A new perspective on cannabinoid signalling: complementary localization of fatty acid amide hydrolase and the CB1 receptor in rat brain. Proc Biol Sci 265 (1410):2081-2085

Egertová M, Simon GM, Cravatt BF, Elphick MR (2008) Localization of N-acyl phosphatidylethanolamine phospholipase D (NAPE-PLD) expression in mouse brain: A new perspective on N-acylethanolamines as neural signaling molecules. J Comp Neurol 506 (4):604-615

Eggan SM, Lewis DA (2007) Immunocytochemical distribution of the cannabinoid CB1 receptor in the primate neocortex: a regional and laminar analysis. Cereb Cortex 17 (1):175-191

Emrich HM, Weber MM, Wendl A, Zihl J, von Meyer L, Hanisch W (1991) Reduced binocular depth inversion as an indicator of cannabis-induced censorship impairment. Pharmacol Biochem Behav 40 (3):689-690

Felder CC, Nielsen A, Briley EM, Palkovits M, Priller J, Axelrod J, Nguyen DN, Richardson JM, Riggin RM, Koppel GA, Paul SM, Becker GW (1996) Isolation and measurement of the endogenous cannabinoid receptor agonist, anandamide, in brain and peripheral tissues of human and rat. FEBS Lett 393 (2-3):231-235

Fitzpatrick D, Usrey WM, Schofield BR, Einstein G (1994) The sublaminar organization of corticogeniculate neurons in layer 6 of macaque striate cortex. Vis Neurosci 11 (2):307-315

Flom MC, Brown B, Adams AJ, Jones RT (1976) Alcohol and marijuana effects on ocular tracking. Am J Optom Physiol Opt 53 (12):764-773

Glass M, Dragunow M, Faull RL (1997) Cannabinoid receptors in the human brain: a detailed anatomical and quantitative autoradiographic study in the fetal, neonatal and adult human brain. Neuroscience 77 (2):299-318

Gómez-Ruiz M, Hernández M, de Miguel R, Ramos JA (2007) An overview on the biochemistry of the cannabinoid system. Mol Neurobiol 36 (1):3-14

Goodale MA, Milner AD (1992) Separate visual pathways for perception and action. Trends Neurosci 15 (1):20-25

Green B, Kavanagh D, Young R (2003) Being stoned: a review of self-reported cannabis effects. Drug and alcohol review 22 (4):453-460

Herkenham M, Lynn AB, Johnson MR, Melvin LS, de Costa BR, Rice KC (1991) Characterization and localization of cannabinoid receptors in rat brain: a quantitative in vitro autoradiographic study. J Neurosci 11 (2):563-583

Hill EL, Gallopin T, Ferezou I, Cauli B, Rossier J, Schweitzer P, Lambolez B (2007) Functional CB1 receptors are broadly expressed in neocortical GABAergic and glutamatergic neurons. J Neurophysiol 97 (4):2580-2589

Huberman AD, Niell CM (2011) What can mice tell us about how vision works? Trends Neurosci 34 (9):464-473.

Jiang B, Sohya K, Sarihi A, Yanagawa Y, Tsumoto T (2010) Laminar-specific maturation of GABAergic transmission and susceptibility to visual deprivation are related to endocannabinoid sensitivity in mouse visual cortex. J Neurosci 30 (42):14261-14272

Jongen-Relo AL, Pitkanen A, Amaral DG (1999) Distribution of GABAergic cells and fibers in the hippocampal formation of the macaque monkey: an immunohistochemical and in situ hybridization study. J Comp Neurol 408 (2):237-271

Kupers R, Ptito M (2014) Compensatory plasticity and cross-modal reorganization following early visual deprivation. Neurosci Biobehav Rev 7634:191-197

Lee BB, Martin PR, Valberg A (1989) Sensitivity of macaque retinal ganglion cells to chromatic and luminance flicker. J Physiol. Jul;414:223-43

Lerner AG, Goodman C, Rudinski D, Bleich A (2011) Benign and time-limited visual disturbances (flashbacks) in recent abstinent high-potency heavy cannabis smokers: a case series study. The Israel journal of psychiatry and related sciences 48 (1):25-29

Levi L, Miller NR (1990) Visual illusions associated with previous drug abuse. Journal of clinical neuro-ophthalmology 10 (2):103-110

Leweke FM, Schneider U, Thies M, Munte TF, Emrich HM (1999) Effects of synthetic delta9-tetrahydrocannabinol on binocular depth inversion of natural and artificial objects in man. Psychopharmacology (Berl) 142 (3):230-235

Marsicano G, Lutz B (1999) Expression of the cannabinoid receptor CB1 in distinct neuronal subpopulations in the adult mouse forebrain. Eur J Neurosci 11 (12):4213-4225.

Maunsell JH, Nealey TA, DePriest DD (1990) Magnocellular and parvocellular contributions to responses in the middle temporal visual area (MT) of the macaque monkey. J Neurosci 10 (10):3323-3334

McCormick DA, von Krosigk M (1992) Corticothalamic activation modulates thalamic firing through glutamate "metabotropic" receptors. Proc Natl Acad Sci U S A 89 (7):2774-2778

Merigan WH, Byrne CE, Maunsell JH (1991) Does primate motion perception depend on the magnocellular pathway? J Neurosci 11 (11):3422-3429

Merigan WH, Maunsell JH (1990) Macaque vision after magnocellular lateral geniculate lesions. Vis Neurosci 5 (4):347-352

Merzouki A, Mesa JM (2002) Concerning kif, a Cannabis sativa L. preparation smoked in the Rif mountains of northern Morocco. Journal of ethnopharmacology 81 (3):403-406

Moldrich G, Wenger T (2000) Localization of the CB1 cannabinoid receptor in the rat brain. An immunohistochemical study. Peptides 21 (11):1735-1742

Morishita J, Okamoto Y, Tsuboi K, Ueno M, Sakamoto H, Maekawa N, Ueda N (2005) Regional distribution and age-dependent expression of N-acylphosphatidylethanolamine-hydrolyzing phospholipase D in rat brain. J Neurochem 94 (3):753-762

Moskowitz H, Sharma S, McGlothlin W (1972) Effect of marihuana upon peripheral vision as a function of the information processing demands in central vision. Percept Mot Skills 35 (3):875-882

Navarrete M, Araque A (2008) Endocannabinoids mediate neuron-astrocyte communication. Neuron 57 (6):883-893

Ohiorhenuan IE, Mechler F, Purpura KP, Schmid AM, Hu Q, Victor JD (2014) Cannabinoid neuromodulation in the adult early visual cortex. PLoS One 9 (2):e87362

Ong WY, Mackie K (1999) A light and electron microscopic study of the CB1 cannabinoid receptor in primate brain. Neuroscience 92 (4):1177-1191

Piomelli D (2003) The molecular logic of endocannabinoid signalling. Nat Rev Neurosci 4 (11):873-884.

Ptito M, Javadi, P, Bouskila J, Casanova C, Bouchard JF (2014), Role of retinal cannabinoid receptors CB1 and CB2, and GPR55 defined by electroretinography in vervet monkeys. FENS -0297-D021

Robbe D, Montgomery SM, Thome A, Rueda-Orozco PE, McNaughton BL, Buzsaki G (2006) Cannabinoids reveal importance of spike timing coordination in hippocampal function. Nat Neurosci 9 (12):1526-1533

Rodriguez JJ, Mackie K, Pickel VM (2001) Ultrastructural localization of the CB1 cannabinoid receptor in mu-opioid receptor patches of the rat Caudate putamen nucleus. J Neurosci 21 (3):823-833

Russo EB, Merzouki A, Mesa JM, Frey KA, Bach PJ (2004) Cannabis improves night vision: a case study of dark adaptometry and scotopic sensitivity in kif smokers of the Rif mountains of northern Morocco. Journal of ethnopharmacology 93 (1):99-104

Schiller PH, Logothetis NK, Charles ER (1990) Role of the color-opponent and broad-band channels in vision. Vis Neurosci 5 (4):321-346

Semple DM, Ramsden F, McIntosh AM (2003) Reduced binocular depth inversion in regular cannabis users. Pharmacol Biochem Behav 75 (4):789-793

Stella N (2004) Cannabinoid signaling in glial cells. Glia 48 (4):267-277

Straiker A, Stella N, Piomelli D, Mackie K, Karten HJ, Maguire G (1999a) Cannabinoid CB1 receptors and ligands in vertebrate retina: localization and function of an endogenous signaling system. Proc Natl Acad Sci U S A 96 (25):14565-14570

Straiker AJ, Maguire G, Mackie K, Lindsey J (1999b) Localization of cannabinoid CB1 receptors in the human anterior eye and retina. Invest Ophthalmol Vis Sci 40 (10):2442-2448

Suárez J, Bermudez-Silva FJ, Mackie K, Ledent C, Zimmer A, Cravatt BF, de Fonseca FR (2008) Immunohistochemical description of the endogenous cannabinoid system in the rat cerebellum and functionally related nuclei. J Comp Neurol 509 (4):400-421

Takahata T, Hashikawa T, Tochitani S, Yamamori T (2010) Differential expression patterns of OCC1-related, extracellular matrix proteins in the lateral geniculate nucleus of macaque monkeys. J Chem Neuroanat. 2010 Oct;40(2):112-22

Tootell RB, Hamilton SL, Switkes E (1988) Functional anatomy of macaque striate cortex. IV. Contrast and magno-parvo streams. J Neurosci 8 (5):1594-1609

Tsou K, Brown S, Sanudo-Pena MC, Mackie K, Walker JM (1998) Immunohistochemical distribution of cannabinoid CB1 receptors in the rat central nervous system. Neuroscience 83 (2):393-411

Van Horn SC, Erisir A, Sherman SM (2000) Relative distribution of synapses in the A-laminae of the lateral geniculate nucleus of the cat. J Comp Neurol 416 (4):509-520

Viveros MP, de Fonseca FR, Bermudez-Silva FJ, McPartland JM (2008) Critical role of the endocannabinoid system in the regulation of food intake and energy metabolism, with phylogenetic, developmental, and pathophysiological implications. Endocrine, metabolic & immune disorders drug targets 8 (3):220-230

Wojcik SM, Rhee JS, Herzog E, Sigler A, Jahn R, Takamori S, Brose N, Rosenmund C (2004) An essential role for vesicular glutamate transporter 1 (VGLUT1) in postnatal development and control of quantal size. Proc Natl Acad Sci U S A. 2004 May 4;101(18):7158-63

Xu X, Ichida JM, Allison JD, Boyd JD, Bonds AB, Casagrande VA (2001) A comparison of koniocellular, magnocellular and parvocellular receptive field properties in the lateral geniculate nucleus of the owl monkey (Aotus trivirgatus). J Physiol 531 (Pt 1):203-218

Zabouri N, Bouchard JF, Casanova C (2011) Cannabinoid receptor type 1 expression during postnatal development of the rat retina. J Comp Neurol 519 (7):1258-1280

Zhou J, Nannapaneni N, Shore S (2007) Vessicular glutamate transporters 1 and 2 are differentially associated with auditory nerve and spinal trigeminal inputs to the cochlear nucleus. J Comp Neurol. 2007 Feb 1;500(4):777-8

CHAPTER 7: Discussion and Conclusion

The importance of cannabinoid research has become more apparent with time. Cannabinoid researchers have diverged from studying the adverse events of recreational cannabis in the sixties to investigating the utility of the endogenous system as a therapeutic target. It has since become clear that the complex eCB system is present throughout the animal kingdom and in almost every organ and cell type. It worth mentioning that there are several research projects that focus mainly on the roles of endocannabinoid system in attention, memory, appetite, stress response, inflammation, immune functions, analgesia, sleep and etc., and reveal many interesting aspects of this polyhedron system. The work presented in this thesis seeks to elaborate on the relationship between the eCB system and vision. Thus, we report here for the first time that:

1. CB2R is present in the retinal layers of the vervet monkey but with striking dissimilar laminar pattern of expression. We show that CB2R is restricted to Müller cell processes with very low staining in the internal limiting membrane and heavy labeling in the external limiting membrane. We conclude that CB2R is indeed present in the retina but exclusively in the retinal glia, whereas CB1R is expressed only in the neuroretina (Bouskila et al., 2013a).

2. The expression of the eCB system components in the tree shrew retina and the distribution of NAPE-PLD, MAGL and DAGLα in the monkey retina (vervet and macaque) were compared. We also verified the expression pattern of eCB system and found that CB1R and FAAH distributions are well preserved among mouse, tree shrews, and vervet and macaque monkeys. By contrast to mice and tree shrews, NAPE-PLD expression in monkeys is circumscribed to the photoreceptor layer. CB2R expression is variable across these species; in

mice, CB2R is found in retinal neurons, in tree shrews, it is expressed in Müller cell processes of the outer retina and in retinal neurons of the inner retina, and in monkeys, CB2R is restricted to Müller cells that span the entire retinal thickness. Expression patterns of MAGL and DAGLα are complementary in the inner retinal layers. Overall, these results provide evidence that the eCB system is differentially expressed in the retina of these mammals and suggest a distinctive role of eCBs in visual processing (Javadi et al., Submitted to Frontiers in Neuroanatomy).

3. The development of a standardized protocol for photopic and scotopic ERG in vervet monkeys to assess the retinal function of the CB1R and CB2R. When testing the protocol, we found that the recordings obtained in healthy Green Monkeys matched very well with those in humans (Marmor et al., 2009) and other non-human primate species (*Macaca mulatta* and *Macaca fascicularis*, reported by (Bee, 2001). Furthermore, the results from the standardized protocol validate the Green Monkey as an excellent non-human primate model, with the potential to serve for testing retinal function after manipulations such as visual deprivation or drug evaluation (Bouskila et al., 2014).

4. Blockade of CB2R increases the amplitude of the photopic ERG a-wave and b-wave at certain higher flash intensities, while at some lower flash intensities, blockade of CB1R reduces the amplitude of both a- and b-waves. In dark-adapted eyes, blockade of the CB1R and CB2R reduces the a-wave amplitudes in the higher intensities and decrease the b-wave in lower intensities. Also the cannabinoid receptors antagonists AM251 and AM630 delayed the time to peak in both a- and b-waves.

5. The expression pattern of the CB1R, FAAH, and NAPE-PLD in the dLGN of the vervet monkey beyond the retina. Our results show that CB1R and FAAH are expressed throughout the dLGN with more prominent labeling in the magnocellular layers. However, the synthesizing enzyme NAPE-PLD is diffused homogenously throughout the magnocellular and parvocellular layers of dLGN. These proteins are weakly expressed in the koniocellular layers. The higher expression of CB1R in the magnocellular layer suggests some of the behavioral effects of cannabinoids associated with the integrity of the dorsal visual pathway that plays a role in visual-spatial localization and motion perception (Javadi et al., In press, Neuroscience).

The activation of the CBRs via exogenous agonists such as THC seldom produces mutual and critical visual symptoms other than IOP reduction and vasodilation; however, the abundance of these receptors throughout the visual system, from retina to visual cortex, suggests that eCBs play a role in normal visual function. Otherwise, spending this quantity of protein and consuming energy to produce such copious receptors without any crucial role, will not be economic for the cell. In case studies and anecdotal reports, chronic marijuana users reported various visual symptoms including visual distortions, distorted perception of distance, illusions of movement, color intensification, dimmed color, dimensional distortion, blending of patterns and objects (Levi and Miller, 1990; Lerner et al., 2011;), impaired performance in tracking a moving point of light (Adams et al., 1975; Adams et al., 1978), increased glare recovery time, blurred vision (Noyes et al., 1975), double vision and vision dimness (Consroe et al., 1997), improved dim light vision (Dawson et al., 1977; Merzouki and Mesa, 2002; Russo et al., 2004), reduced Vernier and Snellen acuity, altered color discrimination, increased photosensitivity, decreased dark adaptation (Kiplinger et al., 1971; Dawson et al., 1977; Russo

et al., 2004), reduction in acuity of moving targets when coordinated eye movements were required (Leweke et al., 1999), and reduction of binocular depth inversion (Semple et al., 2003).

Most of our knowledge about the eCB system and mammalian vision is based on the research that has been performed in rodents (Yazulla, 2008; Casanova et al., 2010; Cécyre et al., 2011; Zabouri et al., 2011a; Zabouri et al., 2011b; Dasilva et al., 2012; Cécyre et al., 2013; Cécyre et al., 2014). Mice exhibit very low resolution of about 20/2000 (Prusky and Douglas, 2004) with eyes and visual pathways of about one to two magnitudes of order smaller than primates. Thus, it is difficult to compare the refraction, chromatic aberration, and retinal illumination of rodents to that of primates (Remtulla and Hallett, 1985). By contrast, the vervet monkey possesses large eyes with high visual acuity and foveal vision. Similar to humans, the vervet visual pathway displays well-segregated parallel pathways in the visual thalamus, six layers dLGN, ocular dominance, and orientation columns in the visual cortex. In addition, vervets and macaques have RGB trichromatic vision (Jacobs, 2008), making them a great animal model for visual research that can be easily translated to humans.

Here, with anatomical and electrophysiological approaches, we tried to speculate on certain roles of the eCB systems in the primate vision.

Expression of CB2R in Müller Cells of the Monkey Retina

First, we assessed the localization of two cannabinoid receptors (CB1R, CB2R), two eCB synthesizing enzymes (NAPE-PLD and DAGLα), and two eCB degrading enzymes (FAAH and MAGL) in the retina and compared expression in three phylogenetically related mammals; mice, tree shrews, and monkeys.

The primary CBR, CB1R, is expressed throughout the retinal layers in all of our animal models, with the exception of the rods and Müller cells in monkey. We show here that in the retina of the vervet monkey, CB2R is specifically present in the Müller cells. This agrees with its glial expression in the CNS and suggests a specific role for each of these receptors. Among the three glial cells of the primate retina (Müller cells, astrocytes, and microglia), Müller cells are the main glial cells with processes that extend from the outer limiting membrane to the inner limiting membrane throughout the retina. The similar expression pattern of CB2R, with higher polarization towards the outer retina and colocalization with GS, supports our finding that CB2R is exclusively expressed in Müller cells. It has been reported that activation of CB2R triggers a series of protective activities (Pacher and Mechoulam, 2011) such as augmentation of microglial cell proliferation (Carrier et al., 2004) and reduction of the release of harmful factors such as tumor necrosis factor and free radicals (Stella, 2009). In human, exposing activated Müller cells to eCBs reduces the production of pro-inflammatory cytokines (Krishnan and Chatterjee, 2012). CB2R activation in Müller cells may protect neurons from exposure to excess neurotransmitters (Placzek et al., 2008), which can play important roles in mediating neurotoxicity, inflammation, and neuroprotection. CB2R expressed in distal Müller cell fibers adjacent to photoreceptor layers

that express CB1R may also mediate light transduction. The junction between the Müller cells and photoreceptors, at outer limiting membrane, represents the outer border of CB2R expression. The neuronal expression of CB1R and glial presence of CB2R suggests a complementary relationship between these two receptors in the monkey's retina. We speculate that the eCBRs are important for light transduction where CB1R plays a role in neurons and CB2R in glia. Based on these anatomical data, we proposed the following model for eCB function in the retina: light increases the K^+ concentration in the extracellular space of the retina. Müller cells release the excess amount of the K^+ ions into vitreous to maintain the electrolytic balance (Newman and Reichenbach, 1996). The b-wave of the ERG is attributed to ON-bipolar and Müller cell interactions and reflects the K^+ level of the Müller cells in such a way that blocking the K^+ channels reduces the ERG b-wave. Based on the role of CB2R activation in the reduction of cAMP and PKA, which indirectly increases the activity of Kir4.1 channels in Müller cells (MacGregor et al., 1998), we proposed that the deactivation of CB2R, as a negative modulator of K^+ channel, increases the amplitude of the b-wave. The functional data we report here supports this model.

Comparison of the Retinal Expression Pattern of the eCB Components

CB1R and CB2R are unique to chordates but the enzymes involved in the synthesis and degradation of eCBs have been discovered throughout the vertebrate and many species in the whole animal kingdom (Elphick, 2012). Thus, it is likely that proteins have evolved as pre- or postsynaptic receptors for eCBs. Although the expression pattern of some components such

as CB1R and FAAH seem to be similar in different species, such is not the case for other eCB components such as CB2R and NAPE-PLD. Considering the differential expression of CB2R in the retina of mice (Cecyre et al., 2013) and vervets (Bouskila et al., 2012), we compared the expression of other components of the eCB system in these two species as well as in a phylogenetically intermediary animal, the tree shrew. Moreover, we verified the similarity in the retinal expression of eCBs in vervets and macaques to demonstrate the utility of these animal models for eCB research in the visual system. The overlapping distribution of CB1R and FAAH suggested that the degrading enzyme might remotely influence CB1R (Egertová et al., 2003). In the monocular, rod dominant visual system of the mouse, CB2R is expressed in the photoreceptor layer, mainly in cones and some rods (Cecyre et al., 2013). The tree shrew, with cone-dominant binocular vision, is an appropriate phylogenetic midpoint, exhibiting expression in all layers (similar to rodents) as well as in Müller cells (as seen in primates). This interspecies pattern is repeated in other eCB components such as NAPE-PLD. Both anandamide and NAEs are biosynthesized from the phospholipids of the cell membrane with NAPE-PLD hydrolysis. Despite the well-preserved sequence of NAPE-PLD among rodents and humans, it exhibits different retinal expression between species. Unlike the mouse but similar to primates, the tree shrew has a higher expression of NAPE-PLD in the photoreceptor layer. This variation may be due to non-eCB related functions of NAPE-PLD; these include diverse physiological roles such as anti-inflammatory effects (Lambert et al., 2002), anorexic effects (Rodriguez de Fonseca et al., 2001), and pro-apoptotic effects (Maccarrone et al., 2002). Moreover, NAE products in axons suggest a role in the regulation of postsynaptic neuron activity as anterograde synaptic signaling molecules (Egertová et al., 2008). This pattern of expression also indicates another direct role of NAEs in primate photo-transduction.

For the first time, we report the expression pattern of DAGLα and MAGL in the retina of the monkey and the tree shrew. Logically, eCB ligands should synthesize and degrade in the vicinity of their receptors; thus DAGLα and MAGL should be expressed near CB2R. Their expression pattern in mouse retina follows this logic as they are in the vicinity of both CB1R and CB2R, meaning that the CBs such as 2-AG are faithfully expressed adjacent to cannabinoid receptors and could be involved in their retinal function. Through evolution, tree shrews and primates have chosen a complementary distribution pattern. It seems that the eCB system has become more highly specialized in species with complex visual systems to adopt a more specific strategy for modulation of their visual activity.

Standard protocol for vervet monkeys

To assess our hypothesis and verify the role of eCB in normal retinal function we utilized the full field ERG as a non-invasive method. The ERG measures the electrical responses of various retinal cells such as photoreceptors (rods and cones) and inner retinal cells (bipolar and amacrine cells) in response to diverse stimuli. The ERG represents a useful tool in toxicology and eye research. The progressive use of vervets as a model in visual research led us to publish our methodology as a standard protocol. Our standard values for vervets were very similar to humans by standard ERG. ISCEV standards provide a consensus for stable comparison between research laboratories and clinical ERG recordings (Marmor et al., 2009). The shape and latency of the primate waves were similar to human; however, their waves tended to show lower amplitude. This decrease in amplitude is due to the smaller diameter of the eye and retinal surface of the monkey.

Blockade of the CB1R, reduces photopic a-waves amplitude; role in photosensitivity

The photopic a-wave amplitude originates from the activity of the cone photoreceptors (Hood and Birch, 1993, 1996). CB1R agonists raise calcium current in rods and decrease it in large single cones. These agonists can also reduce the potassium current in both rods and cones (Straiker and Sullivan, 2003). Light-mediated hyperpolarization of the photoreceptors decreases the calcium current and reduces neurotransmitter release. The CB1R activation differentially modulates the calcium and potassium currents in rods and cones of the goldfish and salamander (Fan and Yazulla, 2003; Straiker and Sullivan, 2003; Fan and Yazulla, 2007). We show that the blockade of the CB1R reduce the photoreceptor responses in lower intensities. This result can be an explanation for the increase of the photosensitivity after the consumption of cannabis (Dawson et al., 1977; Yazulla, 2008).

CB2R antagonist increases the amplitude of b-wave through Müller cells

In chapter 2 of this thesis, we demonstrate the anatomical expression of the CB2R and speculated a function for CB2R. Briefly, we proposed that CB2R in Müller cells uses potassium channel, $K_{IR}4.1$ to modulate the ERG. Given that CB2R coupling via $G_{i/o}$ decreases cAMP and PKA levels (Howlett et al., 2002) and that PKA increases the activity of $K_{IR}4.1$ channels in the Müller cells, we therefore suggest that the blockade of the CB2R will therefore activate the potassium channels and increase the amplitude of the b-wave (Bouskila et al., 2013a). Here, we confirm the proposed model via ERG, that blockade of this receptor increase the b-wave amplitude.

Blockade of CBR decreases scotopic b-wave amplitude in lower intensity; role in dim light vision

Our results demonstrate that both cannabinoid receptors antagonists decrease the amplitude of scotopic b-wave in lower flash intensities. This is in line with the claim that activation of the cannabinoid receptors may cause an increase in rod responses through bipolar cells and/or Müller cells (Straiker and Sullivan, 2003). This reduction can be due to the blockade of the CB1Rs that are mainly expressed in bipolar cells. The fact that CB2R is mainly found in Müller cells, the potassium-buffering role of Müller cells (explained before) could be the reason for this reduction. This can also elucidate the reports on the role of cannabis in improving the night vision (West, 1991, Merzouki and Mesa, 2002, Russo et al., 2004).

Monkeys vs mice results

In their recent ERG study, Cécyre et al revealed that in transgenic mice, while CB1R removal does not affect the ERG responses in scotopic condition, CB2R elimination increased significantly the amplitude of the a-wave in higher intensity (Cécyre et al., 2013). They suggested that the reported alteration of rod sensitivity by cannabinoid agonist in tiger salamander (Straiker and Sullivan, 2003) is mediated by CB2R. Here we show a decrease of a-wave response in higher intensities for mainly CB1R and also CB2R. This controversy can be due to the difference in the visual system of these species and animal models. Firstly, the expression pattern of CB2R in the vervet monkey is dissimilar to rodents. In rodents, CB1R and CB2R have a very similar expression pattern (Zabouri et al., 2011, Cécyre et al., 2013) but in the vervet monkey while CB1R is expressed throughout the retina (Bouskila et al.,

2012), CB2R is mainly detected in Müller cells (Bouskila et al., 2013a). Secondly, transgenic animal without CB1R or CB2R went through an adaptations procedure through their development. This adaptation may result in different physiological responses from the normal animals that their receptors were blocked temporarily with an antagonist.

Limitations on Functional Study of the Cannabinoid Systems

One of the main limitations of cannabinoid research is the dose effect (Yazulla, 2008). Agonists in some dosage can cause complete opposite effects on the cannabinoid receptors activity (Henstridge et al., 2010). A CB1R agonist can be a stimulant at low dose and an inhibitor at high concentrations (Sulcova et al., 1998). In low concentrations, CB1R agonists like anandamide or WIN 55212-2 enhance the current via coupling to $G_{i/o}$ but in higher concentrations, they do inhibit the current by pairing to G_s (Chabre et al., 1994). Although these controversial effects were mainly reported in cannabinoid agonists and not antagonists, that same issue can also be raised for the blockers. In our study, due to lack of any information regarding eCB intravitreal injection dosage in primates, we opted for the lowest possible concentration that would produce an effect on the ERG since no effect was observed at lower doses.

Moreover, since some studies have claimed that AM251, at some concentrations, is an agonist for the orphan G-protein coupled receptor, GPR55, a putative third cannabinoid receptor, one may attribute the effect of AM251 on the ERG responses to GPR55 activation. However, from an anatomical point of view, CB1R and CB2R were slightly detected in the rod photoreceptors of the vervet monkey whereas GPR55 was exclusively expressed in rods (Bouskila et al., 2013b).

Expression of eCB components beyond the retina

Rods and cones transfer visual information to retinal ganglion cells. The presence of CB1R and FAAH in GCL has been previously reported (Zabouri et al., 2011a; Zabouri et al., 2011b; Bouskila et al., 2012). The ganglion cell axons leave the orbit as the optic nerve towards the optic chiasm, including the ganglion cells that output visual information. We assessed the expression of the CB1R, FAAH and NAPE-PLD beyond the retina of the vervet monkey. We found that the track of the CB1R, FAAH and NAPE-PLD in the optic nerve of the vervet is diffused throughout the coronal section.

Two magnocellular layers and the four parvocellular layers of the dLGN receive the input from the parasol and midget ganglion cells, respectively. Both magno- and parvocellular layers target layer 4 of area V1 (4Cα and 4Cβ respectively). Layer 4 of the visual cortex expressed the lowest intensity of the CB1R (Eggan and Lewis 2007). Beside layer 4, the M and P pathways also project to layer 6 of V1 and receive robust corticogeniculate feedback from the same layer, primarily excitatory and glutamatergic signaling (McCormick and von Krosigk 1992; Fitzpatrick et al., 1994). Layer 6 of the V1 shows the highest expression of CB1R (Eggan and Lewis 2007). Here, for the first time, we report that CB1R and FAAH are expressed more abundantly in magnocellular layers and NAPE-PLD is homogeneously expressed in both magno- and parvocellular layers. None of these components are expressed richly in the koniocellular layer. Previous reports have shown slight expression of CB1Rs in the dorsal thalamus of rats (Tsou et al., 1998) but no (Eggan and Lewis 2007) or only moderate (Ong and Mackie 1999) expression in primates and humans (Glass et al., 1997). However, none of these studies focused on the visual pathway and the dLGN *per se*. Argaw *et*

al. reported the presence of CB1R in the dLGN of the rodent; however, due to the fundamental structural difference of the dLGN in rodents and primates, it is impossible to make any conclusions for the human visual pathway based on the rodent results. Moreover, the number of the retinal inputs to the primitive dLGN of the rodents is considerably lower than that of the ganglion cells converging to the dLGN of the primates. About 90% of the dLGN inputs are coming from sites other than retina, and about 30% of them are feedback inputs from V1 (Van Horn et al., 2000).

Since the magnocellular pathway is more sensitive to low spatial frequencies and low luminance contrasts but is chromatically non-opponent, the eCB system may play a role in related functions. In addition, since the MT and MST are motion detection centers that also express the highest level of CB1R in the visual cortex and mainly receive their primary inputs from magnocellular layers, it appears likely that the eCB system plays a role in motion detection.

Compared to CB1R and FAAH, the unusual diffused expression of the NAPE-PLD throughout the vervet dLGN is not unexpected. NAPE-PLD is widely present in the mouse thalamus (Egertová et al., 2008). Rat brain also exhibits high expression of NAPE-PLD in the thalamus (Morishita et al., 2005). NAPE-PLD is not only responsible for anandamide production; it also generates NAEs as the major substrate for mediating various motivational functions (Viveros et al., 2008) besides synthesizing eCB agonist.

From the functional point of view, CB1R and FAAH in the magnocellular layers could regulate the dorsal visual system involved in motion processing and object location ("how/where" pathway) (Goodale and Milner 1992; Kupers and Ptito 2014). The high expression of CB1R in MT and MST areas supports this theorized role of eCB system in motion perception. Case studies and interviews with high-potency, heavy cannabis smokers reported some motion related visual impairments (Levi and Miller 1990) and a reduced ability to track a moving point of light on a screen that requires fine psychomotor control (Adams et al., 1975; Adams et al., 1978).

The magnocellular pathway may also play a role in nystagmus, the rhythmic involuntary movement of the eyes. It has been suggested that alterations of the magnocellular motion-processing pathway and the superior colliculus (SC) may be involved in the production of nystagmus (Hepp et al., 1993; Leigh et al., 2002). Interestingly, several studies reported that cannabis could be effective in suppressing acquired pendular nystagmus (Schon et al., 1999; Dell'Osso 2000; Pradeep et al., 2008). Since the main input signals to the SC rely on activity in the magnocellular geniculostriate pathway (Schiller et al., 1979), in which moderate CB1R expression has been shown in rats (Tsou et al., 1998), we suggest that cannabis may partially modulate nystagmus suppression through magnocellular pathways in the monkey dLGN. Based on the modulatory role of presynaptic eCB receptors and their expression in both excitatory glutamatergic and inhibitory GABAergic neurons, the precise mechanism of action still needs to be verified.

One of the other characteristics of magnocellular neurons is their sensitivity to low luminance contrasts (Tootell et al., 1988). Frequent reports and anecdotes claim that smoking marijuana improves scotopic vision and increases photosensitivity (Dawson et al., 1977; Merzouki and Mesa 2002; Russo et al., 2004). The high expression of CB1R in magnocellular layers suggests a putative role for the eCB system in dim light vision.

The lower expression of the CB1R in parvocellular layers does not mean that the eCB system is absent in this pathway. It is worthy to note that in parvocellular layers, the CB1Rs are spread out over a larger area (four layers) compare to magnocellular layers (two layers). In addition, the scarcity of these receptors in parvocellular layers makes them more sensitive to agonists and antagonists. In other words, a low dosage of ligand can saturate these receptors and trigger related symptoms. However, the abundance of CB1R in the magnocellular layer increases the likelihood that some receptors will not be affected by low concentration of ligands. Hence, if the eCB system plays any role in color perception, it should be through the chromatic properties of parvo cells and retinal cones. One of the most frequently reported symptoms of cannabis consumption is intensification of the perception of colors and their brightness (Green et al., 2003; Lerner et al., 2011), where parvocellular pathway may play a role beside the cones.

Our results also show that there is weak expression of CB1R, FAAH or NAPE-PLD in the koniocellular layers of the dLGN. There are three populations of relay neurons that represent three different visual pathways in primates. Koniocellular neurons make up a third channel in the primate dLGN and are located between and within the principal dLGN layers (Casagrande 1994; Hendry and Yoshioka 1994; Casagrande 1999; Hendry and Reid 2000).

The retinal input of K neurons suggests that they are involved in blue/yellow chromatic processing (Martin et al., 1997). Even though CB1R is present in the retinal ganglion cell layers of vervets, there is a minority of ganglion cells that are not CB1R positive (Bouskila et al., 2012). This could represent the blue/yellow neurons that project to the koniocellular layers of the dLGN.

Conclusion

The physiological systems of a living body tend to follow an elegant economical logic. Evolutionarily, it is highly unlikely that the body would spend a considerable amount of energy and material to produce numerous eCB components in the visual system for no other reason than getting activated after a "joint". Accordingly, the abundance of the eCB system components through the visual system suggests that they play an important role in normal vision. The variation in the pattern of expression of these components such as exclusive expression of CB2R in retinal glia and CB1R in neuroglia demonstrate that CBRs do not play the same role in all species. The eCB expression pattern in the mouse (rod-dominated retina with monocular vision), tree shrew (cone-dominated retina with binocular vision), and monkey (duplex retina with binocular vision) strongly supports the hypothesis that the retinal eCB system plays a fundamental role in mammalian visual processing.

Moreover, alteration of the retinal responses after blockade of these receptors with antagonists supports that eCB system is an important role player in the normal function of the visual system. Based on our ERG results we also endorse some of the eCB system roles in dim light vision and photosensitivity.

Beyond the retina, the neuroanatomy of CB1R, FAAH, and NAPE-PLD in the primate dLGN provides a new standpoint for the visual function of this system. This specific presence in the magnocellular pathway suggests a putative neuromodulatory action that affects the functions of the dorsal visual pathway involved in motion perception, object localization and action-oriented behaviors that depend on the perception of space, dim light vision, and nystagmus.

Chapter 8: Future Direction

Anatomy

The expression pattern of other eCB system components beyond the retina, such as CB2R, MAGL and DAGLα throughout the dLGN, and expression of eCB system components in the visual cortex (V1, V2, V4, MT, MST) needs to be verified. Another important pathway required to assess eCBs presence is saccadic and eye movement structures of vision. CB1R has been detected in human SC (Glass et al., 1997); however, its pattern of expression throughout the SC layers still needs to be clarified to reveal its role. Additionally, the expression pattern of other eCB components in the SC and the pretectal area may suggest new visual functions for eCB system while also explaining some of the symptoms present after marijuana consumption, including impaired performance in tests that require fine psychomotor control such as tracking a moving point of light on a screen (Adams et al., 1975; Adams et al., 1978).

Other than our previous work (for the article see index) (Bouskila et al., 2013b) on the retinal expression of the potential CBR, GPR55, to our knowledge there is no other study that reported its expression in the visual system of monkeys. The orphan GPR55 is thought to be responsible for some of the observed properties of the cannabinoids such as blood pressure lowering (Johns et al., 2007), gastrointestinal functions (Schicho and Storr, 2012), and anti-cancer effects (Farsandaj et al., 2012). These effects have attracted the attention of investigators and have increasingly become the focus of research in the field. The expression pattern of GPR55 in other sections of the visual system will complete our anatomic model in non-human primate and consequently in human.

It has been reported that a 2 day monocular deprivation upregulated the expression level of CB1R in the mouse visual cortex (Yoneda et al., 2013). An interesting future direction would

be to examine eCB expression patterns in blind or visually impaired monkeys compared to normally sighted ones.

Functional

ERG

In our ERG study, we utilized only receptor antagonists; examining receptor agonists and antagonists concurrently would yield a more complete picture of the roles of eCB signaling in normal retinal function. Similarly, recording ERG waves after using an inhibitor (e.g. tetrahydrolipstatin) or enhancer of the NAPE-PLD may enable us to elucidate the function of this enzyme in the retina. Verification of the functional role of NAPE-PLD in retina will be another interesting project.

In humans, comparing the ERG patterns of regular consumers of marijuana with standard ERG may show how consistent activation of the CBRs can affect the retina.

Finally, it is worthy of note that ligand concentration is very important in the cannabinoid system and can have paradoxical effects. In this study, we used only one concentration for blockers. The efficacy and optimal concentration still needs to be defined and examination may yield even more insights to the roles of cannabinoid signaling.

Visual Evoked Potential (VEP)

To assess the function of eCB beyond the retina, a VEP test can be performed with the same equipment and a similar procedure as ERG. We began registering primary VEP results during our data collection in St-Kitts to verify the electrode positions. The electrodes are

placed topically using stereotaxic coordinates close to the Oz point in the occipital lobe to register electrical responses from the visual cortex and dLGN. Classic checkerboards can isolate the activity of dLGN layers to compare their VEP wave patterns before and after blockade of the CBRs. Additionally; VEP can be used as a measure of visual acuity (Hamilton et al., 2010).

Behavioral

For our behavioural studies, we designed a series of easy-to-implement routines to tap the perceptual and cognitive functions of normally developing and adult nonhuman primates based on spontaneously generated behaviour; gaze preference. We developed a protocol to measure preferential looking time at a given stimulus as its position was shifted from the left to the right side of the screen (or vice versa). The amount of looking time was expressed as a proportion of total looking time at the entire display containing both the stimulus and the control (Zangenehpour et al., 2014). These tests can measure visual acuity, chromatic contrast sensitivity, and spatial-temporal contrast sensitivity function. Our experience in implementing this procedure showed that training the monkeys to be attentive to our stimuli was a challenge that required lengthier training periods. However, the same procedure would be useful to compare regular cannabis consumers versus a control group when demonstrating the role of chronic marijuana consumption in visual function.

Brain Imaging

Chronic consumption of cannabis might cause structural changes in brain. Lately, brain imaging studies solidly show alteration or neuroadaptation in activation of higher cognitive part of the brain networks. A lower global cerebellar glucose metabolism in resting brain function of marijuana users has been reported (Volkow et al., 1996). Intravascular THC administration increased cerebellar metabolism as well as cerebellar blood flow (CBF) in frontal cortices, basal ganglia, insula, cingulate cortex and some subcortical regions with higher increase in right hemisphere (Volkow et al., 1996; Mathew et al., 1998). This augmentation is lower in regular users (Volkow et al., 1996, Lindsey et al., 2005). Auditory attention network shows a reduction in activation following smoking marijuana (Chang and Chronicle, 2007). Chronic administration of THC down-regulate and desensitize CB1R in animal (Sim-Selley, 2003). The BOLD contrast of marijuana users in simple tasks showed reduced activation in the supplemental motor area and the cingulate region (Chang and Chronicle, 2007). In complex tasks, brain activation is altered or increased in cannabinoid users (Ganis et al., 2004). Brain activation in attention network (prefrontal, medial, dorsal parietal cortices, medial vermis of cerebellum) is reduced in marijuana users (Dasilva et al., 2012). Higher activation has been found in inferior and middle frontal gyri and right superior temporal gyrus of smokers in visuospatial working memory tasks (Smith et al., 2010). These alterations in regular users are possibly related to down-regulation of CB1R and its mRNA expression in chronic exposure to THC that is reversible (Villares, 2007).

Over the past decade, considerable effort has been devoted to develop a PET ligand to study the CB1R, in vivo. Endogenous ligands of CB1R are highly lipophilic. This lipophilicity is a great challenge to design the PET ligands. Most of the attempts result in high non-specific

binding and low brain penetration. [^{123}I] AM251 brain uptake was low and [^{123}I] AM281was more promising with a higher brain uptake but lower specificity (Li et al., 2005; Lindsey et al., 2005). The CB1R distribution in human and rhesus brain has been identified using specific, high affinity [^{18}F] MK-9470 antagonist (Burns et al., 2007). Some attempt to visualize CB2R has been reported in primates using radioligand [11C] NE40 (Evens et al., 2012).

Comparison of CB1R distribution in sighted and congenital blinds using PET

The successful PET studies that are tracing the CB1R in brain were not attentive to visual pathways and focused more on prefrontal lobe, cerebellum and hippocampus (Burns et al., 2007). Moreover studies on cross-modal plasticity in the congenitally blinds demonstrated the anatomic and functional viability of their primary and associative visual cortices (Ptito et al., 2008). PET studies show a supranormal metabolism at rest state of the occipital lobe in congenitally blind subjects (De Volder et al., 1997; Ptito et al., 2008; Kupers et al., 2011;). The visual lobes are still active in blind subject and respond to somatosensory and auditory inputs (Kupers and Ptito, 2011). Investigating the distribution of this receptor in visual areas of normal sighted subjects compared to that of the congenitally blind brain will shed a light to the role of CB1R in vision. Development of the highly specific [^{18}F] MK-9470 ligand produced remarkable outcomes in the human central nervous system (Burns et al., 2007) and makes it possible to track the CB1R in human and non-human primate visual system.

Comparison of CB1R distribution in control and regular marijuana users using PET

Chronic administration of THC down-regulate and desensitize the CB1R in animal (Villares, 2007). However no association has been found between alteration of the volume of gray matter, white matter, Cerebrospinal fluid, hippocampi and chronic use (Jager et al.,

2006), but voxel-based morphometry reveal reduction of gray matter density in right parahippocampal gyrus and augmentation in right pre-central gyrus and thalamus as well as white matter density (Chang and Chronicle, 2007). *In situ* hybridization demonstrated a significant decrease of CB1R in postmortem human brain in regular cannabis users (Sim-Selley, 2003). Verification of the expression of the CB1R in the visual pathway of the chronic marijuana users using highly specific [18F] MK-9470 ligand can shed a light on the putitative roles of eCB system in vision.

Comparing the visual processing and brain activation before and after administration of CB1R antagonist, rimonabant, in normal subjects under fMRI

Most of our knowledge on the effects of cannabinoids on vision has been studied through the use of marijuana. Rimonabant is an antagonist for CB1R that had been used as an anorectic anti-obesity drug to reduce appetite (Duarte et al., 2004). It had been also used as an anti-addiction drug for smoking cessation therapy and reducing cocaine-seeking habits (Le Foll and Goldberg, 2005; Cahill and Ussher, 2011). The threshold of the visual acuity, chromatic contrast sensitivity, and motion perception subjects before and after blocking the receptors can be compared. Moreover, the effects of the blockers on activations of the visual pathways can be verified with fMRI.

eCB research is a complex but highly promising field. Characterization of eCB components and discovering their role will pave the road to new therapeutics for vision. Finally, in light of the seemingly inevitable wave of cannabis legalization, I concur that accurately quantifying adverse effects and interactions will help us avoid the irrevocable mistakes that had been made with tobacco and cigarettes in the 1960s.

Bibliography

Adams AJ, Brown B, Flom MC, Jones RT, Jampolsky A. 1975. Alcohol and marijuana effects on static visual acuity. Am J Optom Physiol Opt 52(11):729-735.

Adams AJ, Brown B, Haegerstrom-Portnoy G, Flom MC, Jones RT. 1978. Marijuana, alcohol, and combined drug effects on the time course of glare recovery. Psychopharmacology (Berl) 56(1):81-86.

Addy C, Wright H, Van Laere K, Gantz I, Erondu N, Musser BJ, Lu K, Yuan J, Sanabria-Bohorquez SM, Stoch A, Stevens C, Fong TM, De Lepeleire I, Cilissen C, Cote J, Rosko K, Gendrano IN, 3rd, Nguyen AM, Gumbiner B, Rothenberg P, de Hoon J, Bormans G, Depre M, Eng WS, Ravussin E, Klein S, Blundell J, Herman GA, Burns HD, Hargreaves RJ, Wagner J, Gottesdiener K, Amatruda JM, Heymsfield SB. 2008. The acyclic CB1R inverse agonist taranabant mediates weight loss by increasing energy expenditure and decreasing caloric intake. Cell metabol 7(1):68-78.

Andradas C, Caffarel MM, Perez-Gomez E, Salazar M, Lorente M, Velasco G, Guzman M, Sanchez C. 2011. The orphan G protein-coupled receptor GPR55 promotes cancer cell proliferation via ERK. Oncogene 30(2):245-252.

Argaw A, Duff G, Zabouri N, Cecyre B, Chaine N, Cherif H, Tea N, Lutz B, Ptito M, Bouchard JF. 2011. Concerted action of CB1 cannabinoid receptor and deleted in colorectal cancer in axon guidance. J Neurosci 31(4):1489-1499.

Armington JC, Johnson EP, Riggs LA. 1952. The scotopic A-wave in the electrical response of the human retina. J Physiol 118(3):289-298.

Ashton CH. 1999. Adverse effects of cannabis and cannabinoids. Brit J of anaesth 83(4):637-649.

Ashton JC, Friberg D, Darlington CL, Smith PF. 2006. Expression of the cannabinoid CB2 receptor in the rat cerebellum: an immunohistochemical study. Neurosci Lett 396(2):113-116.

Aung MM, Griffin G, Huffman JW, Wu M, Keel C, Yang B, Showalter VM, Abood ME, Martin BR (August 2000). "Influence of the N-1 alkyl chain length of cannabimimetic indoles upon CB1 and CB2)receptor binding". Drug Alcohol Depend 60 (2): 133–40.

Baek JH, Zheng Y, Darlington CL, Smith PF. 2008. Cannabinoid CB2 receptor expression in the rat brainstem cochlear and vestibular nuclei. Acta oto-laryngologica 128(9):961-967.

Balter MB, Uhlenhuth EH. 1992. Prescribing and use of benzodiazepines: an epidemiologic perspective.J Psychoactive Drugs. 1992 Jan-Mar;24(1):63-4.

Basu S, Ray A, Dittel BN. 2011. Cannabinoid receptor 2 is critical for the homing and retention of marginal zone B lineage cells and for efficient T-independent immune responses. J Immunol 187(11):5720-5732.

Bee WH. 2001. Standardized electroretinography in primates: a non-invasive preclinical tool for predicting ocular side effects in humans. Curr Opin Drug Discov Devel. 4(1):81-91.

Bisogno T, Howell F, Williams G, Minassi A, Cascio MG, Ligresti A, Matias I, Schiano-Moriello A, Paul P, Williams EJ, Gangadharan U, Hobbs C, Di Marzo V, Doherty P.

2003. Cloning of the first sn1-DAG lipases points to the spatial and temporal regulation of endocannabinoid signaling in the brain. Journal Cell Biol 163(3):463-468.
Blankman JL, Simon GM, Cravatt BF. 2007. A comprehensive profile of brain enzymes that hydrolyze the endocannabinoid 2-arachidonoylglycerol. Chem Biol 14(12):1347-1356.
Borrelli F, Fasolino I, Romano B, Capasso R, Maiello F, Coppola D, Orlando P, Battista G, Pagano E, Di Marzo V, Izzo AA. 2013. Beneficial effect of the non-psychotropic plant cannabinoid cannabigerol on experimental inflammatory bowel disease. Biochem Pharmacol 85(9):1306-1316.
Bouskila J, Burke MW, Zabouri N, Casanova C, Ptito M, Bouchard JF. 2012. Expression and localization of the cannabinoid receptor type 1 and the enzyme fatty acid amide hydrolase in the retina of vervet monkeys. Neuroscience 202:117-130.
Bouskila J, Javadi P, Casanova C, Ptito M, Bouchard JF. 2013a. Muller cells express the cannabinoid CB2 receptor in the vervet monkey retina. J Comp Neurol.
Bouskila J, Javadi P, Casanova C, Ptito M, Bouchard JF. 2013b. Rod photoreceptors express GPR55 in the adult vervet monkey retina. PLoS One 8(11):e81080.
Bouskila J, Javadi P, Palmour RM, Bouchard JF, Ptito M. 2014. Standardized Full-Field Electroretinography in the Green Monkey (Chlorocebus sabaeus). PLoS One 9(10):e111569.
Bowmaker JK, Dartnall HJ. 1980. Visual pigments of rods and cones in a human retina. J Physiol 298:501-511.
Bringmann A, Pannicke T, Biedermann B, Francke M, Iandiev I, Grosche J, Wiedemann P, Albrecht J, Reichenbach A. 2009. Role of retinal glial cells in neurotransmitter uptake and metabolism. Neurochem Int. 54(3-4):143-160.
Brown AJ, Robin Hiley C. 2009. Is GPR55 an anandamide receptor? Vitam Horm 81:111-137.
Brown B, Adams AJ, Haegerstrom-Portnoy G, Jones RT, Flom MC. 1977. Pupil size after use of marijuana and alcohol. American journal of ophthalmology 83(3):350-354.
Buckley NE, Hansson S, Harta G, Mezey E. 1998. Expression of the CB1 and CB2 receptor messenger RNAs during embryonic development in the rat. Neuroscience 82(4):1131-1149.
Burns HD, Van Laere K, Sanabria-Bohorquez S, Hamill TG, Bormans G, Eng WS, Gibson R, Ryan C, Connolly B, Patel S, Krause S, Vanko A, Van Hecken A, Dupont P, De Lepeleire I, Rothenberg P, Stoch SA, Cote J, Hagmann WK, Jewell JP, Lin LS, Liu P, Goulet MT, Gottesdiener K, Wagner JA, de Hoon J, Mortelmans L, Fong TM, Hargreaves RJ. 2007. [18F]MK-9470, a positron emission tomography (PET) tracer for in vivo human PET brain imaging of the cannabinoid-1 receptor. Proc Natl Acad Sci U S A 104(23):9800-9805.
Burns ME, Baylor DA. 2001. Activation, deactivation, and adaptation in vertebrate photoreceptor cells. Annu Rev Neurosci. 24:779-805.
Cabral GA, Raborn ES, Griffin L, Dennis J, Marciano-Cabral F. 2008. CB2 receptors in the brain: role in central immune function. Br J Pharmacol 153(2):240-251.
Cahill K, Ussher MH. 2011. Cannabinoid type 1 receptor antagonists for smoking cessation. Cochrane Database Syst Rev. (Online)(3):CD005353.
Callen L, Moreno E, Barroso-Chinea P, Moreno-Delgado D, Cortes A, Mallol J, Casado V, Lanciego JL, Franco R, Lluis C, Canela EI, McCormick PJ. 2012. Cannabinoid

receptors CB1 and CB2 form functional heteromers in brain. J Biol Chem 287(25):20851-20865.
Campos AC, Moreira FA, Gomes FV, Del Bel EA, Guimaraes FS. 2012. Multiple mechanisms involved in the large-spectrum therapeutic potential of cannabidiol in psychiatric disorders. Philos Trans R Soc Lond B Biol Sci 367(1607):3364-3378.
Cardin V, Smith AT. 2010. Sensitivity of human visual and vestibular cortical regions to egomotion-compatible visual stimulation. Cereb Cortex 20(8):1964-1973.
Carrier EJ, Kearn CS, Barkmeier AJ, Breese NM, Yang W, Nithipatikom K, Pfister SL, Campbell WB, Hillard CJ. 2004. Cultured Rat Microglial Cells Synthesize the Endocannabinoid 2-Arachidonylglycerol, Which Increases Proliferation via a CB2 Receptor-Dependent Mechanism. Mol Pharmacol 65(4):999-1007.
Casanova C, Zabouri N, Farishta A, Robert C, Vanni M, Belanger S, Minville K, Bouchard JF. 2010. Retinal and cortical functions in adult mice lacking cannabinoid receptors. Acta Ophthalmologica 88: 0. doi: 10.1111/j.1755-3768.2010.2126.x.
Castillo PE, Younts TJ, Chavez AE, Hashimotodani Y. 2012. Endocannabinoid signaling and synaptic function. Neuron 76(1):70-81.
Cécyre B, Zabouri N, Huppe-Gourgues F, Bouchard JF, Casanova C. 2013. Roles of cannabinoid receptors type 1 and 2 on the retinal function of adult mice. Invest Ophthalmol Vis Sci 54(13):8079-8090.
Cécyre B, Thomas S, Ptito M, Casanova C, Bouchard JF.2014a. Evaluation of the specificity of antibodies raised against cannabinoid receptor type 2 in the mouse retina. Naunyn Schmiedebergs Arch Pharmacol.387(2):175-84.
Cécyre B, Monette M, Beudjekian L, Casanova C and Bouchard JF.2014b. Localization of diacylglycerol lipase alpha and monoacylglycerol lipase during postnatal development of the rat retina. Front Neuro 150(8):1-17
Chang L, Chronicle EP. 2007. Functional imaging studies in cannabis users. The Neuroscientist : a review journal bringing neurobiology, neurol Psych 13(5):422-432.
Chang ML, Wu CH, Jiang-Shieh YF, Shieh JY, Wen CY. 2007. Reactive changes of retinal astrocytes and Muller glial cells in kainate-induced neuroexcitotoxicity. J Anat 210(1):54-65.
Chen J, Matias I, Dinh T, Lu T, Venezia S, Nieves A, Woodward DF, Di Marzo V. 2005. Finding of endocannabinoids in human eye tissues: implications for glaucoma. Biochem Biophys Res Commun 330(4):1062-1067.
Cheng Y, Hitchcock SA. 2007. Targeting cannabinoid agonists for inflammatory and neuropathic pain. Expert Opin Investig Drugs. 16(7):951-965.
Chevaleyre V, Castillo PE. 2003. Heterosynaptic LTD of hippocampal GABAergic synapses: a novel role of endocannabinoids in regulating excitability. Neuron 38(3):461-472.
Colasanti BK, Craig CR, Allara RD. 1984. Intraocular pressure, ocular toxicity and neurotoxicity after administration of cannabinol or cannabigerol. Exp eye res 39(3):251-259.
Consroe P, Musty R, Rein J, Tillery W, Pertwee R. 1997. The perceived effects of smoked cannabis on patients with multiple sclerosis. European neurology 38(1):44-48.
Coscas S, Benyamina A, Reynaud M, Karila L. 2013. [Psychiatric complications of cannabis use]. La Revue du praticien 63(10):1426-1428.

Cravatt BF, Giang DK, Mayfield SP, Boger DL, Lerner RA, Gilula NB. 1996. Molecular characterization of an enzyme that degrades neuromodulatory fatty-acid amides. Nature 384(6604):83-87.
Curcio CA, Sloan KR, Kalina RE, Hendrickson AE. 1990. Human photoreceptor topography. J Comp Neurol 292(4):497-523.
Daly CJ, Ross RA, Whyte J, Henstridge CM, Irving AJ, McGrath JC. 2010. Fluorescent ligand binding reveals heterogeneous distribution of adrenoceptors and 'cannabinoid-like' receptors in small arteries. Br J Pharmacol 159(4):787-796.
Dasilva MA, Grieve KL, Cudeiro J, Rivadulla C. 2012. Endocannabinoid CB1 receptors modulate visual output from the thalamus. Psychopharmacology (Berl) 219(3):835-845.
Dawson WW, Jimenez-Antillon CF, Perez JM, Zeskind JA. 1977. Marijuana and vision--after ten years' use in Costa Rica. Invest Ophthalmol Vis Sci 16(8):689-699.
De Volder AG, Bol A, Blin J, Robert A, Arno P, Grandin C, Michel C, Veraart C. 1997. Brain energy metabolism in early blind subjects: neural activity in the visual cortex. Brain Res 750(1-2):235-244.
Demuth DG, Molleman A. 2006. Cannabinoid signalling. Life Sci 78(6):549-563.
Devane WA, Hanus L, Breuer A, Pertwee RG, Stevenson LA, Griffin G, Gibson D, Mandelbaum A, Etinger A, Mechoulam R. 1992. Isolation and structure of a brain constituent that binds to the cannabinoid receptor. Science 258(5090):1946-1949.
DeVries SH. 2000. Bipolar cells use kainate and AMPA receptors to filter visual information into separate channels. Neuron 28(3):847-856.
Di Marzo V. 2006. A brief history of cannabinoid and endocannabinoid pharmacology as inspired by the work of British scientists. Trends in pharmacological sciences 27(3):134-140.
Di Marzo V. 2011. Endocannabinoid signaling in the brain: biosynthetic mechanisms in the limelight. Nat Neurosci 14(1):9-15.
Di Marzo V, Fontana A. 1995. Anandamide, an endogenous cannabinomimetic eicosanoid: 'killing two birds with one stone'. Prostaglandins, leukotrienes, and essential fatty acids 53(1):1-11.
Di Marzo V, Fontana A, Cadas H, Schinelli S, Cimino G, Schwartz JC, Piomelli D. 1994. Formation and inactivation of endogenous cannabinoid anandamide in central neurons. Nature 372(6507):686-691.
Dinh TP, Carpenter D, Leslie FM, Freund TF, Katona I, Sensi SL, Kathuria S, Piomelli D. 2002. Brain monoglyceride lipase participating in endocannabinoid inactivation. Proceedings of the National Academy of Sciences 99(16):10819-10824.
Distler C, Dreher Z. 1996. Glia Cells of the Monkey Retina—II. Müller Cells. Vision Research 36(16):2381-2394.
Duarte C, Alonso R, Bichet N, Cohen C, Soubrie P, Thiebot MH. 2004. Blockade by the cannabinoid CB1 receptor antagonist, rimonabant (SR141716), of the potentiation by quinelorane of food-primed reinstatement of food-seeking behavior. Neuropsychopharmacology : official publication of the American College of Neuropsychopharmacology 29(5):911-920.
Duff G, Argaw A, Cecyre B, Cherif H, Tea N, Zabouri N, Casanova C, Ptito M, Bouchard JF. 2013. Cannabinoid Receptor CB2 Modulates Axon Guidance. PLoS One 8(8):e70849.

Dursteler MR, Wurtz RH, Newsome WT. 1987. Directional pursuit deficits following lesions of the foveal representation within the superior temporal sulcus of the macaque monkey. J Neurophysiol 57(5):1262-1287.
Egertová M, Cravatt BF, Elphick MR. 2003. Comparative analysis of fatty acid amide hydrolase and cb(1) cannabinoid receptor expression in the mouse brain: evidence of a widespread role for fatty acid amide hydrolase in regulation of endocannabinoid signaling. Neuroscience 119(2):481-496.
Egertová M, Elphick MR. 2000. Localisation of cannabinoid receptors in the rat brain using antibodies to the intracellular C-terminal tail of CB. J Comp Neurol 422(2):159-171.
Eggan SM, Lewis DA. 2007. Immunocytochemical distribution of the cannabinoid CB1 receptor in the primate neocortex: a regional and laminar analysis. Cereb Cortex 17(1):175-191.
Elphick MR, Egertová M. 2001. The neurobiology and evolution of cannabinoid signalling. Philos Trans R Soc Lond B Biol Sci 356(1407):381-408.
Evens N, Vandeputte C, Coolen C, Janssen P, Sciot R, Baekelandt V, Verbruggen AM, Debyser Z, Van Laere K, Bormans GM. 2012. Preclinical evaluation of [11C]NE40, a type 2 cannabinoid receptor PET tracer. Nuc Med Biol 39(3):389-399.
Fan Y, Huang ZY, Cao CC, Chen CS, Chen YX, Fan DD, He J, Hou HL, Hu L, Hu XT, Jiang XT, Lai R, Lang YS, Liang B, Liao SG, Mu D, Ma YY, Niu YY, Sun XQ, Xia JQ, Xiao J, Xiong ZQ, Xu L, Yang L, Zhang Y, Zhao W, Zhao XD, Zheng YT, Zhou JM, Zhu YB, Zhang GJ, Wang J, Yao YG. 2013. Genome of the Chinese tree shrew. Nat comm 4:1426.
Farsandaj N, Ghahremani MH, Ostad SN. 2012. Role of cannabinoid and vanilloid receptors in invasion of human breast carcinoma cells. J Environ Pathol Toxicol Oncol. 31(4):377-387.
Felder CC, Joyce KE, Briley EM, Mansouri J, Mackie K, Blond O, Lai Y, Ma AL, Mitchell RL. 1995. Comparison of the pharmacology and signal transduction of the human cannabinoid CB1 and CB2 receptors. Mol Pharmacol 48(3):443-450.
Felleman DJ, Van Essen DC. 1991. Distributed hierarchical processing in the primate cerebral cortex. Cereb Cortex 1(1):1-47.
Fernández-Ruiz J, Berrendero F, Hernández ML, Ramos JA. 2000. The endogenous cannabinoid system and brain development. Trends Neurosci 23(1):14-20.
Flom MC, Adams AJ, Jones RT. 1975. Marijuana smoking and reduced pressure in human eyes: drug action or epiphenomenon? Inves Ophthal 14(1):52-55.
Fong TM, Heymsfield SB. 2009. Cannabinoid-1 receptor inverse agonists: current understanding of mechanism of action and unanswered questions. Int J Obes (2005) 33(9):947-955.
Franze K, Grosche J, Skatchkov SN, Schinkinger S, Foja C, Schild D, Uckermann O, Travis K, Reichenbach A, Guck J. 2007. Muller cells are living optical fibers in the vertebrate retina. Proc Natl Acad Sci U S A 104(20):8287-8292.
Galiègue S, Mary S, Marchand J, Dussossoy D, Carrière D, Carayon P, Bouaboula M, Shire D, Le Fur G, Casellas P. 1995. Expression of Central and Peripheral Cannabinoid Receptors in Human Immune Tissues and Leukocyte Subpopulations. Eur J Biochem 232(1):54-61.
Ganis G, Thompson WL, Kosslyn SM. 2004. Brain areas underlying visual mental imagery and visual perception: an fMRI study. Brain Res Cogn Brain Res 20(2):226-241.

Gao Y, Vasilyev DV, Goncalves MB, Howell FV, Hobbs C, Reisenberg M, Shen R, Zhang MY, Strassle BW, Lu P, Mark L, Piesla MJ, Deng K, Kouranova EV, Ring RH, Whiteside GT, Bates B, Walsh FS, Williams G, Pangalos MN, Samad TA, Doherty P. 2010. Loss of retrograde endocannabinoid signaling and reduced adult neurogenesis in diacylglycerol lipase knock-out mice. J Neurosci 30(6):2017-2024.

Gawienowski AM, Chatterjee D, Anderson PJ, Epstein DL, Grant WM. 1982. Effect of delta 9-tetrahydrocannabinol on monoamine oxidase activity in bovine eye tissues, in vitro. Invest Ophthalmol Vis Sci 22(4):482-485.

Gerdeman GL, Ronesi J, Lovinger DM. 2002. Postsynaptic endocannabinoid release is critical to long-term depression in the striatum. Nat Neurosci 5(5):446-451.

Glaser ST, Deutsch DG, Studholme KM, Zimov S, Yazulla S. 2005. Endocannabinoids in the intact retina: 3 H-anandamide uptake, fatty acid amide hydrolase immunoreactivity and hydrolysis of anandamide. Vis Neurosci 22(6):693-705.

Glass M, Dragunow M, Faull RL. 1997. Cannabinoid receptors in the human brain: a detailed anatomical and quantitative autoradiographic study in the fetal, neonatal and adult human brain. Neuroscience 77(2):299-318.

Goddard E, Mannion DJ, McDonald JS, Solomon SG, Clifford CW. 2011. Color responsiveness argues against a dorsal component of human V4. J Visi 11(4).

Gold MS, Gebhart GF. 2010. Nociceptor sensitization in pain pathogenesis. Nature medicine 16(11):1248-1257.

Gong JP, Onaivi ES, Ishiguro H, Liu QR, Tagliaferro PA, Brusco A, Uhl GR. 2006. Cannabinoid CB2 receptors: immunohistochemical localization in rat brain. Brain Res 1071(1):10-23.

Goodman M, Porter CA, Czelusniak J, Page SL, Schneider H, Shoshani J, Gunnell G, Groves CP. 1998. Toward a phylogenetic classification of Primates based on DNA evidence complemented by fossil evidence. Mol Phylogenet Evol. 9(3):585-598.

Green B, Kavanagh D, Young R. 2003. Being stoned: a review of self-reported cannabis effects. Drug Alcohol Rev. 22(4):453-460.

Green K. 1979. The ocular effects of cannabinoids. Curr Top Eye Res 1:175-215.

Griffin G, Tao Q, Abood ME. 2000. Cloning and pharmacological characterization of the rat CB(2) cannabinoid receptor. J Pharmacol Exp Ther 292(3):886-894.

Hamilton R, McGlone L, MacKinnon JR, Russell HC, Bradnam MS, Mactier H. 2010. Ophthalmic, clinical and visual electrophysiological findings in children born to mothers prescribed substitute methadone in pregnancy. Br J Ophthalmol. 94(6):696-700.

Han J, Kesner P, Metna-Laurent M, Duan T, Xu L, Georges F, Koehl M, Abrous DN, Mendizabal-Zubiaga J, Grandes P, Liu Q, Bai G, Wang W, Xiong L, Ren W, Marsicano G, Zhang X. 2012. Acute cannabinoids impair working memory through astroglial CB1 receptor modulation of hippocampal LTD. Cell 148(5):1039-1050.

Haring M, Kaiser N, Monory K, Lutz B. 2011. Circuit specific functions of cannabinoid CB1 receptor in the balance of investigatory drive and exploration. PLoS One 6(11):e26617.

Herkenham M, Lynn AB, Johnson MR, Melvin LS, de Costa BR, Rice KC. 1991. Characterization and localization of cannabinoid receptors in rat brain: a quantitative in vitro autoradiographic study. J Neurosci 11(2):563-583.

Hillard, CJ; Manna, S; Greenberg, MJ; Dicamelli, R; Ross, RA; Stevenson, LA; Murphy, V; Pertwee, RG; Campbell, WB (1999). "Synthesis and characterization of potent and

selective agonists of the neuronal cannabinoid receptor (CB1)". The Journal of Pharmacology and Experimental Therapeutics 289 (3): 1427–33.
Hillig KW, Mahlberg PG. 2004. A chemotaxonomic analysis of cannabinoid variation in Cannabis (Cannabaceae). Am J Botany 91(6):966-975.
Hu G, Ren G, Shi Y. 2011. The putative cannabinoid receptor GPR55 promotes cancer cell proliferation. Oncogene 30(2):139-141.
Huxlin KR, Sefton AJ, Furby JH. 1992. The origin and development of retinal astrocytes in the mouse. J Neurocytol 21(7):530-544.
Iversen L. 2003. Cannabis and the brain. Brain : a journal of neurology 126(Pt 6):1252-1270.
Jacobs GH. 2008. Primate color vision: A comparative perspective. Vis Neurosci 25(5-6):619-633.
Jager G, Kahn RS, Van Den Brink W, Van Ree JM, Ramsey NF. 2006. Long-term effects of frequent cannabis use on working memory and attention: an fMRI study. Psychopharmacology (Berl) 185(3):358-368.
Jasinska AJ, Schmitt CA, Service SK, Cantor RM, Dewar K, Jentsch JD, Kaplan JR, Turner TR, Warren WC, Weinstock GM, Woods RP, Freimer NB. 2013. Systems biology of the vervet monkey. ILAR J. 54(2):122-143.
Johns DG, Behm DJ, Walker DJ, Ao Z, Shapland EM, Daniels DA, Riddick M, Dowell S, Staton PC, Green P, Shabon U, Bao W, Aiyar N, Yue TL, Brown AJ, Morrison AD, Douglas SA. 2007. The novel endocannabinoid receptor GPR55 is activated by atypical cannabinoids but does not mediate their vasodilator effects. Br J Pharmacol 152(5):825-831.
Kaminski NE. 1998. Inhibition of the cAMP signaling cascade via cannabinoid receptors: a putative mechanism of immune modulation by cannabinoid compounds. Toxicol lett 102-103:59-63.
Kandel ER, Schwartz JH, Jessell TM 2000. Principles of Neural Science, 5th ed. McGraw-Hill, New York. ISBN 0-07-139011-1
Kanayama G, Rogowska J, Pope HG, Gruber SA, Yurgelun-Todd DA. 2004. Spatial working memory in heavy cannabis users: a functional magnetic resonance imaging study. Psychopharmacology (Berl) 176(3-4):239-247.
Kim J, Alger BE. 2010. Reduction in endocannabinoid tone is a homeostatic mechanism for specific inhibitory synapses. Nat Neurosci 13(5):592-600.
Kiplinger GF, Manno JE, Rodda BE, Forney RB. 1971. Dose-response analysis of the effects of tetrahydrocannabinol in man. Clin Pharmacol Ther 12(4):650-657.
Koch M, Habazettl I, Dehghani F, Korf HW. 2008. The rat pineal gland comprises an endocannabinoid system. J Pineal Res. 45(4):351-360.
Koyasu T, Kondo M, Miyata K, Ueno S, Miyata T, Nishizawa Y, Terasaki H. 2008. Photopic electroretinograms of mGluR6-deficient mice. Curr Eye Res 33(1):91-99.
Kreitzer AC, Regehr WG. 2001. Retrograde inhibition of presynaptic calcium influx by endogenous cannabinoids at excitatory synapses onto Purkinje cells. Neuron 29(3):717-727.
Krishnan G, Chatterjee N. 2012. Endocannabinoids alleviate proinflammatory conditions by modulating innate immune response in muller glia during inflammation. Glia 60(11):1629-1645.
Kupers R, Pietrini P, Ricciardi E, Ptito M. 2011. The nature of consciousness in the visually deprived brain. Front Psychol 2:19.

Kupers R, Ptito M. 2011. Insights from darkness: what the study of blindness has taught us about brain structure and function. Prog Brain Res. 192:17-31.
Lan R, Liu Q, Fan P, Lin S, Fernando SR, McCallion D, Pertwee R, Makriyannis A. 1999. Structure-activity relationships of pyrazole derivatives as cannabinoid receptor antagonists. Journal of medicinal chemistry 42(4):769-776.
Laprevote V, Schwitzer T, Giersch A, Schwan R. 2015. Flash electroretinogram and addictive disorders. Prog Neuropsychopharmacol Biol Psychiatry. 56:264.
Lauckner JE, Jensen JB, Chen HY, Lu HC, Hille B, Mackie K. 2008. GPR55 is a cannabinoid receptor that increases intracellular calcium and inhibits M current. Proc Natl Acad Sci U S A 105(7):2699-2704.
Le Foll B, Goldberg SR. 2005. Cannabinoid CB1 receptor antagonists as promising new medications for drug dependence. J Pharmacol Exp Ther 312(3):875-883.
Lerner AG, Goodman C, Rudinski D, Bleich A. 2011. Benign and time-limited visual disturbances (flashbacks) in recent abstinent high-potency heavy cannabis smokers: a case series study. Isr J Psychiatry Relat Sci. 48(1):25-29.
Lerner TN, Kreitzer AC. 2012. RGS4 is required for dopaminergic control of striatal LTD and susceptibility to parkinsonian motor deficits. Neuron 73(2):347-359.
Levi L, Miller NR. 1990. Visual illusions associated with previous drug abuse. J Clin Neuroophthalmol. 10(2):103-110.
Leweke FM, Schneider U, Thies M, Munte TF, Emrich HM. 1999. Effects of synthetic delta9-tetrahydrocannabinol on binocular depth inversion of natural and artificial objects in man. Psychopharmacology (Berl) 142(3):230-235.
Li Z, Gifford A, Liu Q, Thotapally R, Ding YS, Makriyannis A, Gatley SJ. 2005. Candidate PET radioligands for cannabinoid CB1 receptors: [18F]AM5144 and related pyrazole compounds. Nucl Med Biol. 32(4):361-366.
Lindsey KP, Glaser ST, Gatley SJ. 2005. Imaging of the brain cannabinoid system. Handb Exp Pharmacol. (168):425-443.
Lopez EM, Tagliaferro P, Onaivi ES, Lopez-Costa JJ. 2011. Distribution of CB2 cannabinoid receptor in adult rat retina. Synapse 65(5):388-392.
Lydon J, Teramura AH, Coffman CB. 1987. UV-B radiation effects on photosynthesis, growth and cannabinoid production of two Cannabis sativa chemotypes. Photochem Photobiol. 46(2):201-206.
Lynn AB, Herkenham M. 1994. Localization of cannabinoid receptors and nonsaturable high-density cannabinoid binding sites in peripheral tissues of the rat: implications for receptor-mediated immune modulation by cannabinoids. J Pharmacol Exp Ther 268(3):1612-1623.
Maccarrone M, Gasperi V, Catani MV, Diep TA, Dainese E, Hansen HS, Avigliano L. 2010. The endocannabinoid system and its relevance for nutrition. Ann Rev Nut 30:423-440.
MacGregor GG, Xu JZ, McNicholas CM, Giebisch G, Hebert SC. 1998. Partially active channels produced by PKA site mutation of the cloned renal K+ channel, ROMK2 (kir1.2). Am J Physiol. 275(3 Pt 2):F415-422.
MacNeil MA, Masland RH. 1998. Extreme diversity among amacrine cells: implications for function. Neuron 20(5):971-982.
Marmor MF, Fulton AB, Holder GE, Miyake Y, Brigell M, Bach M. 2009. ISCEV Standard for full-field clinical electroretinography (2008 update). Doc Ophthalmol. 118(1):69-77.

Marsicano G, Lutz B. 1999. Expression of the cannabinoid receptor CB1 in distinct neuronal subpopulations in the adult mouse forebrain. Eur J Neurosci 11(12):4213-4225.
Marsicano G, Wotjak CT, Azad SC, Bisogno T, Rammes G, Cascio MG, Hermann H, Tang J, Hofmann C, Zieglgansberger W, Di Marzo V, Lutz B. 2002. The endogenous cannabinoid system controls extinction of aversive memories. Nature 418(6897):530-534.
Martin PR, White AJ, Goodchild AK, Wilder HD, Sefton AE. 1997. Evidence that blue-on cells are part of the third geniculocortical pathway in primates. Eur J Neurosci 9(7):1536-1541.
Masland RH. 2001. The fundamental plan of the retina. Nat Neurosci 4(9):877-886.
Masland RH. 2012. The neuronal organization of the retina. Neuron 76(2):266-280.
Mathew RJ, Wilson WH, Turkington TG, Coleman RE. 1998. Cerebellar activity and disturbed time sense after THC. Brain Res 797(2):183-189.
Matias I, Wang JW, Moriello AS, Nieves A, Woodward DF, Di Marzo V. 2006. Changes in endocannabinoid and palmitoylethanolamide levels in eye tissues of patients with diabetic retinopathy and age-related macular degeneration. Prostaglandins Leukot Essent Fatty Acids. 75(6):413-418.
Matsuda LA. 1997. Molecular aspects of cannabinoid receptors. Crit Rev Neurobiol. 11(2-3):143-166.
Matsuda LA, Lolait SJ, Brownstein MJ, Young AC, Bonner TI. 1990. Structure of a cannabinoid receptor and functional expression of the cloned cDNA. Nature 346(6284):561-564.
Mattes RD, Engelman K, Shaw LM, Elsohly MA. 1994. Cannabinoids and appetite stimulation. Pharmacol Biochem Behav 49(1):187-195.
Mechoulam R. 1986. Interview with Prof. Raphael Mechoulam, codiscoverer of THC.. Interview by Stanley Einstein. Int J Addict.
Mechoulam R. 2002. Discovery of endocannabinoids and some random thoughts on their possible roles in neuroprotection and aggression. Prostaglandins Leukot Essent Fatty Acids. 66(2-3):93-99.
Mechoulam R, Ben Shabat S, Hanus L, Ligumsky M, Kaminski NE, Schatz AR, Gopher A, Almog S, Martin BR, Compton DR. 1995. Identification of an endogenous 2-monoglyceride, present in canine gut, that binds to cannabinoid receptors. Biochem pharmacol 50(1):83-90.
Mechoulam R, Gaoni Y. 1965. A Total Synthesis of Dl-Delta-1-Tetrahydrocannabinol, the Active Constituent of Hashish. J Am Chem Soc 87:3273-3275.
Mechoulam R, Gaoni Y. 1967. Recent advances in the chemistry of hashish. Fortschr Chem Org Naturst. 25:175-213.
Merzouki A, Mesa JM. 2002. Concerning kif, a Cannabis sativa L. preparation smoked in the Rif mountains of northern Morocco. J ethnopharmacol 81(3):403-406.
Miller RF, Dowling JE. 1970. Intracellular responses of the Muller (glial) cells of mudpuppy retina: their relation to b-wave of the electroretinogram. J Neurophysiol 33(3):323-341.
Moreno-Navarrete JM, Catalan V, Whyte L, Diaz-Arteaga A, Vazquez-Martinez R, Rotellar F, Guzman R, Gomez-Ambrosi J, Pulido MR, Russell WR, Imbernon M, Ross RA, Malagon MM, Dieguez C, Fernandez-Real JM, Fruhbeck G, Nogueiras R. 2012. The L-alpha-lysophosphatidylinositol/GPR55 system and its potential role in human obesity. Diabetes 61(2):281-291.

Morishita J, Okamoto Y, Tsuboi K, Ueno M, Sakamoto H, Maekawa N, Ueda N. 2005. Regional distribution and age-dependent expression of N-acylphosphatidylethanolamine-hydrolyzing phospholipase D in rat brain. J Neurochem 94(3):753-762.
Mouslech Z, Valla V. 2009. Endocannabinoid system: An overview of its potential in current medical practice. Neuro Endocrinol Lett 30(2):153-179.
Mukherjee S, Adams M, Whiteaker K, Daza A, Kage K, Cassar S, Meyer M, Yao BB. 2004. Species comparison and pharmacological characterization of rat and human CB2 cannabinoid receptors. Eur J Pharmacol 505(1-3):1-9.
Muller B, Peichl L. 1993. Horizontal cells in the cone-dominated tree shrew retina: morphology, photoreceptor contacts, and topographical distribution. J Neurosci 13(8):3628-3646.
Munro S, Thomas KL, Abu-Shaar M. 1993. Molecular characterization of a peripheral receptor for cannabinoids. Nature 365(6441):61-65.
Nair G, Kim M, Nagaoka T, Olson DE, Thule PM, Pardue MT, Duong TQ. 2011. Effects of common anesthetics on eye movement and electroretinogram. Doc Ophthalmol. 122(3):163-176.
Newman E, Reichenbach A. 1996. The Müller cell: a functional element of the retina. Trends Neurosci 19(8):307-312.
Newsome WT, Pare EB. 1988. A selective impairment of motion perception following lesions of the middle temporal visual area (MT). J Neurosci 8(6):2201-2211.
Noyes R, Jr., Brunk SF, Avery DA, Canter AC. 1975. The analgesic properties of delta-9-tetrahydrocannabinol and codeine. Clin Pharmacol Ther 18(1):84-89.
O'Shaughnessy WB. 1840 On the preparations of the Indian hemp (Cannabis indica); their effects on the animal system in health, and their utility in the treatment of tetanus and other convulsive diseases. Transactions of the Medical and Physical Society, Bengal 71–102 :421–426.
Ohno-Shosaku T, Kano M. 2014. Endocannabinoid-mediated retrograde modulation of synaptic transmission. Curr Opin Neurobiol. 29C:1-8.
Oka S, Nakajima K, Yamashita A, Kishimoto S, Sugiura T. 2007. Identification of GPR55 as a lysophosphatidylinositol receptor. Biochem Biophys Res Commun 362(4):928-934.
Oka S, Toshida T, Maruyama K, Nakajima K, Yamashita A, Sugiura T. 2009. 2-Arachidonoyl-sn-glycero-3-phosphoinositol: a possible natural ligand for GPR55. J Biochem 145(1):13-20.
Okamoto Y, Morishita J, Tsuboi K, Tonai T, Ueda N. 2004. Molecular characterization of a phospholipase D generating anandamide and its congeners. J Biol Chem 279(7):5298-5305.
Onaivi ES. 2006. Neuropsychobiological evidence for the functional presence and expression of cannabinoid CB2 receptors in the brain. Neuropsychobiology 54(4):231-246.
Onaivi ES, Ishiguro H, Gong JP, Patel S, Perchuk A, Meozzi PA, Myers L, Mora Z, Tagliaferro P, Gardner E, Brusco A, Akinshola BE, Liu QR, Hope B, Iwasaki S, Arinami T, Teasenfitz L, Uhl GR. 2006. Discovery of the presence and functional expression of cannabinoid CB2 receptors in brain. Ann N Y Acad Sci. 1074:514-536.
Pacher P, Mechoulam R. 2011. Is lipid signaling through cannabinoid 2 receptors part of a protective system? Prog Lipid Res. 50(2):193-211.

Pagotto U, Marsicano G, Cota D, Lutz B, Pasquali R. 2006. The emerging role of the endocannabinoid system in endocrine regulation and energy balance. Endocr Rev. 27(1):73-100.
Palmour RM, Mulligan J, Howbert JJ, Ervin F. 1997. Of monkeys and men: vervets and the genetics of human-like behaviors. Am J Hum Genet. 61(3):481-488.
Pertwee RG. 2005. Inverse agonism and neutral antagonism at cannabinoid CB1 receptors. Life Sci 76(12):1307-1324.
Pertwee RG. 2006. The pharmacology of cannabinoid receptors and their ligands: an overview. Int J Obes (Lond). 30 Suppl 1:S13-18.
Pertwee RG. 2007. GPR55: a new member of the cannabinoid receptor clan? Br J Pharmacol 152(7):984-986.
Pertwee RG. 2008. The diverse CB1 and CB2 receptor pharmacology of three plant cannabinoids: delta9-tetrahydrocannabinol, cannabidiol and delta9-tetrahydrocannabivarin. Br J Pharmacol 153(2):199-215.
Petkov CI, Jarvis ED. 2012. Birds, primates, and spoken language origins: behavioral phenotypes and neurobiological substrates. Front Evol Neurosci 4:12.
Pillay SS, Rogowska J, Kanayama G, Jon DI, Gruber S, Simpson N, Cherayil M, Pope HG, Yurgelun-Todd DA. 2004. Neurophysiology of motor function following cannabis discontinuation in chronic cannabis smokers: an fMRI study. Drug Alcohol Depend.76(3):261-271.
Pineiro R, Maffucci T, Falasca M. 2011. The putative cannabinoid receptor GPR55 defines a novel autocrine loop in cancer cell proliferation. Oncogene 30(2):142-152.
Pini A, Mannaioni G, Pellegrini-Giampietro D, Passani MB, Mastroianni R, Bani D, Masini E. 2012. The role of cannabinoids in inflammatory modulation of allergic respiratory disorders, inflammatory pain and ischemic stroke. Curr Drug Targets.13(7):984-993.
Piomelli D. 2003. The molecular logic of endocannabinoid signalling. Nat Rev Neurosci 4(11):873-884.
Pisanti S, Picardi P, D'Alessandro A, Laezza C, Bifulco M. 2013. The endocannabinoid signaling system in cancer. Trends Pharmacol Sci. 34(5):273-282.
Placzek EA, Okamoto Y, Ueda N, Barker EL. 2008. Mechanisms for recycling and biosynthesis of endogenous cannabinoids anandamide and 2-arachidonylglycerol. J Neurochem 107(4):987-1000.
Porcella A, Casellas P, Gessa GL, Pani L. 1998. Cannabinoid receptor CB1 mRNA is highly expressed in the rat ciliary body: implications for the antiglaucoma properties of marihuana. Molecular Brain Research 58(1-2):240-245.
Porcella A, Maxia C, Gessa GL, Pani L. 2000. The human eye expresses high levels of CB1 cannabinoid receptor mRNA and protein. Eur J Neurosci. 12(3):1123-1127.
Prusky GT, Douglas RM. 2004. Characterization of mouse cortical spatial vision. Vision Res 44(28):3411-3418.
Ptito M, Schneider FC, Paulson OB, Kupers R. 2008. Alterations of the visual pathways in congenital blindness. Exp Brain Res 187(1):41-49.
Purves D, Augustine GJ, Fitzpatrick D, et al., editors. Neuroscience. 2nd edition. Sunderland (MA): Sinauer Associates; 2001. Available from: http://www.ncbi.nlm.nih.gov/books/NBK1079
Remtulla S, Hallett PE. 1985. A schematic eye for the mouse, and comparisons with the rat. Vision Res 25(1):21-31.

Rinaldi-Carmona M, Barth F, Millan J, Derocq JM, Casellas P, Congy C, Oustric D, Sarran M, Bouaboula M, Calandra B, Portier M, Shire D, Brelière JC, Le Fur GL. 1998. SR 144528, the first potent and selective antagonist of the CB2 cannabinoid receptor. J Pharmacol Exp Ther. Feb;284(2):644-50.

Rodríguez de Fonseca F, Del Arco I, Bermudez-Silva FJ, Bilbao A, Cippitelli A, Navarro M. 2005. The endocannabinoid system: physiology and pharmacology. Alcohol 40(1):2-14.

Romero-erbo SY, Rafacho A, Diaz-Arteaga A, Suarez J, Quesada I, Imbernon M, Ross RA, Dieguez C, Rodriguez de Fonseca F, Nogueiras R, Nadal A, Bermudez-Silva FJ. 2011. A role for the putative cannabinoid receptor GPR55 in the islets of Langerhans. J Endocrinol. 211(2):177-185.

Rosolen SG, Kolomiets B, Varela O, Picaud S. 2008. Retinal electrophysiology for toxicology studies: applications and limits of ERG in animals and ex vivo recordings. Exp Toxicol Pathol. 60(1):17-32.

Rosolen SG, Rigaudiere F, LeGargasson JF, Chalier C, Rufiange M, Racine J, Joly S, Lachapelle P. 2004. Comparing the photopic ERG i-wave in different species. Vet Ophthalm 7(3):189-192.

Russo EB. 2008. Clinical endocannabinoid deficiency (CECD): can this concept explain therapeutic benefits of cannabis in migraine, fibromyalgia, irritable bowel syndrome and other treatment-resistant conditions? Neuro Endocrinol Lett 29(2):192-200.

Russo EB, Merzouki A, Mesa JM, Frey KA, Bach PJ. 2004. Cannabis improves night vision: a case study of dark adaptometry and scotopic sensitivity in kif smokers of the Rif mountains of northern Morocco. J Ethnopharmacol 93(1):99-104.

Ryberg E, Larsson N, Sjogren S, Hjorth S, Hermansson NO, Leonova J, Elebring T, Nilsson K, Drmota T, Greasley PJ. 2007. The orphan receptor GPR55 is a novel cannabinoid receptor. Br J Pharmacol 152(7):1092-1101.

Schicho R, Storr M. 2012. A potential role for GPR55 in gastrointestinal functions. Curr Opin Pharmacol.12(6):653-658.

Schiller PH. 1992. The ON and OFF channels of the visual system. Trends Neurosci 15(3):86-92.

Schon F, Hart PE, Hodgson TL, Pambakian AL, Ruprah M, Williamson EM, Kennard C. 1999. Suppression of pendular nystagmus by smoking cannabis in a patient with multiple sclerosis. Neurology. Dec 10;53(9):2209-10.

Schlicker E, Timm J, Gothert M. 1996. Cannabinoid receptor-mediated inhibition of dopamine release in the retina. Naunyn Schmiedebergs Arch Pharmacol. 354(6):791-795.

Semple DM, Ramsden F, McIntosh AM. 2003. Reduced binocular depth inversion in regular cannabis users. Pharmacol Biochem Behav 75(4):789-793.

Sharir H, Abood ME. 2010. Pharmacological characterization of GPR55, a putative cannabinoid receptor. Pharmacol Ther 126(3):301-313.

Shen W, Fruttiger M, Zhu L, Chung SH, Barnett NL, Kirk JK, Lee S, Coorey NJ, Killingsworth M, Sherman LS, Gillies MC. 2012. Conditional Mullercell ablation causes independent neuronal and vascular pathologies in a novel transgenic model. J Neurosci 32(45):15715-15727.

Shoemaker JL, Ruckle MB, Mayeux PR, Prather PL. 2005. Agonist-directed trafficking of response by endocannabinoids acting at CB2 receptors. J Pharmacol Exp Ther 315(2):828-838.
Showalter VM, Compton DR, Martin BR, Abood ME. 1996. Evaluation of binding in a transfected cell line expressing a peripheral cannabinoid receptor (CB2): identification of cannabinoid receptor subtype selective ligands. J Pharmacol Exp Ther 278(3):989-999.
Sim-Selley LJ. 2003. Regulation of cannabinoid CB1 receptors in the central nervous system by chronic cannabinoids. Crit Rev Neurobiol. 15(2):91-119.
Sincich LC, Park KF, Wohlgemuth MJ, Horton JC. 2004. Bypassing V1: a direct geniculate input to area MT. Nat Neurosci 7(10):1123-1128.
Skaper SD, Buriani A, Dal Toso R, Petrelli L, Romanello S, Facci L, Leon A. 1996. The ALIAmide palmitoylethanolamide and cannabinoids, but not anandamide, are protective in a delayed postglutamate paradigm of excitotoxic death in cerebellar granule neurons. Proc Natl Acad Sci U S A 93(9):3984-3989.
Skosnik PD, Krishnan GP, Vohs JL, O'Donnell BF. 2006. The effect of cannabis use and gender on the visual steady state evoked potential. Clin Neurophysiol 117(1):144-156.
Smith AM, Longo CA, Fried PA, Hogan MJ, Cameron I. 2010. Effects of marijuana on visuospatial working memory: an fMRI study in young adults. Psychopharmacology (Berl) 210(3):429-438.
Steinberg R, Linsenmeier R, Griff E. 1985. Retinal pigment epithelial cell contributions to the electroretinogram and electrooculogram. Prog Retin Res 4:33-66.
Stell WK, Ishida AT, Lightfoot DO. 1977. Structural basis for on-and off-center responses in retinal bipolar cells. Science 198(4323):1269-1271.
Stella N. 2009. Endocannabinoid signaling in microglial cells. Neuropharmacology 56 Suppl 1:244-253.
Straiker A, Stella N, Piomelli D, Mackie K, Karten HJ, Maguire G. 1999. Cannabinoid CB1 receptors and ligands in vertebrate retina: localization and function of an endogenous signaling system. Proc Natl Acad Sci U S A 96(25):14565-14570.
Struik ML, Yazulla S, Kamermans M. 2006. Cannabinoid agonist WIN 55212-2 speeds up the cone response to light offset in goldfish retina. Vis Neurosci 23(2):285-293.
Stumpff F, Boxberger M, Krauss A, Rosenthal R, Meissner S, Choritz L, Wiederholt M, Thieme H. 2005. Stimulation of cannabinoid (CB1) and prostanoid (EP2) receptors opens BKCa channels and relaxes ocular trabecular meshwork. Exp Eye Res. 80(5):697-708.
Sugiura T, Kondo S, Sukagawa A, Nakane S, Shinoda A, Itoh K, Yamashita A, Waku K. 1995. 2-Arachidonoylglycerol: a possible endogenous cannabinoid receptor ligand in brain. Biochemical and biophysical research communications 215(1):89-97.
Sugiura T, Waku K. 2002. Cannabinoid receptors and their endogenous ligands. J Biochem 132(1):7-12.
Sutphen R, Xu Y, Wilbanks GD, Fiorica J, Grendys EC, Jr., LaPolla JP, Arango H, Hoffman MS, Martino M, Wakeley K, Griffin D, Blanco RW, Cantor AB, Xiao YJ, Krischer JP. 2004. Lysophospholipids are potential biomarkers of ovarian cancer. Cancer Epidemiol Biomarkers Prev. 13(7):1185-1191.
Tanimura A, Uchigashima M, Yamazaki M, Uesaka N, Mikuni T, Abe M, Hashimoto K, Watanabe M, Sakimura K, Kano M. 2012. Synapse type-independent degradation of

the endocannabinoid 2-arachidonoylglycerol after retrograde synaptic suppression. Proc Natl Acad Sci U S A 109(30):12195-12200.
Tolon RM, Nunez E, Pazos MR, Benito C, Castillo AI, Martinez-Orgado JA, Romero J. 2009. The activation of cannabinoid CB2 receptors stimulates in situ and in vitro beta-amyloid removal by human macrophages. Brain Res 1283:148-154.
Toth A, Blumberg PM, Boczan J. 2009. Anandamide and the vanilloid receptor (TRPV1). Vitam Horm 81:389-419.
Tramer MR, Carroll D, Campbell FA, Reynolds DJ, Moore RA, McQuay HJ. 2001. Cannabinoids for control of chemotherapy induced nausea and vomiting: quantitative systematic review. BMJ (Clinical research ed) 323(7303):16-21.
Tsou K, Brown S, Sanudo-Pena MC, Mackie K, Walker JM. 1998. Immunohistochemical distribution of cannabinoid CB1 receptors in the rat central nervous system. Neuroscience 83(2):393-411.
Van Horn SC, Erisir A, Sherman SM. 2000. Relative distribution of synapses in the A-laminae of the lateral geniculate nucleus of the cat. J Comp Neurol 416(4):509-520.
Villares J. 2007. Chronic use of marijuana decreases cannabinoid receptor binding and mRNA expression in the human brain. Neuroscience 145(1):323-334.
Volkow ND, Gillespie H, Mullani N, Tancredi L, Grant C, Valentine A, Hollister L. 1996. Brain glucose metabolism in chronic marijuana users at baseline and during marijuana intoxication. Psych Res 67(1):29-38.
Wang J, Ueda N. 2009. Biology of endocannabinoid synthesis system. Prostaglandins Other Lipid Mediat 89(3-4):112-119.
Whyte LS, Ryberg E, Sims NA, Ridge SA, Mackie K, Greasley PJ, Ross RA, Rogers MJ. 2009. The putative cannabinoid receptor GPR55 affects osteoclast function in vitro and bone mass in vivo. Proc Natl Acad Sci U S A 106(38):16511-16516.
Wilson RI, Nicoll RA. 2001. Endogenous cannabinoids mediate retrograde signalling at hippocampal synapses. Nature 410(6828):588-592.
Wong KY, Dunn FA, Berson DM. 2005. Photoreceptor adaptation in intrinsically photosensitive retinal ganglion cells. Neuron 48(6):1001-1010.
Wotherspoon G, Fox A, McIntyre P, Colley S, Bevan S, Winter J. 2005. Peripheral nerve injury induces cannabinoid receptor 2 protein expression in rat sensory neurons. Neuroscience 135(1):235-245.
Yazulla S. 2008. Endocannabinoids in the retina: from marijuana to neuroprotection. Prog Retin Eye Res 27(5):501-526.
Yazulla S, Studholme KM. 2001. Neurochemical anatomy of the zebrafish retina as determined by immunocytochemistry. J Neurocytol 30(7):551-592.
Yazulla S, Studholme KM, McIntosh HH, Deutsch DG. 1999. Immunocytochemical localization of cannabinoid CB1 receptor and fatty acid amide hydrolase in rat retina. J Comp Neurol 415(1):80-90.
Yee R, Liebman PA. 1978. Light-activated phosphodiesterase of the rod outer segment. Kinetics and parameters of activation and deactivation. J Biol Chem 253(24):8902-8909.
Yiangou Y, Facer P, Durrenberger P, Chessell IP, Naylor A, Bountra C, Banati RR, Anand P. 2006. COX-2, CB2 and P2X7-immunoreactivities are increased in activated microglial cells/macrophages of multiple sclerosis and amyotrophic lateral sclerosis spinal cord. BMC Neurology 6:12.

Yoneda T, Kameyama K, Esumi K, Daimyo Y, Watanabe M, Hata Y. 2013. Developmental and visual input-dependent regulation of the CB1 cannabinoid receptor in the mouse visual cortex. PLoS One 8(1):e53082.
Zabouri N, Bouchard JF, Casanova C. 2011a. Cannabinoid receptor type 1 expression during postnatal development of the rat retina. J Comp Neurol 519(7):1258-1280.
Zabouri N, Ptito M, Casanova C, Bouchard JF. 2011b. Fatty acid amide hydrolase expression during retinal postnatal development in rats. Neuroscience 195:145-165.
Zangenehpour S, Javadi P, Ervin FR, Palmour RM, Ptito M. 2014. A Deficit in Face-Voice Integration in Developing Vervet Monkeys Exposed to Ethanol during Gestation. PLoS One 9(12):e114100.